Negative cell autotropisms in *Aspergillus fumigatus*

A thesis submitted to The University of Manchester for the degree of Doctor of Philosophy in the Faculty of Biology, Medicine and Health

2018

Pavlos Geranios

School of Biological Sciences

Infection, Immunity and Respiratory Medicine

Manchester Fungal Infection Group

[Blank page]

List of Contents

Word count: 50,763

List of Figures

List of Tables

List of Abbreviations

ABPA: Allergic Bronchopulmonary Aspergillosis

ACMA: *Aspergillus* Complete Medium Agar

AGC: Protein Kinase A, G and C group

AmB: Amphotericin B

AMM: *Aspergillus* Minimal Medium

AMMA: *Aspergillus* Minimal Medium Agar

ANOVA: Analysis of Variance

BLAST: Basic Local Alignment Search Tool

blastp: protein-protein BLAST

BTH: budded-to-hyphal (form)

Ca^{2+}: Calcium ion

CAMK: Calcium/Calmodulin Modulation Kinase activity group

CCD: Charge-coupled Device

Cd: Cadmium

CDK: Cyclin-dependent kinase

CFW: Calcofluor White

CK1: Casein Kinase 1 group

CLSM: Confocal LASER-Scanning Microscopy

CMGC: Kinase group of CDKs, MAPKs, GSK and CDK-like kinases

CNPA: chronic necrotic pulmonary aspergillosis

CO$_2$: Carbon dioxide

CPA: chronic pulmonary aspergillosis

Cu: Copper

CWI: Cell Wall Integrity pathway

DIC: Differential Interference Contrast

DMSO: Dimethyl Sulfoxide

DSCAM: Down's Syndrome Cell Adhesion Molecule

E$_r$: Reduced modulus

FGSC: Fungal Genetics Stock Centre

Fiji: Fiji is just ImageJ

FOV: Field of view

GAG: Galactosaminogalactan

GAP: GTPase activating proteins

GEF: Guanine nucleotide exchange factor

GFP: Green Fluorescent Protein

GM: Genetic Modified

GMO: Genetically Modified Organism

GPCR: G-protein coupled receptor

GSK: Glygogen-synthase kinases

h: hour(s)

HKI: Hans Knöll Institute

HOG: High-osmolarity glycerol

hpi: hours post-inoculation

IMS: Industrial Methylated Spirit

IQR: Interquartile Range

KEGG: Kyoto Encyclopedia of Genes and Genomes

kg: kilogram(s)

KO: knock-out (strain)

kPa: kiloPascal

LAS X: Leica Application Suite X

LASER: Light Amplification by Stimulated Emission of Radiation

LSFM: Light Sheet Fluorescence Microscopy

MAPK: Mitogen-activated protein kinases

MFIG: Manchester Fungal Infection Group

min: minute(s)

ml: millilitre(s)

mol: mole(s) – SI Unit

MW: Molecular Weight

NA: (Lens) Numerical Aperture

NIST: National Institute of Standards and Technology

nm: nanometre(s)

º: degree(s)

OCTIN: octahedral crystal matrix protein

PABA: 4-aminobenzoic acid

PAQR: Progestin and adipoQ receptor family

Pcdh: Protocadherin

Pcdh: Protocadherin(s)

PDHK: pyruvate dehydrogenase kinase group

PDMS: Polydimethylsiloxane

pH: Potential of Hydrogen

PI: Propidium iodide

PIKK: Phosphatidyl-inositol 3' kinase-related kinases

PKA: Protein Kinase A

PKC: Protein Kinase C

PTFE: Polytetrafluoroethylene

PTIO: 2-Phenyl-4,4,5,5-tetramethylimidazoline-1-oxyl 3-oxide

Ret. Time: Retention time

RGS: Regulation of G-protein signalling

RIO: "right open reading frame" kinase group

RNS: Reactive Nitrogen Species

ROS: Reactive Oxygen Species

RT: Room Temperature

SAFS: severe asthma with fungal sensitisation

SDA: Sabouraud Dextrose Agar

SEM: Scanning Electron Microscopy

SPIM: Selective Plane Illumination Microscopy

Spk: Spitzenkörper

STE: Kinase group including many kinases in the MAPK cascades

tblastn: protein-nucleotide BLAST

TD-GC/TOF-MS: Thermal Desorption-Gas Chromatography/Time-of-Flight-Mass Spectrometry

Tenax TA: registered trademark of poly(2,6-diphenyl-p-phenylene oxide)

TK: Tyrosine kinase group

TORC: Target of Rapamycin complex

UV: Ultraviolet

VMM: Vogel's Minimal Media

VOC: Volatile Organic Compound

WASP: Wiskott-Aldrich syndrome protein

µM: micromolar(s)

Abstract

Negative cell autotropisms are ubiquitous in true filamentous fungi. Three clear examples are: (1) determination of the site of germ tube emergence from a spore away from surrounding spores; (2) avoidance of growing adjacent germ tubes during colony initiation; and (3) avoidance of growing adjacent vegetative hyphae and branches at the colony periphery. These tropisms may be important in reducing the competition of neighbouring germ tubes/hyphae for nutrients. Despite their widespread occurrence, in fungi, little is known about the signalling processes governing these negative tropisms. The overall aim of the research described in this thesis was to analyse negative autotropisms in the human pathogen *Aspergillus fumigatus* in order to understand their mechanistic basis.

High resolution confocal microscopy was used to analyse negative autotropisms during conidial germination, germ tube growth, vegetative hyphal growth in *A. fumigatus*. The interaction between living cells was found to be a prerequisite for self-avoidance. A novel 3D image analysis method was developed which allowed the quantification of angles formed between germ tubes to measure self-avoidance. Results from this quantification showed the angles are narrower than expected due to the propensity of germ tubes to invade their substratum by means of an unknown mechanism. Self-avoidance in vegetative leading hyphae may play a role in the formation of barrier zone between two approaching colonies.

NO was found not to influence negative autotropisms based on experiments using the NO-scavenger PTIO. Ten chemical compounds, previously found to cause germination self-inhibition, were also found not to influence the self-avoidance responses. However, one of these compounds, nonanoic acid, induced the formation of specialised asexual hyphal aggregates known as synnemata (coremia) after 48 hours, the first such report in *A. fumigatus* to-date. Using gas chromatography-mass spectrometry, a fungal headspace analysis above colonies of the wild type, and a secondary metabolism defective strain (*ΔpptA*) which exhibits self-avoidance, revealed six common volatile organic compounds (VOCs) between the two strains. The potential self-avoidance activities of these six VOCs remain to be analysed.

A non-biased phenotypic screen of 16 G-protein coupled receptor (GPCR) deletion mutants and 90 protein kinase deletion mutants revealed that 7 of the GPCR mutants and 13 of the kinase mutants were defective in self-avoidance by undergoing hyphal aggregation. The GPCRs belong to four classes of fungal receptors involved in pheromone-, carbon-sensing, nitrogen-, and steroid-sensing. The kinase mutant screen identified homologues of *Saccharomyces cerevisiae* in the mitogen-activated protein (MAP) kinase cascade that belongs to the mating pheromone response pathway, along with other kinase homologues involved in nutrient sensing, that may be involved in self-avoidance responses.

My results indicate that negative, self-avoidance autotropisms are probably responses to a combination of multiple, extracellular stimuli which activate multiple signalling pathways in germinating spores, germ tubes and hyphae. Some of these signals (e.g. pheromones) may be derived from these cells whilst others are probably derived from the microenvironment around the growing cells. It is proposed that, based on the balance between the combination of signals received, the fungal cell "decides" where to grow in the form of a self-avoidance response, thus maximising its growth efficiency and therefore fitness to the external environment.

Declaration

No portion of the work referred to in this thesis has been submitted in support of an application for another degree or qualification of this or any other university or other institute of learning.

_____

Pavlos Geranios

Manchester, March 2018

Copyright Statement

    i. The author of this thesis (including any appendices and/or schedules to this thesis) owns certain copyright or related rights in it (the "Copyright") and he has given The University of Manchester certain rights to use such Copyright, including for administrative purposes.

    ii. Copies of this thesis, either in full or in extracts and whether in hard or electronic copy, may be made **only** in accordance with the Copyright, Designs and Patents Act 1988 (as amended) and regulations issued under it or, where appropriate, in accordance with licensing agreements which the University has from time to time. This page must form part of any such copies made.

    iii. The ownership of certain Copyright, patents, designs, trademarks and other intellectual property (the "Intellectual Property") and any reproductions of copyright works in the thesis, for example graphs and tables ("Reproductions"), which may be described in this thesis, may not be owned by the author and may be owned by this parties. Such Intellectual Property and Reproductions cannot and must not be made available for use without the prior written permission of the owner(s) of the relevant Intellectual Property and/or Reproductions.

    iv. Further information on the conditions under which disclosure, publication and commercialisation of this thesis, the Copyright and Intellectual Property and/or Reproductions described in it may take place is available in the University IP Policy (see http://documents.manchester.ac.uk/DocuInfo.aspx?DocID=24420), in any relevant Thesis restriction declarations deposited in the University Library, The University Library's regulations (see http://www.library.manchester.ac.uk/about/regulations/) and in the University's Policy on Presentation of Theses.

Epigraph

Ἰθάκη

Σὰ βγεῖς στὸν πηγαιμὸ γιὰ τὴν Ἰθάκη,
νὰ εὔχεσαι νᾶναι μακρὺς ὁ δρόμος,
γεμάτος περιπέτειες, γεμάτος γνώσεις.

Τοὺς Λαιστρυγόνας καὶ τοὺς Κύκλωπας,
τὸν θυμωμένο Ποσειδῶνα μὴ φοβᾶσαι,
τέτοια στὸν δρόμο σου ποτέ σου δὲν θὰ βρεῖς,
ἂν μέν᾽ ἡ σκέψις σου ὑψηλή, ἂν ἐκλεκτὴ
συγκίνησις τὸ πνεῦμα καὶ τὸ σῶμα σου ἀγγίζει.

Τοὺς Λαιστρυγόνας καὶ τοὺς Κύκλωπας,
τὸν ἄγριο Ποσειδῶνα δὲν θὰ συναντήσεις,
ἂν δὲν τοὺς κουβανεῖς μὲς στὴν ψυχή σου,
ἂν ἡ ψυχή σου δὲν τοὺς στήνει ἐμπρός σου.

Νὰ εὔχεσαι νά ᾽ναι μακρὺς ὁ δρόμος.
Πολλὰ τὰ καλοκαιρινὰ πρωϊὰ νὰ εἶναι
ποὺ μὲ τί εὐχαρίστηση, μὲ τί χαρὰ
θὰ μπαίνεις σὲ λιμένας πρωτοειδωμένους·

νὰ σταματήσεις σ᾽ ἐμπορεῖα Φοινικικά,
καὶ τὲς καλὲς πραγμάτειες ν᾽ ἀποκτήσεις,
σεντέφια καὶ κοράλλια, κεχριμπάρια κ᾽ ἔβενους,
καὶ ἡδονικὰ μυρωδικὰ κάθε λογῆς,
ὅσο μπορεῖς πιὸ ἄφθονα ἡδονικὰ μυρωδικά.

Σὲ πόλεις Αἰγυπτιακὲς πολλὲς νὰ πᾶς,
νὰ μάθεις καὶ νὰ μάθεις ἀπ᾽ τοὺς
σπουδασμένους.
Πάντα στὸ νοῦ σου νἄχῃς τὴν Ἰθάκη.
Τὸ φθάσιμον ἐκεῖ εἶν᾽ ὁ προορισμός σου.

Ἀλλὰ μὴ βιάζῃς τὸ ταξείδι διόλου.
Καλλίτερα χρόνια πολλὰ νὰ διαρκέσει.
Καὶ γέρος πιὰ ν᾽ ἀράξῃς στὸ νησί,
πλούσιος μὲ ὅσα κέρδισες στὸν δρόμο,
μὴ προσδοκώντας πλούτη νὰ σὲ δώσῃ ἡ Ἰθάκη.

Ἡ Ἰθάκη σ᾽ ἔδωσε τ᾽ ὡραῖο ταξίδι.
Χωρὶς αὐτὴν δὲν θἄβγαινες στὸν δρόμο.
Ἄλλα δὲν ἔχει νὰ σὲ δώσει πιά.

Κι ἂν πτωχικὴ τὴν βρῇς, ἡ Ἰθάκη δὲν σὲ γέλασε.
Ἔτσι σοφὸς ποὺ ἔγινες, μὲ τόση πείρα,
ἤδη θὰ τὸ κατάλαβες ἡ Ἰθάκες τί σημαίνουν.

Ithaka

When as you set about on the passage to Ithaca
do wish for the journey to be long,
full of adventures, full of learnings.

The Lestrygonians and the Cyclopes,
the enraged Poseidon, don't fear them,
suchlike you will not encounter in your journey,
if your thought, remains high, if your body
and mind are touched by excellent excitement.

The Lestrygonians and the Cyclopes,
the fierce Poseidon, you will not meet them,
if you don't carry them within your soul,
if your soul doesn't place them before you.

Do wish for the journey to be long;
for the summery mornings to be many,
whereas with what pleasure, with what joy
will you enter in first seen ports.

Do stop by the Phoenician markets,
and do acquire the fine commodities
nacres and corals, amber and ebony pieces,
and luscious perfumes of all kinds,
as abundant luscious perfumes as you can.

Do go to many Egyptian cities,
do learn and do learn by the scholars.
Always do keep your mind on Ithaca,
the arrival there is your destination.

But do not hasten the trip at all.
It'd be better if it lasted many years;
and you old man by then moor at the island,
rich with the lot you earned on the journey,
without expecting Ithaca to give you riches.

Ithaca gave you the nice trip.
Without her you wouldn't have set about the journey.
But now she does have nothing to give you anymore.

And should you find her poor, Ithaca did not deceive you.
As wise as you became, with such experience.
you would have understood by now what do
the Ithacas stand for.

K. Π. Καβάφης

Acknowledgements

A PhD project is a strenuous journey of self-discipline, self-motivation, self-reflection and, with a certain amount of luck, fulfilment and satisfaction. Even though a single name is written on the spine of this thesis, the exchange of ideas and collaboration is a necessary requirement for the fruition of any academic project, rendering it, even indirectly, a collective effort. In this aspect, this PhD is no different, therefore there are quite a few people which I would like to express my gratitude to.

First, I would like to thank my main supervisor Nick Read for his constant help, attention and general attitude. Since the first time we meet on late January 2012 in Edinburgh you have been nothing but supportive. Even when you had a lot of personal distress, you always found some time for me and my crazy ideas or expectations. Your optimism and positive mentorship have been truly inspiring throughout these four years. I would also like to thank my second supervisor, Mike Bromley who knew when to put a stop to my presence in the lab, so I could start writing, and for his invaluable input when I needed him most. I thoroughly enjoyed our conversations and have gained a lot from your advice. The same goes for Colette Inkson-Webb, who first helped me settle in the UK, and gave her insightful feedback above and beyond her call of duty as the Project Manager of the FungiBrain project. It may have looked that I did not pay attention to what you said, but I always took and take your advice into account. I would also like to thank Elaine Bignell for always having her door open to me and my questions, even when she had to juggle through dozens of other more important responsibilities. Also, for trusting me with responsibilities that involved the externalisation of MFIG to the public. It was a huge experience and honour. Paul Bowyer for being supportive and keen on discussing everything new regarding my research ideas. Thank you for placing your trust in me to design and carry out the experiments with the 16HBE cell lines!

My gratitude goes also to Sergio David Moreno Velasquez and Constanze Seidel, for their support in and outside the lab, and their scientific feedback. You both know that in your faces I did not gain friends, but an extension of my family. I am looking forward to meeting with you again very soon, maybe in a remote beach watching the sunset while drinking our freddo cappuccinos! Special mention should go to Narjes Al-Furaiji, for her amazing beyond-selfless generosity. Without your knockout strains,

significant portion of this PhD would not have been made possible. I cannot begin to express how I will miss your spectacular catering services!

<u>Waqar Ahmed</u>, <u>Craig Portsmouth</u>, <u>Iain White</u> and <u>Stephen Fowler</u> from the Manchester Institute of Biotechnology (MIB) for their massive help while we set up (and analysed the data of) the GC-MS experiments. You acquainted me with a branch of science that I would never have thought I would cross in my career and for this I am grateful! It would be an understatement to say that our collaboration has been pure joy. <u>Sara Gago</u> for the splendid collaboration (and her patience) during the analysis of volatome of infected cell lines and for teaching me how to handle the latter! It has been a pleasure to work with you and gain valuable research experience by your side.

<u>All members from the Read group</u>, past and present. Notably, <u>Can Zhao</u> for always been keen to answer any weird chemistry-related question I had. <u>Darren Thomson</u> for his advice on the refinement of several microscopy techniques, and his patience whenever I left the confocal PC turned on! <u>Alberto Munoz</u> on helping me settle in the Manchester Fungal Infection Group (MFIG) and for his advice on the preliminary experiments during my first year of this project. <u>Patricia Hernandez-Ortiz</u> (also a FungiBrain fellow) for all help related to *Neurospora crassa* experiments, which unfortunately did not make it in the final text. <u>Nagwa Ben Ghazzi</u> for her vast amounts of patience with me during some very stressed times.

All members of the MFIG during my time there but more specifically: <u>Jorge Amich Elias</u> for his amazing attitude, sharing of excellent music taste, scientific feedback, and interest in my research since the day he arrived. <u>Sayema Khan</u> for being extremely patient with me and helping me out file in consumable orders whenever I needed her. <u>Aiah Khateb</u> for our unofficial PGA (Post-Grads Anonymous) meetings, general support, and for providing a small window to see through at an intriguing different culture than the one I was brought up in. <u>Margherita Bertuzzi</u> for her eagerness to help every single time I asked her, despite her being overwhelmingly busy with her own work. <u>Fabio Gsaller</u> for the solid advice and of course the great trip we shared towards Asilomar 2017. <u>Jennifer Scott</u> for putting up with all my silly pranks when she first arrived at MFIG and for making me feel that I am funny. I wish you the best in your future, but judging by your eagerness and hard work, it is pretty much guaranteed.

Dedication

The research, writing and completion of this PhD thesis would have been impossible without the continuous support and love of the pillar of my life; Παναγιώτα Σταθοπούλου (Panagiota Stathopoulou). For all the nights I have been away, either isolated in the lab or at the PC writing, for all the times you needed me and I was not there, for all the sacrifices you have made, so I could finish this. This life milestone is as much yours as it is mine. I also dedicate this thesis to my daughter Ευτυχία (Eftychia), one of the earliest and, most surely, the best result I have had during this PhD. Your smile and mental acuity never fail to amaze me, and I cannot wait to see you grow and blossom! I love you both from the depths of my heart.

Chapter 1

General introduction

[Blank page]

1.1 The Kingdom of Fungi

The three-domain system of life (Woese et al., 1990), which classifies three main domains of life (Bacteria, Archaea, Eucarya), has undergone many revisions since it was proposed. One of the latest revisions suggests that life can be classified into a two-superkingdom (Prokaryota and Eukaryota) further divided into seven-kingdom system (Archaea, Bacteria, Protozoa, Chromista, Fungi, Plantae, Animalia) (Ruggiero et al., 2015). The kingdom of Fungi comprises of ~99,000 described species (Kirk et al., 2008) with a recent estimate of the total species number ranging from 2.2 to 3.8 million (Hawksworth and Lücking, 2017). Fungi diverged more recently from animals than plants, which was 1.538 billion years ago (animal-fungus) compared to 1.547 billion years ago (animal-plants), based on data obtained from comparison of 75 genes present in plants, animals and fungi (Wang et al., 1999).

Further classification of the fungal kingdom is based primarily upon their sexual structures. Thus, the kingdom is divided into two subkingdoms: Dicarya (Neomycota) and Eomycota. Dicarya consist of the phyla Ascomycota, fungi whose meiotic spore products are contained in asci (sacks), and Basidiomycota, fungi which produce specialised support cells for their spores (basidia). Eumycota contains more primitive fungal life forms, and, notably, the only fungal phylum with a motile life stage cycle, the Chytridiomycota (James et al., 2006).

Fungi are a very diverse group of heterotrophic organisms; able to occupy a wide range of niches across the globe ranging from extreme conditions such as nuclear reactors and the Antarctic up to survival in the International Space Station (reviewed by Newsham, 2012). This high adaptability can be partly attributed to the diverse capabilities of nutrient assimilation in the fungal kingdom. Fungi have adapted a diverse range of metabolic pathways which has resulted in them being major participants in the carbon, nitrogen, sulphur and phosphate biogeochemical cycles (Hawksworth, 1991).

A defining characteristic of the majority of species in the fungal kingdom is the presence of a glucan-chitinous cell wall, as opposed to the cellulose cell wall in plants. A dynamic organelle, its presence is vital for many morphological and functional processes in the fungal cell cycle. The fungal cell wall's components are predominantly glycoproteins and polysaccharides, mostly glucan (mainly 1,3-glucan) and chitin (reviewed by Bowman and Free, 2006).

1.2 The genus *Aspergillus*

The *Aspergillus* genus consists of approximately 250 species. However, due to the complex taxonomy of the genus this number might be smaller because of conflicting references on the agreed number of accepted species (Peterson, 2008). The *Aspergillus* genus belongs to the taxonomic Order Eurotiales (Eurotiomycetidae/ Eurotiomycetes/ Pezizomycotina/ Ascomycetes) which includes fungi with a wide range of metabolic functions. Many species of this Order are highly important for the food industry (e.g. *Aspergillus oryzae* is used to produce sake by rice fermentation). Furthermore, it includes species that have a significant negative impact on human health, such as *A. flavus* and *A. parasiticus* which produce aflatoxins and neurotoxins respectively, or species responsible for infectious diseases such as aspergillosis by *A. fumigatus* and *A. niger* and in immunocompromised patients (Kirk et al., 2008).

The subphylum of Pezizomycotina consists of ascomycetes that grow and reproduce by producing hyphae and ascospores in their sexual cycle. The ascospores are located in one of the four specialised species-dependent, differentiated multi-hyphall structures called ascocarps: cleistothecia, perithecia, apothecia or pseudothecia. These structures differ in size, shape and the location of asci within them (Poggeler et al., 2006). The ascocarp of the members of the *Aspergillus* genus is the cleistothecium.

The species of the *Aspergillus* genus are identified by the presence of a common morphological trait, the reproductive structure of the asexual cycle. This structure consists of the conidiophore which results in specialised lines of cells: the metulae and phialides. The latter cells produce the conidiospores through mitosis. The name *Aspergillus* originates from the botanist Pietro Antonio Micheli who in 1729 described the fungus for the first time. The chains of conidia growing radially from the conidiophores resemble the aspergillum, an instrument used in the Catholic church for sprinkling holy water during communion (Fig. 1.1).

For most of the species belonging to the *Aspergillus* genus a sexual cycle stage has not been described, despite them being in the Ascomycota phylum. The *Aspergillus* genus contains many fungal anamorphs, i.e. fungi that have no known sexual cycle. These anamorphs are connected to twelve distinct teleomorphic species, on which production of ascospores by meiosis can be observed (Dyer and O'Gorman, 2012). Usually the taxonomy of the teleomorph, if it is known, predates the one of the
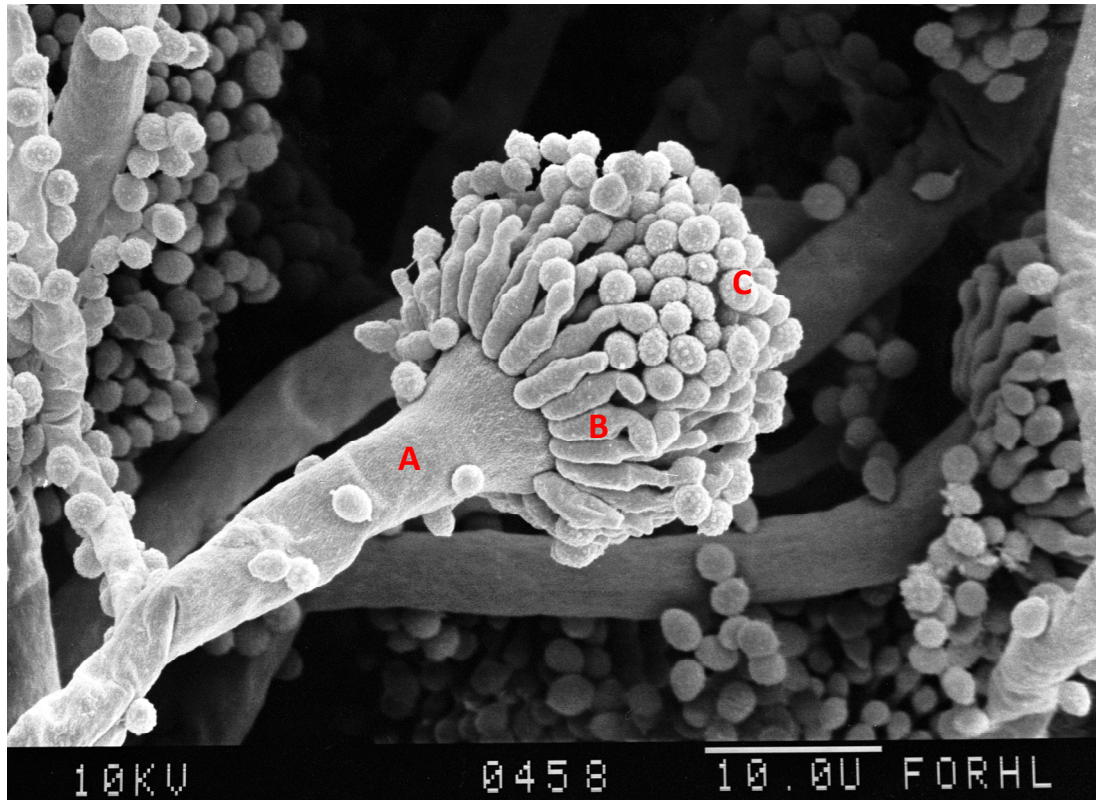
Figure 1.1 Scanning-electron microscopy image of the *A. fumigatus* conidiophore. The stalk (A) is a differentiated supporting hyphal structure upon which grow the phiallides (B), bottle-shaped differentiated cells. Phiallides divide mitotically to produce conidiospores (or conidia) (C). A distinguishing feature of the *A. fumigatus* conidiophore is the lack of basal cells between the stalk and the phialides called metualae (singular metula) which are a common in other *Aspergilli* (eg. *A. nidulans)*. Reproduced from https://wellcomecollection.org.

anamorph. This rule does not apply by convention to the fungi belonging to the *Aspergillus* genus (as voted during the International Commission of *Penicillium* and *Aspergillus*, Amsterdam, Netherlands, April 2012). Instead the genus retains its name (*sensu* Raper and Fennell, 1965) and other names are treated as optional when they have meaning, e.g. when genes of sexual development are described.

1.2.1 Biology of *Aspergillus fumigatus*

The first description of *A. fumigatus* was detailed by Fresenius (1850) after observing isolates from air sacs and bronchi of a bustard. It is an opportunistic saprotrophic fungus found in soil where it participates in the carbon and nitrogen cycles by decomposing organic matter (Mullins et al., 1976). It's genome has been sequenced and consists of 9,926 predicted genes distributed in eight chromosomes (Fedorova et al., 2008; Nierman et al., 2005). In their ecological niche *Aspergilli* encounter a highly competitive environment; having to compete against ~4,000 prokaryotic and eukaryotic species per gram of soil (Montesinos, 2003). The competition for nutrients necessitates

Table 1.1 The taxonomy of *Aspergillus fumigatus* (NCBI taxonomy, 2018)

Taxonomy	
Kingdom	Fungi
Phylum	Ascomycota
Subphylum	Pezizomycotina
Class	Eurotiomycetes
Family	Aspergillaceae
Genus	*Neosartorya*

a complex signalling machinery which would interact with and sense the external environment guiding growth towards optimal, or away from adverse, conditions for the fungus to optimise its fitness to best compete within its microhabitat (tropic responses, examined in section 1.3).

The life cycle of *Aspergillus fumigatus* consists of an asexual and a, recently described, sexual stage (O'Gorman et al., 2009) and shares many similarities with *Aspergillus nidulans* life cycle (Casselton and Zolan, 2002). The discovery of the sexual stage has resulted in a re-evaluation of the *A. fumigatus* taxonomy, attributing the name *Neosartorya fumigata* to the teleomorph. The asexual cycle is divided in three stages (Adams et al., 1998): a) germination of the conidiospore, b) hyphal growth and c) production of specialised structures for spore production. The germination of the airborne conidia occurs after their establishment on a substrate. If the conditions are suitable enough (abundance of nutrients and humidity) the conidia start to swell in an almost uniform manner (isotropic growth) and then germinate. The germination rate is dependent on the concentration of conidia as well as the temperature of the environment, with optimal growth conditions range from 25 °C to 37 °C (Araujo and Rodrigues, 2004). The main fungal structure, post-germination, is the septate filamentous hypha. All hyphae are characterised by polarised growth, extending apically while branching at the same time to produce the vegetative mycelium. The third stage includes the differentiation of aerial hyphae into conidiophores which in turn produce the mitotic products of the asexual cycle, the conidia, which are dispersed in air (Fig. 1.2).

The wild type strain of *A. fumigatus* produces greenish to grey colonies on solid media, a factor based on the colour of the highly abundant conidia in the colony. The conidiospores are spherical in shape with a size ranging from 2.5 to 3 μm in diameter, a trait which allows the conidia to enter the lung alveoli easily (Latgé, 2001). Once the conidium germinates it produces a small specialized hypha called the germ tube. The conidium combined with its germ tube, which is initially multinucleate lacking a septum, is defined as the germling. As the hypha grows the first septum is usually formed between the spore and germ tube marking the first compartmentalisation event in the
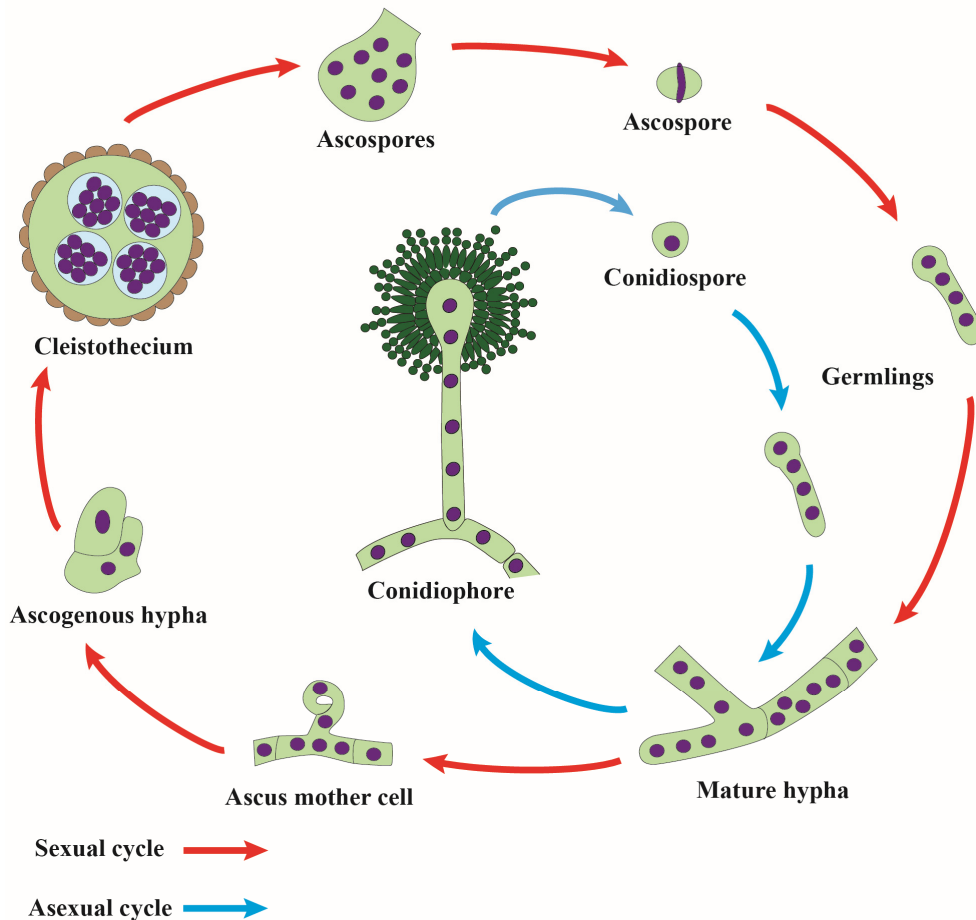
Figure 1.2 The life cycle of *Aspergillus fumigatus*. Hyphae are multinucleate compartmentalized structures, which can differentiate into conidiophores or asci. The former produce multiple chains of conidia (mitotic reproduction), the latter contain the ascospores (produced meiotically). Asci are contained inside a specialized structure, the cleistothecium. Successful gemination leads to the formation of new hyphae. Details on specific structures in main text. Reproduced with permission from Moreno-Velasquez, 2017.

cell. Subsequent septation and changes in the cell wall composition results in the multinucleate, mature hyphae (Fig. 1.2).

1.2.2 Fungal diseases caused by *Aspergillus fumigatus*

Although 100-10,000 *Aspergillus fumigatus* conidia are estimated to be inhaled daily by humans (Latgé, 1999), they have little effect on healthy individuals as they are removed by cilia on airway epithelial cells and alveolar macrophages (Fig 1.3). However, in the case of immunodeficient hosts its effects can be dramatic. *Aspergillus*-related diseases occur frequently with 2.3 million episodes alone documented in Europe annually. The vast majority of those cases (approx. 2 million) are allergic disease in asthma and cystic fibrosis patients (Kleinkauf et al., 2013), while more than 200,000 cases of invasive aspergillosis (IA) are documented annually, mortality rates of IA range from 30-95%

(Brown et al., 2012). The worldwide numbers of aspergillosis cases are even greater: chronic pulmonary aspergillosis (CPA) is estimated to affect more than 3 million patients every year. Severe asthma with fungal sensitisation (SAFS) is believed to affect 3.25-14 million adults, while allergic bronchopulmonary aspergillosis (ABPA) is estimated to affect 4 million individuals with asthma and cystic fibrosis (reviewed by Brown et al., 2012).

The common requirement in all *Aspergillus*-related diseases is the inhalation of *Aspergillus* spores; the most common species (due to larger conidia dispersal) being *A. fumigatus*. Conidia can attach to the epithelium of damaged areas in the lung and if they escape the immune response germinate and establish fungal colonies. The reasons for *A. fumigatus* being a highly successful ubiquitous fungal pathogen are attributed to its physical and metabolic characteristics (Kwon-Chung and Sugui, 2013). More specifically, *A. fumigatus*
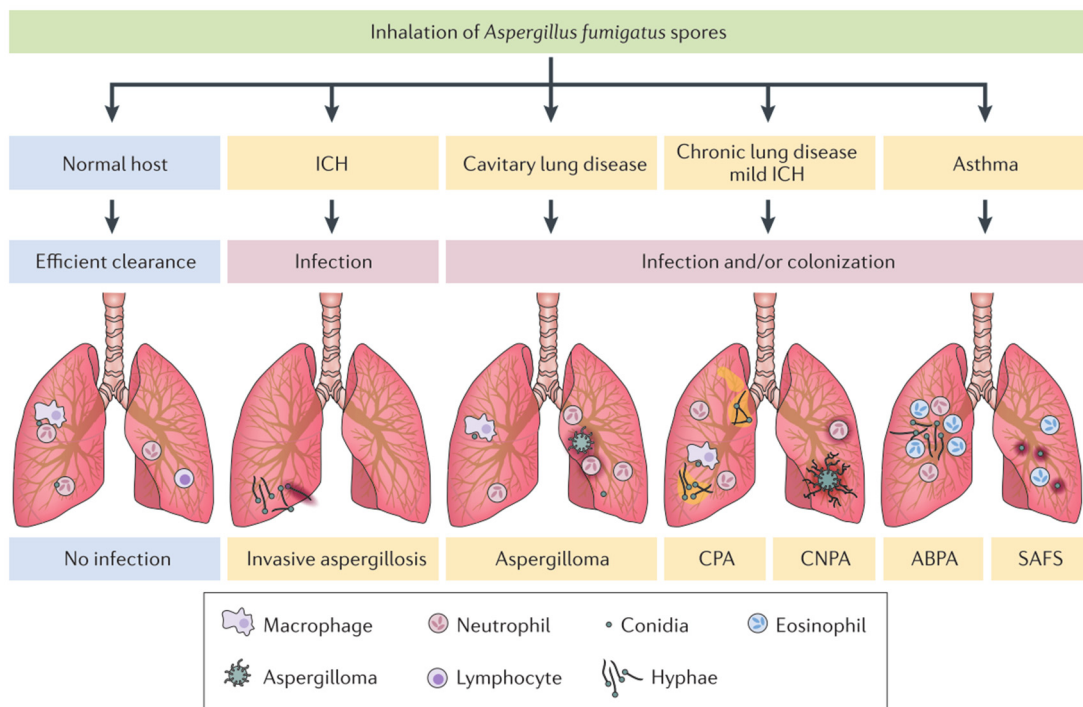
Figure 1.3 Types of Aspergillosis diseases. In normal hosts *Aspergillus* conidia do not have any effect. In immunocompromised hosts (ICH) conidia can germinate and disrupt the epithelial cell layer causing invasive aspergillosis (IA). A particular case is that of Aspergilloma where a biomass of differentiated mycelium ("a fungal ball") is formed in lung cavities which have resulted by previous damage due to illness or injury (acute cases). More chronic forms of infection and/or colonization include chronic pulmonary aspergillosis and chronic necrotic pulmonary aspergillosis (CPA and CNPA, respectively). Asthma and cystic fibrosis patients can have fungal burdens which results in secondary conditions such as severe asthma with fungal sensitisation (SAFS) or allergic bronchopulmonary aspergillosis (ABPA). Host natural defences besides the immune system leukocytes include cilia of the epithelial layers lining the bronchioles and alveolae. Reproduced from Van de Veerdonk *et al.*, 2017.

has a wide metabolic range which allows for the successful establishment in different environmental conditions. Moreover, its conidia are so small that are easily dispersed through air and can reach the lung bronchioles through the respiratory tract. Last but not least, the optimal temperature of the fungus' growth is 37 °C, the same as human body temperature which results in rapid growth in immunocompromised patients.

Among cystic fibrosis and asthma suffers a secondary inflicted condition is ABPA, an inflammatory lung disease characterised by hypersensitivity to fungal products. ABPA has been the most severe allergic pulmonary complication caused by *A. fumigatus* and has five distinct stages: the acute, remission, exacerbation, glucocorticoid dependent and fibrotic stage. There are at least 21 known allergens from *A. fumigatus* that cause ABPA reviewed in Singh *et al.* (2014). Severe cases of ABPA are found in cystic fibrosis patients, in which anti-IgE treatment has been tested (Jat et al., 2013). However, no successful therapy has been identified for treating ABPA.

Invasive aspergillosis is the most severe form of *Aspergillus* infection. Denning (1998) reviewed the different most common forms of IA which include: invasive pulmonary aspergillosis, *Aspergillus* tracheobronchitis, invasive sinusitis, disseminated, cutaneous and cerebral aspergillosis. Successful aspergillosis treatment with antifungals remains elusive. Previous strategies for managing aspergillosis included treatment with azoles, yet fungal strains have developed resistance to these drugs (Chowdhary et al., 2014; Seyedmousavi et al., 2014). However there are many factors affecting virulence, participating in different cellular functions, which can serve as potential targets (reviewed in Abad *et al.*, 2010).

The most common form of IA is pulmonary aspergillosis. Airborne conidia are inhaled by the host and establish in the alveoli. The adherence of *A. fumigatus* to host cells is dependent on several molecules, mainly the carbohydrates located in the fungal cell wall (Sheppard, 2011). The hyphal cell-wall exopolysaccharide galactosaminogalactan (GAG) has been shown to mediate adherence of *A. fumigatus* hyphae to fibronectin and epithelial cells and conceal the hyphal β-glucan from the immune system (Gravelat et al., 2013). Post-adherence there are two potential developments during fungal establishment: 1) either the fungus grows on top of the respiratory epithelium, or 2) conidia are internalised by epithelial cells and germinate internally. The epithelial responses and interactions with the fungal cells depend on the fungal morphotype and

host cell origin (Bertuzzi et al., 2018). It has been shown that dormant inhaled conidia possess a coherent outer layer of densely packed hydrophobic proteins, called hydrophobins, which mask the underlying immunogenic cell wall and result in the absence of immune response, even in healthy hosts (Aimanianda et al., 2009; Aimanianda and Latge, 2010). Once the conidia undergo isotropic growth prior to germination, the hydrophobin layer is disrupted, presenting antigens that stimulate an immune response. Another line of defence against the host's immune system is the ability to scavenge the Reactive Oxygen Species (ROS) produced by macrophages either by the production of melanin or by inducing apoptosis of the macrophages in the first place (Dagenais and Keller, 2009; Van De Veerdonk et al., 2017).

In immunocompromised hosts germlings can further grow and disrupt endothelial and epithelial cells. Further progression of the infection results in hyphae invading the lung tissue, entering the circulatory system through blood capillaries and further dissemination to other organs. The signals and precise process that leads to tissue invasion by hyphae have yet to be determined.

1.3 Fungal cell tropisms

A tropism is defined as the directional growth of a cell in response to an external (environmental) stimulus. Fungal tropic responses are important since they maximise the survivability and the successful establishment of a fungus in its niche. These tropisms can: assist successful invasion of a host and facilitate the avoidance of intra- and inter-species competition for nutrients necessary for growth while attracting the same species for mating at the same time. More specifically, by employing a signalling machinery which can sense external stimuli and modulate the fungal growth pattern, fungal tropic responses ensure that the fungus a) avoids potentially harmful interactions (e.g. negative tropisms) or b) is attracted to beneficial sources for nutrient assimilation, reproduction and growth (i.e. positive tropisms). Essentially, the equilibrium of all the external signals and the corresponding responses in a wild-type cell is what defines the growth patterns and sporulation of the fungus. Tropisms identified to date in fungi include thigmotropism, galvanotropism, phototropism, chemotropism and tropisms towards nutrients. Although significant progress has been made, knowledge on tropisms and their signalling machinery in *A. fumigatus* is still rather limited. Cases of such studied tropisms are examined in the corresponding subsections.

1.3.1 Thigmotropisms

A thigmotropism is the adjusted directional growth of an organism in response to the variation of a substrate's physical properties, such as its microtopography and hardness. The first report of touch-sensing response in fungi was made in *Arthobotrys oligospora*, a nematode-trapping fungus, which creates a cellular capture loop that swells upon touch, constricting any nematode which passes through (Drechsler, 1937). Thigmotropisms have also been well-described in phytopathogenic fungi. Different species have developed two basic strategies for locating the leaves' stomata in order to infect the plant: some species like *Cymadothea trifolii* grow along the peripheries of the epidermal cells (Roderick, 1993) while others cross the junctions between adjacent cells on the leaf surface at a 90° angle which improves their chances of locating stomata through which they invade their host (Hoch et al., 1993; Read et al., 1997).

Thigmotropism in human fungal pathogens, such as *C. albicans,* has previously been reported (Gow, 2004, 1993; Piérard et al., 2007). Despite the fact that thigmotropism is well-recognised in pathogenesis, it seems that it is not a prerequisite for successful infection. Brand *et al.* (2008) have shown that non-thigmotropic mutants of *Candida albicans* are not so successful during infection. However, the mutations affecting thigmotropism in these strains are pleiotropic and as a result the observed phenotype cannot be linked exclusively to them.

To date, there is no definite protein or complex which has been shown to be contact-induced and thus mechanosensory in fungi. However, investigation of thigmotropism and galvanotropism (section 1.3.2) in *C. albicans* revealed the participation of Ca^{2+} in these tropisms (Brand et al., 2007) (Fig. 1.4). The data in the referenced study predict a model in which extracellular calcium enters the cell through the Mid1-Cch1p calcium channel complex. This subsequently leads to hyphal re-orientation in accordance with the localization of Ca^{2+} influx. It seems that thigmotropic responses require the presence of two signals to happen: physical contact and a chemical signal which would then initiate the appropriate response. The former can be transduced by different signalling pathways in the cell such as intracellular Ca^{2+}-signalling, the cell wall integrity pathway, and via integrin-like proteins. Diffusible signals can be sensed by seven-transmembrane receptor to induce specific downstream cascades. As a result, distinct pathways may be involved in the recognition of thigmotropic signals and the activation of thigmotropic responses. A comprehensive review discussing fungal thigmotropisms

and their molecular regulation has been recently presented by Almeida and Brand (2017).

The homologue proteins of Cch1p and Mid1 (CchA and MidA, respectively) have been identified in *A. fumigatus*. Restriction of extracellular Ca^{2+} by the addition of chelating agents results inhibits growth of the null mutants of those proteins (De Castro et al., 2014). However, their direct involvement in thigmotropic responses has yet to be tested.

1.3.2 Galvanotropisms

A galvanotropism is cellular growth in a specific direction in response to an imposed direct current of electricity. Different fungi respond differently to changes in the electric fields' charge. Directional growth responses of filamentous fungi to fields of >2-5 V/cm have been observed, although zoospores of oomycetes are able to sense and respond to much weaker electric fields. Galvanotropism occurs naturally during recruitment of these zoospores from plant roots that produce sufficient electrical currents to attract them (Miller and Gow, 1989; van West et al., 2002).
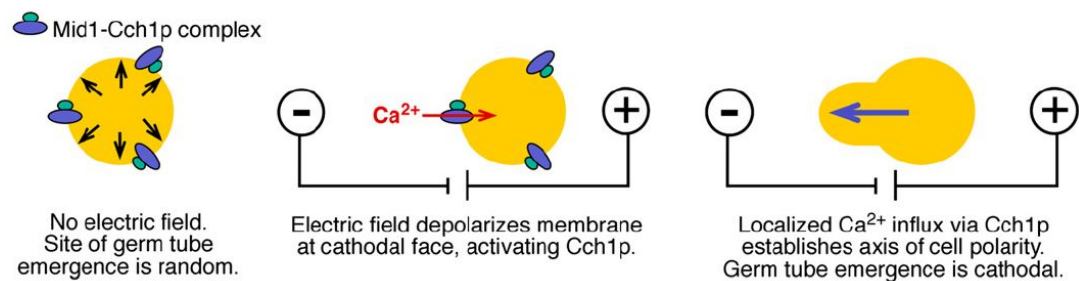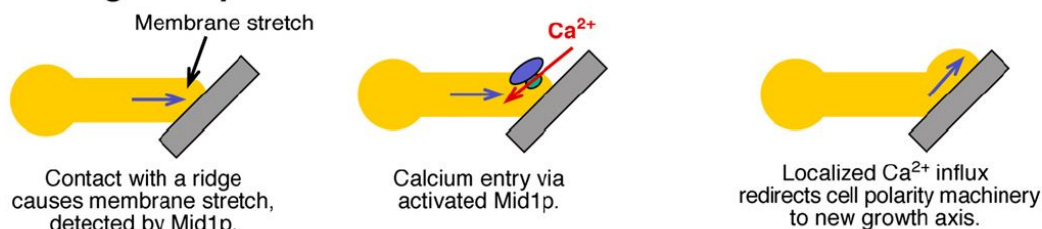
Figure 1.4 Suggested model for galvanotropism (A) and thigmotropism (B) in *C. albicans*. Cch1 is a high-affinity calcium channel and Mid1 is a transmembrane protein that is necessary for Ca^{2+} during pheromone response. After Ca^{2+} enters the cell calcineurin is activated that leads to a cascade leading to the change in hyphal orientation. Reproduced from Brand *et al.* (2007).

Experiments done with *C. albicans* have demonstrated that the fungus reorients its hyphae to the electric current, growing towards the negative pole (cathode) of the electric field (Brand *et al.*, 2007). This phenomenon is calcium-dependent as it was shown when the fungus was incubated with extracellular calcium (1mM). Presence of calcium chelators (BAPTA) disrupts this orientation, unless larger concentrations (up to ~3 mM) of calcium are added. The model on how calcium has been suggested to regulate orientated growth is shown in Fig. 1.4. The role of calcium in the rearrangement of apical growth direction is believed to involve that Ca^{2+}-dependent actin polymerisation and depolymerisation. Interestingly when incubating microtubules on a kinesin-coated surface, appliance of electric current forces the microtubules to rearrange their axis in parallel to the current (Kim et al., 2007).

Galvanotropism in *Neurospora crassa* is pH-dependent, an indication that different membrane components such as ion channels contribute to the sensing of the stimulus. Notably an isoelectric point has been described by Lever et al. (1994) in which the fungus displays grows perpendicular to the electric current. In *A. fumigatus* galvanotropisms are also dependent on extracellular Ca^{2+} with germ tubes growing towards the anode in electrical fields of 25 V/cm (Lever et al., 1994). In general, filamentous fungal pathogens do not display strong galvanotropic responses in their hosts, indicating that they are not sensitive enough to detect the weak electric fields in host tissue.

1.3.3 Phototropisms

Phototropisms, the directed growth in response to light, was reported very early in fungi in the *Phycomyces* genus (Castle, 1930). *Phycomyces blakesleeanus* reacts to light by bending its fruiting body stem (sporiangiophore) towards white light or by avoiding ultraviolet wavelengths. Phototropism in *P. blakesleeanus* requires the products of the *madA* and *madB* genes which form a complex (Sanz et al., 2009). The *madA* gene encodes for a protein that is similar to the blue-light photoreceptor in *N. crassa* WC-1 which contains a zinc-finger domain (Ballario et al., 1996).

Additionally, the conidiophores of *Aspergillus giganteus* have been observed to react positively towards white light, with the tropism effect being reversed when they are stimulated with ultraviolet wavelengths (Trinci and Banbury, 1968). This kind of tropism in a saprotrophic species, which mainly inhabits soil where sunlight is scarce,

could be explained by the molecular mechanism guiding its life cycle. The life cycle in several *Aspergillus* species is regulated by the complex governed by the VeA protein (Bayram et al., 2008; Kim et al., 2002). In wild type strains light inhibits the VeA protein which normally induces the production of sexual structures. Thus, in conditions where light is present, asexual reproduction is promoted which is metabolically less complex and produces a vast number of spores. *A. fumigatus* has recently been shown to regulate growth, metabolism and stress resistance in response to blue and red light (Fuller et al., 2013).

1.3.4 Chemotropisms

A chemotropism is defined as the directed growth responding to a signalling chemical molecule. A well-studied type of positive chemotropism in lower eukaryotes is their response to the species' mating pheromones. One of the simpler systems investigated is the chemotaxis of *Dictyostelium discoideum* cells to cAMP gradients that result in formation of a multicellular cell aggregation called a 'slug'. The yeast *Saccharomyces cerevisiae* has also been used for its well-defined pheromone tropism system. During the initiation of its life cycle sexual stage *S. cerevisiae* cells grow towards the pheromone gradient of the opposite mating type cells in order to mate (reviewed by Merlini et al., 2013). A review detailing the necessary proteins and presenting model pathways on these two systems has also been presented by Arkowitz (1999).

In summary, there is a requirement for a receptor to the signal. Once the receptor has been activated, signal transduction cascade takes place activating corresponding cellular functions. One of the most important of these functions is actin polymerization so as to rearrange the cells' growth towards the gradient. The intracellular turnover rate of the chemoattractant is also important to maintain the sensing of environmental signal gradient constant and avoid desensitization towards it.

Pheromones have also been described in *N. crassa* which is a heterothallic fungus with two mating types, *mat a* and *mat A* (Metzenberg and Glass, 1990). Two of them (peptides CCG-4 and MFA-1) are crucial for male fertility in the organism, while the CCG-4 peptide is important for the polarized growth of trichogynes, the receptive hyphae during sexual cycle of *N. crassa* (Kim and Borkovich, 2006). Another type of self-tropism described first in *N. crassa* is the oriented growth of conidial anastomosis tubes (CATs, section 1.3.4.1).

Oxygen has also been suggested to be a positive chemotropic factor for fungi by Robinson (1973). Despite clearly showing that there is directed growth in densely populated conidia of *Geotrichum candidum*, this study does not conclusively show that oxygen is without a doubt as Robinson's conclusions are speculative based on the limitations of perforated-plate assay used.

An important fungal tropism is the tropism towards nutrients. It has been observed that during starvation the typical symmetrical shape in *S. cerevisiae* is disrupted and the fungus produces invasive pseudohyphae in search for the restricting nutrients (Gimeno et al., 1992).

1.3.4.1 Conidial Anastomosis Tubes (CATs)

A particular case of positive chemotropisms are the formation of Conidial Anastomosis Tubes (CATs, Roca et al., 2004; Fig. 1.5). CATs are cell protrusions emerging from conidia and which are thinner and shorter than regular germ tubes. CATs home towards each other, in contrast to the negative chemotropism observed in vegetative hyphae. It has been shown that even if conidia are rearranged in relation to each other using optical tweezers CATs still home towards each other's' tips. This provides convincing evidence that that the signal inducing this positive chemotropism is both released and sensed at CAT tips (Roca et al., 2005a). Since their discovery, many fungal species have been verified to produce CATs (Roca et al., 2005b).
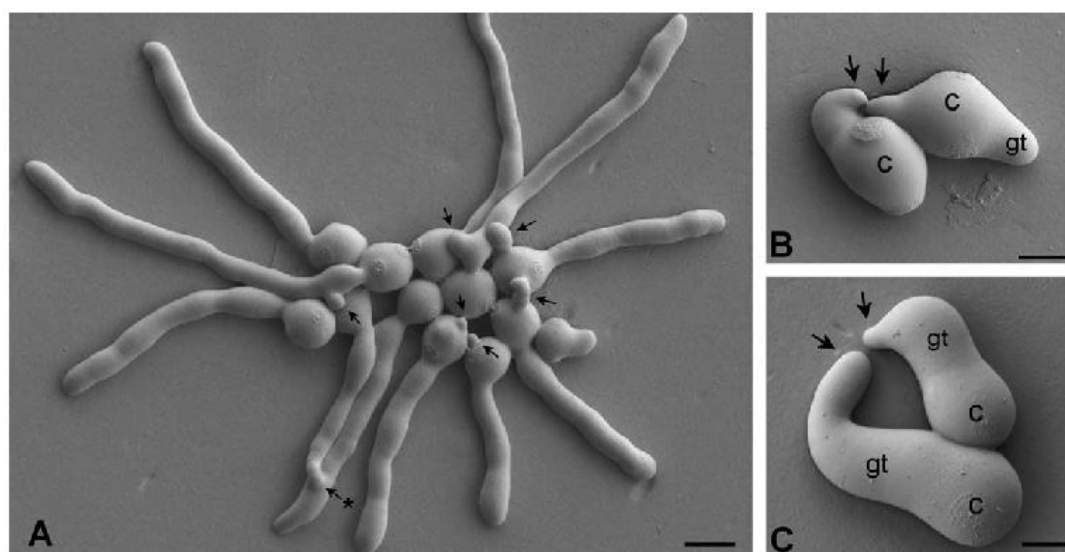
Figure 1.5 (A) CATs in *N. crassa* shown by arrowheads. (B, C) CATs protruding and homing towards each other from conidia, Bar scale = 5 μm. Reproduced from Roca *et al.* (2005b)

The presence of CATs could potentially provide at least three main advantages for the fungus: a) faster colony establishment due to early formation of hyphal network, b) sharing of nutrients and water between fused germlings and c) horizontal gene exchange, which may be particularly important in fungi that have no known sexual cycle (Read et al., 2010). In the latter case, genetic diversity in a species may be secured even though there is no efficient meiotic recombination (Ishikawa et al., 2012). The signalling pathways that regulate CAT formation and fusion are detailed in section 1.4.1.

Negative self-chemotropisms in fungi were also described very early and have been proposed to be more dominant than any positive tropism to nutrient availability (Clark, 1902; Fulton, 1906). Despite that, and contrary to positive chemotropism, little is known about negative self-tropisms regarding the chemical signals and/or pathways governing the phenomenon in filamentous fungi. A study using *Mucor* and *Aspergillus* has verified that there is a ubiquitous inhibitory substance secreted by hyphae which is responsible for the inhibition of germination in fresh conidia and inability of growing hyphae to grow towards it (Bottone et al., 1998). This substance has not been characterized yet, although the self-inhibition during growth that subsequently leads to radial growth of a fungal culture is widely-observed and well-known. No CATs have been observed in *A. fumigatus* to date. In fact, hyphal fusion occurs very rarely in the fungus but is induced highly stressful conditions (Read and Bromley, personal communication).

1.3.5 Other fungal tropisms

Other fungal tropisms have also been described. These include gravitropism and tropisms towards nutrients. Gravitropism is the directed growth as a response to earth's gravitational pull and has been studied extensively in the *Phycomyces* genus, which displays negative gravitropism (Dennison and Shropshire Jr., 1984). A recent study has unveiled that during fungus gravistimulation a major shift in the Ca^{2+} and H^+ ion flux from the tip to the base of the zygomycete sporangiophore is observed (Zivanovic, 2012). This change in the ion flux pattern during sporiangophore formation is absent in a mutant that has no gravitropic response. It has recently been shown in *Phycomyces blakesleeanus* that an octahedral crystal matric protein (OCTIN) makes up sedimenting vacuolar crystals to activate signalling pathways that modulate the tropic growth of sporangiophores which bear sporangia containing asexual sporangiophores.

Interestingly, OCTIN originated by horizontal gene transfer from gram-negative bacteria (Anh Nguyen et al., 2018).

Gravisensation and gravitropism are highly important to basidiomycetes as they have to organise their lamellae in the most efficient way for dispersing their spores by positively responding to gravity. Hyphae in the toadstool stalk, on the other hand, respond negatively to gravity (Grolig et al., 2006; Kern, 1999). A study with *Flammulina velutipes* toadstools suggested that each gravity-sensing hypha has its own gravisensor which results in the regulated secretion of a growth factor resulting in the bending of the hypha in appropriate ways (Kern et al., 1997). All in all, tropisms are a fundamentally and ubiquitous aspect of fungal polarized growth. This suggests that they are governed by conserved similar signalling pathways and regulatory mechanics.

1.3.6 Negative cell autotropisms (self-avoidance)

Negative cell autotropisms in fungi were first described at the end of the 19th century. Miyoshi (1894) showed that fungal hyphae can avert their growth in response to specific nutrient extracts, and poisons. In his study, Clark (1902) concluded that *Rhizopus* displayed negative chemotropism in response to a secreted factor from its own mycelium; the phenomenon overcame any positive chemotropism which may have been induced by food sources or oxygen. He also noted that his tested methodology did not verify whether negative tropisms are a result of copper sensing or not. Recent work involving *Geotrichum candidum, Gliocladium roseum, Humicola grisea* and *Trichoderma viride* as test organisms showed that negative chemotropisms are induced by copper (Cu), and cadmium (Cd) treatment in all tested fungi (Fomina et al., 2000).

Previous work had suggested that exhibited negative autotropisms during germination in arthrospore pairs of *G. candidum*, were a result of oxygen availability instead of the accumulation of the fungus's own metabolites (Robinson, 1973a). These findings contradicted the conclusions presented by Clark (1902) and Fulton (1906). Data obtained with early microfluidics experiments also suggested that the factor inducing negative cell tropisms is a self-secreted component which is diffusible, unstable and locally effective (Müller and Jaffe, 1965). This suggests that signalling may be induced by a volatile organic compound (VOC), something discussed in further detail in section 1.5 and Chapter 5. The model would also suggest that the governing factor is uniformly secreted in the extracellular environment with pulsatile or more rapid secretions taking

place at specific cell points. Further study of autotropisms in *B. cirenea* revealed that different pH caused by citrate buffers do not affect negative germination autotropisms in *B. cinerea* (Jaffe, 1966). Data from the same study suggested that saturation with CO_2 (0.3%-3%) reversed any chemoattraction between spores.

Surprisingly, little research has been carried out on negative fungal autotropisms in the recent years. Simulations and flow experiments in *S. cerevisiae* showed that the protease Bar1 secreted by *MAT***a** cells degrades the α-factor creating a gradient towards the *MATa* cells. This gradient results in avoidance of neighbouring *MAT***a** cells and growth towards *MATa* cells (Jin et al., 2011). Computational simulations have also been carried out to estimate the percentage of negative autotropisms taking place in a hyphal fungal colony (Meskauskas et al., 2004b) using a Neighbour-Sensing algorithm (Meskauskas et al., 2004a).

In summary, two main models have been proposed to explain the causal factors of self-avoidance in fungi: (a) the "staling reaction" caused by a self-secreted agent or environmental molecule which accumulates around hyphae and instigates outward growth or aversion (Müller and Jaffe, 1965; Stadler, 1952), and (b) the "limiting nutrient factor or agent" model which causes hyphae to search for higher concentrations away from neighbouring cells (Jin et al., 2011; Robinson, 1973b, 1973a).

In the context of disease, negative (auto)tropisms are crucial for the successful infection of the host by a fungal pathogen. It has been showing that *A. fumigatus* cells interacting with neutrophils stimulate evasive hyphal branching and avoidance of the interaction point. This responses has been shown to be independent of neutrophil NADPH oxidase activity (Ellett et al., 2017). Therefore, it is crucial to understand the mechanism(s) of growth avoidance in the fungus.

1.3.6.1 Negative autotropisms in neuron cells of higher eukaryotic organisms

The phenomenon of negative autotropisms has been extensively studied in neuron cells of higher eukaryotes. Negative cell autotropisms are essential for the correct formation and establishment of dendrite networks in higher eukaryotes (Kise and Schmucker, 2013). The first report of self-avoidance in neurons was made by Kramer and Stent

(1985) when they observed that some neuron axons in the leech *Haementeria ghilianii* did not overlap leading to hypothesis of neuron self-recognition and repulsion.

In the past two decades, significant steps have been made towards the understanding of self-avoidance and its role in neuronal networking in *Drosophila* and mice. The first breakthrough towards understanding the signalling machinery responsible was made when Slit proteins were identified as ligands for the Roundabout (Robo) receptor (Brose et al., 1999; Kidd et al., 1999; Li et al., 1999). These studies verified that there is an evolutionarily conserved, extracellular signal mediator (Slit peptide) which affects growth direction of neuron axons when it binds to its corresponding Robo receptor. The Slit-Robo pathway functions through the Rho GTPases Cdc42 and Rac1 (Fan et al., 2003; Wong et al., 2001) while receptor tyrosine phosphatases serve as positive regulators of the pathway (Sun et al., 2000). Netrin signalling is another type of signalling demanding a secreted cue to induce self-avoidance. Netrin-1 has been shown to bind to the <u>D</u>eleted in <u>C</u>olorectal <u>C</u>ancer (DCC) receptor and induce repulsion (Hamelin et al., 1993; Hong et al., 1999).

Another molecular strategy adopted for dendrite self-avoidance is the use of contact-mediated recognition and avoidance. In *Drosophila*, this is achieved by *Dscam* (Down's syndrome Cell Adhesion Molecule, Kidd and Condron, 2007; Matthews et al., 2007; Millard and Zipursky, 2008; Soba et al., 2007), a gene cluster which encodes (through alternative splicing) a set of immunoglobulin superfamily adhesion receptors located on the cell surface. In the case of two neurons expressing the same isoform of the Dscam1 receptor, the homophilic interaction of the dimer is not stable and thus the neuronal branches tilt away from each other. Mutant *Drosophila* larvae which carried strong loss-of-function allelles of *Dscam* due to modification of their cytoplasmic ends, showed branch aggregation (clumping) of their neurons (Matthews et al., 2007; Fig. 1.6). In vertebrates, deletion of the PDZ-interacting C-terminus of DSCAM resulted in variable phenotypes of self-avoidance, ranging from normal to complete loss-of-function, depending on the type of neuronal cell (Garrett et al., 2016). DSCAM has also been associated with the netrin signalling pathway (Purohit et al., 2012).

In mice the prominent molecules involved in contact-mediated self-avoidance are the cadherin adhesion molecules encoded by the cluster of the γ-protocadherin (*pcdhcγ*) genes (Hayashi and Takeichi, 2015; Hoang and Grueber, 2013; Keeler et al., 2015;
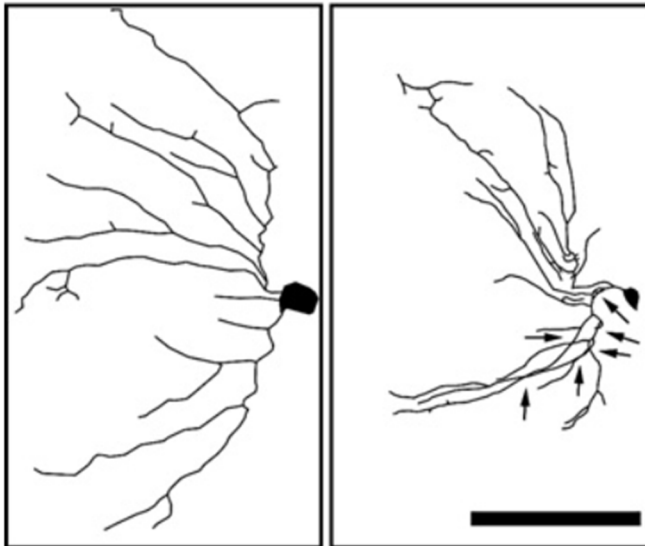
Figure 1.6 Neuron cells with wild type functioning Dscam1 (left) and loss-of-function allele (right) in *Drosophila*. The loss-of-function mutants result in the neuron axons aggregating and/or overlapping during growth contrary to the wild type in which they spread away from one another. Scale bar = 50 µm. Reproduced from Matthews *et al.* (2007).

Rubinstein et al., 2015). A study in a specific type of cerebellar cortex neuron cells (Purkinje cells) has revealed that the Slit-Robo pathway is autonomous to the Phdhγ one, while both result in self-avoidance. Although *Dscams* and *Pcdhs* are evolutionary distinct gene clusters, it is notable that self-avoidance is achieved through mainly three conserved functions: a) both gene clusters produce multiple isoforms of transmembrane molecules, b) isoforms of both clusters are a result of random combinatorial gene expression, and c) homophilic adhesion between those isoforms is what guides the self/non-self discrimination and results in self-avoidance or successful synapse respectively.

The research carried out in neurons shows that recognition signalling pathways converge towards the same signalling cascades and that self-avoidance is in fact a multifactorial response. A general categorisation of self-avoidance responses in neurons divides them into the following major groups: a) those depending on a soluble extracellular signal, and b) those dependent on contact-based recognition and repulsion.

1.4 Molecular mechanisms and signalling pathways during tropisms

Tropisms are largely regulated by three overlapping signalling pathways: the MAPK signalling pathway, signalling by small-GTPases and signalling by calcium. Components of all systems have been shown to be present in *A. fumigatus,* as described in the following sections.

1.4.1 MAP kinases signalling and fungal cell tropisms

Fungal cells encounter a wide range of environmental obstacles during their growth and development. The response to those signal cues and the coordination of their responses involves the interaction of different signal transduction pathways.

The MAP (<u>M</u>itogen-<u>A</u>ctivated <u>P</u>rotein) kinase pathways have been studied extensively in *S. cerevisiae* and govern several cellular functions in response to external stimuli (Fig. 1.7). In the instance of the pheromone MAP kinase response pathway, in order for the pathway to be initialised a signal (protein pheromone) Mat-a or Mat-α, and a cognate G-coupled protein receptor (GPCR), Ste2 or Ste3, are required. Once the receptor is activated by the necessary signal it further activates the downstream G-protein subunits Ste4 and Ste18. In turn, they activate the Ste20 which regulates the activation of the MAP kinases cascade through phosphorylation. Once the cascade is activated it in turn activates transcription factors in the nucleus and readjust actin polymerisation in the cytoplasm, as a response to the initial signal which results in a positive cell tropism (asymmetrically polarized yeast cells called 'shmoos' homing towards each other). Bardwell (2004) reviews the MAPK pheromone response in *S. cerevisiae* in detail.

Besides the pheromone response pathway involved in mating, the cell wall integrity (CWI), and high osmolarity stress response (HOG) MAP kinase pathways also play key roles regulating filamentous and invasive growth, (Hamel et al., 2012; Fig. 1.7). These pathways are crucial for the maintenance of the fungal lifestyle as they are the first line of defence for fungi to cope with stresses. The fungal cell wall is crucial as it contributes to cell morphology, maintenance and provides physical support amongst its many other functions. For these reasons, the cell wall and the CWI described components are appealing drug targets in *A. fumigatus* (Valiante et al., 2015). The HOG-MAPK pathway is also involved in adaptation to stress by transmission of environmental osmotic signals and has been described in *A. fumigatus* (Ma and Li, 2013). Besides acting as stress-coping mechanisms, MAP kinase pathways have also been identified to be important in influencing virulence during infection in a range of pathogenic fungi (reviewed by Turrà et al., 2014).

In *N.crassa*, MAP kinase signalling is involved during CAT fusion, sharing some common stages with the pathway in *S. cerevisiae*. The MAPK pathway still induces cell-cycle arrest at G1, actin reorganization and transcription of relevant genes. It is
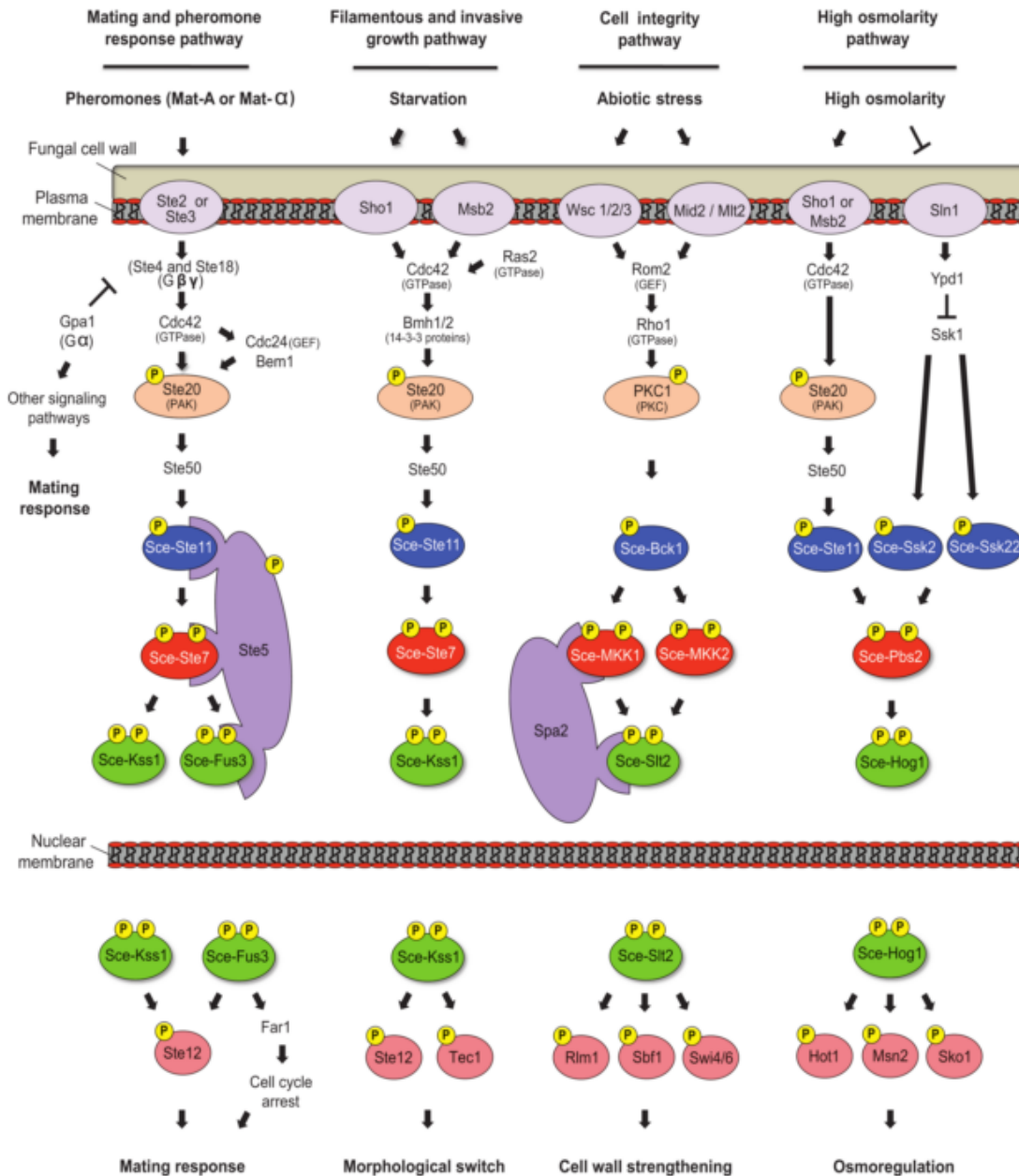
Figure 1.7 Overview of main MAPK signaling pathways in *S. cerevisiae*. It is evident that there are common kinase components in pathways regulating responses to different types of stress/signals (cross-talk). The consensus of the MAPK pathways is the necessity of a stimulus, which is sensed by a receptor. During signal transduction it is common that an upstream kinase (such as Ste20) regulates the MAPK cascade, the final kinase of which phosphorylates the appropriate transcription factor to initiate a response. Reproduced from Hamel *et al.* (2012).

suggested that the whole signalling pathway is governed by a "ping-pong" mechanism, in which the self-signalling molecule is alternately secreted in a pulsatile fashion from CAT tips homing towards each other. This oscillation period of MAPK recruitment is very short (6-12 min), contrary to that in *S. cerevisiae* during the pheromone response (~150 min) (Read et al., 2009). This short time indicates that no transcriptional events can take place during the signalling.
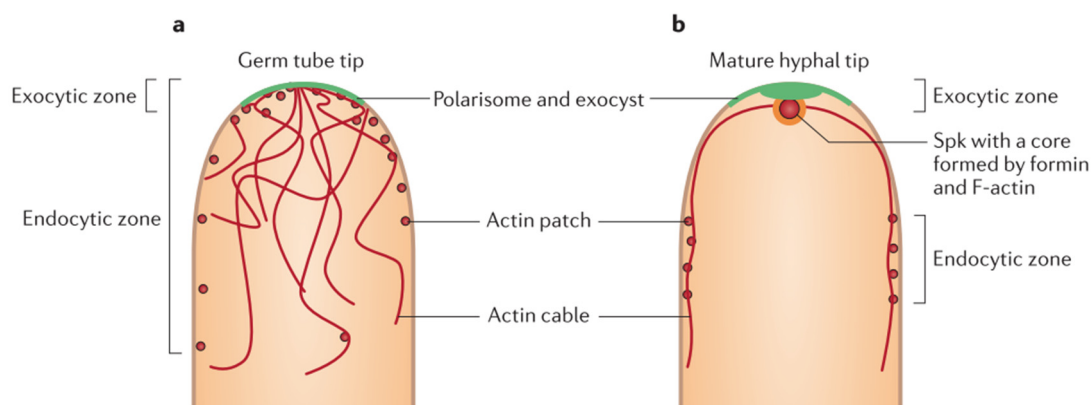
Figure 1.8 Organisation of hyphal tip polarity apparatus in (a) germ tubes and (b) mature hyphae. In germlings, the polarisome is distributed under the plasma membrane and is regulated by the MAPK signalling pathways and small GTPases, promoting nucleation of actin in the region. In mature hyphae the polarisome interacts downstream with the Spitzenkörper (Spk) which acts as a vesicle supply centre (VSC) to the tip. Hyphal tip extension and polarity maintenance rely on the balanced action between cell wall-loosening enzymes and cell wall-synthesizing enzymes delivered through vesicles at the apical region. Reproduced from Berepiki et al. (2011).

MAP kinases interact with the polarisome through their downstream effectors, such as the small GTPase Cdc42 (Atay and Skotheim, 2017). The polarisome is a key multiprotein complex involved in regulating the actin cytoskeleton and secretory machinery required for polarized hyphal growth. The associated exocyst is composed of proteins that regulate secretory vesicle docking and fusion with the plasma membrane (Riquelme et al, 2018). These protein complexes are in turn associated with the Spitzenkörper (Spk; Araujo-Palomares et al., 2009, Fig 1.8) which is a multi-component structure dominated by vesicles. It plays an intimate and crucial role regulating the morphogenesis and direction of growth of hyphal tip growth by regulating vesicle delivery to and from the apical regions of the hypha by regulating cell wall turnover in the region (Read, 2017; Riquelme et al., 2018; Riquelme and Martínez-Núñez, 2016). The Spk is present in mature *A. fumigatus* hyphae (personal observations). It is believed that tropic responses involving MAPK signalling pathways can affect the polarisome and Spk via downstream effectors thus changing the polarity axis of an extending hyphal cell.

1.4.2 Small GTPase signalling and fungal cell tropisms

It has been shown that an essential factor for establishment of cell polarity in filamentous fungi and yeasts is the small Rho-family small GTPase, Cdc42 (Harris, 2011; Johnson and Pringle, 1990) by regulating the organization of the actin

cytoskeleton (Spiering and Hodgson, 2011; Tapon and Hall, 1997). The Rho-family GTPases are anchored to the membrane lipid bilayer. They are activated by a guanine nucleotide exchange factor (GEF) and deactivated by a GTPase-activating protein (GAP). Among the targets of the activated Cdc42/Rho complex is the Ste20 component of the MAPK signalling pathway (Tapon and Hall, 1997).

In other fungal species there have been recent breakthroughs that shed some light to Cdc42 function and how it affects tropic growth. In *C. albicans*, Cdc42 along with Ca^{2+} influx are essential for the polarised growth during thigmotropisms and galvanotropisms (Brand et al., 2014). During galvanotropisms, Cch1 is activated, raising locally the influx of Ca^{2+}. This leads to reinforcement of weak Cdc42 polarity signals resulting in change of growth towards the cathode (Fig. 1.9).

In true filamentous fungi apart from the presence of the homologue to Cdc42, a Rac1
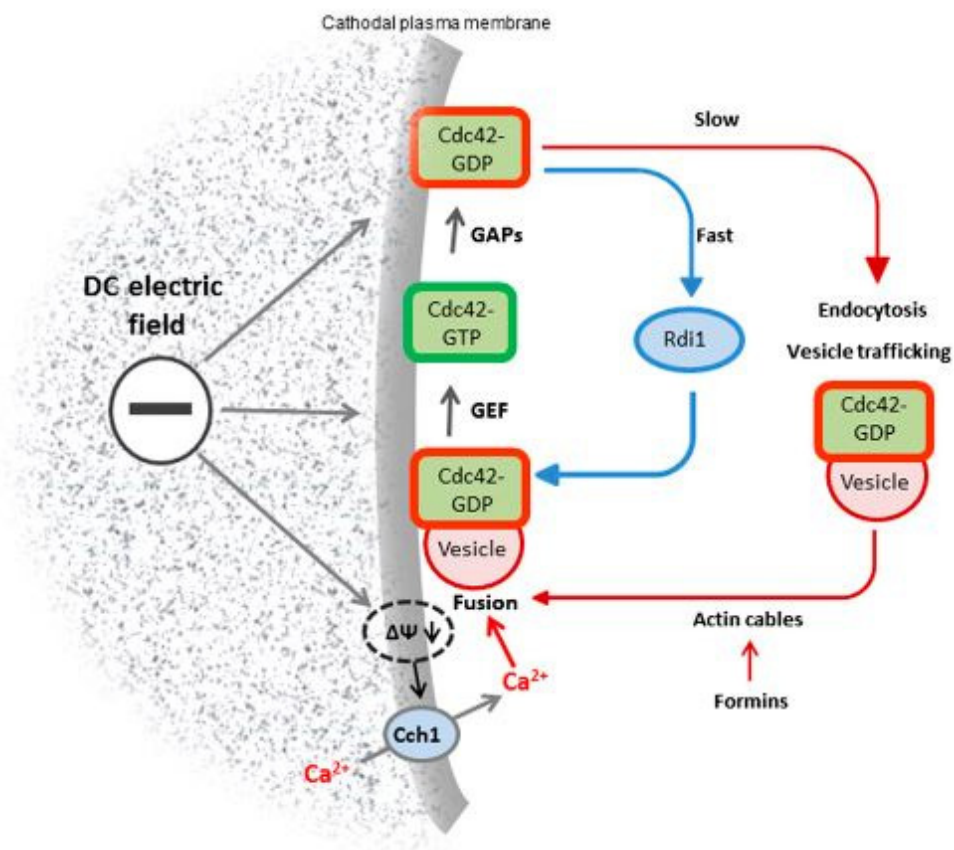
Figure 1.9 Cdc42 signaling during galvanotropism. Cdc42-GDP is recycled in the cytosol, by Rdi1 or endocytosis and vesicle trafficking. During the latter case it is recruited back to the membrane by formin-nucleated actin cables to the membrane. Depolarisation of the membrane leads to accumulation of Cdc42 in the membrane, which leads to actin reorganisation and directed growth. Reproduced from Brand *et al.* (2014)

homologue also exists (Kwon et al., 2011). Rac1 is similar to Cdc42 and is responsible for regulation of morphogenesis functions in animal cells. Possibly due to the presence of Rac1, *cdc42* null strains are not lethal, i.e. Cdc42 is not essential, while the *cdc42 rac1* double mutants are. A recent study has provided insight into the CDC-42 and RAC-1 functionality during chemotropic responses in *N. crassa* (Lichius et al., 2014). In a wild type strain CDC-42 and RAC-1 are located in the apex of the tips of growing germ tubes, whereas in mature hyphae CDC-42 is more confinely localised to the apex in contrast to RAC-1 which forms an apical ring outside that region (Araujo-Palomares et al., 2011). Both deletion mutants show defects in polarity establishment during vegetative hyphal growth, however these mutations display distinct growth phenotypes. In Δ*rac-1* cells, initiation and maintenance of polarised growth of elongated germ tubes and mature hyphae could be observed. However, this is not the case in Δ*cdc-42* cells which are unable to establish and maintain a polar axis. Both mutants show an inability in forming CATs (Lichius et al., 2014). The conclusion of the later study was that while CDC-42 is sufficient for germ tube formation and growth while retaining self-avoidance (negative chemotropism), RAC-1 is essential for CAT formation and fusion (positive chemotropism).

Another important small GTPase in hyphal morphogenesis is Ras. In *A. fumigatus*, RasA regulates hyphal morphogenesis, polarity establishment and maintenance and stress response (Fortwendel et al., 2008, 2005, 2004). Its function is controlled similarly to the Rho GTPases with its own GEFs and GAPs and has been suggested that to regulate signalling through the Cdc42 and Rac1 pathways (Harris, 2011). A recent study has shown that the correct localisation of RasA in the plasma membrane is crucial for *A. fumigatus* growth, hyphal morphogenesis, cell wall integrity and virulence (Al Abdallah and Fortwendel, 2015). Spatial regulation of RasA is achieved through a series of post-translation modification steps, such as farnesylation, palmitoylation and carboxymethylation.

1.4.3 Calcium signalling

Calcium signalling is a ubiquitous pathway in organisms which is being found to be involved in many cellular functions in fungi including growth, cell wall integrity and drug resistance.

As far as fungi are concerned, calcium signalling has been well-studied in *S. cerevisiae*. An increase in the intracellular Ca^{2+} concentration activates its primary intracellular chelator calmodulin. Once bound to Ca^{2+}, calmodulin regulates are a large number of other proteins. One of its main target proteins is the Ca^{2+}/calmodulin-dependent phosphatase calcineurin. The increase of the intracellular Ca^{2+} can be a result of ion influx through the Ca^{2+} transporter Cch1 or by release of calcium ions from internal stores such as the endoplasmic reticulum. Calcineurin's substrate is the transcription factor Crz1 (<u>c</u>alcineurin-<u>r</u>esponsive <u>z</u>inc finger 1), which is normally phosphorylated and located in the cytosol in its inactive form. Once it has been dephosphorylated by calcineurin it enters the nucleus and induces the Crz1-dependent genes (Thewes, 2014; Fig. 1.10).

Studies in *A. fumigatus* have revealed an orthologue to Crz1, CrzA which is responsible for increased tolerance to high calcium and manganese concentrations (Soriani et al.,
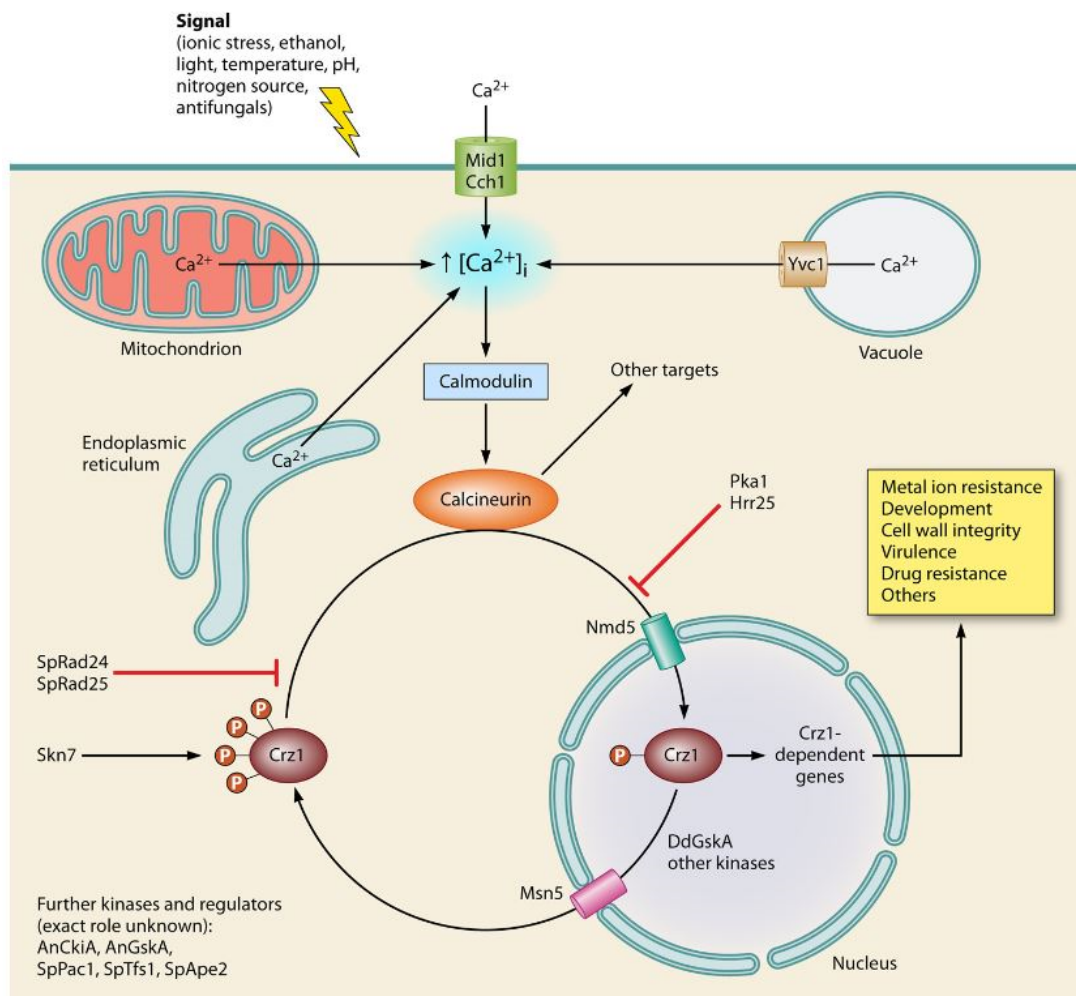
Figure 1.10 Calcium signalling pathway in *S. cerevisiae*. Reproduced from Thewes (2014).

2008). Additionally, CrzA regulates conidial germination and hyphal growth as well as being an important virulence factor for the pathogenicity of the fungus (Cramer et al., 2008). Even though CrzA is an important calcineurin substrate, it is not the only one affected during calcium signalling. The results from Almeida et al. (2013), investigating three genes that suppress the calcium intorelance in a *crzAΔ* strain, indicate that in *Aspergillus nidulans* there are responses that are calcineurin-dependent yet CrzA-independent. Furthermore, the CkiA essential casein kinase transporter protein (Apostolaki et al., 2012) is implicated to participate in the calcium signalling pathway, yet its role is not yet fully understood. All in all, the final target of different signalling pathways during tropisms is the rearrangement of the actin microfilaments in response to the primary external signal.

Evidence for calcium signalling in fungal cell tropisms have been found in relation to thigmotropisms, and galvanotropisms in *Candida albicans* (Fig. 1.3), as well as positive CAT tropisms (Hernandez-Ortiz et al., in prep).

1.5 Volatile Organic Compounds (VOCs) as signal molecules in fungal development and growth

As it has already been stated in section 1.3.6, Müller and Jaffe (1965) suggested that the signal molecule inducing negative autotropisms in *Botrytis* should be a diffusible, unstable and locally-effective compound. These properties are intrinsic to volatile organic compounds (VOCs), a class of low molecular weight, carbon-containing chemical compounds (Herrmann, 2010). In their review, Pennerman et al. (2016) summarise the diverse roles *Aspergillus* that VOCs have in the fungus' lifestyle (Fig 1.11).

In recent years there has been rising interest in identifying volatiles which affect fungal growth and development (Leeder et al., 2011; Ugalde, 2006; Ugalde and Rodriguez-Urra, 2014) and microbial interactions (Jones and Elliot, 2017). Notable cases of the latter involve the stimulation of growth of *Aspergillus fumigatus* by volatiles emitted by the Gram negative bacterium *Pseudomonas aeruginosa*, possibly through dimethyl sulfide (Briard et al., 2016). On the contrary, co-cultivation of *A. nidulans* with *C. albicans* results in growth inhibition of the former in a way that resembles farnesol-induced apoptosis (Semighini et al., 2006). These findings are of significant importance for three main reasons: a) they show that microbes can interact at a distance through the air via
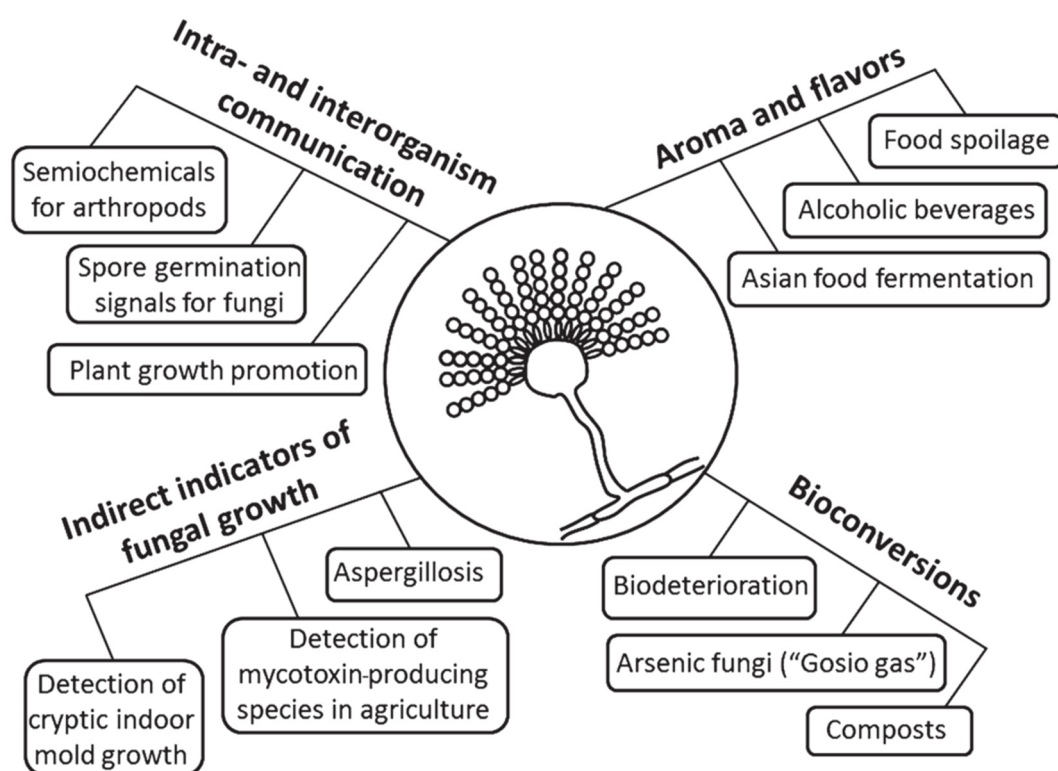
Figure 1.11 VOCs in *Aspergillus* are primarily studied for the application in industry, but interest has arisen in their role in inter-microbial communication. Reproduced from Pennerman et al. (2016)

volatiles, b) this communication can be intra- or inter-kingdom, c) in the context of fungal infections, this communication has implications on how we understand fungal interactions during the infection and disease, as they can potentially be signal initiators for the formation of biofilms, a developmental stage in which fungi can thrive and survive. The biofilm phenotype of the fungus is refractory to most conventional antifungal treatment options, due to the inability of agents to properly kill the fungal biomass inside the biofilm (Mowat et al., 2008).

All in all, although steps have been made towards the identification of VOCs involved in fungal development, their implications in cell-cell communication and what downstream signalling pathways they activate are only now beginning to be understood.

1.6 Research aims of this thesis

It is evident that despite the fact the negative cell autotropisms in filamentous fungi are ubiquitous, having first been observed and described in the late 19th century, little knowledge has been gathered regarding the signalling machinery responsible for this kind of response. The main objective of the research described in this PhD thesis was

to investigate negative autotropisms in *A. fumigatus* and elucidate the signalling which is responsible for these responses. The main questions addressed in the research described in were:

(1) Are negative cell tropisms observed in *A. fumigatus*? If so, at which developmental stage(s) are they prevalent?

(2) Can any small extracellular molecules be identified that act as signals for this tropism?

(3) What is the downstream signalling machinery involved in this kind of tropic response?

Chapter 2 describes the materials and methods used in my thesis research.

Chapter 3 describes the approach undertaken during this PhD project with the aim to establish a consistent quantification method for the self-avoidance phenomenon during the emergence of germ tubes from conidia of *A. fumigatus*. The approach was also applied to quantifying germ tubes invading the agar substratum by *A. fumigatus* germinating hyphae under different conditions. All experiments were carried out using live-cell imaging.

Chapter 4 focuses on attempts to identify the signal molecule responsible for self-avoidance. Different chemical compounds with reported roles in the fungal germination and development were screened and assessed for their impact, if any, on self-avoidance. Secondly, I analysed the volatome of *A. fumigatus* in culture using mass spectroscopy. I also describe the development of a new sampling methodology for mass spectroscopy to assess the qualities of the fungal headspace. By sampling the wild type and a mutant fungal strain with metabolic deficiencies I aimed to answer what the candidate signal molecules would be, by analysing if there are any qualitative similarities between the volatomes of *A. fumigatus* wild type and a metabolically deficient strain which exhibits self-avoidance.

Chapter 5 details the mechanistic investigation of the signalling mechanism involved in self-avoidance. My aim was to screen known homologue proteins from genomic knock-out libraries of *A. fumigatus* and find whether the self-avoidance response is severely hindered, indicating the likely participation of the corresponding signalling pathway. To this end, the full kinase KO library of *A. fumigatus* was screened, along with select G-protein coupled receptor (GPCR) knockout mutants, using live-cell imaging.

1.7 References

Abad, A., Fernandez-Molina, J. V, Bikandi, J., Ramirez, A., Margareto, J., Sendino, J., Hernando, F.L., Ponton, J., Garaizar, J., Rementeria, A., 2010. What makes *Aspergillus fumigatus* a successful pathogen? Genes and molecules involved in invasive aspergillosis. Rev Iberoam Micol 27, 155–182. https://doi.org/10.1016/j.riam.2010.10.003

Adams, T.H., Wieser, J.K., Yu, J.H., 1998. Asexual sporulation in *Aspergillus nidulans*. Microbiol Mol Biol Rev 62, 35–54.

Aimanianda, V., Bayry, J., Bozza, S., Kniemeyer, O., Perruccio, K., Elluru, S.R., Clavaud, C., Paris, S., Brakhage, A.A., Kaveri, S. V, Romani, L., Latgé, J.-P., 2009. Surface hydrophobin prevents immune recognition of airborne fungal spores. Nature 460, 1117–21. https://doi.org/10.1038/nature08264

Aimanianda, V., Latge, J.P., 2010. Fungal hydrophobins form a sheath preventing immune recognition of airborne conidia. Virulence 1, 185–187. https://doi.org/10.4161/viru.1.3.11317

Al Abdallah, Q., Fortwendel, J.R., 2015. Exploration of *Aspergillus fumigatus* Ras pathways for novel antifungal drug targets. Front. Microbiol. 6, 1–6. https://doi.org/10.3389/fmicb.2015.00128

Almeida, M.C., Brand, A.C., 2017. Thigmo Responses: The Fungal Sense of Touch. Microbiol. Spectr. 5, 487–507. https://doi.org/10.1128/microbiolspec.FUNK-0040-2016

Almeida, R.S., Loss, O., Colabardini, A.C., Brown, N.A., Bignell, E., Savoldi, M., Pantano, S., Goldman, M.H., Arst Jr., H.N., Goldman, G.H., 2013. Genetic bypass of *Aspergillus nidulans* crzA function in calcium homeostasis. G3 3, 1129–1141. https://doi.org/10.1534/g3.113.005983

Anh Nguyen, T., Greig, J., Khan, A., Goh, C., Jedd, G., 2018. Evolutionary novelty in gravity sensing through horizontal gene transfer and high- order protein assembly. PLOS Biol. 16, e2004920. https://doi.org/10.1371/journal.pbio.2004920

Apostolaki, A., Harispe, L., Calcagno-Pizarelli, A.M., Vangelatos, I., Sophianopoulou, V., Arst, H.N., Peñalva, M.A., Amillis, S., Scazzocchio, C., 2012. *Aspergillus nidulans* CkiA is an essential casein kinase I required for delivery of amino acid transporters to the plasma membrane. Mol. Microbiol. 84, 530–549. https://doi.org/10.1111/j.1365-2958.2012.08042.x

Araujo-Palomares, C.L., Richthammer, C., Seiler, S., Castro-Longoria, E., 2011. Functional Characterization and Cellular Dynamics of the CDC-42 – RAC – CDC-24 Module in *Neurospora crassa*. PLoS One 6, e27148. https://doi.org/10.1371/journal.pone.0027148

Araujo-Palomares, C.L., Riquelme, M., Castro-Longoria, E., 2009. The polarisome component SPA-2 localizes at the apex of *Neurospora crassa* and partially colocalizes with the Spitzenkörper. Fungal Genet. Biol. 46, 551–563. https://doi.org/10.1016/j.fgb.2009.02.009

Araujo, R., Rodrigues, A.G., 2004. Variability of germinative potential among pathogenic species of *Aspergillus*. J. Clin. Microbiol. 42, 4335–4337. https://doi.org/10.1128/JCM.42.9.4335-4337.2004

Arkowitz, R.A., 1999. Responding to attraction: chemotaxis and chemotropism in *Dictyostelium* and yeast. Trends Cell Biol 9, 20–27.

Atay, O., Skotheim, J.M., 2017. Spatial and temporal signal processing and decision making by MAPK pathways. J. Cell Biol. 216, 317–330. https://doi.org/10.1083/jcb.201609124

Ballario, P., Vittorioso, P., Magrelli, A., Talora, C., Cabibbo, A., Macino, G., 1996. White collar-1, a central regulator of blue light responses in *Neurospora*, is a zinc finger protein. EMBO J. 15, 1650–7.

Bardwell, L., 2004. A walk-through of the yeast mating pheromone response pathway. Peptides 25, 1465–1476. https://doi.org/10.1016/j.peptides.2003.10.022

Bayram, O., Krappmann, S., Ni, M., Bok, J.W., Helmstaedt, K., Valerius, O., Braus-

Stromeyer, S., Kwon, N.-J., Keller, N.P., Yu, J.-H., Braus, G.H., 2008. VelB/VeA/LaeA Complex Coordinates Light Signal with Fungal Development and Secondary Metabolism. Science (80-.). 320, 1504–1506. https://doi.org/10.1126/science.1155888

Berepiki, A., Lichius, A., Read, N.D., 2011. Actin organization and dynamics in filamentous fungi. Nat. Rev. Microbiol. 9, 876–887. https://doi.org/10.1038/nrmicro2666

Bertuzzi, M., Hayes, G., Icheoku, U., van Rhijn, N., Denning, D., Osherov, N., Bignell, E., 2018. Anti-*Aspergillus* Activities of the Respiratory Epithelium in Health and Disease. J. Fungi 4, 8. https://doi.org/10.3390/jof4010008

Bottone, E.J., Nagarsheth, N., Chiu, K., 1998. Evidence of self-inhibition by filamentous fungi accounts for unidirectional hyphal growth in colonies. Can J Microbiol 44, 390–393.

Bowman, S.M., Free, S.J., 2006. The structure and synthesis of the fungal cell wall. BioEssays 28, 799–808. https://doi.org/10.1002/bies.20441

Brand, A., Shanks, S., Duncan, V.M.S., Yang, M., Mackenzie, K., Gow, N.A.R., 2007. Hyphal Orientation of *Candida albicans* Is Regulated by a Calcium-Dependent Mechanism. Curr. Biol. 17, 347–352. https://doi.org/10.1016/j.cub.2006.12.043

Brand, A., Vacharaksa, A., Bendel, C., Norton, J., Haynes, P., Henry-Stanley, M., Wells, C., Ross, K., Gow, N.A.R., Gale, C.A., 2008. An internal polarity landmark is important for externally induced hyphal behaviors in *Candida albicans*. Eukaryot. Cell 7, 712–720. https://doi.org/10.1128/EC.00453-07

Brand, A.C., Morrison, E., Milne, S., Gonia, S., Gale, C. a, Gow, N. a R., 2014. Cdc42 GTPase dynamics control directional growth responses. Proc. Natl. Acad. Sci. U. S. A. 111, 811–6. https://doi.org/10.1073/pnas.1307264111

Briard, B., Heddergott, C., Latgé, J.-P., 2016. Volatile Compounds Emitted by *Pseudomonas aeruginosa* Stimulate Growth of the Fungal Pathogen *Aspergillus*

fumigatus. MBio 7, e00219-16. https://doi.org/10.1128/mBio.00219-16

Brose, K., Bland, K.S., Kuan, H.W., Arnott, D., Henzel, W., Goodman, C.S., Tessier-Lavigne, M., Kidd, T., 1999. Slit proteins bind robo receptors and have an evolutionarily conserved role in repulsive axon guidance. Cell 96, 795–806. https://doi.org/10.1016/S0092-8674(00)80590-5

Brown, G.D., Denning, D.W., Gow, N.A.R., Levitz, S.M., Netea, M.G., White, T.C., 2012. Hidden killers: Human fungal infections. Sci. Transl. Med. 4, 1–10. https://doi.org/10.1126/scitranslmed.3004404

Casselton, L., Zolan, M., 2002. The art and design of genetic screens: filamentous fungi. Nat. Rev. Genet. 3, 683–697. https://doi.org/10.1038/nrg889

Castle, E.S., 1930. Phototropism and the Light-Sensitive System of *Phycomyces*. J Gen Physiol 13, 421–435.

Chowdhary, A., Sharma, C., Hagen, F., Meis, J.F., 2014. Exploring azole antifungal drug resistance in *Aspergillus fumigatus* with special reference to resistance mechanisms. Futur. Microbiol 9, 697–711. https://doi.org/10.2217/fmb.14.27

Clark, J.F., 1902. On the Toxic Properties of Some Copper Compounds with Special Reference to Bordeaux Mixture. Bot. Gaz. 33, 26–48.

Cramer Jr., R.A., Perfect, B.Z., Pinchai, N., Park, S., Perlin, D.S., Asfaw, Y.G., Heitman, J., Perfect, J.R., Steinbach, W.J., 2008. Calcineurin target CrzA regulates conidial germination, hyphal growth, and pathogenesis of *Aspergillus fumigatus*. Eukaryot Cell 7, 1085–1097. https://doi.org/10.1128/EC.00086-08

Dagenais, T.R., Keller, N.P., 2009. Pathogenesis of *Aspergillus fumigatus* in Invasive Aspergillosis. Clin Microbiol Rev 22, 447–465. https://doi.org/10.1128/CMR.00055-08

De Castro, P.A., Chiaratto, J., Winkelströter, L.K., Bom, V.L.P., Ramalho, L.N.Z., Goldman, M.H.S., Brown, N.A., Goldman, G.H., 2014. The involvement of the

Mid1/Cch1/Yvc1 calcium channels in *Aspergillus fumigatus* virulence. PLoS One 9. https://doi.org/10.1371/journal.pone.0103957

Denning, D.W., 1998. Invasive aspergillosis. Clin Infect Dis 26, 781–785.

Dennison, D.S., Shropshire Jr., W., 1984. The gravireceptor of *Phycomyces*. Its development following gravity exposure. J Gen Physiol 84, 845–859.

Drechsler, C., 1937. Some Hyphomycetes That Prey on Free-Living Terricolous Nematodes. Mycologia 29, 447. https://doi.org/10.2307/3754331

Dyer, P.S., O'Gorman, C.M., 2012. Sexual development and cryptic sexuality in fungi: insights from *Aspergillus* species. FEMS Microbiol Rev 36, 165–192. https://doi.org/10.1111/j.1574-6976.2011.00308.x

Ellett, F., Jorgensen, J., Frydman, G.H., Jones, C.N., Irimia, D., 2017. Neutrophil Interactions Stimulate Evasive Hyphal Branching by *Aspergillus fumigatus*. PLoS Pathog. 13, 1–22. https://doi.org/10.1371/journal.ppat.1006154

Fan, X., Labrador, J.P., Hing, H., Bashaw, G.J., 2003. Slit stimulation recruits Dock and Pak to the roundabout receptor and increases Rac activity to regulate axon repulsion at the CNS midline. Neuron 40, 113–127. https://doi.org/10.1016/S0896-6273(03)00591-9

Fedorova, N.D., Khaldi, N., Joardar, V.S., Maiti, R., Amedeo, P., Anderson, M.J., Crabtree, J., Silva, J.C., Badger, J.H., Albarraq, A., Angiuoli, S., Bussey, H., Bowyer, P., Cotty, P.J., Dyer, P.S., Egan, A., Galens, K., Fraser-Liggett, C.M., Haas, B.J., Inman, J.M., Kent, R., Lemieux, S., Malavazi, I., Orvis, J., Roemer, T., Ronning, C.M., Sundaram, J.P., Sutton, G., Turner, G., Venter, J.C., White, O.R., Whitty, B.R., Youngman, P., Wolfe, K.H., Goldman, G.H., Wortman, J.R., Jiang, B., Denning, D.W., Nierman, W.C., 2008. Genomic islands in the pathogenic filamentous fungus *Aspergillus fumigatus*. PLoS Genet. 4. https://doi.org/10.1371/journal.pgen.1000046

Fomina, M., Ritz, K., Gadd, G.M., 2000. Negative fungal chemotropism to toxic

metals. FEMS Microbiol. Lett. 193, 207–211. https://doi.org/10.1016/S0378-1097(00)00477-8

Fortwendel, J.R., Fuller, K.K., Stephens, T.J., Bacon, W.C., Askew, D.S., Rhodes, J.C., 2008. *Aspergillus fumigatus* RasA regulates asexual development and cell wall integrity. Eukaryot Cell 7, 1530–1539. https://doi.org/10.1128/EC.00080-08

Fortwendel, J.R., Panepinto, J.C., Seitz, A.E., Askew, D.S., Rhodes, J.C., 2004. *Aspergillus fumigatus* rasA and rasB regulate the timing and morphology of asexual development. Fungal Genet Biol 41, 129–139.

Fortwendel, J.R., Zhao, W., Bhabhra, R., Park, S., Perlin, D.S., Askew, D.S., Rhodes, J.C., 2005. A fungus-specific ras homolog contributes to the hyphal growth and virulence of *Aspergillus fumigatus*. Eukaryot Cell 4, 1982–1989. https://doi.org/10.1128/EC.4.12.1982-1989.2005

Fresenius, G., 1850. Beiträge zur Mykologie. Heinrich Ludwig Brömmer Verlag, Frankfurt.

Fuller, K.K., Ringelberg, C.S., Loros, J.J., Dunlap, J.C., 2013. The Fungal Pathogen *Aspergillus fumigatus* Regulates Growth, Metabolism, and Stress Resistance in Response to Light. MBio 4, e00142-13-e00142-13. https://doi.org/10.1128/mBio.00260-13

Fulton, H.R., 1906. Chemotropism of Fungi. Bot. Gaz. 41, 81–108.

Garrett, A.M., Tadenev, A.L., Hammond, Y.T., Fuerst, P.G., Burgess, R.W., 2016. Replacing the PDZ-interacting C-termini of DSCAM and DSCAML1 with epitope tags causes different phenotypic severity in different cell populations. Elife 5, 1–24. https://doi.org/10.7554/eLife.16144

Gimeno, C.J., Ljungdahl, P.O., Styles, C.A., Fink, G.R., 1992. Unipolar cell divisions in the yeast *S. cerevisiae* lead to filamentous growth: Regulation by starvation and RAS. Cell 68, 1077–1090. https://doi.org/10.1016/0092-8674(92)90079-R

Gow, N.A., 2004. New angles in mycology: studies in directional growth and directional motility. Mycol Res 108, 5–13.

Gow, N.A.R., 1993. Nonchemical signals used for host location and invasion by fungal pathogens. Trends Microbiol. 1, 45–50. https://doi.org/10.1016/0966-842X(93)90031-L

Gravelat, F.N., Beauvais, A., Liu, H., Lee, M.J., Snarr, B.D., Chen, D., Xu, W., Kravtsov, I., Hoareau, C.M.Q., Vanier, G., Urb, M., Campoli, P., Al Abdallah, Q., Lehoux, M., Chabot, J.C., Ouimet, M.-C., Baptista, S.D., Fritz, J.H., Nierman, W.C., Latgé, J.P., Mitchell, A.P., Filler, S.G., Fontaine, T., Sheppard, D.C., 2013. *Aspergillus* Galactosaminogalactan Mediates Adherence to Host Constituents and Conceals Hyphal β-Glucan from the Immune System. PLoS Pathog. 9, e1003575. https://doi.org/10.1371/journal.ppat.1003575

Grolig, F., Döring, M., Galland, P., 2006. Gravisusception by buoyancy: A mechanism ubiquitous among fungi? Protoplasma 229, 117–123. https://doi.org/10.1007/s00709-006-0218-7

Hamel, L.-P., Nicole, M.-C., Duplessis, S., Ellis, B.E., 2012. Mitogen-Activated Protein Kinase Signaling in Plant-Interacting Fungi: Distinct Messages from Conserved Messengers. Plant Cell 24, 1327–1351. https://doi.org/10.1105/tpc.112.096156

Hamelin, M., Zhou, Y., Su, M.-W., Scott, I.M., Culotti, J.G., 1993. Expression of the UNC-5 guidance receptor in the touch neurons of *C. elegans* steers their axons dorsally. Nature 364, 327–330. https://doi.org/10.1038/364327a0

Harris, S.D., 2011. Cdc42/Rho GTPases in fungi: variations on a common theme. Mol Microbiol 79, 1123–1127. https://doi.org/10.1111/j.1365-2958.2010.07525.x

Hawksworth, D.L., 1991. The fungal dimension of biodiversity: magnitude, significance, and conservation. Mycol. Res. 95, 641–655. https://doi.org/10.1016/S0953-7562(09)80810-1

Hawksworth, D.L., Lücking, R., 2017. Fungal Diversity Revisited: 2.2 to 3.8 Million

Species, in: The Fungal Kingdom. American Society of Microbiology, pp. 79–95. https://doi.org/10.1128/microbiolspec.FUNK-0052-2016

Hayashi, S., Takeichi, M., 2015. Emerging roles of protocadherins: from self-avoidance to enhancement of motility. J. Cell Sci. 128, 1455–1464. https://doi.org/10.1242/jcs.166306

Herrmann, A., 2010. The chemistry and biology of volatiles. Wiley.

Hoang, P., Grueber, W.B., 2013. Dendritic self-avoidance: protocadherins have it covered. Cell Res. 23, 323–5. https://doi.org/10.1038/cr.2012.137

Hoch, H., Bojko, R., Comeau, G., 1993. Integrating microfabrication and biology. Circuits Devices … 9, 17–22. https://doi.org/10.1109/101.180737

Hong, K., Hinck, L., Nishiyama, M., Poo, M.M., Tessier-Lavigne, M., Stein, E., 1999. A ligand-gated association between cytoplasmic domains of UNC5 and DCC family receptors converts netrin-induced growth cone attraction to repulsion. Cell 97, 927–941. https://doi.org/10.1016/S0092-8674(00)80804-1

Ishikawa, F.H., Souza, E.A., Shoji, J.Y., Connolly, L., Freitag, M., Read, N.D., Roca, M.G., 2012. Heterokaryon incompatibility is suppressed following conidial anastomosis tube fusion in a fungal plant pathogen. PLoS One 7. https://doi.org/10.1371/journal.pone.0031175

Jaffe, L.F., 1966. On Autotropism in *Botrytis*: Measurement Technique and Control by CO2. PLANT Physiol. 41, 303–306. https://doi.org/10.1104/pp.41.2.303

James, T.Y., Kauff, F., Schoch, C.L., Matheny, P.B., Hofstetter, V., Cox, C.J., Celio, G., Gueidan, C., Fraker, E., Miadlikowska, J., Lumbsch, H.T., Rauhut, A., Reeb, V., Arnold, A.E., Amtoft, A., Stajich, J.E., Hosaka, K., Sung, G.H., Johnson, D., O'Rourke, B., Crockett, M., Binder, M., Curtis, J.M., Slot, J.C., Wang, Z., Wilson, A.W., Schüßler, A., Longcore, J.E., O'Donnell, K., Mozley-Standridge, S., Porter, D., Letcher, P.M., Powell, M.J., Taylor, J.W., White, M.M., Griffith, G.W., Davies, D.R., Humber, R.A., Morton, J.B., Sugiyama, J., Rossman, A.Y., Rogers, J.D.,

Pfister, D.H., Hewitt, D., Hansen, K., Hambleton, S., Shoemaker, R.A., Kohlmeyer, J., Volkmann-Kohlmeyer, B., Spotts, R.A., Serdani, M., Crous, P.W., Hughes, K.W., Matsuura, K., Langer, E., Langer, G., Untereiner, W.A., Lücking, R., Büdel, B., Geiser, D.M., Aptroot, A., Diederich, P., Schmitt, I., Schultz, M., Yahr, R., Hibbett, D.S., Lutzoni, F., McLaughlin, D.J., Spatafora, J.W., Vilgalys, R., 2006. Reconstructing the early evolution of Fungi using a six-gene phylogeny. Nature 443, 818–822. https://doi.org/10.1038/nature05110

Jat, K.R., Walia, D.K., Khairwa, A., 2013. Anti-IgE therapy for allergic bronchopulmonary aspergillosis in people with cystic fibrosis. Cochrane Database Syst Rev 9, CD010288. https://doi.org/10.1002/14651858.CD010288.pub2

Jin, M., Errede, B., Behar, M., Mather, W., Nayak, S., Hasty, J., Dohlman, H.G., Elston, T.C., 2011. Yeast dynamically modify their environment to achieve better mating efficiency. Sci. Signal. 4, ra54.

Johnson, D.I., Pringle, J.R., 1990. Molecular characterization of CDC42, a *Saccharomyces cerevisiae* gene involved in the development of cell polarity. J Cell Biol 111, 143–152.

Jones, S.E., Elliot, M.A., 2017. Streptomyces Exploration: Competition, Volatile Communication and New Bacterial Behaviours. Trends Microbiol. 25, 522–531. https://doi.org/10.1016/j.tim.2017.02.001

Keeler, A.B., Molumby, M.J., Weiner, J.A., 2015. Protocadherins branch out: Multiple roles in dendrite development. Cell Adhes. Migr. 9, 214–226. https://doi.org/10.1080/19336918.2014.1000069

Kern, V.D., 1999. Gravitropism of basidiomycetous fungi - On earth and in microgravity. Adv. Sp. Res. 24, 697–706. https://doi.org/10.1016/S0273-1177(99)00401-9

Kern, V.D., Mendgen, K., Hock, B., 1997. Flammulina as a model system for fungal graviresponses. Planta 203, S23-32.

Kidd, T., Bland, K.S., Goodman, C.S., 1999. Slit is the midline repellent for the Robo receptor in *Drosophila*. Cell 96, 785–794. https://doi.org/10.1016/S0092-8674(00)80589-9

Kidd, T., Condron, B., 2007. Avoiding the SCAMs. Neuron 54, 350–352. https://doi.org/10.1016/j.neuron.2007.04.018

Kim, H., Borkovich, K.A., 2006. Pheromones are essential for male fertility and sufficient to direct chemotropic polarized growth of trichogynes during mating in *Neurospora crassa*. Eukaryot Cell 5, 544–554. https://doi.org/10.1128/EC.5.3.544-554.2006

Kim, H., Han, K., Kim, K., Han, D., Jahng, K., Chae, K., 2002. The veA gene activates sexual development in Aspergillus nidulans. Fungal Genet Biol 37, 72–80.

Kim, T., Kao, M.T., Hasselbrink, E.F., Meyhofer, E., 2007. Active alignment of microtubules with electric fields. Nano Lett 7, 211–217. https://doi.org/10.1021/nl061474k

Kirk Paul M, Cannon Paul F, Minter David W, Stalpers Joost A, 2008. Dictionary of the Fungi, 10th ed. CAB International.

Kise, Y., Schmucker, D., 2013. Role of self-avoidance in neuronal wiring. Curr. Opin. Neurobiol. 23, 983–989. https://doi.org/10.1016/j.conb.2013.09.011

Kleinkauf, N., Verweij, P., Arendrup, M., Donnelly, P., Cuenca-Estrella, M., Fraaije, B., Melchers, W., Adriaenssens, N., Kema, G., Ullmann, A., 2013. Risk Assessment on the Impact of Environmental Usage of Triazoles on the Development and Spread of Resistance to Medical Triazoles in Aspergillus Species, in: European Centre for Disease Prevention and Control (ECDC). Stockholm, Sweden, pp. 1–17. https://doi.org/10.1016/S0007-8506(07)90004-9

Kramer, A.P., Stent, G.S., 1985. Developmental arborization of sensory neurons in the leech *Haementeria ghilianii*. II. Experimentally induced variations in the branching pattern. J. Neurosci. 5, 768–75.

Kwon-Chung, K.J., Sugui, J.A., 2013. *Aspergillus fumigatus*—What Makes the Species a
Ubiquitous Human Fungal Pathogen? PLoS Pathog. 9, e1003743.
https://doi.org/10.1371/journal.ppat.1003743

Kwon, M.J., Arentshorst, M., Roos, E.D., van den Hondel, C.A.M.J.J., Meyer, V., Ram,
A.F.J., 2011. Functional characterization of Rho GTPases in *Aspergillus niger*
uncovers conserved and diverged roles of Rho proteins within filamentous fungi.
Mol. Microbiol. 79, 1151–1167. https://doi.org/10.1111/j.1365-
2958.2010.07524.x

Latgé, J.P., 2001. The pathobiology of *Aspergillus fumigatus*. Trends Microbiol. 9, 382–
389. https://doi.org/10.1016/S0966-842X(01)02104-7

Latgé, J.P., 1999. *Aspergillus fumigatus* and aspergillosis. Clin. Microbiol. Rev. 12, 310–50.
https://doi.org/0893-8512

Leeder, A.C., Palma-Guerrero, J., Glass, N.L., 2011. The social network: deciphering
fungal language. Nat. Rev. Microbiol. 9, 440–451.
https://doi.org/10.1038/nrmicro2580

Lever, M.C., Robertson, B.E.M., Buchan, A.D.B., Miller, P.F.P., Gooday, G.W., Gow,
N.A.R., 1994. pH and Ca2+dependent galvanotropism of filamentous fungi:
implications and mechanisms. Mycol. Res. 98, 301–306.
https://doi.org/10.1016/S0953-7562(09)80458-9

Li, H. shun, Chen, J. hui, Wu, W., Fagaly, T., Zhou, L., Yuan, W., Dupuis, S., Jiang, Z.
hong, Nash, W., Gick, C., Ornitz, D.M., Wu, J.Y., Rao, Y., 1999. Vertebrate slit, a
secreted ligand for the transmembrane protein roundabout, is a repellent for
olfactory bulb axons. Cell 96, 807–818. https://doi.org/10.1016/S0092-
8674(00)80591-7

Lichius, A., Goryachev, A.B., Fricker, M.D., Obara, B., Castro-Longoria, E., Read,
N.D., 2014. CDC-42 and RAC-1 regulate opposite chemotropisms in *Neurospora
crassa*. J. Cell Sci. 127, 1953–65. https://doi.org/10.1242/jcs.141630

Ma, D., Li, R., 2013. Current Understanding of HOG-MAPK Pathway in *Aspergillus fumigatus*. Mycopathologia 175, 13–23. https://doi.org/10.1007/s11046-012-9600-5

Matthews, B.J., Kim, M.E., Flanagan, J.J., Hattori, D., Clemens, J.C., Zipursky, S.L., Grueber, W.B., 2007. Dendrite Self-Avoidance Is Controlled by Dscam. Cell 129, 593–604. https://doi.org/10.1016/j.cell.2007.04.013

Merlini, L., Dudin, O., Martin, S.G., 2013. Mate and fuse: how yeast cells do it. Open Biol. 3, 130008–130008. https://doi.org/10.1098/rsob.130008

Meskauskas, A., Fricker, M.D., Moore, D., 2004a. Simulating colonial growth of fungi with the Neighbour-Sensing model of hyphal growth. Mycol. Res. 108, 1241–56. https://doi.org/10.1017/S0953756204001261

Meskauskas, A., McNulty, L.J., Moore, D., 2004b. Concerted regulation of all hyphal tips generates fungal fruit body structures: experiments with computer visualizations produced by a new mathematical model of hyphal growth. Mycol. Res. 108, 341–353. https://doi.org/10.1017/S0953756204009670

Metzenberg, R.L., Glass, N.L., 1990. Mating type and mating strategies in *Neurospora*. BioEssays 12, 53–59. https://doi.org/10.1002/bies.950120202

Millard, S.S., Zipursky, S.L., 2008. Dscam-mediated repulsion controls tiling and self-avoidance. Curr. Opin. Neurobiol. 18, 84–89. https://doi.org/10.1016/j.conb.2008.05.005

Miller, A.L., Gow, N.A., 1989. Correlation between Root-Generated Ionic Currents, pH, Fusicoccin, Indoleacetic Acid, and Growth of the Primary Root of Zea mays. Plant Physiol 89, 1198–1206.

Miyoshi, M., 1894. Über chemotropismus der Pilze. Bot. Zeitung 52, 1–28.

Montesinos, E., 2003. Plant-associated microorganisms: A view from the scope of microbiology. Int. Microbiol. 6, 221–223. https://doi.org/10.1007/s10123-003-

0141-0

Mowat, E., Lang, S., Williams, C., McCulloch, E., Jones, B., Ramage, G., 2008. Phase-dependent antifungal activity against *Aspergillus fumigatus* developing multicellular filamentous biofilms. J. Antimicrob. Chemother. 62, 1281–1284. https://doi.org/10.1093/jac/dkn402

Müller, D., Jaffe, L., 1965. A Quantitative Study of Cellular Rheotropism. Biophys. J. 5, 317–335. https://doi.org/10.1016/S0006-3495(65)86719-4

Mullins, J., Harvey, R., Seaton, A., 1976. Sources and incidence of airborne *Aspergillus fumigatus* (Fres). Clin Allergy 6, 209–217.

Newsham, K.K., 2012. Fungi in extreme environments. Fungal Ecol. 5, 379–380. https://doi.org/10.1016/j.funeco.2012.04.003

Nierman, W.C., Pain, A., Anderson, M.J., Wortman, J.R., Kim, H.S., Arroyo, J., Berriman, M., Abe, K., Archer, D.B., Bermejo, C., Bennett, J., Bowyer, P., Chen, D., Collins, M., Coulsen, R., Davies, R., Dyer, P.S., Farman, M., Fedorova, N., Fedorova, N., Feldblyum, T. V, Fischer, R., Fosker, N., Fraser, A., García, J.L., García, M.J., Goble, A., Goldman, G.H., Gomi, K., Griffith-Jones, S., Gwilliam, R., Haas, B., Haas, H., Harris, D., Horiuchi, H., Huang, J., Humphray, S., Jiménez, J., Keller, N., Khouri, H., Kitamoto, K., Kobayashi, T., Konzack, S., Kulkarni, R., Kumagai, T., Lafon, A., Latgé, J.-P., Li, W., Lord, A., Lu, C., Majoros, W.H., May, G.S., Miller, B.L., Mohamoud, Y., Molina, M., Monod, M., Mouyna, I., Mulligan, S., Murphy, L., O'Neil, S., Paulsen, I., Peñalva, M.A., Pertea, M., Price, C., Pritchard, B.L., Quail, M.A., Rabbinowitsch, E., Rawlins, N., Rajandream, M.-A., Reichard, U., Renauld, H., Robson, G.D., Rodriguez de Córdoba, S., Rodríguez-Peña, J.M., Ronning, C.M., Rutter, S., Salzberg, S.L., Sanchez, M., Sánchez-Ferrero, J.C., Saunders, D., Seeger, K., Squares, R., Squares, S., Takeuchi, M., Tekaia, F., Turner, G., Vazquez de Aldana, C.R., Weidman, J., White, O., Woodward, J., Yu, J.-H., Fraser, C., Galagan, J.E., Asai, K., Machida, M., Hall, N., Barrell, B., Denning, D.W., 2005. Genomic sequence of the pathogenic and allergenic filamentous fungus *Aspergillus fumigatus*. Nature 438, 1151–1156. https://doi.org/10.1038/nature04332

O'Gorman, C.M., Fuller, H., Dyer, P.S., 2009. Discovery of a sexual cycle in the opportunistic fungal pathogen *Aspergillus fumigatus*. Nature 457, 471–474. https://doi.org/10.1038/nature07528

Pennerman, K.K., AL-Maliki, H.S., Lee, S., Bennett, J.W., 2016. Fungal Volatile Organic Compounds (VOCs) and the Genus *Aspergillus*, New and Future Developments in Microbial Biotechnology and Bioengineering. Elsevier B.V. https://doi.org/10.1016/B978-0-444-63505-1.00007-5

Peterson, S.W., 2008. Phylogenetic analysis of Aspergillus species using DNA sequences from four loci. Mycologia 100, 205–226. https://doi.org/10.3852/mycologia.100.2.205

Piérard, G.E., Piérard-Franchimont, C., Quatresooz, P., 2007. Fungal thigmotropism in onychomycosis and in a clear hydrogel pad model. Dermatology 215, 107–113. https://doi.org/10.1159/000104260

Poggeler, S., Nowrousian, M., Ringelberg, C., Loros, J.J., Dunlap, J.C., Kuck, U., 2006. Microarray and real-time PCR analyses reveal mating type-dependent gene expression in a homothallic fungus. Mol Genet Genomics 275, 492–503. https://doi.org/10.1007/s00438-006-0107-y

Purohit, A.A., Li, W., Qu, C., Dwyer, T., Shao, Q., Guan, K.-L., Liu, G., 2012. Down syndrome cell adhesion molecule (DSCAM) associates with uncoordinated-5C (UNC5C) in netrin-1-mediated growth cone collapse. J. Biol. Chem. 287, 27126–38. https://doi.org/10.1074/jbc.M112.340174

Raper, K.B.; Fennell, D.I., 1965. The Genus *Aspergillus*, 1st ed. Williams and Wilkins.

Read, N.D., 2017. Fungal cell structure and organization, in: Kibbler, C., Barton, R., Gow, N.A.R., Howell, S., MacCallum, D., Manuel, R. (Eds.), Oxford Textbook in Medical Mycology. Oxford University Press, p. 400.

Read, N.D., Fleiβner, A., Roca, M.G., Louise Glass, N., 2010. Cellular and Molecular Biology of Filamentous Fungi, Cellular and Molecular Biology of Filamentous

Fungi. American Society of Microbiology.
https://doi.org/10.1128/9781555816636

Read, N.D., Kellock, L.J., Collins, T.J., Gundlach, A.M., 1997. Role of topography
sensing for infection-structure differentiation in cereal rust fungi. Planta 202, 163–
170. https://doi.org/10.1007/s004250050115

Read, N.D., Lichius, A., Shoji, J.Y., Goryachev, A.B., 2009. Self-signalling and self-
fusion in filamentous fungi. Curr Opin Microbiol 12, 608–615.
https://doi.org/10.1016/j.mib.2009.09.008

Riquelme, M., Aguirre, J., Bartnicki-García, S., Braus, G.H., Feldbrügge, M., Fleig, U.,
Hansberg, W., Herrera-Estrella, A., Kämper, J., Kück, U., Mouriño-Pérez, R.R.,
Takeshita, N., Fischer, R., 2018. Fungal Morphogenesis, from the Polarized
Growth of Hyphae to Complex Reproduction and Infection Structures. Microbiol.
Mol. Biol. Rev. 82, e00068-17. https://doi.org/10.1128/MMBR.00068-17

Riquelme, M., Martínez-Núñez, L., 2016. Hyphal ontogeny in *Neurospora crassa*: a model
organism for all seasons. F1000Research 5, 2801.
https://doi.org/10.12688/f1000research.9679.1

Robinson, P.M., 1973a. Oxygen-positive chemotropic factor for fungi? New Phytol. 72,
1349–1356. https://doi.org/10.1111/j.1469-8137.1973.tb02113.x

Robinson, P.M., 1973b. Chemotropism in fungi. Trans. Br. Mycol. Soc. 61, 303-IN13.
https://doi.org/10.1016/S0007-1536(73)80153-6

Roca, M.G., Arlt, J., Jeffree, C.E., Read, N.D., 2005. Cell biology of conidial
anastomosis tubes in *Neurospora crassa*. Eukaryot Cell 4, 911–919.
https://doi.org/10.1128/EC.4.5.911-919.2005

Roca, M.G., Davide, L.C., Davide, L.M.C., Mendes-Costa, M.C., Schwan, R.F., Wheals,
A.E., 2004. Conidial anastomosis fusion between *Colletotrichum* species. Mycol. Res.
108, 1320–1326. https://doi.org/10.1017/S0953756204000838

Roca, M.G., Read, N.D., Wheals, A.E., 2005. Conidial anastomosis tubes in filamentous fungi. FEMS Microbiol. Lett. 249, 191–198. https://doi.org/10.1016/j.femsle.2005.06.048

Roderick, H.W., 1993. The infection of white clover (Trifolium repens) by conidia of *Cymadothea trifolii*. Mycol. Res. 97, 227–232. https://doi.org/10.1016/S0953-7562(09)80245-1

Rubinstein, R., Thu, C.A., Goodman, K.M., Wolcott, H.N., Bahna, F., Mannepalli, S., Ahlsen, G., Chevee, M., Halim, A., Clausen, H., Maniatis, T., Shapiro, L., Honig, B., 2015. Molecular Logic of Neuronal Self-Recognition through Protocadherin Domain Interactions. Cell 163, 629–642. https://doi.org/10.1016/j.cell.2015.09.026

Ruggiero, M.A., Gordon, D.P., Orrell, T.M., Bailly, N., Bourgoin, T., Brusca, R.C., Cavalier-Smith, T., Guiry, M.D., Kirk, P.M., 2015. A higher level classification of all living organisms. PLoS One 10, 1–60. https://doi.org/10.1371/journal.pone.0119248

Sanz, C., Rodríguez-Romero, J., Idnurm, A., Christie, J.M., Heitman, J., Corrochano, L.M., Eslava, A.P., 2009. *Phycomyces* MADB interacts with MADA to form the primary photoreceptor complex for fungal phototropism. Proc. Natl. Acad. Sci. U. S. A. 106, 7095–100. https://doi.org/10.1073/pnas.0900879106

Semighini, C.P., Hornby, J.M., Dumitru, R., Nickerson, K.W., Harris, S.D., 2006. Farnesol-induced apoptosis in *Aspergillus nidulans* reveals a possible mechanism for antagonistic interactions between fungi. Mol. Microbiol. 59, 753–764. https://doi.org/10.1111/j.1365-2958.2005.04976.x

Seyedmousavi, S., Mouton, J.W., Melchers, W.J., Bruggemann, R.J., Verweij, P.E., 2014. The role of azoles in the management of azole-resistant aspergillosis: from the bench to the bedside. Drug Resist Updat 17, 37–50. https://doi.org/10.1016/j.drup.2014.06.001

Sheppard, D.C., 2011. Molecular mechanism of *Aspergillus fumigatus* adherence to host

constituents. Curr Opin Microbiol 14, 375–379.
https://doi.org/10.1016/j.mib.2011.07.006

Singh, B., Singh, S., Asif, A.R., Oellerich, M., Sharma, G.L., 2014. Allergic aspergillosis
and the antigens of *Aspergillus fumigatus*. Curr Protein Pept Sci 15, 403–423.

Soba, P., Zhu, S., Emoto, K., Younger, S., Yang, S.J., Yu, H.H., Lee, T., Jan, L.Y., Jan,
Y.N., 2007. Drosophila Sensory Neurons Require Dscam for Dendritic Self-
Avoidance and Proper Dendritic Field Organization. Neuron 54, 403–416.
https://doi.org/10.1016/j.neuron.2007.03.029

Soriani, F.M., Malavazi, I., da Silva Ferreira, M.E., Savoldi, M., Von Zeska Kress, M.R.,
de Souza Goldman, M.H., Loss, O., Bignell, E., Goldman, G.H., 2008. Functional
characterization of the *Aspergillus fumigatus* CRZ1 homologue, CrzA. Mol Microbiol
67, 1274–1291. https://doi.org/10.1111/j.1365-2958.2008.06122.x

Spiering, D., Hodgson, L., 2011. Dynamics of the rho-family small GTPases in actin
regulation and motility. Cell Adhes. Migr. 5, 170–180.
https://doi.org/10.4161/cam.5.2.14403

Stadler, D.R., 1952. Chemotropism in *Rhizopus nigricans*: The staling reaction. J. Cell.
Comp. Physiol. 39, 449–474. https://doi.org/10.1002/jcp.1030390308

Sun, Q., Bahri, S., Schmid, a, Chia, W., Zinn, K., 2000. Receptor tyrosine phosphatases
regulate axon guidance across the midline of the *Drosophila* embryo. Development
127, 801–812.

Tapon, N., Hall, A., 1997. Rho, Rac and Cdc42 GTPases regulate the organization of
the actin cytoskeleton. Curr. Opin. Cell Biol. 9, 86–92.
https://doi.org/10.1016/S0955-0674(97)80156-1

Thewes, S., 2014. Calcineurin-Crz1 signaling in lower eukaryotes. Eukaryot Cell 13,
694–705. https://doi.org/10.1128/EC.00038-14

Trinci, A.P., Banbury, G.H., 1968. Phototropism and light-growth responses of the tall

conidiophores of *Aspergillus giganteus*. J Gen Microbiol 54, 427–438.

Turrà, D., Segorbe, D., Di Pietro, A., 2014. Protein Kinases in Plant-Pathogenic Fungi: Conserved Regulators of Infection. Annu. Rev. Phytopathol. 52, 267–288. https://doi.org/10.1146/annurev-phyto-102313-050143

Ugalde, U., 2006. Autoregulatory signals in mycelial fungi. Growth, Differ. Sex. 203–213. https://doi.org/10.1007/3-540-28135-5_11

Ugalde, U., Rodriguez-Urra, A.B., 2014. The Mycelium Blueprint: insights into the cues that shape the filamentous fungal colony. Appl. Microbiol. Biotechnol. 98, 8809–8819. https://doi.org/10.1007/s00253-014-6019-6

Valiante, V., Macheleidt, J., Föge, M., Brakhage, A.A., 2015. The *Aspergillus fumigatus* cell wall integrity signalling pathway: Drug target, compensatory pathways and virulence. Front. Microbiol. 6, 1–12. https://doi.org/10.3389/fmicb.2015.00325

Van De Veerdonk, F.L., Gresnigt, M.S., Romani, L., Netea, M.G., Latgé, J.P., 2017. *Aspergillus fumigatus* morphology and dynamic host interactions. Nat. Rev. Microbiol. 15, 661–674. https://doi.org/10.1038/nrmicro.2017.90

van West, P., Morris, B.M., Reid, B., Appiah, A.A., Osborne, M.C., Campbell, T.A., Shepherd, S.J., Gow, N.A.R., 2002. Oomycete plant pathogens use electric fields to target roots. Mol. Plant-Microbe Interact. 15, 790–798. https://doi.org/10.1094/MPMI.2002.15.8.790

Wang, D.Y.-C., Kumar, S., Hedges, S.B., 1999. Divergence time estimates for the early history of animal phyla and the origin of plants, animals and fungi. Proc. R. Soc. B Biol. Sci. 266, 163–171. https://doi.org/10.1098/rspb.1999.0617

Woese, C.R., Kandler, O., Wheelis, M.L., 1990. Towards a natural system of organisms: proposal for the domains Archaea, Bacteria, and Eucarya. Proc. Natl. Acad. Sci. 87, 4576–4579. https://doi.org/10.1073/pnas.87.12.4576

Wong, K., Ren, X.R., Huang, Y.Z., Xie, Y., Liu, G., Saito, H., Tang, H., Wen, L., Brady-

Kalnay, S.M., Mei, L., Wu, J.Y., Xiong, W.C., Rao, Y., 2001. Signal transduction in neuronal migration: Roles of GTPase activating proteins and the small GTPase Cdc42 in the Slit-Robo pathway. Cell 107, 209–221. https://doi.org/10.1016/S0092-8674(01)00530-X

Zivanovic, B.D., 2012. Surface tip-to-base Ca2+ and H+ ionic fluxes are involved in apical growth and graviperception of the *Phycomyces* stage I sporangiophore. Planta 236, 1817–1829. https://doi.org/10.1007/s00425-012-1738-3

Chapter 2

Materials and methods

[Blank page]

2.1 Chemicals

All chemicals and reagents used in this study were purchased from Sigma (http://www.sigmaaldrich.com/united-kingdom.html), unless otherwise stated.

2.2 Handling of microorganisms

The wild type and all genetically modified (GM) *Aspergillus fumigatus* strains were considered class 2 containment level organisms for the purposes of handling and manipulations. Microbiological handling was carried out using established techniques under fully sterile conditions following the general guidelines and regulations set by the Health and Safety Executive (http://www.hse.gov.uk/biosafety/GMO/) and applied by the University of Manchester. Decontamination of the microbiological laminar flow cabinet Bio2+ (ENVAIR, UK) before and after handling of microorganisms was achieved by thorough wiping with 1:100 Chemgene HDL_4H (Medimark Scientific, UK) and subsequent wiping with 70% w/w industrial methylated spirit (IMS, Fischer Scientific, UK).

2.3 Fungal strains

All strains used in this work are listed in Table 2.1. The wild type strain used for this study was *A. fumigatus* CEA10 (Fedorova et al., 2008; Girardin et al., 1993; Monod et al., 1993). The *gfp::pyrG* strain is a strain which expresses the Green Fluorescent Protein (GFP) constitutively in the cytoplasm under control of the *A. fumigatus* β-tubulin promoter (*benA^p*). Its parental strain is CEA17 a strain which carries mutations in it orotidine-5'-decarboxylase gene (*pyrG)* resulting in the strain being auxotrophic for uracil and uridine (D'Enfert, 1996). Strains with assigned numbers 4-94 are kinase knockout mutants generated by Furaiji *et al.* (unpublished) in the Manchester Fungal Infection Group (MFIG). Their parental strain was FGSC A1160p+ (*⌐akuB^{KU80}::pyrG1 pyrG$^-$ MAT1-1*) (Fraczek et al., 2013). The deletion of *akuB^{KU80}* gene encodes for a DNA repair protein which promotes non-homologous end joining of DNA strands; its deletion results in high percentage of homologous DNA recombination (da Silva Ferreira et al., 2006). Deletion of the genes encoding for the predicted kinases was achieved by insertion of the *hph* cassette encoding for the hygromycin B phosphotransferase gene (the knockout mutants are resistant to hygromycin B). Strains 95-110 are seven-transmembrane G-protein coupled receptor knockout mutants of *A. fumigatus*, which were kindly provided by the Axel Brakhage group (Hans Knöll

Institute, Jena). The *ΔpptA* strain is a mutant strain carrying a deletion of the phosphopantetheinyl transferase, PptA, as well as being auxotrophic to lysine and iron ions (Allen et al., 2011; Johns et al., 2017).

Table 2.1 Fungal strains used during this study.

#	Strain	Locus	Genotype	Source
1	CEA10	-	Wild type, *MAT1-1*	MFIG Collection
2	gfp::pyrG	-	*pyrG⁻ benAᵖ::gfp::pyrG1*	MFIG Collection
3	FGSC A1152 (CEA17)	-	*pyrG⁻*	MFIG Collection
4	FGSC A1160	-	*ΔakuB^{KU80}::pyrG1 pyrG⁻ MAT1-1*	MFIG Collection
5	-	AFUB_045810	*ΔAFUB_045810::hph* *ΔakuB^{KU80}::pyrG1 pyrG⁻ MAT1-1*	MFIG Collection
6	-	AFUB_021710	*ΔAFUB_021710::hph* *ΔakuB^{KU80}::pyrG1 pyrG⁻ MAT1-1*	MFIG Collection
7	-	AFUB_053300	*ΔAFUB_053300::hph* *ΔakuB^{KU80}::pyrG1 pyrG⁻ MAT1-1*	MFIG Collection
8	-	AFUB_032300	*ΔAFUB_032300::hph* *ΔakuB^{KU80}::pyrG1 pyrG⁻ MAT1-1*	MFIG Collection
9	-	AFUB_026400	*ΔAFUB_026400::hph* *ΔakuB^{KU80}::pyrG1 pyrG⁻ MAT1-1*	MFIG Collection
10	-	AFUB_044560	*ΔAFUB_044560::hph* *ΔakuB^{KU80}::pyrG1 pyrG⁻ MAT1-1*	MFIG Collection
11	-	AFUB_030660	*ΔAFUB_030660::hph* *ΔakuB^{KU80}::pyrG1 pyrG⁻ MAT1-1*	MFIG Collection
12	-	AFUB_052450	*ΔAFUB_052450::hph* *ΔakuB^{KU80}::pyrG1 pyrG⁻ MAT1-1*	MFIG Collection
13	-	AFUB_041010	*ΔAFUB_041010::hph* *ΔakuB^{KU80}::pyrG1 pyrG⁻ MAT1-1*	MFIG Collection
14	-	AFUB_043130	*ΔAFUB_043130::hph* *ΔakuB^{KU80}::pyrG1 pyrG⁻ MAT1-1*	MFIG Collection
15	-	AFUB_010510	*ΔAFUB_010510::hph* *ΔakuB^{KU80}::pyrG1 pyrG⁻ MAT1-1*	MFIG Collection
16	-	AFUB_029710	*ΔAFUB_029710::hph* *ΔakuB^{KU80}::pyrG1 pyrG⁻ MAT1-1*	MFIG Collection
17	-	AFUB_018770	*ΔAFUB_018770::hph* *ΔakuB^{KU80}::pyrG1 pyrG⁻ MAT1-1*	MFIG Collection
18	-	AFUB_020560	*ΔAFUB_020560::hph* *ΔakuB^{KU80}::pyrG1 pyrG⁻ MAT1-1*	MFIG Collection
19	-	AFUB_029320	*ΔAFUB_029320::hph* *ΔakuB^{KU80}::pyrG1 pyrG⁻ MAT1-1*	MFIG Collection
20	-	AFUB_025560	*ΔAFUB_025560::hph* *ΔakuB^{KU80}::pyrG1 pyrG⁻ MAT1-1*	MFIG Collection
21	-	AFUB_038630	*ΔAFUB_038630::hph* *ΔakuB^{KU80}::pyrG1 pyrG⁻ MAT1-1*	MFIG Collection
22	-	AFUB_029240	*ΔAFUB_029240::hph* *ΔakuB^{KU80}::pyrG1 pyrG⁻ MAT1-1*	MFIG Collection
23	-	AFUB_016170	*ΔAFUB_016170::hph* *ΔakuB^{KU80}::pyrG1 pyrG⁻ MAT1-1*	MFIG Collection
24	-	AFUB_048440	*ΔAFUB_048440::hph* *ΔakuB^{KU80}::pyrG1 pyrG⁻ MAT1-1*	MFIG Collection

#	Strain	Locus	Genotype	Source
25	-	AFUB_013090	*⊿AFUB_013090::hph* *⊿akuB^{KU80}::pyrG1 pyrG- MAT1-1*	MFIG Collection
26	-	AFUB_006780	*⊿AFUB_006780::hph* *⊿akuB^{KU80}::pyrG1 pyrG- MAT1-1*	MFIG Collection
27	-	AFUB_053440	*⊿AFUB_053440::hph* *⊿akuB^{KU80}::pyrG1 pyrG- MAT1-1*	MFIG Collection
28	-	AFUB_039620	*⊿AFUB_039620::hph* *⊿akuB^{KU80}::pyrG1 pyrG- MAT1-1*	MFIG Collection
29	-	AFUB_045840	*⊿AFUB_045840::hph* *⊿akuB^{KU80}::pyrG1 pyrG- MAT1-1*	MFIG Collection
30	-	AFUB_051750	*⊿AFUB_051750::hph* *⊿akuB^{KU80}::pyrG1 pyrG- MAT1-1*	MFIG Collection
31	-	AFUB_026080	*⊿AFUB_026080::hph* *⊿akuB^{KU80}::pyrG1 pyrG- MAT1-1*	MFIG Collection
32	-	AFUB_029820	*⊿AFUB_029820::hph* *⊿akuB^{KU80}::pyrG1 pyrG- MAT1-1*	MFIG Collection
33	-	AFUB_027640	*⊿AFUB_027640::hph* *⊿akuB^{KU80}::pyrG1 pyrG- MAT1-1*	MFIG Collection
34	-	AFUB_038060	*⊿AFUB_038060::hph* *⊿akuB^{KU80}::pyrG1 pyrG- MAT1-1*	MFIG Collection
35	-	AFUB_001600	*⊿AFUB_001600::hph* *⊿akuB^{KU80}::pyrG1 pyrG- MAT1-1*	MFIG Collection
36	-	AFUB_053500	*⊿AFUB_053500::hph* *⊿akuB^{KU80}::pyrG1 pyrG- MAT1-1*	MFIG Collection
37	-	AFUB_018600	*⊿AFUB_018600::hph* *⊿akuB^{KU80}::pyrG1 pyrG- MAT1-1*	MFIG Collection
38	-	AFUB_010360	*⊿AFUB_010360::hph* *⊿akuB^{KU80}::pyrG1 pyrG- MAT1-1*	MFIG Collection
39	-	AFUB_044400	*⊿AFUB_044400::hph* *⊿akuB^{KU80}::pyrG1 pyrG- MAT1-1*	MFIG Collection
40	-	AFUB_028770	*⊿AFUB_028770::hph* *⊿akuB^{KU80}::pyrG1 pyrG- MAT1-1*	MFIG Collection
41	-	AFUB_036500	*⊿AFUB_036500::hph* *⊿akuB^{KU80}::pyrG1 pyrG- MAT1-1*	MFIG Collection
42	-	AFUB_023730	*⊿AFUB_023730::hph* *⊿akuB^{KU80}::pyrG1 pyrG- MAT1-1*	MFIG Collection
43	-	AFUB_027480	*⊿AFUB_027480::hph* *⊿akuB^{KU80}::pyrG1 pyrG- MAT1-1*	MFIG Collection
44	-	AFUB_030570	*⊿AFUB_030570::hph* *⊿akuB^{KU80}::pyrG1 pyrG- MAT1-1*	MFIG Collection
45	-	AFUB_053520	*⊿AFUB_053520::hph* *⊿akuB^{KU80}::pyrG1 pyrG- MAT1-1*	MFIG Collection
46	-	AFUB_039100	*⊿AFUB_039100::hph* *⊿akuB^{KU80}::pyrG1 pyrG- MAT1-1*	MFIG Collection
47	-	AFUB_007300	*⊿AFUB_007300::hph* *⊿akuB^{KU80}::pyrG1 pyrG- MAT1-1*	MFIG Collection
48	-	AFUB_014350	*⊿AFUB_014350::hph* *⊿akuB^{KU80}::pyrG1 pyrG- MAT1-1*	MFIG Collection
49	-	AFUB_006320	*⊿AFUB_006320::hph* *⊿akuB^{KU80}::pyrG1 pyrG- MAT1-1*	MFIG Collection
50	-	AFUB_052630	*⊿AFUB_052630::hph* *⊿akuB^{KU80}::pyrG1 pyrG- MAT1-1*	MFIG Collection
51	-	AFUB_035220	*⊿AFUB_035220::hph* *⊿akuB^{KU80}::pyrG1 pyrG- MAT1-1*	MFIG Collection
52	-	AFUB_019930	*⊿AFUB_019930::hph* *⊿akuB^{KU80}::pyrG1 pyrG- MAT1-1*	MFIG Collection

#	Strain	Locus	Genotype	Source
53	-	AFUB_017750	*⊿AFUB_017750::hph* *⊿akuB^{KU80}::pyrG1 pyrG- MAT1-1*	MFIG Collection
54	-	AFUB_011380	*⊿AFUB_011380::hph* *⊿akuB^{KU80}::pyrG1 pyrG- MAT1-1*	MFIG Collection
55	-	AFUB_027890	*⊿AFUB_027890::hph* *⊿akuB^{KU80}::pyrG1 pyrG- MAT1-1*	MFIG Collection
56	-	AFUB_056020	*⊿AFUB_056020::hph* *⊿akuB^{KU80}::pyrG1 pyrG- MAT1-1*	MFIG Collection
57	-	AFUB_089870	*⊿AFUB_089870::hph* *⊿akuB^{KU80}::pyrG1 pyrG- MAT1-1*	MFIG Collection
58	-	AFUB_059390	*⊿AFUB_059390::hph* *⊿akuB^{KU80}::pyrG1 pyrG- MAT1-1*	MFIG Collection
59	-	AFUB_059540	*⊿AFUB_059540::hph* *⊿akuB^{KU80}::pyrG1 pyrG- MAT1-1*	MFIG Collection
60	-	AFUB_059090	*⊿AFUB_059090::hph* *⊿akuB^{KU80}::pyrG1 pyrG- MAT1-1*	MFIG Collection
61	-	AFUB_066150	*⊿AFUB_066150::hph* *⊿akuB^{KU80}::pyrG1 pyrG- MAT1-1*	MFIG Collection
62	-	AFUB_071620	*⊿AFUB_071620::hph* *⊿akuB^{KU80}::pyrG1 pyrG- MAT1-1*	MFIG Collection
63	-	AFUB_056110	*⊿AFUB_056110::hph* *⊿akuB^{KU80}::pyrG1 pyrG- MAT1-1*	MFIG Collection
64	-	AFUB_082700	*⊿AFUB_082700::hph* *⊿akuB^{KU80}::pyrG1 pyrG- MAT1-1*	MFIG Collection
65	-	AFUB_072650	*⊿AFUB_072650::hph* *⊿akuB^{KU80}::pyrG1 pyrG- MAT1-1*	MFIG Collection
66	-	AFUB_073970	*⊿AFUB_073970::hph* *⊿akuB^{KU80}::pyrG1 pyrG- MAT1-1*	MFIG Collection
67	-	AFUB_078810	*⊿AFUB_078810::hph* *⊿akuB^{KU80}::pyrG1 pyrG- MAT1-1*	MFIG Collection
68	-	AFUB_093160	*⊿AFUB_093160::hph* *⊿akuB^{KU80}::pyrG1 pyrG- MAT1-1*	MFIG Collection
69	-	AFUB_075210	*⊿AFUB_075210::hph* *⊿akuB^{KU80}::pyrG1 pyrG- MAT1-1*	MFIG Collection
70	-	AFUB_090090	*⊿AFUB_090090::hph* *⊿akuB^{KU80}::pyrG1 pyrG- MAT1-1*	MFIG Collection
71	-	AFUB_078920	*⊿AFUB_078920::hph* *⊿akuB^{KU80}::pyrG1 pyrG- MAT1-1*	MFIG Collection
72	-	AFUB_066030	*⊿AFUB_066030::hph* *⊿akuB^{KU80}::pyrG1 pyrG- MAT1-1*	MFIG Collection
73	-	AFUB_095720	*⊿AFUB_095720::hph* *⊿akuB^{KU80}::pyrG1 pyrG- MAT1-1*	MFIG Collection
74	-	AFUB_060320	*⊿AFUB_060320::hph* *⊿akuB^{KU80}::pyrG1 pyrG- MAT1-1*	MFIG Collection
75	-	AFUB_087320	*⊿AFUB_087320::hph* *⊿akuB^{KU80}::pyrG1 pyrG- MAT1-1*	MFIG Collection
76	-	AFUB_078980	*⊿AFUB_078980::hph* *⊿akuB^{KU80}::pyrG1 pyrG- MAT1-1*	MFIG Collection
77	-	AFUB_053960	*⊿AFUB_053960::hph* *⊿akuB^{KU80}::pyrG1 pyrG- MAT1-1*	MFIG Collection
78	-	AFUB_070630	*⊿AFUB_070630::hph* *⊿akuB^{KU80}::pyrG1 pyrG- MAT1-1*	MFIG Collection
79	-	AFUB_072800	*⊿AFUB_072800::hph* *⊿akuB^{KU80}::pyrG1 pyrG- MAT1-1*	MFIG Collection
80	-	AFUB_072000	*⊿AFUB_072000::hph* *⊿akuB^{KU80}::pyrG1 pyrG- MAT1-1*	MFIG Collection

#	Strain	Locus	Genotype	Source
81	-	AFUB_095640	⊿*AFUB_095640::hph* ⊿*akuB^{KU80}::pyrG1 pyrG^- MAT1-1*	MFIG Collection
82	-	AFUB_087120	⊿*AFUB_087120::hph* ⊿*akuB^{KU80}::pyrG1 pyrG^- MAT1-1*	MFIG Collection
83	-	AFUB_075350	⊿*AFUB_075350::hph* ⊿*akuB^{KU80}::pyrG1 pyrG^- MAT1-1*	MFIG Collection
84	-	AFUB_054020	⊿*AFUB_054020::hph* ⊿*akuB^{KU80}::pyrG1 pyrG^- MAT1-1*	MFIG Collection
85	-	AFUB_081540	⊿*AFUB_081540::hph* ⊿*akuB^{KU80}::pyrG1 pyrG^- MAT1-1*	MFIG Collection
86	-	AFUB_055480	⊿*AFUB_055480::hph* ⊿*akuB^{KU80}::pyrG1 pyrG^- MAT1-1*	MFIG Collection
87	-	AFUB_056640	⊿*AFUB_056640::hph* ⊿*akuB^{KU80}::pyrG1 pyrG^- MAT1-1*	MFIG Collection
88	-	AFUB_074550	⊿*AFUB_074550::hph* ⊿*akuB^{KU80}::pyrG1 pyrG^- MAT1-1*	MFIG Collection
89	-	AFUB_098230	⊿*AFUB_098230::hph* ⊿*akuB^{KU80}::pyrG1 pyrG^- MAT1-1*	MFIG Collection
90	-	AFUB_099170	⊿*AFUB_099170::hph* ⊿*akuB^{KU80}::pyrG1 pyrG^- MAT1-1*	MFIG Collection
91	-	AFUB_096030	⊿*AFUB_096030::hph* ⊿*akuB^{KU80}::pyrG1 pyrG^- MAT1-1*	MFIG Collection
92	-	AFUB_096080	⊿*AFUB_096080::hph* ⊿*akuB^{KU80}::pyrG1 pyrG^- MAT1-1*	MFIG Collection
93	-	AFUB_099990	⊿*AFUB_099990::hph* ⊿*akuB^{KU80}::pyrG1 pyrG^- MAT1-1*	MFIG Collection
94	-	AFUB_006190	⊿*AFUB_006190::hph* ⊿*akuB^{KU80}::pyrG1 pyrG^- MAT1-1*	MFIG Collection
95	-	AFUB_089280	⊿*AFUB_089280::hph* ⊿*akuB^{KU80}::pyrG1 pyrG^- MAT1-1*	MFIG Collection
96	⊿*gprA*	AFUB_034900	⊿*gprA::AnpyrG* ⊿*akuBKU80 pyrG^-*	Hans Knöll Institute (HKI)
97	⊿*gprB*	AFUB_055410	⊿*gprB::AnpyrG* ⊿*akuBKU80 pyrG^-*	Hans Knöll Institute (HKI)
98	⊿*gprC*	AFUB_090350	⊿*gprC::AnpyrG* ⊿*akuBKU80 pyrG^-*	Hans Knöll Institute (HKI)
99	⊿*gprD*	AFUB_028290	⊿*gprD::AnpyrG* ⊿*akuBKU80 pyrG^-*	Hans Knöll Institute (HKI)
100	⊿*gprF*	AFUB_052610	⊿*gprF::AnpyrG* ⊿*akuBKU80 pyrG^-*	Hans Knöll Institute (HKI)
101	⊿*gprG*	AFUB_011350	⊿*gprG::AnpyrG* ⊿*akuBKU80 pyrG^-*	Hans Knöll Institute (HKI)
102	⊿*gprJ*	AFUB_007220	⊿*gprJ::AnpyrG* ⊿*akuBKU80 pyrG^-*	Hans Knöll Institute (HKI)
103	⊿*gprH*	AFUB_052640	⊿*gprH::AnpyrG* ⊿*akuBKU80 pyrG^-*	Hans Knöll Institute (HKI)
104	⊿*gprI*	AFUB_047630	⊿*gprI::AnpyrG* ⊿*akuBKU80 pyrG^-*	Hans Knöll Institute (HKI)
105	⊿*gprL*	AFUB_046660	⊿*gprL::AnpyrG* ⊿*akuBKU80 pyrG^-*	Hans Knöll Institute (HKI)
106	⊿*gprK*	AFUB_101830	⊿*gprK::AnpyrG* ⊿*akuBKU80 pyrG^-*	Hans Knöll Institute (HKI)
107	⊿*gprM*	AFUB_090880	⊿*gprM::AnpyrG* ⊿*akuBKU80 pyrG^-*	Hans Knöll Institute (HKI)
108	⊿*gprO*	AFUB_038590	⊿*gprO::AnpyrG* ⊿*akuBKU80 pyrG^-*	Hans Knöll Institute (HKI)

#	Strain	Locus	Genotype	Source
109	⊿gprP	AFUB_073100	⊿gprP::AnpyrG ⊿akuBKU80 pyrG⁻	Hans Knöll Institute (HKI)
110	⊿gprT	AFUB_096360	⊿gprT::AnpyrG ⊿akuBKU80 pyrG⁻	Hans Knöll Institute (HKI)
111	⊿nopA	AFUB_088000	⊿nopA::AnpyrG ⊿akuBKU80 pyrG⁻	Hans Knöll Institute (HKI)
112	⊿pptA	AFUB_024520A	⊿AFUB_024520A::hph ⊿akuB^{KU80}::pyrG1 pyrG⁻ MAT1-1	MFIG Collection

2.4 Culture media and growth conditions

Handling of microorganisms is described in section 2.2. Nutrient media for *A. fumigatus* were prepared according to Table 2.2 (Vogel, 1956). *Aspergillus* media were based on protocols detailed by Arst and Cove, 1973 and Pontecorvo et al., 1953. For experiments involving solid media, 1.5% w/v agar (Oxoid No1, ThermoScientific, UK) was added before autoclaving. Salt, vitamin and trace elements solutions were kept refrigerated for preservation and used as needed. For the cultivation of the ⊿pptA strain lysine and iron sulphate (FeSO$_4$) were added as supplements to the medium to a final concentration of 100 µM and 10 µM, respectively.

To obtain *A. fumigatus* spores, strain isolates were streaked in tissue culture flasks containing up to 10 ml of either *Aspergillus* Complete Media Agar (ACMA) or Sabouraud Dextrose Agar (SDA, OXOID, Thermo Fischer Scientific, UK), and incubated for 5 days at 37 ºC or until confluent mycelial growth was observed. Subsequently, 10 ml of sterile saline-Tween20 solution (0.9% NaCl, 0.05% v/v Tween20) was pipetted into each flask, followed by vigorous shaking of the sealed-tight flask to obtain a saturated spore suspension. Spore suspensions were subsequently filtered through two layers of sterile Miracloth® (Calbiochem, UK) into 15 ml Corning™ Falcon™ conical centrifuge tubes and were centrifuged at 4,000 rpm for 10 min at room temperature (RT). The supernatant was discarded, and the precipitate was resuspended in 1 ml of 0.05% Saline-Tween20. Spore concentration was measured using a 0.200 mm depth haemocytometer (Fuchs-Rosenthal, VWR) with a conventional benchtop optical microscope and adjusted according to requirements of individual experiments.

For short term storage, tissue culture flasks containing confluent mycelium or Corning™ Falcon™ tubes with spore suspensions were stored at 4 ºC. Long term storage of strains was achieved by mixing 1 ml of spore suspension with 500 µl of

100% sterile glycerol in sterile CryoTubes (Nunc, Thermo Fischer Scientific, UK) and stored at -80 ºC.

Table 2.2 Media and stock solutions for culturing of fungal strains

Media/Stock solution (final volume)	Component	Quantity
Aspergillus Complete Medium (ACM) (1 L)	Adenine (add, until completely dissolved)	0.075 g
	Glucose	25 g
	Yeast extract	1 g
	Bacteriological Peptone	2 g
	Casamino acids	1 g
	100x Vitamin Solution	10 ml
	50x Salt Solution	20 ml
	Ammonium tartrate (from 500mM stock)	10 ml
	pH 6.5 with 10 M NaOH	
Aspergillus Minimal Medium (AMM) (1 L)	Glucose	10 g
	Biotin Solution (0.1 mg/ml, 4 C)	10 ml
	Salt Solution	20 ml
	Ammonium tartrate (from 500mM stock)	10 ml
	pH 6.5 with 10 M NaOH	
50x *Aspergillus* Salt solution (1 L)	KCl (Potassium chloride)	26 g
	$MgSO_4 \cdot 7H_2O$ (Magnesium dihydrogen heptahydrate)	26 g
	KH_2PO_4 (Potassium dihydrogen orthophosphate)	76 g
	Trace element solution	50 ml
	Chloroform (functions as preservative)	1.5 ml
100x Vitamin Solution (1 L)	4-aminobenzoic acid (PABA)	400 mg
	Thiamine	50 mg
	Biotin	1 mg
	Inositol	24 g
	Nicotinic acid	100 mg
	Panto (DL-pantothenic acid)	200 mg
	Pyridoxine	250 mg
	Riboflavin	100 mg
	Choline chloride	1.4 g
Trace Elements Solution (1 L)	$Na_2B_4O_7 \cdot 10H_2O$ (di-sodium tetraborate decahydrate)	40 mg
	$CuSO_4 \cdot 5H_2O$ (cupric sulphate pentahydrate)	400 mg
	$FePO_4 \cdot 2H_2O$ (ferric orthophosphate dihydrate)	800 mg
	$MnSO_4 \cdot 2H_2O$ (manganese sulphate dihydrate)	800 mg
	$Na_2MoO_4 \cdot 2H_2O$ (sodium molybdate dihydrate)	800 mg
	$ZnSO_4 \cdot 7H_2O$ (zinc sulphate heptahydrate)	8 g
Vogel's Medium (VM) (1 L)	50x Vogel's Salts	20 ml
	Sucrose	15 g

Media/Stock solution (final volume)	Component	Quantity
50x Vogel's Salts (1 L)	$Na_3Citrate \cdot 5.5H_2O$	150 g
	KH_2PO_4 (Potassium dihydrogen orthophosphate)	250 g
	NH_4NO_3 (Ammonium nitrate)	100 g
	$MgSO_4 \cdot 7H_2O$ (Magnesium dihydrogen heptahydrate)	10 g
	$CaCl_2 \cdot 2H_2O$ (Calcium chloride dihydrate)	5 g
	Vogel's Trace Elements	5 ml
	Biotin Solution (0.1 mg/ml, 4 C)	2.5 ml
	Chloroform (functions as preservative)	2 ml
Vogel's Trace Elements (100 ml)	Citric acid monohydrate	5 g
	$ZnSO_4 \cdot 7H_2O$ (zinc sulphate heptahydrate)	5 g
	$Fe(NH_4)_2(SO_4)_2 \cdot 6H_2O$ (Ammonium iron(II) sulphate)	1 g
	$CuSO_4 \cdot 5H_2O$ (copper sulphate pentahydrate)	0.25 g
	$MnSO_4 \cdot 1H_2O$ (manganese sulphate monohydrate)	0.05 g
	H_3BO_3 (boric acid)	0.05 g
	$Na_2MoO_4 \cdot 2H_2O$ (sodium molybdate dihydrate)	0.05 g
	Chloroform	2 ml

2.5 Live-cell imaging

2.5.1 Sample preparation

All live-cell imaging experiments were carried out either using the "inverted agar block method" or by imaging spores grown in liquid media in 8-well μ-slide culture chambers (Ibidi USA Inc.).

For the inverted agar block method (Hickey et al., 2002; Fig 2.1), 4-5 μl droplets containing $3x10^5$ fungal spores/ml were inoculated in a 35mm x 10mm treated polystyrene petri dish (Corning Inc.) containing 3 ml of either AMMA or VMA (to limit substrate autofluorescence). The spore concentration was chosen for optimal germination rates according to Araujo and Rodrigues (2004). Plates were incubated for 8-12 h at 37 °C, depending on the purpose of individual experiments. An agar block of approximately 1 cm³ was cut with a scalpel and was placed inverted on top of approximately 40 μl of medium placed on a 48 mm x 64 mm No 1.5 glass coverslip (Agar Scientific, UK). If the droplet contained any fluorescent stains (section 2.6.2), the block was left for 10 minutes for the stain to take effect before imaging.

Imaging of 8-well μ-slide culture chambers were conducted by injecting 200 μl of media containing fungal spores (final concentration $3x10^5$) in each well. The μ-slide culture
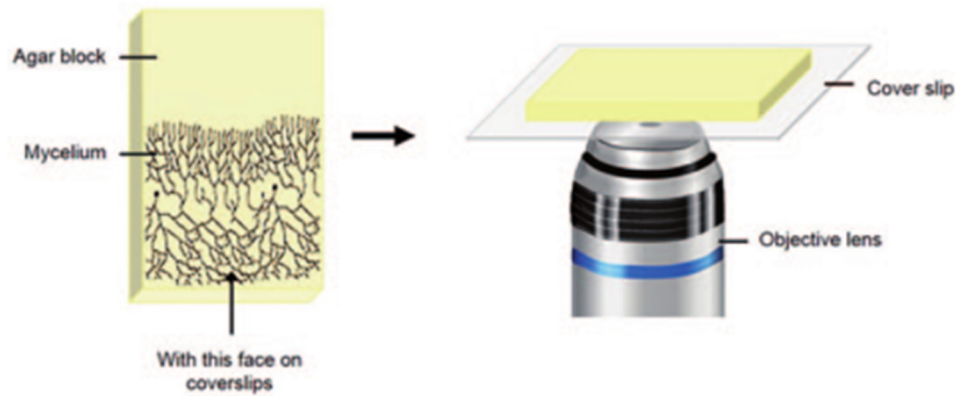
Figure 2.1 The inverted agar block method for live-cell imaging of fungal cells. Reproduced from Dahms and Czymmek (2015)

chambers were subsequently incubated for 8-12 h at 37 °C. Staining of cells, when required, was achieved by slowly dropping 100 µl of the stain (3X of the final concentration) in the desired well and incubating for 20 min, before imaging.

In experiments involving fluorescent microbeads, Flash Red Microspheres (nominal diameter = 7.5 µm, exc./emm. = 660/690, cat. No. FSFR007, Bangs Laboratories, Inc) were mixed at a 1:1 ratio with spores giving a final combined spore/microbead concentration of 3 x 10^5. These samples were then incubated for 8-10 h at 37 °C, before imaging. In nitric oxide (NO) scavenging experiments, spores were inoculated as described and the NO scavenger 2-Phenyl-4,4,5,5-tetramethylimidazoline-1-oxyl 3-oxide (PTIO) was injected in the mixture at the desired concentration (50-500 µM). Spore germination was subsequently imaged at 37 °C at a time-lapse experiment.
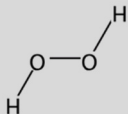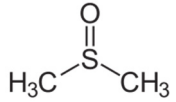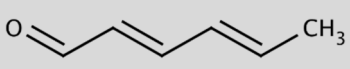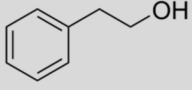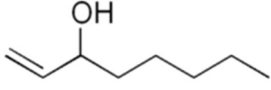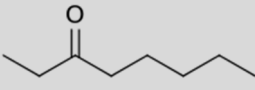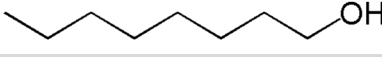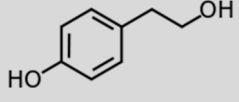
2.5.1.1 Chemical gradient plate assays
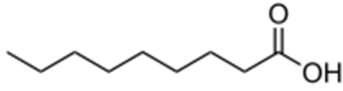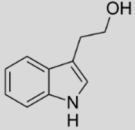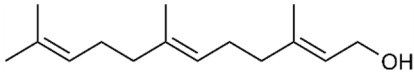
To assess the effects of chemical compounds on the germination of spores and induction of avoidance by young hyphae, a chemical compound gradient assay was generated in a 9 cm Petri dish containing *Aspergillus* Minimal Medium Agar (AMMA). To this end, 3 x 10^5 spores (final volume = 0.5 ml) were spread on AMMA with the use of a plastic spreader and left to dry. Subsequently, a Whatman® Antibiotic Assay Disc (6 mm, Sigma-Aldrich) was placed securely at the centre of the inoculated Petri dish. This filter disc contained 10 µl of the compound to be assayed (Table 2.3). All chemical compounds were diluted in appropriate organic solvents (either ethanol or chloroform which also served as controls) to a final concentration of 1 M. The Petri dishes were incubated at 37 °C for 24 h and observed using stereomicroscopy. For conventional

photography of fungal colonies an Olympus OM-D E-M1 camera with an attached Olympus M.Zuiko Digital ED, 12-40 mm, f/2.8 Pro lens was fixed on a column 35 cm above the plates. The lens focal length was adjusted at 25 mm to minimize spherical aberrations (ISO200, f/5.6, aperture priority mode).

To test if the chemical gradients affected leading vegetative hyphae at the periphery of a colony, 5 µl of AMM containing $3x10^5$ spores/ml were inoculated on a Petri dish containing AMMA and incubated for at least 48 h at 37 °C. Subsequently, a Whatman® Antibiotic Assay Disc (6 mm, Sigma-Aldrich), containing 10 µl of 1M the compound to be tested, was placed 1 cm away from the edge of the colony, and the fungal colonies further incubated for 24 h at 37 °C. Petri dishes with the fungal colonies were imaged using stereomicroscopy and conventional photography.

Table 2.3 Chemical compounds used for gradient plate assays

Molecule	Structure	Group	MW (g/mol)
Hydrogen Peroxide		Reactive Oxygen Species	34.014
Dimethyl sulfoxide (DMSO)		Sulfoxide	78.129
trans,trans-2,4-hexadienal		Aldehyde	96.129
phenylethyl alcohol		Aromatic alcohol	122.167
1-Octen-3-ol		Fatty alcohol	128.215
3-Octanone		Ketone	128.215
1-Octanol		Fatty alcohol	130.231
2-(4hydroxyphenyl) ethanol		Aromatic alcohol	138.166

Molecule	Structure	Group	MW (g/mol)
Nonanoic acid		Carboxylic acid	158.241
Tryptophol		Aromatic alcohol	161.20
Farnesol		Sesquiterpene alcohol	222.37

2.5.2 Proteins and dyes used for fluorescence microscopy

A variant of the wild type Green Fluorescent Protein (GFP) was used in the *gfp::pyrG* strain. This superfolder GFP (sGFP, Cava et al., 2008) displays excitation/emission maxima at 489 nm and 509 nm respectively, and was constitutively expressed in the cytoplasm (section 2.3).

Fluorescent dyes serving as specific markers for cell compartments were used to stain fungal cells depending on experimental needs (Hickey et al., 2004). Stock solutions were prepared in the organic solvent dimethyl sulfoxide (DMSO), and further diluted when applied to cells before imaging. Dyes used in this study along with their properties and targets are summarised in Table 2.4. Concentration denotes the final concentration in the cell suspension for each dye. As a general principle, staining with dyes was achieved by incubation for at least 20 min prior to observation. Excitation and emission spectra for all fluorescent proteins and dyes were validated using the λΛ-scan function (lambda-Lambda-scan) of the Leica TCS SP8X confocal microscope.

Table 2.4 Fluorescent dyes used in this study.

Dye	Target/Marker of	Concentrations	Excitation wavelengths (nm)	Emission wavelengths (nm)
Calcofluor White (Fluorescent brightener 28)	Cell wall chitin	1 µg/ml	405	450-550
Propidium iodide	Cell death	5 µg/ml	543	>550
FM4-64	Lipid membranes	5 µM	515	>550

2.5.3 Confocal Laser-Scanning Microscopy (CLSM)

Live-cell imaging of fungal cells at high resolution was performed using a laser-scanning confocal microscope (Leica, TCS SP8X), which was mounted on an inverted microscope and equipped with a blue diode 405 laser, argon ion laser (457 nm, 476 nm, 488 nm and 514 nm), and a tuneable white light laser (400 nm-700 nm). Simultaneous brightfield images were captured with a transmitted light detector. The laser intensity and laser exposure to the cells were kept to a minimum to reduce photobleaching and phototoxic effects. A 40x/0.85 Numerical Aperture (NA) dry, a 63x/1.4 NA water, and a 63x/1.4 HC PL AP CS2 Oil objective lens were used. Imaging was carried out at room temperature, and for time-lapse experiments at 37°C in a microscope temperature-controlled chamber (Cube & Box, CH). Confocal images were captured using the Leica Application Suite X (LAS X).

For medium to high-throughput imaging of cells grown in 8-well chamber slides, the MATRIXscreener module of the Leica SP8 was used. This allowed the capture of multiple fields of view (FOV) in a single well-based on the algorithm chosen. For my experimental purposes, the Multiple Regular Matrices pattern was chosen which allowed the scanning of multiple equidistant scan-fields in a single well and across multiple equidistant wells. The 40x/0.85 NA dry lens was used for the MATRIX screen exclusively to minimise image aberrations caused by the evaporation of the immersion liquid.

2.5.4 Stereomicroscopy

A Leica MZ FLIII optical stereomicroscope was used for low magnification imaging of hyphae at the periphery of fungal colonies. Magnification used ranged from 0.75X to 6.3X. Mirrors and lighting were adjusted appropriately to generate a shadow effect resembling differential interference contrast (DIC). Images were captured using an attached Retiga6000 Monochrome CCD (charge-coupled device) camera (QImaging, Can) controlled by the MicroManager v1.4.22 programme (open-source software based on ImageJ). Images were saved as 12-bit lossless TIFF format.

2.5.5 Light Sheet Fluorescence Microscopy (LSFM)

To image germinated spores inside solidified agar Light Sheet Fluorescence Microscopy (LSFM) was used. Since a thin slice of the sample is illuminated by a sheet of light, the

main advantage of LSFM over CLSM is that it allows deep penetration of the excitation (provided that the sample is clear), has significantly higher acquisition speeds (100-1000 times faster) and causes reduced damage by irradiation of the samples (Fadero et al., 2018). For my experimental purposes a 2 mm agar column sample was imaged in its entirety.

Sample were prepared as follows: 2 mm suction capillary columns (Zeiss) were used to suck liquid AMMA containing low gelling point agarose instead of agar (4% w/v). The reasons for choosing low gelling point agarose was because a) it does not polymerise rapidly/immediately when making contract with the capillary walls, b) it produces images of far superior optical clarity than agar in LSFM due to limited interference with the light sheet. The nutrient substrate was left to solidify and then the upper tip was cut with a sharp razor blade to cut off the meniscus formed to produce a flat surface. Subsequently, 3 μl of AMM (liquid) containing 3 x 10^5 *gfp::pyrG* spores/ml were placed
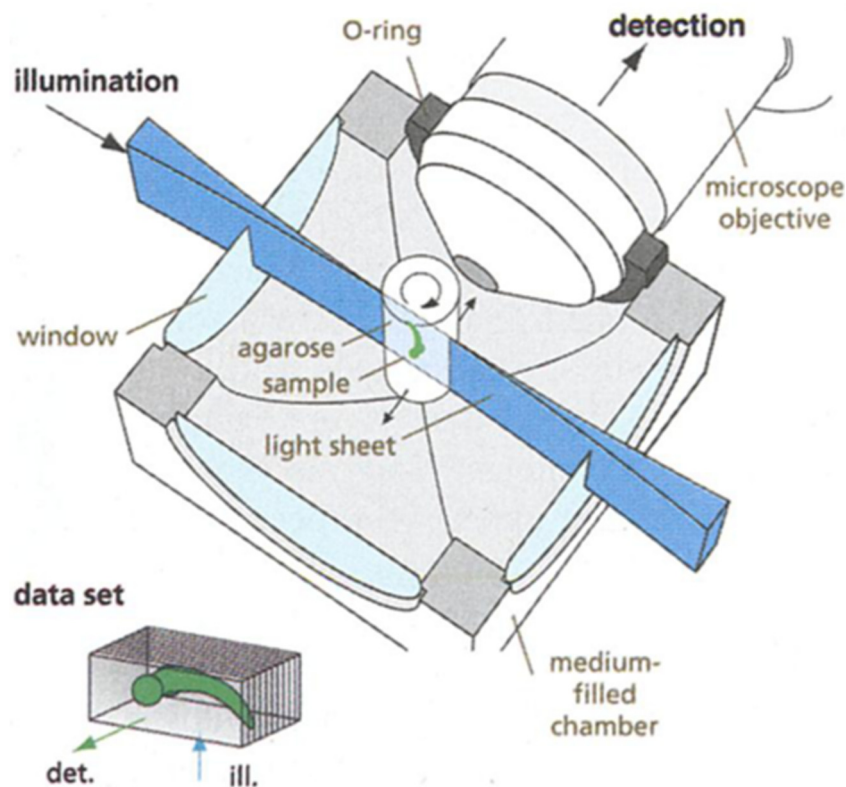
Figure 2.2 Selective plane illumination microscopy (SPIM) during light sheet microscopy imaging. The medium with agarose (2 mm thick in diameter) was pushed outside the capillary and was exposed in a chamber filled with media. Light sheet illumination was used for excitation of the sample with the microscope objective being perpendicular to the light sheet at all times. The sample was rotated to image from all sides, and the image was reconstructed using the ZEN software. Reproduced from Huisken et al. (2004).

at the top of the capillary and left to dry. Afterwards, AMMA (with low gelling point agarose 1.5% w/v) was sucked into the capillary and left to solidify. With this preparation the spore suspension became concentrated at the interface of the two media with different agarose concentrations, thus different stiffness.

Imaging of the capillary samples was performed in a Zeiss Z.1 Light Sheet Microscope using the selective/single plane illumination microscopy method (SPIM, Huisken et al., 2004; Fig. 2.2). The chamber in which the sample was immersed was filled with fresh, sterile AMM. The W Plan-Apochromat 20x/1.0 NA lens was used, along with a 488-60 nm LASER and LBF 405/488/561 beam splitter filter. An AxioCam ICm1, controlled by the ZEN software (Zeiss) was used to detect fluorescence signals.

2.5.6 Microscopy Image Analysis

All images acquired by CLSM and LSFM were processed and analysed using the Imaris 4D image analysis suite v8.0 (Bitplane AG) or Leica Application Suite X (LAS X). Segmentation of 4D-stacks obtained by CLSM was achieved using the FilamentTracer, Spots, or Surfaces functionalities in Imaris, with default settings, fine tuning the thresholds to reduce background when needed.

Stereomicroscopy images were processed with the FIJI freeware software suite. Images were converted to from 12-bit to 8-bit and adjustments were made in the brightness/contrast ratio and dynamic range. Gamma was not adjusted in any image. All images and photos were further processed and sorted without any retouching in Adobe Photoshop CS6 and Adobe Illustrator CS6.

2.6 Mass spectroscopy methods

2.6.1 Fungal headspace analysis

A novel method of headspace extraction and analysis involving mass spectroscopy was developed to investigate the Volatile Organic Compounds (VOCs) secreted by *A. fumigatus*. The methodology is summarised in Figure 2.5 at the end this section.

2.6.1.1 Headspace sampling apparatus

For the headspace sampling, 50 ml Büchner filter flasks (Scientific Glass Laboratories Limited, Stoke-on-Trent, UK) containing 10 mL of solid *Aspergillus* minimal media (AMMA) were inoculated with 1 mL of conidial suspension containing a total of 3 x 10^5 spores. After gentle shaking to ensure the suspension has covered the entirety of the medium surface, the flasks were sealed and placed in incubation at 37 °C.

The headspace sampling apparatus was made of inert material. The headspace chamber was composed of the glass flasks, where the flask opening was sealed with a polytetrafluoroethylene (PTFE) stopper (Sigma Aldrich, Gillingham, UK). A hollow stainless-steel tube was fixed through the PTFE stopper and exposed within the headspace chamber. VOC samples were trapped on a sorbent tube fixed onto a three-way stainless-steel ball valve (Thames Restek, Saunderton, UK) attached to the outside part of the exposed hollow tube. In addition to quartz wool and gauzes within the hollow tube (Sigma Aldrich, Gillingham, UK), this set up prevented any fungal conidia from attaching to the outside of the sample sorbent tube. PTFE tape was used to seal and prevent gas leaks (Fig. 2.3).

Figure 2.3 Experimental setup of the headspace sampling apparatus. A flask (1) containing the media with the fungal samples was sealed with a PTFE stopper (2) to prevent any gas leaks. The three-way stainless valve (3) was used to direct flow accordingly. A tube was placed to gather any VOCs passively up until the sampling time point (4) at which point the valve was switched to permit flow to the active sampling tube (5). Active sampling was achieved by vacuum suction by the Acti-VOC low-flow pump at 50 ml/min to avoid turbulence and VOC degradation.

Stainless steel sorbent tubes packed with a multi-sorbent bed consisting of Tenax TA, a registered trademark of the poly(2,6-diphenyl-p-phenylene oxide) porous polymer resin, and Carbograph 5TD (medium/strong sorbent of light hydrocarbons) were used for capturing headspace and quality control samples (Fig. 2.4). The detection range of VOCs for such tubes is C_2-C_{30}. Tubes were conditioned between use at 330 °C for 60 min with a constant dry N_2 flow of 100 ml/min through the tubes and limited to a maximum number of 100 thermal cycles. Sorbent tubes were tightly sealed with brass caps outside of sampling, conditioning, and desorption. Tubes were transported to and from the fungal laboratory in a protected container and were stored at 4°C after sample collection for no longer than one week before desorption.

2.6.1.2 Headspace sampling

During active sampling, headspace gas was drawn out using a low-flow pump (Acti-VOC, Markes International, Llantrisant, UK) at a flow rate of 50 mL/min for 2 min (expected total volume sampled was up to 100 ml). Headspace was sampled at two time points for germination (0 to 8 h) and maturation or conidiation (12-24 h) for all fungal strains and media samples. Passive sampling (i.e. diffusive sampling) was performed between 0 and 8 h, and 12-24 h. Passive sampling relied upon reaching a pressure-dependant equilibrium i.e. between the atmospheric pressure within the headspace chamber and the external atmospheric pressure. In theory, headspace gas is drawn out of the chamber with minimal flow (generated by increased pressure), where VOCs are adsorbed onto the sorbent material.

After culture headspace sampling flasks were treated with Chemgene HLD₄D
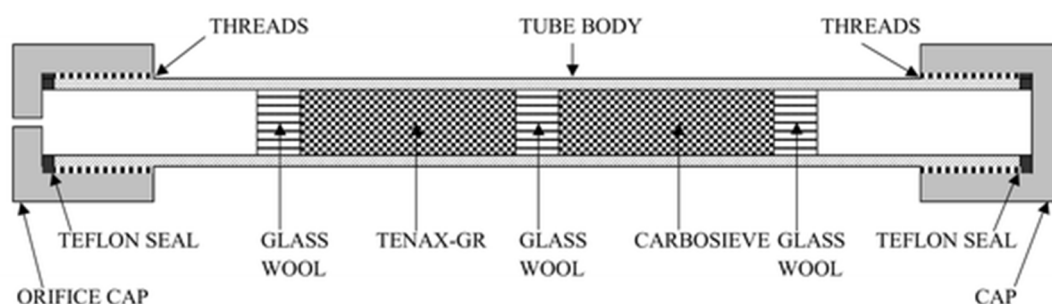
Figure 2.4 Stainless steel sorbent tubes used during the fungal headspace sampling and analysis. The orifice caps were removed during sampling, and headspace gas was collected either passively or sucked through the tube and bound to the TenaxTA (here Tenax-GR) resin (reproduced from Markes website).

(Medimark Scientific, UK) for 24 h. After heating to bring the contained medium to a melting point, the medium was discarded, the flasks thoroughly washed with tap water, rinsed with Milli-Q water and autoclaved to be used for subsequent sampling experiments.

2.6.2 Sample analysis

All sample analysis was carried out by Dr Iain White (Fowler Group, Manchester Institute of Biotechnology, University of Manchester). Samples were analysed in randomised intra-experimental blocks by TD-GC-ToF-MS (GCT Premier, Waters Corporation, Manchester, UK). Briefly, sorbent tubes were heated to 320 °C (5 min hold) before being purged with helium (1 ml/min). Compounds were transferred onto a cold trap (kept at 0 °C) before being desorbed a second time to 330 °C (3 min hold) and transferred into the GC column for separation. The DB-5ms Ultra Inert GC column (30 m length, 0.25 mm internal diameter, 0.25 µm film thickness) had a helium carrier gas flow set to a constant pressure method (69 kPa), and was subjected to a temperature ramped program starting at 40 °C, first ramp to 170 °C at 6 °C/min, and the second ramp to 250 °C at 15 °C/min (total GC run time of 27 min).

After chromatographic separation, VOCs were transferred to the mass spectrometer and subjected to electron ionisation in positive mode (70eV) before further separation in the time-of-flight mass analyser. Mass spectra were acquired in centroid format, at a rate of 10 scans/s over an m/z range of 40 to 500 Da. Each sample included an internal standard (4-bromofluorobenzene in N_2) and each run included a minimum of two external standard mixtures at the start and end of a run, or every block of 10 samples in a continuous run. All samples were desorbed twice to prevent carry-over.

2.6.3 Data analysis

Raw gas chromatography-mass spectroscopy (GC-MS) data files were converted to mzXML format. Samples were pre-processed (peak integration and smoothing, baseline correction, and retention time alignment) using both the *XCMS* package (Smith et al., 2006) through R software (R Core Development team, version 3.4.2) and Chromalynx batch analysis using the ApexTrack peak integration algorithm (Masslynx software, Waters Corporation, Manchester, UK). XCMS and Chromalynx parameters were tuned using the VOC standards mixture (Table 2.5). The NIST14 mass spectral library was

used for compound identification. Peak areas were normalised by the internal standard for each sample. To test statistical significance between two different sample groups, the non-parametric Mann Whitney-U test was used ($\alpha \leq 0.05$). Chemical compounds and their related metabolic pathways were looked up in the Kyoto Encyclopedia of Genes and Genomes (KEGG, Ogata et al., 1999). The automated data analysis was carried out by Waqar Ahmed and cross-validated by manual analysis by myself.

1. Fungal culture
37 °C for 24h

Media   CEA10 $\Delta pptA$
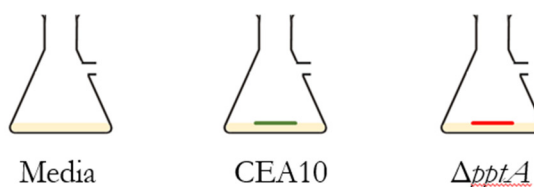
2. Headspace sampling
Germination: 0-8h
Early conidiation: 12-24h
Flow rate 50 ml/min (2 min)

Passive sampling   Active sampling
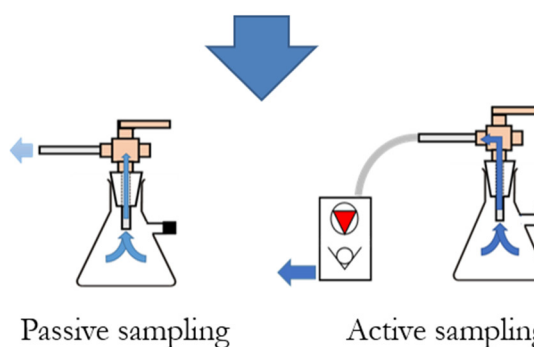
3. Sample analysis by TD-GC-MS
Sorbent tube: Tenax TA-Carbograph 5TD

TA:5TD   TD-GC-ToF-MS

4. Data analysis
Masslynx peak integration
ID with NIST14
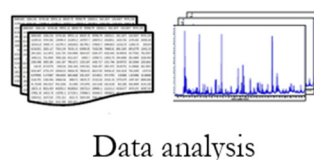
Data analysis

Figure 2.5 Fungal headspace sampling and analysis process. Headspace sampling (2) was carried out over the course of 24 hpi (1) using media as control and other fungal strains CEA10 and $\Delta pptA$. This included the passive collection of headspace over the course and active sampling of the whole headspace to a different Tenax TA-Carbograph 5TD tube which was analysed by Iain White in the Manchster Institute of Biotechnology (TD-GC-ToF-MS). Acquired data was then matched against a NIST14 library and further analysed (4). Please refer to text for further details.

Table 2.5 Standards used to tune XCMS and Chromalynx parameters.

Mixture	Compounds
VOC standards mix	Acetone, Isoprene, Benzene, 3-pentanone, 1,4-dioxane, Toluene, Octane, Butyl acetate, p-xylene, Nonane, Benzaldehyde, 1-heptanol, Decane, 3-carene, Limonene, Undecane, Nonanal, Tetralin, Dodecane, Methyl indole, Tridecane, Tetradecane, Pentadecane
External standards	Styrene, a-pinene, Camphene, Pyrazine, Humulene, Longifolene, Valencene, Bergamot oil, Farnesene

2.7 DNA and protein homology analyses

To identify homologue DNA and protein orthologue sequences of the kinase knockout mutant strains (section 2.3) *in silico* analysis was carried out using the Basic Local Alignment Search Tool (BLAST; Altschul et al., 1990). Two algorithms were used for the same kinases: protein-protein similarity (blastp) and protein-DNA database (tblastn). The results were cross-referenced and search returns ("hits") with the highest similarity (% identities and number of positives), lowest E-value, as well as conserved domains. The BLAST analysis was performed in the EnsemblFungi webpage of *A. fumigatus* A1163 (http://fungi.ensembl.org/Aspergillus_fumigatusa1163/Info/Index) against the sequenced and annotated genomes of *Neurospora crassa* OR74A (Galagan et al., 2003), *Candida albicans* SC5314 (Fonzi and Irwin, 1993; Odds et al., 2004) and *Saccharomyces cerevisiae* S288C (Goffeau et al., 1996). Further investigation of homologue gene and protein sequences functions was performed in the corresponding organism genome webpage: *N. crassa* (https://www.ncbi.nlm.nih.gov/genome/19), *C. albicans* (http://www.candidagenome.org/), and *S. cerevisiae* (https://www.yeastgenome.org/).

2.8 Statistical analysis

Unless otherwise state, all data sets were analysed using either Student's t-test or one-way analysis of variance (ANOVA) statistical comparison with 95% confidence intervals. All statistical analyses were performed using GraphPad Prism software v7.04 (GraphPad Software, Inc.). All comparisons were deemed significant if their *p*-value was lower than 0.05. All experiments were conducted at least in triplicate.

2.9 References

Allen, G., Bromley, M., Kaye, S.J., Keszenman-Pereyra, D., Zucchi, T.D., Price, J., Birch, M., Oliver, J.D., Turner, G., 2011. Functional analysis of a mitochondrial phosphopantetheinyl transferase (PPTase) gene pptB in *Aspergillus fumigatus*. Fungal Genet. Biol. 48, 456–464. https://doi.org/10.1016/J.FGB.2010.12.006

Altschul, S.F., Gish, W., Miller, W., Myers, E.W., Lipman, D.J., 1990. Basic local alignment search tool. J. Mol. Biol. 215, 403–410. https://doi.org/10.1016/S0022-2836(05)80360-2

Araujo, R., Rodrigues, A.G., 2004. Variability of germinative potential among pathogenic species of *Aspergillus*. J. Clin. Microbiol. 42, 4335–4337. https://doi.org/10.1128/JCM.42.9.4335-4337.2004

Arst, H.N., Cove, D.J., 1973. Nitrogen metabolite repression in *Aspergillus nidulans*. MGG Mol. Gen. Genet. 126, 111–141. https://doi.org/10.1007/BF00330988

Cava, F., de Pedro, M.A., Blas-Galindo, E., Waldo, G.S., Westblade, L.F., Berenguer, J., 2008. Expression and use of superfolder green fluorescent protein at high temperatures in vivo: a tool to study extreme thermophile biology. Environ. Microbiol. 10, 605–613. https://doi.org/10.1111/j.1462-2920.2007.01482.x

D'Enfert, C., 1996. Selection of multiple disruption events in *Aspergillus fumigatus* using the orotidine-5'-decarboxylase gene, pyrG, as a unique transformation marker. Curr. Genet. 30, 76–82. https://doi.org/10.1007/s002940050103

da Silva Ferreira, M.E., Kress, M.R.V.Z., Savoldi, M., Goldman, M.H.S., Hartl, A., Heinekamp, T., Brakhage, A.A., Goldman, G.H., 2006. The akuBKU80 Mutant Deficient for Nonhomologous End Joining Is a Powerful Tool for Analyzing Pathogenicity in *Aspergillus fumigatus*. Eukaryot. Cell 5, 207–211. https://doi.org/10.1128/EC.5.1.207-211.2006

Fadero, T.C., Gerbich, T.M., Rana, K., Suzuki, A., DiSalvo, M., Schaefer, K.N., Heppert, J.K., Boothby, T.C., Goldstein, B., Peifer, M., Allbritton, N.L., Gladfelter, A.S., Maddox, A.S., Maddox, P.S., 2018. LITE microscopy: Tilted

light-sheet excitation of model organisms offers high resolution and low photobleaching. J. Cell Biol. jcb.201710087. https://doi.org/10.1083/jcb.201710087

Fedorova, N.D., Khaldi, N., Joardar, V.S., Maiti, R., Amedeo, P., Anderson, M.J., Crabtree, J., Silva, J.C., Badger, J.H., Albarraq, A., Angiuoli, S., Bussey, H., Bowyer, P., Cotty, P.J., Dyer, P.S., Egan, A., Galens, K., Fraser-Liggett, C.M., Haas, B.J., Inman, J.M., Kent, R., Lemieux, S., Malavazi, I., Orvis, J., Roemer, T., Ronning, C.M., Sundaram, J.P., Sutton, G., Turner, G., Venter, J.C., White, O.R., Whitty, B.R., Youngman, P., Wolfe, K.H., Goldman, G.H., Wortman, J.R., Jiang, B., Denning, D.W., Nierman, W.C., 2008. Genomic islands in the pathogenic filamentous fungus *Aspergillus fumigatus*. PLoS Genet. 4. https://doi.org/10.1371/journal.pgen.1000046

Fonzi, W.A., Irwin, M.Y., 1993. Isogenic strain construction and gene mapping in *Candida albicans*. Genetics 134, 717–728. https://doi.org/10.1111/j.1834-7819.1995.tb03122.x

Fraczek, M.G., Bromley, M., Buied, A., Moore, C.B., Rajendran, R., Rautemaa, R., Ramage, G., Denning, D.W., Bowyer, P., 2013. The cdr1B efflux transporter is associated with non-cyp51a-mediated itraconazole resistance in *Aspergillus fumigatus*. J. Antimicrob. Chemother. 68, 1486–1496. https://doi.org/10.1093/jac/dkt075

Galagan, J., Calvo, S., Borkovich, K., Selker, E., Read, N., Jaffe, D., FitzHugh, W., Ma, L.-J., Smirnov, S., Purcell, S., Rehman, B., Elkins, T., Engels, R., Wang, S., Nielsen, C., Butler, J., Endrizzi, M., Qui, D., Ianakiev, P., Bell-Pedersen, D., Nelson, M., Werner-Washburne, M., Selitrennikoff, C., Kinsey, J., Braun, E., Zelter, A., Schulte, U., Kothe, G., Jedd, G., Mewes, W., Staben, C., Marcotte, E., Greenberg, D., Roy, A., Foley, K., Naylor, J., Stange-Thomann, N., Barrett, R., Gnerre, S., Kamal, M., Kamvysselis, M., Mauceli, E., Bielke, C., Rudd, S., Frishman, D., Krystofova, S., Rasmussen, C., Metzenberg, R., Perkins, D., Kroken, S., Cogoni, C., Macino, G., Catcheside, D., Li, W., Pratt, R., Osmani, S., DeSouza, C., Glass, L., Orbach, M., Berglund, A., Voelker, R., Yarden, O., Plamann, M., Seiler, S., Dunlap, J., Radford, A., Aramayo, R., Natvig, D., Alex, L., Mannhaupt, G.,

Ebbole, D., Freitag, M., Paulsen, I., Sachs, M., Lander, E., Nusbaum, C., Birren, B., 2003. The genome sequence of the filamentous fungus *Neurospora crassa*. Nature 422, 859–868. https://doi.org/doi: 10.1038/nature01554

Girardin, H., Latge, J.-P., Srikantha, T., Morrow, B., Soll, D.R., 1993. Development of DNA Probes for Fingerprinting *Aspergillus fumigatus*. J. Clin. Microbiol. 31, 1547–1554.

Goffeau, A., Barrell, B.G., Bussey, H., Davis, R.W., Dujon, B., Feldmann, H., Galibert, F., Hoheisel, J.D., Jacq, C., Johnston, M., Louis, E.J., Mewes, H.W., Murakami, Y., Philippsen, P., Tettelin, H., Oliver, S.G., 1996. Life with 6000 Genes conveniently among the different interna- Old Questions and New Answers The genome . At the beginning of the se- of its more complex relatives in the eukary- cerevisiae has been completely sequenced *Schizosaccharomyces pombe* indicate. Science (80-.). 274, 546–567. https://doi.org/jyu

Hickey, P.C., Jacobson, D.J., Read, N.D., Louise Glass, N., 2002. Live-cell imaging of vegetative hyphal fusion in *Neurospora crassa*. Fungal Genet. Biol. 37, 109–119. https://doi.org/10.1016/S1087-1845(02)00035-X

Hickey, P.C., Swift, S.R., Roca, M.G., Read, N.D., 2004. Live-cell Imaging of Filamentous Fungi Using Vital Fluorescent Dyes and Confocal Microscopy. Methods Microbiol. 34, 63–87. https://doi.org/10.1016/S0580-9517(04)34003-1

Huisken, J., Swoger, J., Del Bene, F., Wittbrodt, J., Stelzer, E.H.K., 2004. Optical sectioning deep inside live embryos by selective plane illumination microscopy. Science (80-.). 305, 1007–1009. https://doi.org/10.1126/science.1100035

Johns, A., Scharf, D.H., Gsaller, F., Schmidt, H., Heinekamp, T., Straßburger, M., Oliver, J.D., Birch, M., Beckmann, N., Dobb, K.S., Gilsenan, J., Rash, B., Bignell, E., Brakhage, A.A., Bromley, M.J., 2017. A Nonredundant Phosphopantetheinyl Transferase, PptA, Is a Novel Antifungal Target That Directs Secondary Metabolite, Siderophore, and Lysine Biosynthesis in *Aspergillus fumigatus* and Is Critical for Pathogenicity. MBio 8, e01504-16. https://doi.org/10.1128/mBio.01504-16

Monod, M., Paris, S., Sarfati, J., Jaton-Ogay, K., Ave, P., Latgé, J.-P., 1993. Virulence of alkaline protease-deficient mutants of *Aspergillus fumigatus*. FEMS Microbiol. Lett. 106, 39–46. https://doi.org/10.1111/j.1574-6968.1993.tb05932.x

Odds, F.C., Brown, A.J.P., Gow, N.A.R., 2004. Candida albicans genome sequence: A platform for genomics in the absence of genetics. Genome Biol. 5, 5–7. https://doi.org/10.1186/gb-2004-5-7-230

Ogata, H., Goto, S., Sato, K., Fujibuchi, W., Bono, H., Kanehisa, M., 1999. KEGG: Kyoto encyclopedia of genes and genomes. Nucleic Acids Res. 27, 29–34. https://doi.org/10.1093/nar/27.1.29

Pontecorvo, G., Roper, J.A., Chemmons, L.M., Macdonald, K.D., Bufton, A.W.J., 1953. The Genetics of *Aspergillus nidulans*. Adv. Genet. 5, 141–238. https://doi.org/10.1016/S0065-2660(08)60408-3

Smith, C., Elizabeth, J., O'Maille, G., Abagyan, R., Siuzdak, G., 2006. XCMS: processing mass spectrometry data for metabolite profiling using Nonlinear Peak Alignment,Matching,and Identification. ACS Publ. 78, 779–787. https://doi.org/10.1021/ac051437y

Vogel, H.J., 1956. A convenient growth medium for *Neurospora crassa*. Microb. Genet. Bull. 13, 42–43.

[Blank page]

Chapter 3

Analysis of negative tropisms in

A. fumigatus

[Blank page]

3.1 Introduction

One of the characteristics of a fungal mycelium is that it grows uniformly outwards, resulting in a circular colony if there are no local restrictions on growth (e.g. nutrient availability, competition, or growth inhibition factors). This macroscopic observation is effectively a manifestation of the growth taking place at the microscopic level and results from processes initiated during the germination of the fungus. Another observation of the growth patterns during this early stage of colony establishment is that germlings seem to be more-or-less equally spaced between themselves (Fig. 3.1). There are is little understanding of how this mycelial growth pattern, which results in uniform radial growth, is achieved. The main hypothesis used to explain this phenomenon of radial growth is that it results of from negative cell tropisms (self-avoidance) between adjacent germ tubes in the young colony and between mature hyphae and their branches in older colonies.
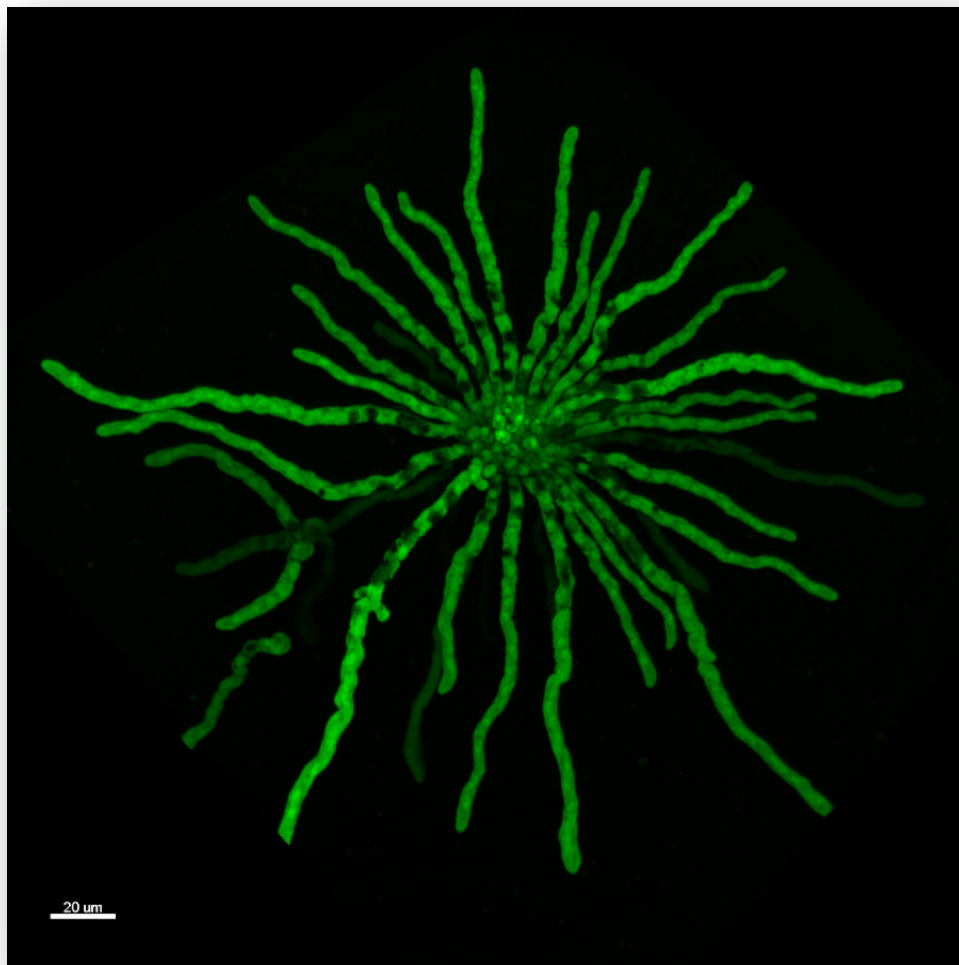
Figure 3.1 Self-avoidance is evident in a fungal microcolony. Fungal hyphae grow uniformly outwards from the original germination site and arrange their growth direction depending on the position of neighbouring cells. Scale bar = 20 μm.

Current knowledge of negative cell tropisms in fungi and neuron cells of higher eukaryotes has been summarised in section 1.3.6. Trinci *et al.* (1979) performed the first simple quantification of avoidance in three filamentous fungal species *Aspergillus nidulans, Mucor hiemalis* and *N. crassa* (Table 3.1). In their study, the measured distances between pairs of approaching hyphae showed that there is great variability of the avoidance: a) between species, and b) between pairs of the same species. This great variability was the first indicator that self-avoidance has intrinsic difficulties in its quantification using vegetative hyphae. This is almost certainly a result of the changes in a hypha's polarity being a result of many, complex and different factors/signals which may or may not be related to negative autotropisms. Thus, the probability of falsely identifying polarity changes as a result of self-avoidance is high (false positive results). All these combined, dictate the necessity for a quantitative assay of avoidance which is fast, simple, relevant to the biology of the fungus and provides reproducible and comparable results.

Virtually all previous studies involving self-avoidance in filamentous fungi have been limited to the responses of vegetative hyphae. However, it has actually been found to occur much earlier during colony development with (a) the sites of emergence of germ tubes from spores, and (b) during germ tube interactions (Lichius et al., 2014). In the latter study it was shown that the active small GTPase, CDC42, in adjacent germ tube tips approaching each other became correspondingly repositioned in each of these tips away from each other and that this repositioning occurred before a repulsive growth response was observed. Previously, CDC42 had been shown to involved in polarity establishment and polarity regulation in hyphae of *N. crassa* (Lichius *et al.,* 2014). These results indicate that the morphology of the initial microcolony is very much influenced by self-avoidance.

Table 3.1 Distances separating pairs of hyphae when autotropic responses were first observed. Each result is a mean of 10-24 observations along with its standard deviation. Distances displayed may not necessarily represent the time when the self-avoidance response is initiated in the observed fungal species (reproduced from Trinci et al., 1979).

	Mean distance between pairs of hyphae when autotropic responses were observed (µm)	Minimum and maximum distances between pairs of hyphae when autotropic responses were first observed (µm)	
		Minimum	Maximum
Neurospora crassa	30±11	15	51
Aspergillus nidulans	27±16	4	68
Mucor hiemalis	24±10	11	46

One potential problem with studying self-avoidance in probably the majority of ascomycete species, including *N. crassa*, is that germ tubes and mature hyphae undergo vegetative cell fusion involving positive chemotropisms (section 1.3.4.1), which could potentially complicate the analysis of self-avoidance. However, there have been no published reports of cell fusion during the early and late stages of colony development in *A. fumigatus*. This property, along with its medical importance as a pathogen, makes *A. fumigatus* an ideal experimental system in which to analyse the mechanistic basis of self-avoidance in a filamentous fungus.

For potential mechanisms involved in self-avoidance, some insight can be extracted from the research on neuron self-avoidance (section 1.3.6.1). Two main mechanisms are prevalent in neurons: a) communication through extracellular signal secretion or b) touch-sensing during establishment of neuron cell synapses. These two mechanisms are necessary to secure two important processes: cell self-sensing and recognition. In nature, cell self-sensing is highly important as it ensures the cells recognise one another and avoid non-optimal interactions.

In fungal biology, self-recognition has been studied extensively and involves vegetative compatibility groups (VCGs) which have been described in numerous hyphomycetes and basidiomycetes (Glass and Kuldau, 1992; Leslie, 1993). Incompatibility between two strains is dependent on allelic and nonallelic genetic systems and regulates whether strains from the same species can fuse to form heterokaryons (hyphae with genetically different nuclei). The *het* locus first described in *N. crassa* (Mylyk, 1976) is crucial for these interactions. Incompatibility is triggered when two strains with different alleles in one or more *het* loci fuse. Whereas allelic incompatibility does not affect sexual function, nonallelic interactions (genetic differences in two separate loci) result in incompatability. Strains from the same species are distributed into different groups according to their compatibility; species in the same VCG are compatible with each another. Incompatible strains typically produce a barrage reaction where the two colonies meet; hyphae in that zone are degenerated or dying, hence growth is stalled. Genes related to self-recognition and incompatibility have been identified through comparative genomic hybridisation and *in silico* analysis in *Aspergilli* (Fedorova et al., 2009, 2005; Pál et al., 2007). Heterokaryon incompatibility can be considered a self-avoidance response which ensures the successful mating and reproduction in filamentous fungi.

3.1.1 Aims of the research described in this chapter

These were to:

(1) Assess the presence of self-avoidance in *A. fumigatus* at different developmental stages (germination, germ tube growth, mature hyphal growth, and the approach towards each other of two colonies).

(2) Elucidate whether spore-spore contact is a determining factor in defining the initial germination site from a spore, and whether self-avoidance is exclusively dependent upon the latter.

(3) Determine whether germ tubes avoid inert objects.

(4) Determine whether self-avoidance responses require the interaction between living and metabolising cells.

(5) Develop and apply a novel approach to quantify self-avoidance during early growth of *A. fumigatus* post-germination. This included an analysis of substrate invasion by young fungal hyphae.

(6) Image avoidance responses in the barrier zone between two approaching colonies.

3.2 Results

3.2.1 Self-avoidance occurs early during germination

As discussed in the introduction of this chapter, filamentous fungi grow in a uniform, radial manner. This general observation applies to the fungal colony at both the macroscopic and microscopic levels. To produce this growth pattern, two hypotheses can be proposed:

(1) *Hypothesis 1: Self-avoidance is a touch-mediated process.* The growth pattern and distribution of germ tubes in a microcolony, formed from a group of ungerminated spores in contact with each other, is a direct result of a touch-sensing mechanism. With this mechanism the initial site of germ protrusion is formed away from the touching surfaces of spores and then germ tubes grow outwards post-germination uninfluenced by adjacent cells. An extension of this hypothesis is that the growth direction of germ tubes is influenced by a further touch-sensing mechanism which would predict that the pattern of subsequent growth should be unable to discriminate between suitably sized objects that are living or inert.

(2) *Hypothesis 2: Self-avoidance is influenced partly by sites of germination and subsequent non-touch mediated interaction between adjacent germ tubes.* The pattern of germ tube self-

avoidance during early colony formation are primarily achieved by a combination of their sites of germ tube emergence and signalling between adjacent germ tubes in the absence of a touch-sensing mechanism.

To test whether the microcolony formation is a dynamic process taking effect after germination or it is only defined by a touch-sensing mechanism occurring before germination, spores were examined in CLSM time-course experiments at 6 hours post-inoculation (hpi) in AMM. During the latter germination stages, which usually take place between 6-7 hpi in AMM, or 8-9 hpi in AMMA, the germ tubes grew from the original cell protrusion sites on the spore. Figure 3.2 provides evidence that the spacing occurring between germ tubes in a group of spores is the result of self-avoidance and can be quantified. It is evident that the germ tubes rearrange their growth axis depending on whether their initial protrusion site is ideally placed away from neighbouring cells. This observation provides evidence that the form of a fungal microcolony is a result of micro-adjustments in polarity during germ tube extension.
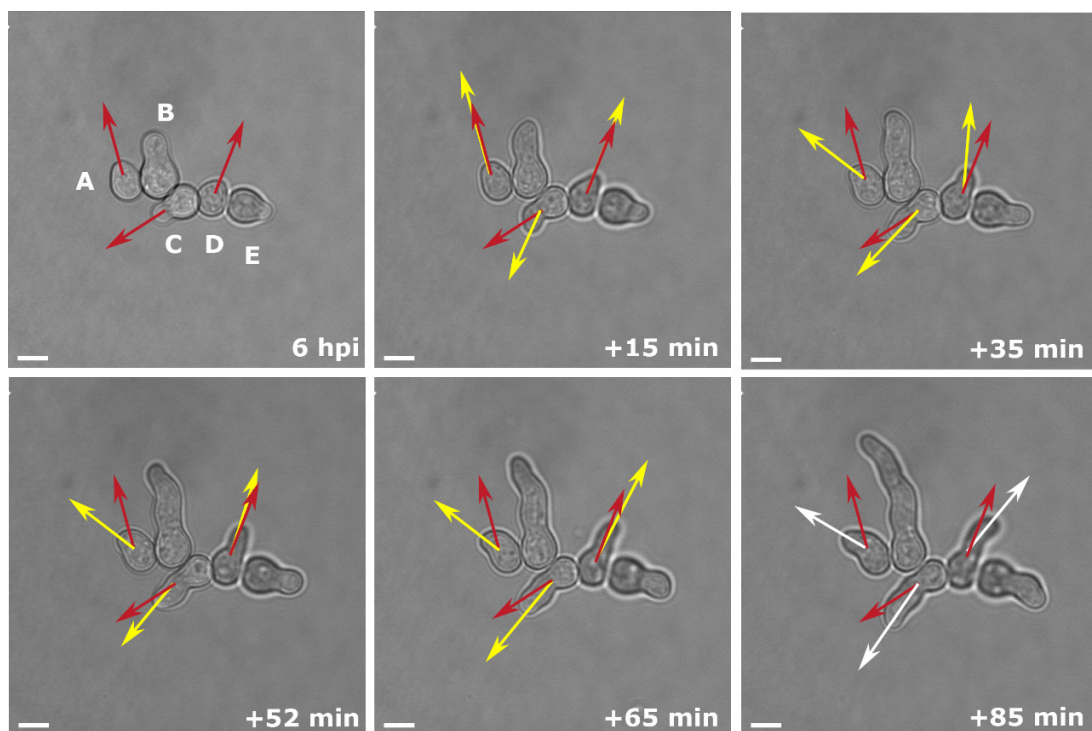
Figure 3.2 Self-avoidance during the latter stages of conidial germination. CLSM images of conidia grown in liquid Vogel's media (VM). Spores are defined as A-E in the group. Red arrows mark the central tip point of the original germ tube protrusion. Yellow arrows mark the subsequent tip central growth axis (as described in Lichius *et al.*, 2014). It is evident that the main tip growth axis is constantly being rearranged depending on its relative position to adjacent cells. White arrows show the final growth axis from the time lapse images germ tubes compared to the projected growth (marked during the protrusion) if no self-avoidance occurred. The angle of reorientation (angle between red-white vectors) was estimated to be 39.9°±7.3° (n = 20 measurements). Scale bar = 5 μm.

These micro-adjustments can be considered a result of negative autotropisms which take place post-germination. The mean minimum distance of sensing adjacent cells is 5 µm (n=20 measurements). These results, however, do not preclude the possibility that a touch-sensing mechanism does not have some role in determining the early stages of directional growth by germ tubes emerging from a group of aggregated spores.

3.2.2 Contact is a determining factor for the initial germination site

To further test hypothesis 1 of whether contact between adjacent cells determines the site of germination establishment thus determining the future pattern of outward growth, freshly harvested spores were mixed with inert red fluorescent microbeads (exc./em. = 660/690, Bangs Laboratories, Inc) at a 1:1 ratio and germinated overnight. Samples were imaged with CLSM using the inverted agar method (section 2.5.1). Angles were measured for single microbead-germling pairs that lacked any surrounding cells/beads (n=17). The angle measured was that of the line connecting the centre of the microbead, the centre of the original spore (germling head) and the germ tube. If hypothesis 1 is correct then the angle formed between the germ tube and the centre of the microbead should ideally be within the 270º of the non-touch zone, as the germination site would be as far away as possible from the microbead as an avoidance response due to contact.

The results actually showed that the germination site of conidia was influenced by whether they touched neighbouring inanimate objects, such as microbeads. Figure 3.3 provides a representative example of one these experiments. While germlings are in contact with the fluorescent microbeads the germ tube does not avert its growth axis (Fig. 3.3A). This is partly consistent with the results shown in Fig 3.2, in which both the germination site and subsequent angle between emerging germ tubes was dependent on the location of touching adjacent spores. In 87.5% of the cases (35/40 pairs measured) the germ tube did not redirect its growth until it came in touch with the microbead, in which case it either subtly redirected it growth or grew tangentially to the sphere surface. Furthermore, in Fig. 3.3B-C avoidance of the sites of germination between adjacent spores can be observed even though there was no contact.

These results reveal that the angles formed between the germ tubes and the microbeads is significantly lower than that theoretically ideally predicted in our hypothesis (~180º).

Although there are rare occasions in which the angle can reach up to 150 degrees, this falls into the extreme end of the Gaussian distribution ($+3\sigma$). The statistical analysis suggests that there is 95% probability that the mean angle is in the range of ~71°-98°. Since the substratum (AMMA) on which the spores are germinating is a homogenous
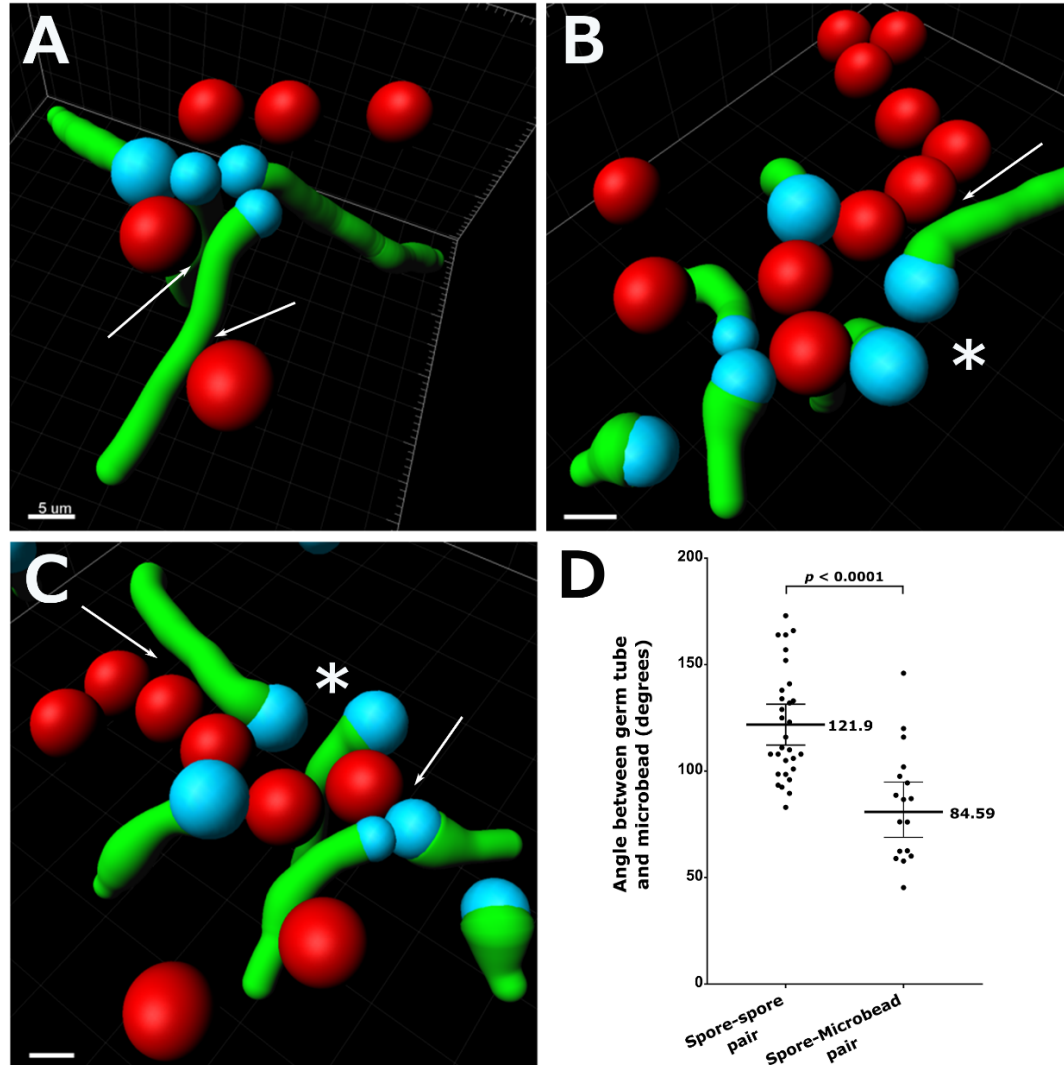
Figure 3.3 Segmented confocal images showing that the sites of germination were influenced by inanimate objects such as fluorescent microbeads (arrows in **A-C**), but the direction of germ tube growth was not. Neighbouring germlings continued to affect the sites of germination and self-avoidance is evident as shown in **(A)**. In **(B)** and **(C)** the same dataset is displayed from different 3D perspectives. The asterisk shows two germlings where self-avoidance at the germination site was observed even though it was not induced by contact. Furthermore, the growing germ tube seemed to be insensitive to the neighbouring microbeads (arrows) until contact, when it bounces off and away from them. The graph **(D)** summarises the quantification of the angles formed between the germ tube and the line connecting the centres of microbead-spore head. The scatter plot displays the mean value of 84.59° (n=17), which is significantly lower than the mean angle (121.9°) formed between a spore-spore pair quantified in the same way (n=30). Error bars display the upper and lower 95% confidence intervals (CI) of the mean. The p-value was calculated by a Student's unpaired t-test. Scale bar = 5 μm

mixture of culture medium components, we can reject that there is any kind of external stimulus providing a gradient which would affect the polarity of germination other than the contact with adjacent microbeads. Thus, since the estimated mean angle formed between the germ tube and the microbead is significantly lower (84°.6) than the angle formed between a germling and an adjacent spore head (122°.0, Fig. 3.3D), contact does not exclusively affect the initial protrusion site location during germination.

In summary, results presented in this section are consistent with contact between a spore and an inanimate object mimicking a spore (a polystyrene microbead) being able to influence the sites of germ tube emergence from the spore although the sites of germination were not dependent on a touch-mediated mechanism. Furthermore, little or no avoidance response of a germ tube growing in close proximity to an inanimate microbead was observed. These results combined would suggest that the interaction between living cells plays a primary role in causing the self-avoidance to occur, hence I proceeded to test this hypothesis.

3.2.3 Self-avoidance requires interaction between living cells

The next question addressed was whether the interacting cells both required to be living. For this purpose, an experiment was conducted with a mixed population of living and dead *A. fumigatus* conidia. Conidia of *A. fumigatus* CEA17 expressing cytosolic GFP were killed by first allowing them to germinate in AMM at 37 °C (8-10 hours) and killing by incubating them for 20 min at 80 °C. They were subsequently mixed in a 1:1 ratio with living spores of the same strain, to a final combined concentration of 3×10^5 spores/ml. Propidium iodide (PI) was added to the spore suspension (final concentration 5 µM) to serve as a marker for dead cells (the damaged plasma membranes of dead cells are permeable to the dye and stain red, whereas living cells remain unstained). Cell germination was imaged over a ten-hour time-course with CLSM at 37 °C (Fig. 3.4 and 3.5).

Figure 3.4 shows that the initial site of protrusion is not influenced by contact between a living spore and a dead spore. Furthermore, the germ tube did not avert its axis away from the dead cells post-germination but ran along their surfaces instead. Figure 3.5 provides another example of live cells being unaware of the dead hyphae, as they germinate towards the dead cells and do not avert their germ tubes until contact or at
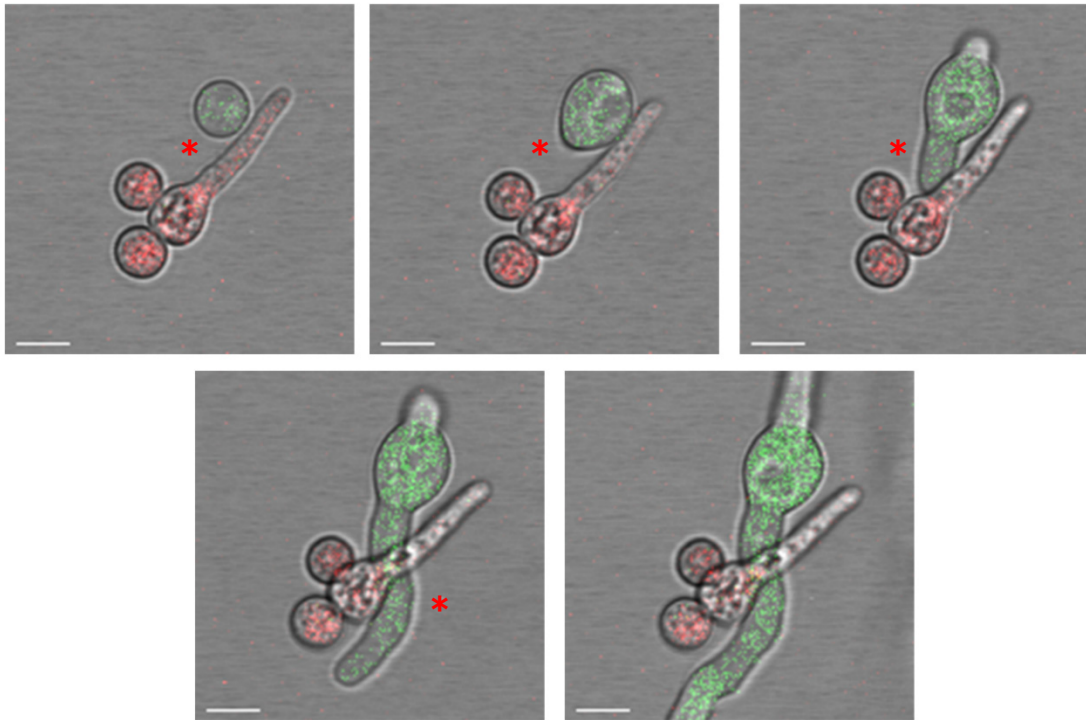
Figure 3.4 Lack of self-avoidance between a living germling (expressing GFP in the cytosol) and 3 heat-killed cells (propidium iodide staining, red) during germination of the former. The living germling was not influenced by the positions of the adjacent dead cells and did not avoid them; instead its germ tube (asterisk) grew along the surface of the dead cells, unaffected by their presence. Scale bar = 5 μm

all. The hypothesis that cell-cell communication is necessary is supported since no negative autotropisms were displayed by living cells in close proximity to either dead spores or dead germlings. However, the alternative hypothesis that contact is crucial for self-avoidance cannot be either validated or rejected due to the nature of the experiment. More specifically, heat-treated cells would most likely have their membrane proteins denaturated to the point where they would not be functional, thus no interaction would be possible in the first place.

To provide convincing evidence that two interacting living cells are required for self-avoidance responses, a second experiment was performed. This involved using spores of the CEA17 strain which are auxotrophic for uracil and uridine (Table 2.1). When incubated in AMM without uracil and uridine these remain in a non-metabolising dormant state. They were mixed in a 1:1 ratio with WT spores (final combined concentration: 3×10^5 spores) and incubated in AMM without any supplements and imaged over a ten-hour time-course with CLSM at 37 °C (Fig. 3.6).
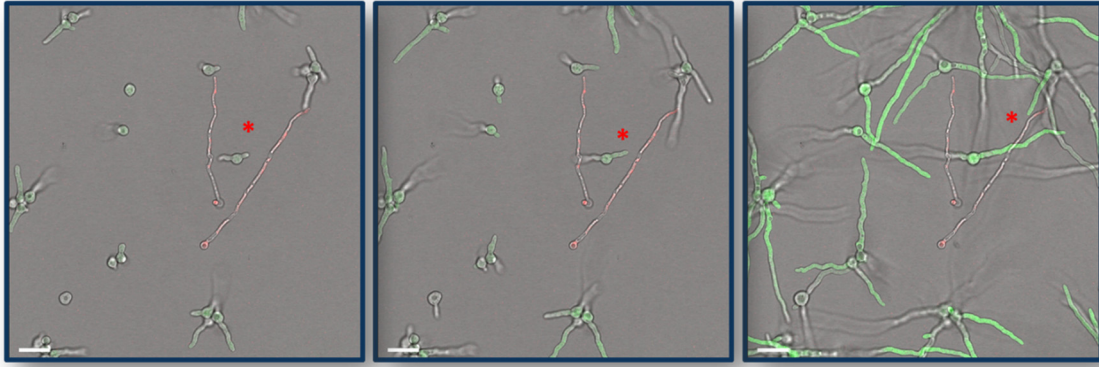
Figure 3.5 Lack of self-avoidance between living cells (expressing GFP in the cytosol) and heat-killed, grown germlings (propidium iodide staining, red). The living cells are unaffected by previously grown hyphae; its germ tubes grow towards the dead hyphae and do not change their course (asterisks). Interactions between cells were measured to test whether the observation is significant. Analysis showed that 18 out of 20 approaching events (90%) between living and dead hyphae, a crossover took place (no self-avoidance). This is compared to 6/20 between living hyphae (30%). Scale bar = 10 μm
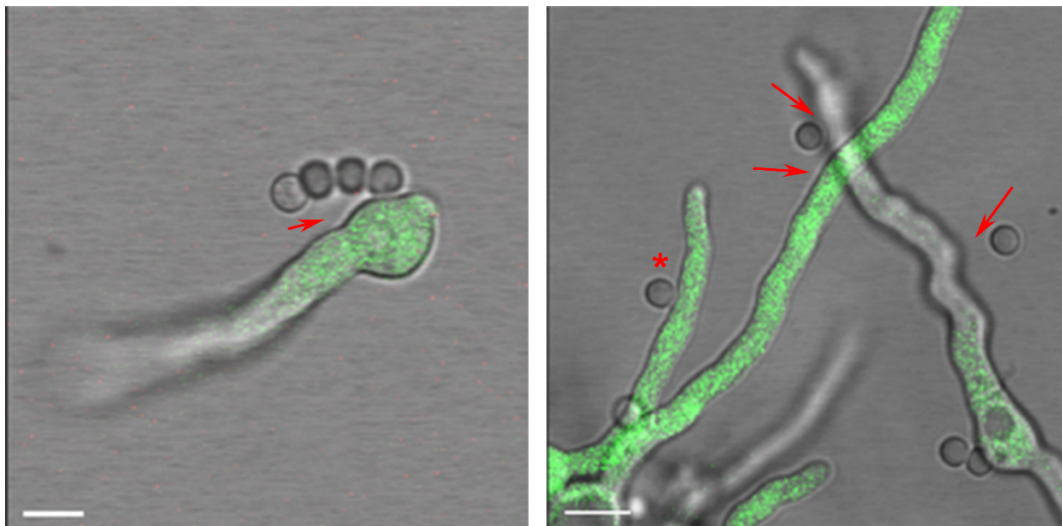
Figure 3.6 Negative tropisms between cells require that they are both living. Living WT conidia mixed with conidia of the *pyrG1* auxotroph in AMM without uracil/uridine. Only the prototrophic conidia have undergone isotropic growth and germinated. Their germ tubes avoid (arrows) the auxotrophic conidia which are dormant and non-metabolising, although there are cases where they ignore them (asterisk). Scale bar = 5 μm

The auxotrophic CEA17 conidia were unable to undergo isotropic growth and germinate in AMM without uracil and uridine. However, they were not dead, just non-metabolising and in a dormant state. The WT germ tubes exhibited avoidance of dormant spores (Fig. 3.6) indicating that both interacting cells required to be living. Due to the lack of swelling the hydrophobin outer layer of the cell is intact (Dague *et al.*, 2008) thus any interaction between live and dormant cells would be a result of a response to an external signal or plain simple contact without the involvement of

surface receptors. This result would suggest that although CEA17 spores are not able to germinate, they can produce a faint but sufficient signal for wild type-like cells to register as an avoidance cue. Taken together, these results provide evidence that self-avoidance involves the communication of at least two living cells.

3.2.4 Development of a quantification method to measure negative autotropisms

Sections 3.2.1 and 3.2.7 show that self-avoidance can occur in different developmental stages of *A. fumigatus* by influencing the site of germ tube emergence from conidia and the growth of germ tubes. The negative autotropisms of germ tubes occurred after 6-12 hours after inoculation. To analyse this latter process, a quantification method was developed using the Imaris 4D image analysis software (Bitplane) for segmentation and measurements using *A. fumigatus* germlings incubated on AMMA for 8-10 hours at 37 °C. The basic principle of the quantification method was to convert each hypha into a vector defined by two points: one point in the middle of the germling head and another up to 20 µm along the hypha's axis; the result being a line which passes through the centre of the hyphal tube. Figure 3.7 (B-D) provides an example of a fungal microcolony and describes the process of obtaining the resulting vectors attributed to each of the germlings. The angles between adjacent tubes were measured based on standard vector analysis (Gibbs and Wilson, 1901) as follows: in a three-dimensional Euclidean space, $\mathbb{R}^3$, a point A has three coordinates (x_A, y_A, z_A). A vector $\overrightarrow{AB}$ is the vector defined by points A (x_A, y_A, z_A) and B (x_B, y_B, z_B). Hence, the coordinates of vector $\overrightarrow{AB}$ can be defined as:

$$(1) \quad \overrightarrow{AB} = (x_B - x_A)\, \vec{\imath} + (x_B - x_A)\, \vec{\jmath} + (x_B - x_A)\, \vec{k} = AB_x\vec{\imath} + AB_y\vec{\jmath} + AB_z\vec{k},$$

Where $\vec{\imath}, \vec{\jmath}, \vec{k}$ are the unit vectors for the x, y, z axes respectively

The cosine of the angle θ between two vectors $\overrightarrow{AB}$ and $\overrightarrow{CD}$ can be calculated by their dot product equation, hence we can calculate the angle itself:

$$(2) \quad cos\theta = \frac{\overrightarrow{AB} \cdot \overrightarrow{CD}}{\|\overrightarrow{AB}\|\|\overrightarrow{CD}\|} = \frac{AB_x CD_x + AB_y CD_y + AB_z CD_z}{\sqrt{AB_x{}^2 + AB_y{}^2 + AB_z{}^2}\sqrt{CD_x{}^2 + CD_y{}^2 + CD_z{}^2}}$$

$$(3) \quad \theta_{(radians)} = \arccos\theta = \cos\theta^{-1}$$

$$(4) \quad \theta_{(degrees)} = \theta_{(radians)} \times 180°/\pi$$

The data coordinates for each point were analysed on and extracted from Imaris and were further processed on Microsoft Excel and GraphPad Prism 7 as detailed in section 2.8.
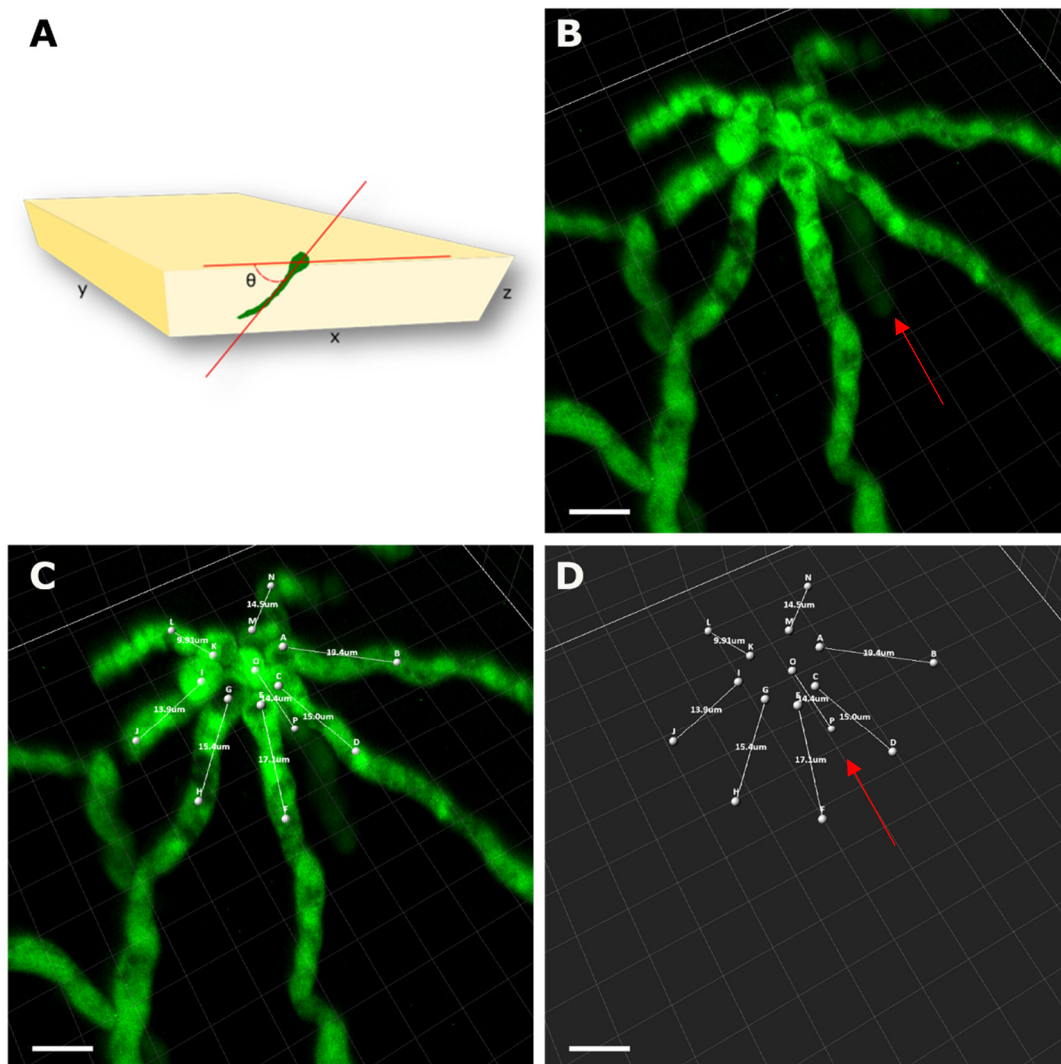
Figure 3.7 Process of quantification of germ tube emergence from conidia. The basic principle is to convert the fungal hypha into a vector which has specific coordinates that can be extracted digitally. The relative position of the germ tubes to one another and their position in the block of agar can then be determined **(A).** A group of eight germlings as can be visualised in Imaris. The arrow points at a germling which has grown into the agar block **(B)**. The same group of germlings with generated vectors running through the germ tubes along their axis of growth **(C).** Final image of the vectors if the digital volume is removed **(D).**

3.2.5 Angles formed between germ tubes can provide an estimate of avoidance in hyphal cells

For the quantitative analysis of self-avoidance responses during germination, germlings 8-10 hours post-inoculation, were grown on 1.5% w/v agar AMMA, imaged using the inverted agar method and the angles of a total of 400 pairs were measured using the approach presented in section 3.2.4. Pairs were distributed to groups based on the number of spores in the group they belonged to (from a pair of spores up to seven spores per group; Fig. 3.8). Angles were measured for both the raw 3D data and their 2D-projections in the XY plane, which were obtained by running the corresponding Matlab script provided by the Imaris XT module.

Fig. 3.9A demonstrates that there is a large variance in the angle of avoidance between
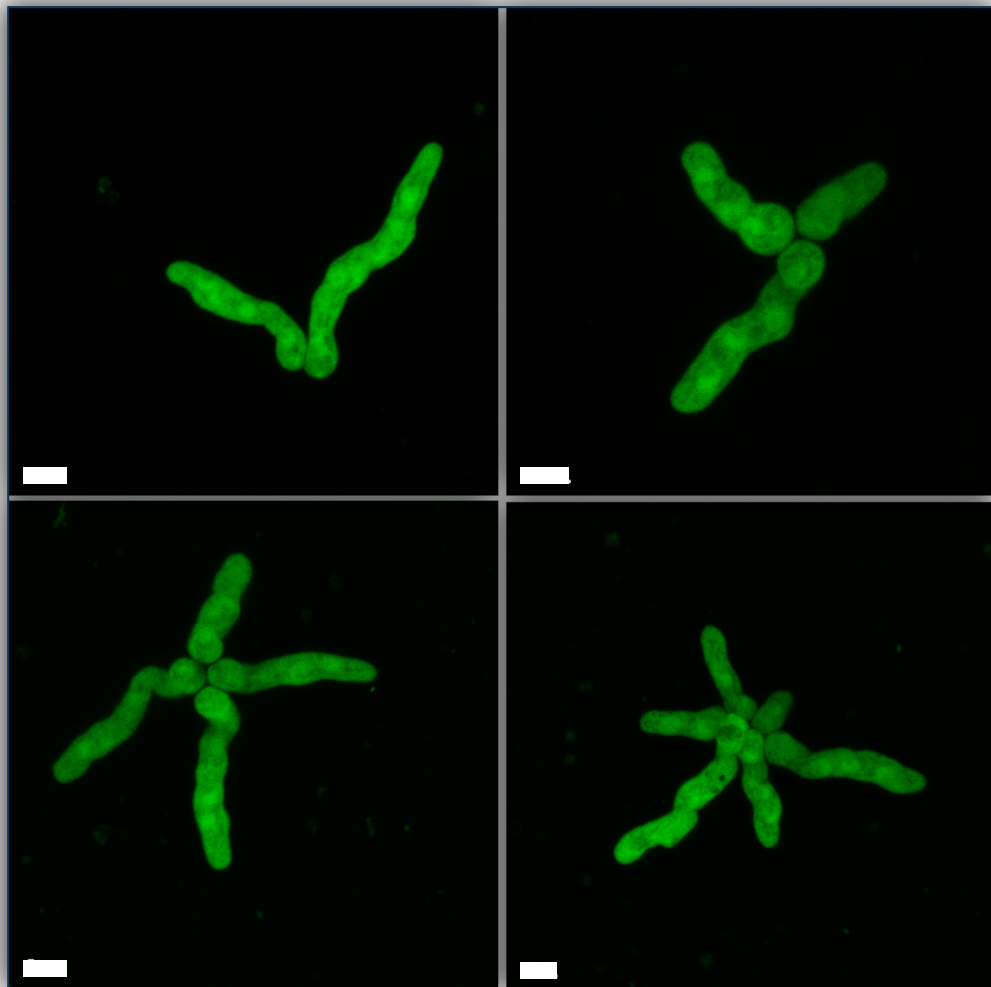
Figure 3.8 Germ tubes tend to be equally spaced from one another in a group of germlings. This phenotype can be attributed to negative cell autotropisms as it is shown in section 3.2.1. CLSM images of *pyrG::gfp* strain, 8 hpi at 37 ℃. Scale bar = 5 μm

germ tubes in fungal microconies. However, when adjusted to further predict the mean values of the corresponding measurements (Fig. 3.9B), it is evident that the mean size of the angles is inversely proportionate to the number of spores in each corresponding group; the more the spores are, the smaller the angles between them get. This is as expected as cells have less space to orientate their hyphae out of the original inoculation and germination area. With the exception of angles in a pair of germlings set, angles measured in the 2D projections are almost equal to the quotient of the division of 360° (full circle) to the number of cells in the group. This would correspond to the angles as the microcolony is observed from above.

Interestingly, in the 3D sets the angles were narrower than their corresponding 2D projections. What is particularly interesting is that the mean angles in the 3D sets are no wider than 80° (in groups consisting of three spores; Table 3.2); the maximum angle of avoidance during germination was no greater than 80° in the wild type. The largest mean angle could be observed in the group of three spores, possibly because the potential avoidance signal is coming and sensed from all directions by the cell, while the number of cells is still quite small to allow maximum spacing between them. Table 3.2 summarises the statistical data for all measurements.

The results of negative cell tropism quantification have raised the question of whether the resulting angles are an exclusive result of self-avoidance or if there are other tropisms involved in the growth of the fungal microcolony during germination.

Table 3.2 Summary of the mean values, their confidence interval (95%) range and standard deviation (SD) for the data presented in Figure 3.9.

Spores in group	2D projection		3D raw stacks	
	Mean angle (°)	SD	Mean angle (°)	SD
2	94.85 ± 9.02	42.85	70.18 ± 5.39	26.63
3	120.78 ± 6.78	33.82	75.95 ± 5.94	29.79
4	90.073 ± 7.83	36.12	69.26 ± 4.78	23.10
5	70.78 ± 6.59	26.50	55.52 ± 5.06	19.62
6	61.80 ± 8.49	20.10	50.09 ± 6.24	16.70
7	48.92 ± 15.3	26.64	38.42 ± 12.74	22.06
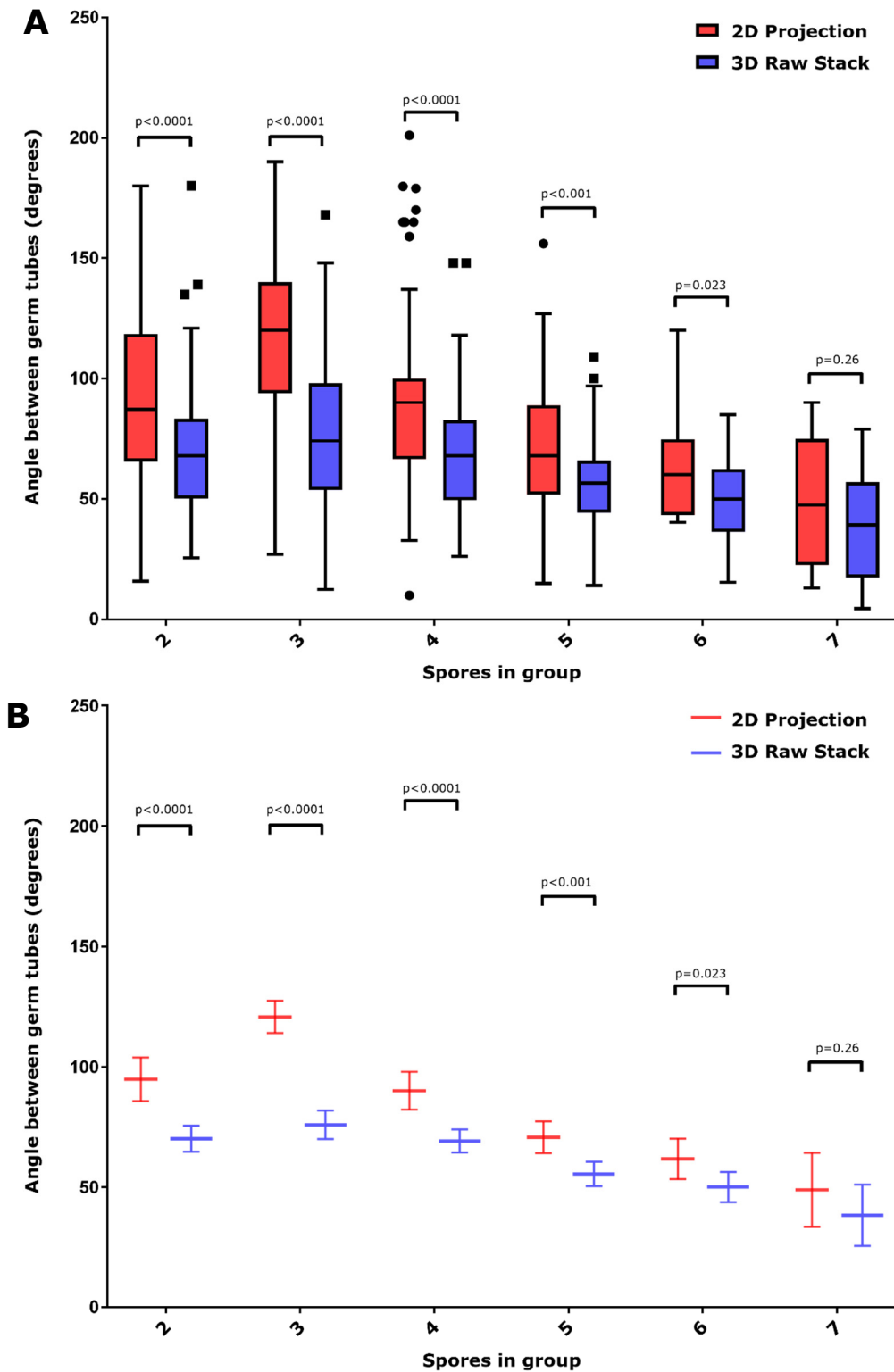
Figure 3.9 Angles of avoidance between germ tubes differ significantly between acquired 3D stacks and their 2D projections **(A).** These show that the z-coordinate is crucial when quantifying the phenomenon. Despite the significant variance in acquired values, the confidence intervals (95%) of the mean are well defined **(B).** Data values are summarised in Table 3.2

3.2.6 *A. fumigatus* has a propensity to invade its substrate

A. fumigatus germ tubes have a propensity to invade their substratum (Nick Read, and Geoff Robson, personal communications), a quality which may be directly involved with virulence. Initially it was thought this might be a response to gravity (i.e. a geotropic response). However, multiple experimental replicates revealed that *A. fumigatus* tends to invade its substratum (1.5% w/v agar) regardless of the direction of the gravity vector (data not shown). A second experiment was then designed to demonstrate whether substrate stiffness is a determining factor of fungal invasion. To this end conidia were inoculated onto AMM with different agar concentrations (0.7%,
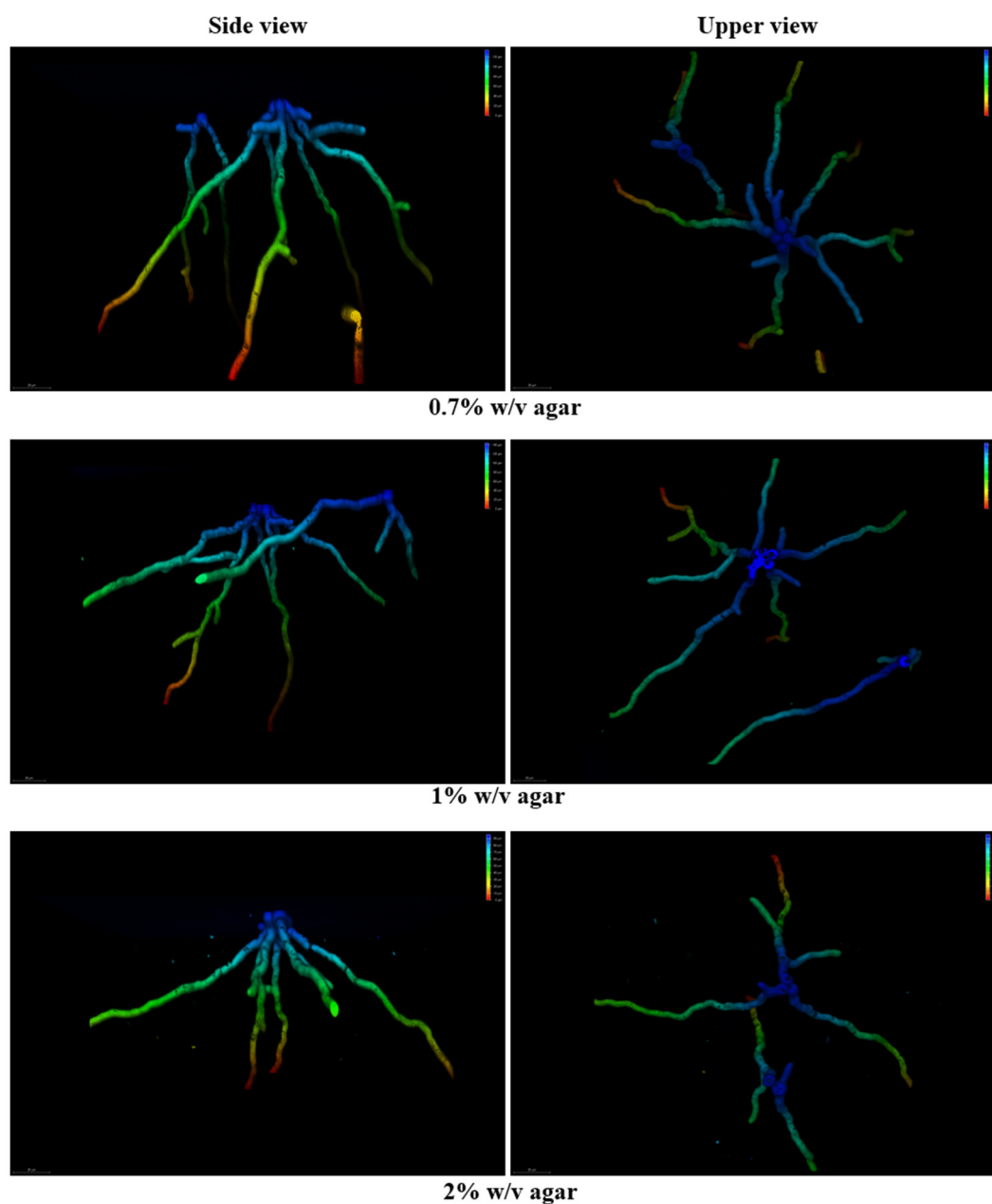
Figure 3.10 *Aspergillus fumigatus* has a propensity to invade its substratum. The stiffness is a factor which influences the fungus invasiveness.

1%, 2%, 3%, 4%, and 5% w/v); increasing concentrations of agar result in increased stiffness of the substratum. Germlings were observed with CLSM using the inversed agar method.

Figures 3.10 and 3.11 demonstrate that stiffness influences the ability of the fungus to invade its substrate. Up to and including 2% w/v agar concentrations, the fungus can penetrate the medium and grow inside it. Interestingly, the fungus was not able to
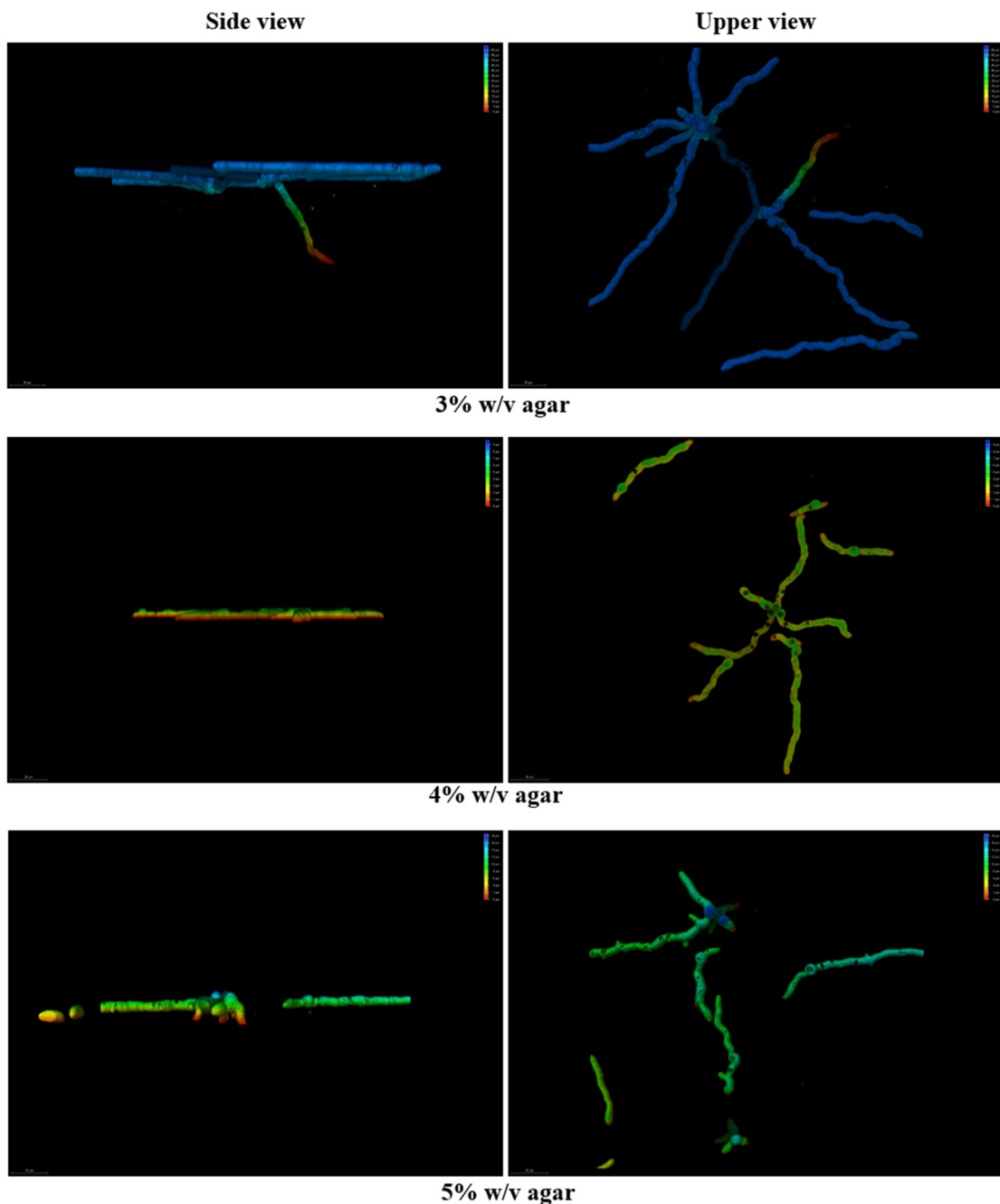
Figure 3.11 Higher agar concentrations prevented the fungus' ability to significantly invade the medium other than by forming very short protrusions into it. Pseudocolour scale runs from blue for germ tubes growing on the agar surface through to red which is the deepest depth reached into the agar.

penetrate substrates with agar concentrations equal to or greater than 3% (w/v) but grew on their surface. This indicates that although the fungus can assimilate nutrients from such substrates, it does not have the strength to breach the medium surface and grow into it. The angles of invasion were quantified according to the methodology presented in section 3.2.4 and the results are summarised in Figure 3.12. The mean angles of invasion ranged from 55° to 62° (Table 3.3). In stiffer substrates (3% w/v agar), a few germ tubes had a limited ability to penetrate the agar surface (Fig. 3.11), with the median value (disregarding those extreme cases) reaching as low as ~ 3° for 3% and 4% w/v agar. When the fungus was grown on 5% w/v agar, its ability to invade was completely prevented. To verify whether the inability to invade was due to mechanical restrictions, an experiment was conducted in which spores were 'sandwiched' between two types of AMMA media; 1% and 4% w/v agar. The setup used was inside an appropriate capillary tube, and the germling was imaged 12 hpi using Light Sheet Fluorescence Microscopy (LSFM). LSFM was used because it can image at depths of 100-500 μm into a tissue sample (Andilla et al., 2017). With the experimental capillary set up used here (section 2.5.5) imaging was made possible up to 1 mm into the sample. Spores grown at the interface of the two types of media exhibit ability of invasion towards the 1% w/v agar but no invasion at 4% w/v agar. Figure 3.13 details one such example, where the growing germ tube germinates in the 1% w/v agar but cannot penetrate the 4% w/v agar interface once it encounters it.

Table 3.3 Statistical values for Figure 3.12

Agar concentration	0.7% w/v	2% w/v	3% w/v	4% w/v	5% w/v
Mean	55.27± 3.36	61.98± 5.00	11.54± 10.28	10.64± 10.48	1.997± 0.76
Median	53.43	62.6	3.064	3.691	1.588
Std. Deviation	11.19	11.29	17.01	19.66	1.659
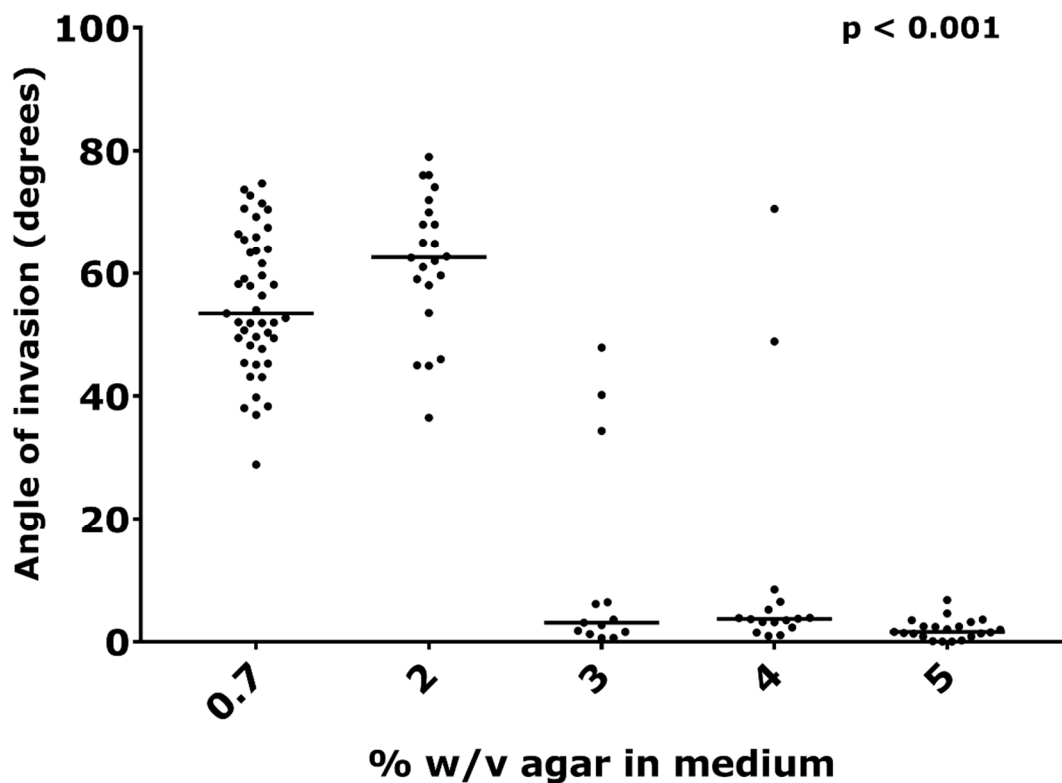
Figure 3.12 Angle of invasion of germ tubes in varying concentrations w/v of agar in media. Up to 2% w/v agar invasion was unhindered. Stiff substrates (3% w/v agar or more) had a severe impact on the fungus' ability to penetrate the substratum, with the angle of invasion being no more than 10 degrees. Measurements of at least 20 single germlings per condition. Bars represent the median value for each sample. The *p*-value was calculated by a one-way analysis of variance (ANOVA).
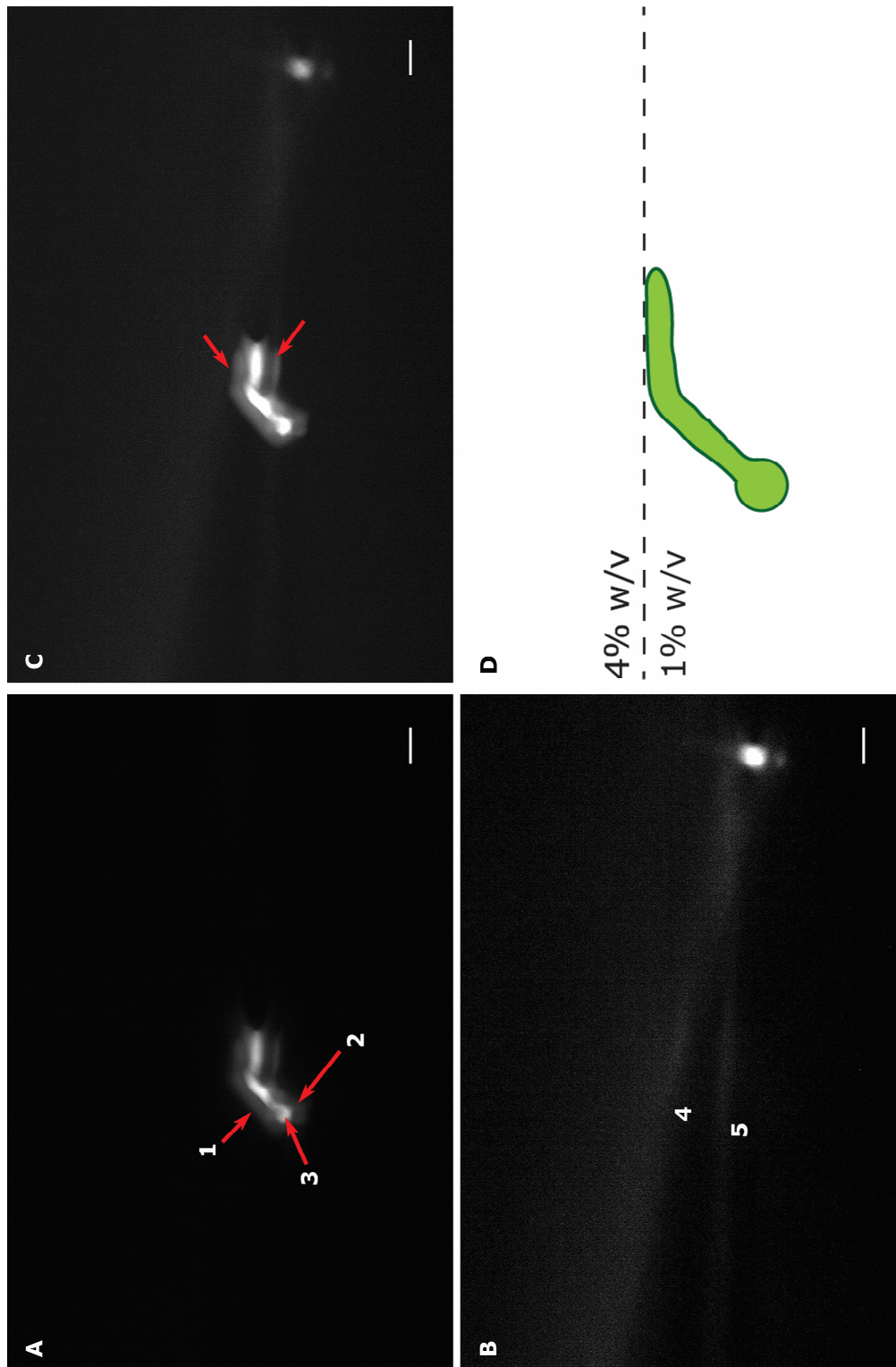
Figure 3.13 Germ tubes have limited ability to invade stiff surfaces. LSFM images showing germlings growing approx. 1 mm deep inside solid AMM at the interface of agarose at 1 and 4% concentrations. Arrows 1 and 2 point at the shadow around the germling which is produced by light-sheet during image acquisition when it meets the germling (arrow 3, **A**). In **(B)** the light sheet diffraction effect allows the visualisation of the interface where the 1% and 4% w/v agarose media meet in the capillary. Merge of the two images (A) and (B) to produce **(C)** shows that the spore germinates and grows normally in 1% w/v agar but redirects its axis along the interface when it meets the stiffer surface, because it cannot successfully penetrate it. **(D)** Graphic representation summarising the concept of A-C.

3.2.7 Self-avoidance during colony approach

A characteristic of slow growing colonies approaching each other is the formation of a barrier zone (Porter, 1924; Skidmore and Dickinson, 1976). The characteristics of the zone is a lagging growth of the leading hyphae of the colony; the mechanisms responsible for this phenomenon are poorly understood. To analyse whether the 'barrier effect' of two colonies of *A. fumigatus* is a result of negative tropism interactions between the hyphae of the neighbouring fungal colonies, the following experiment was
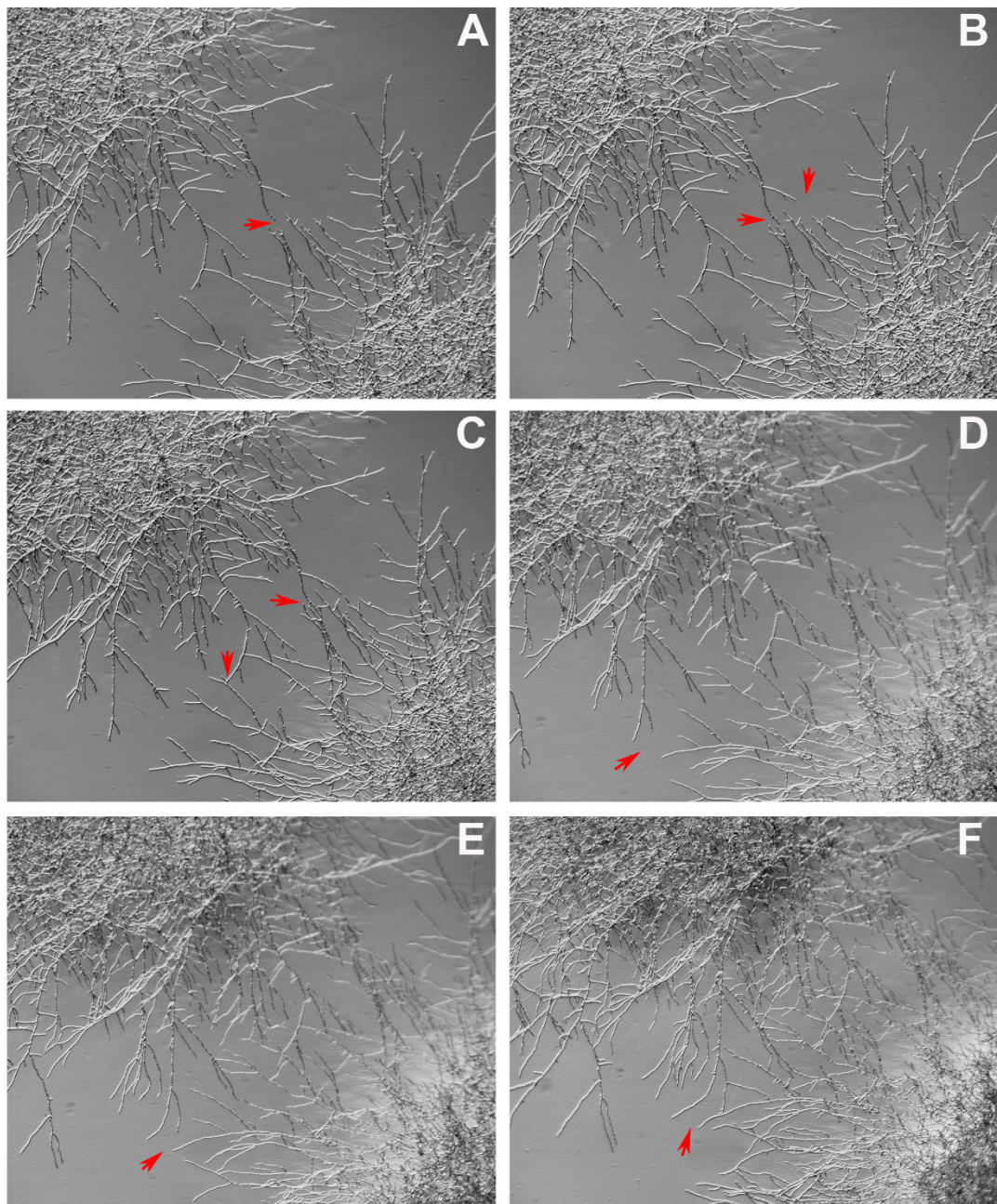
Figure 3.14 Self-avoidance during two colonies approaching each other. Hyphae approaching horizontally or vertically are insensitive to one another, indicated by arrows in A-C. Hyphae at the edge of the colonies (arrows) display negative tropisms from a long distance (~ 1 mm), and adjust their growth to avoid each other (D-F).

performed.

Two drops of 2 µl AMM containing 10^3 spores were inoculated 2 cm apart on a Petri dish containing AMMA. Cells were incubated for 24 hours at 37 °C and imaged at room temperature using stereomicroscopy. Figure 3.14 shows a five-hour time-lapse demonstrating the hyphal interactions between the two colonies at the centre and the edge of the barrier zone. Hyphae which are growing directly towards each other at the centre are 'self-avoidance insensitive', i.e. they do not change the course of their growth, but touch and climb over one another instead. Hyphae at the sides of the barrier zone exhibit avoidance, probably due to the less steep angle of approach, as it can be seen from Fig 3.14 (D-F).

3.3 Discussion

Negative autotropisms in fungi have been observed since the turn of the 19th to the 20th century (Clark, 1902; Fulton, 1906; Miyoshi, 1894). Although the phenomenon is ubiquitous in all filamentous fungi, and fungi producing pseudohyphae or shmoos (Jin et al., 2011), only few advancements have been made in quantifying the phenomenon (Trinci et al., 1979) and understanding its mechanistic basis. The overall aim of the research described this chapter was to describe the range of negative autotropisms in *A. fumigatus* and develop quantitative image analysis methods to facilitate the experimental determination of their mechanistic basis.

3.3.1 Negative autotropisms during germination require cell-cell interactions between living cells

A common characteristic in filamentous fungi is the unidirectional, radial pattern of their mycelial growth which has been attributed to the apical extension of leading hyphae, resulting in the circular morphology of the colonies (Trinci, 1971). I first tested the hypothesis whether this characteristic is a result of apical growth extension of the first protrusion site from germinating conidia or the germ tubes readjusting their growth in relation to neighbouring cells.

In *N. crassa*, the tip-to-tip homing followed by avoidance occurs after the re-localisation of active small-GTPases (imaged by a fluorescent CRIB-reporter) at the hyphal tip Polarity is also established when the uniform localisation of small-GTPases below the

cell membrane changes to a more concentrated region of the cell (Lichius et al., 2014). Time-lapse experiments monitoring germination (Fig. 3.1) provide evidence that rearrangement of the growth axis occurs very early post-germination in *A. fumigatus*. Any germ tubes which are at a critically close distance from neighbouring cells subtly rearrange their growth to grow as far as possible, i.e. they avoid cells of the same type. Thus, the unidirectional, radial growth pattern is not a direct result of hyphal extension from the initial polarity establishment event when the germ tube emerges from a spore. Negative autotropisms (self-avoidance) between cells contribute to the adjustment and correction of the hyphal growth direction even at the early developmental stages post-germination.

I also tested the hypothesis of whether the initial germ tube protrusion site produced at the end of the isotropic growth stage of conidia prior to germination is a self-avoidance response initiated by touch (i.e. contact with adjacent conidia). The results from the quantitative experiments performed on spore germination in the presence of microbeads (section 3.2.2) showed that germ tubes were able to sense inanimate objects in terms of autotropic responses. When a germ tube came in touch with a fluorescent microbead it either grew tangentially without any visible redirection or slightly readjusted its growth direction. Investigation of the phenomenon in *C. albicans* has revealed that hyphae of the fungus follow the contour of hard surfaces with its Spitzenkörper (Spk) located asymmetrically towards the underlying surface it is in contact with (Thomson et al., 2015). My results indicated that touch-responses can contribute to the initial polarity site during spore germination or the precise direction of a germ tube that comes into contact with another spore/germ tube sized object. However, the negative self-avoidance autotropisms in *A. fumigatus* are not dependent on contact-mediated responses and primarily involve cell-cell communication which is not dependent on touch-sensing.

To analyse the nature of the cell-cell communication involved in the self-avoidance experiments further, I performed the following two experiments. The first involved mixing living wild type spores with heat-killed, dead wild type spores. The second involved mixing living wild type spores with those of an auxotroph grown on AMM in the absence of the supplements uridine and uracil with which it requires to germinate and grow normally. Under these conditions the auxotrophic spores were living but remained dormant, and were unable to undergo isotropic growth prior to germination,

because they are unable to metabolise. The outcome of these experiments was that wild type germ tubes did not respond to the dead cells (spores or germ tubes) but did avoid the autotrophic cells (dormant spores). It was thus concluded that the interacting cells needed to be living for self-avoidance responses to occur. Lack of swelling would also indicate that the hydrophobin layer of the spore has not been broken (Aimanianda et al., 2009; Dague et al., 2008; Wösten, 2001). The hydrophobin layer reduces the surface tension of the medium in which the fungal spores germinate and grow, while maintaining permeability to gaseous exchange of molecules smaller than 200 Da (Wang et al., 2005). These findings would indicate that any communication between the prototrophic and auxotrophic cells is mediated through a small, gaseous signal. This hypothesis is tested in Chapter 4.

3.3.2 Germ tubes invade their substratum by an unknown mechanism

To further understand negative autotropisms during the germination of *A. fumigatus*, a novel quantification method was developed. This enabled, in a reproducible manner, the measurement of angles formed between germ tubes derived from adjacent spores in 3D space and in 2D projections of the corresponding CLSM-acquired datasets. My results showed that there were significant differences between the 3D stacks and the 2D projections of the same dataset revealing that the z-coordinate is a crucial factor which needs to be considered when quantifying self-avoidance responses. This observation verifies that germlings have a propensity to invade the substratum (i.e. they do not only grow on top of the agar surface). The angle of germ tube avoidance was never greater than 75.95° ± 5.94°, in the case of 3 spores, while pairs of germ tubes had a slightly narrower mean angle (70.18° ± 5.39°). A possible explanation for this result would be that whatever signal induces self-avoidance, it is potent only to certain degree. Thus, the germ tubes cannot avert their growth any more than the region over which signal has its effect. Another influencing factor to take into consideration when interpreting adjacent germ tubes avoiding each other is that their site of emergence from the spore will influence the initial direction of germ tube growth before this is overcome by self-avoidance signalling between the germ tubes themselves.

However, what seems to be the most important factor influencing these measurements is the fungus' propensity to invade its substratum, almost immediately post-germination. An initial experiment revealed that *A. fumigatus* tends to invade its

substratum (1.5% w/v agar) regardless of gravity. Subsequent experiments assessed the influence of the hardness/stiffness of the agar substratum on this invasive capability. When grown on up 2% w/v agar, *A. fumigatus* retained its ability to invade its substratum, with a significant restriction occurring at 3% w/v agar onwards. Light-sheet fluorescence microscopy experiments showed that the fungus has a preference of growing in soft media composed of agarose and nutrients and will grow along the interface with a stiffer surface, a finding which has already been reported in *C. albicans* (Thomson et al., 2015). Interestingly, the hyphal form of the dimorphic fungus *Schizosaccharomyces japonicus* can penetrate much stiffer substrata consisting of 5% w/v agar (Sophie Martin, personal communication).

Previous studies have assessed the reduced modulus (E_r) as a measure of agar stiffness using depth-sensing nanoindentation (Nayar et al., 2012) and have found that 0.5% w/v agar has an E_r of 30 kPa while 5% w/v agar has an estimated reduced modulus of 650 kPa. These results are well below or within the turgor pressure range (400-800 kPa) reported in filamentous fungi (Howard and Valent, 1996; Lew, 2005). To put this into the context of possible penetration of mammalian cells by fungal hypha, the 0.5% w/v agar stiffness is greater than the stiffness encountered in endothelial cells (Mathur et al., 2001, 2000). Tip-pressure experiments in *A. nidulans* revealed that a pressure gradient of 60 MPa/m is needed to stall tip growth (González-Bermúdez et al., 2017). Such local gradients are hardly encountered in the human body. These facts, coupled with the general propensity for germ tubes to invade the substratum they are growing on, may provide significant insights into the ability of fungi to invade mammalian host tissue.

It is not clear what the mechanism by which germ tubes exhibit penetration into agar substrata of 2% (w/v) or lower. Possibilities include that it is:

(1) a negative tropism to a gaseous signal which forms a gradient with its highest concentration on the agar surface and then decreasing with increasing depth from the surface because of its reduced diffusion through the agar medium. In this respect it could be the same volatile self-avoidance signal that is involved in germ tube avoidance.

(2) a positive thigmotropic response to a substratum with this range of stiffness. This needs to be tested with different types of media of same stiffness (i.e. different hardening polymers besides agar/agarose). More appropriately atomic force

microscopy could be used to verify the stiffness of such media, before experimentation.

(3) an 'agar-philic' tropism due to the specific hydrophilic chemistry coating the germ tube surface which prefers to grow in a hydrophilic agar environment than at the agar-air interface. It should be taken into consideration that *Aspergillus* nidulans has been shown to use agar as a carbon source (Payton et al., 1976; Payton and Roberts, 1979), so this agar-philic tropism may be in fact be a tropism towards a rich carbon source, which is inverted at higher agar concentrations due to a change of physiochemical properties of the substrate (hydrophobicity, xerophilicity etc.).

If mechanisms (2) or (3) are operating, then competition with self-avoidance signals will be influencing the angles in 3D down into the agar substratum that the germ tubes would be growing in.

3.3.3 Self-avoidance is observed between different colonies of the same species

Approaching colonies of *A. fumigatus* demonstrate a zone of growth 'inhibition' in the region they meet facing (data not shown). This barrier effect closely resembles the same phenomenon encountered in fungal species exhibiting heterokaryon incompatibility (Ishikawa et al., 2012) with the difference that the gap is ultimately closed and mycelia mesh in together. Using time-lapse live-cell imaging I observed the growth patterns of vegetative hyphae at the edge of approaching *A. fumigatus* colonies. My results showed that vegetative hyphae in the centre of the arc facing the neighbouring colony at a steep angle did not avert their growth axis but grew unhindered towards the opposite colony. This occurred even in regions where no mycelium was observable with naked eye. Interestingly, hyphae that approached one another at much broader angles seem to sense and respond better to their neighbouring leading hyphae of the confronting colony, by readjusting tip and thus growth direction. No hyphal degeneration was observed suggesting that no incompatibility self-recognition response took effect. Similar observations have been made with *N. crassa* during when leading hyphae of two colonies approached each other when they were grown on cellophane (Robson G., personal communication). Another study using *N. crassa* showed that perpendicular approach to a 2 μm microfabricated ridge resulted in no hyphal re-orientation in contrast to hyphae approaching at a 45° angle which did result in re-orientation along the path of least resistance next to the ridge (Stephenson et al., 2014). These

observations combined with my results would implicate that the angle of approach is crucial for tip-sensing and tip growth redirection as a negative autotropic response.

Although negative autotropisms between leading hyphae of two interacting colonies seem to play an important role in developing the barrier zone, another possibility which could result in fungal self-avoidance is sensing of nutrient gradients. As nutrients are depleted the closer they are to the hyphae a nutrient gradient is formed. This gradient is proportional to the distance from the hyphae (the further it is from cells, the higher the gradient). This would mean that fungal hyphae arrange their growth towards nutrients (positive chemotropism) away from other hyphae, which is perceived as self-avoidance. Thus, increased nutrient depletion in this region of interaction may also play a role in causing some inhibition or aversion of hyphal growth in this region. This mechanism would also contribute the variance in quantification of self-avoidance and the heterogeneity of responses.

3.4 Summary

The main findings of the research described in this chapter can be summarised as follows:

(1) Self-avoidance has been described and analysed at different developmental stages of *A. fumigatus*: conidial germination, germ tube growth, mature hyphal growth, and the approach towards each other of two colonies).

(2) Self-avoidance autotropisms during conidial germination, germ tube growth and the growth of mature vegetative hyphae and branches primarily involve cell-cell communication and the interaction between living cells.

(3) The self-avoidance responses in *A. fumigatus* are not dependent on touch-sensing although touch-responses can contribute to the initial polarity site during spore germination or the precise growth direction of a germ tube that comes into contact with another spore/germ tube sized object.

(4) A novel 3D image analysis approach to quantifying self-avoidance during the early stages of the growth of *A. fumigatus* following germination was developed.

(5) Germ tubes of *A. fumigatus* have a propensity to invade their agar by an unknown mechanism. This facility may be important during host tissue invasion.

(6) Self-avoidance responses of the leading hyphae of approaching hyphae from two colonies play a role in giving rise to a form of barrier zone in the region in which they interact but this does not involve a self-incompatibility response.

3.5 References

Aimanianda, V., Bayry, J., Bozza, S., Kniemeyer, O., Perruccio, K., Elluru, S.R., Clavaud, C., Paris, S., Brakhage, A.A., Kaveri, S. V, Romani, L., Latgé, J.-P., 2009. Surface hydrophobin prevents immune recognition of airborne fungal spores. Nature 460, 1117–21. https://doi.org/10.1038/nature08264

Andilla, J., Jorand, R., Olarte, O.E., Dufour, A.C., Cazales, M., Montagner, Y.L.E., Ceolato, R., Riviere, N., Olivo-Marin, J.C., Loza-Alvarez, P., Lorenzo, C., 2017. Imaging tissue-mimic with light sheet microscopy: A comparative guideline. Sci. Rep. 7, 1–14. https://doi.org/10.1038/srep44939

Clark, J.F., 1902. On the Toxic Properties of Some Copper Compounds with Special Reference to Bordeaux Mixture. Bot. Gaz. 33, 26–48.

Dague, E., Alsteens, D., Latgé, J.P., Dufrêne, Y.F., 2008. High-resolution cell surface dynamics of germinating *Aspergillus fumigatus* conidia. Biophys. J. 94, 656–660. https://doi.org/10.1529/biophysj.107.116491

Fedorova, N.D., Badger, J.H., Robson, G.D., Wortman, J.R., Nierman, W.C., 2005. Comparative analysis of programmed cell death pathways in filamentous fungi. BMC Genomics 6, 1–14. https://doi.org/10.1186/1471-2164-6-177

Fedorova, N.D., Harris, S., Chen, D., Denning, D.W., Yu, J., Cotty, P.J., Nierman, W.C., 2009. Using aCGH to study instraspecific genetic variability in two pathogenic molds, *Aspergillus fumigatus* and *Aspergillus*. Med. Mycol. 47. https://doi.org/10.1080/13693780802354029

Fulton, H.R., 1906. Chemotropism of Fungi. Bot. Gaz. 41, 81–108.

Gibbs, J.W., Wilson, E.B., 1901. Vector Analysis; a text-book for the use of students of mathematics and physics. C. Scribner's Sons, New York.

Glass, N.L., Kuldau, G.A., 1992. Mating Type and Vegetative Incompatibility in Filamentous Ascomycetes. Annu. Rev. Phytopathol. 30, 201–224. https://doi.org/10.1146/annurev.py.30.090192.001221

González-Bermúdez, B., Li, Q., Guinea, G. V., Peñalva, M.A., Plaza, G.R., 2017. Probing the effect of tip pressure on fungal growth: Application to *Aspergillus nidulans*. Phys. Rev. E 96, 1–9. https://doi.org/10.1103/PhysRevE.96.022402

Howard, R.J., Valent, B., 1996. BREAKING AND ENTERING: Host Penetration by the Fungal Rice Blast Pathogen *Magnaporthe grisea*. Annu. Rev. Microbiol. 50, 491–512. https://doi.org/10.1146/annurev.micro.50.1.491

Ishikawa, F.H., Souza, E.A., Shoji, J.Y., Connolly, L., Freitag, M., Read, N.D., Roca,

M.G., 2012. Heterokaryon incompatibility is suppressed following conidial anastomosis tube fusion in a fungal plant pathogen. PLoS One 7. https://doi.org/10.1371/journal.pone.0031175

Jin, M., Errede, B., Behar, M., Mather, W., Nayak, S., Hasty, J., Dohlman, H.G., Elston, T.C., 2011. Yeast dynamically modify their environment to achieve better mating efficiency. Sci. Signal. 4, ra54.

Leslie, J.F., 1993. Fungal Vegetative Compatibility. Annu. Rev. Phytopathol. 31, 127–150. https://doi.org/10.1146/annurev.py.31.090193.001015

Lew, R.R., 2005. Mass flow and pressure-driven hyphal extension in *Neurospora crassa*. Microbiology 151, 2685–2692. https://doi.org/10.1099/mic.0.27947-0

Lichius, A., Goryachev, A.B., Fricker, M.D., Obara, B., Castro-Longoria, E., Read, N.D., 2014. CDC-42 and RAC-1 regulate opposite chemotropisms in *Neurospora crassa*. J. Cell Sci. 127, 1953–65. https://doi.org/10.1242/jcs.141630

Lichius, A., Goryachev, A.B., Fricker, M.D., Obara, B., Castro-Longoria, E., Read, N.D., 2014. CDC-42 and RAC-1 regulate opposite chemotropisms in *Neurospora crassa*. J Cell Sci 127, 1953–1965. https://doi.org/10.1242/jcs.141630

Mathur, A.B., Collinsworth, A.M., Reichert, W.M., Kraus, W.E., Truskey, G.A., 2001. Endothelial, cardiac muscle and skeletal muscle exhibit different viscous and elastic properties as determined by atomic force microscopy. J. Biomech. 34, 1545–53. https://doi.org/10.1016/S0021-9290(01)00149-X

Mathur, A.B., Truskey, G.A., Reichert, W.M., 2000. Atomic force and total internal reflection fluorescence microscopy for the study of force transmission in endothelial cells. Biophys. J. 78, 1725–1735. https://doi.org/10.1016/S0006-3495(00)76724-5

Miyoshi, M., 1894. Über chemotropismus der Pilze. Bot. Zeitung 52, 1–28.

Mylyk, O.M., 1976. Heteromorphism for heterokaryon incompatibility genes in natural populations of *Neurospora crassa*. Genetics 83, 275–284.

Nayar, V.T., Weiland, J.D., Nelson, C.S., Hodge, A.M., 2012. Elastic and viscoelastic characterization of agar. J. Mech. Behav. Biomed. Mater. 7, 60–68. https://doi.org/10.1016/j.jmbbm.2011.05.027

Pál, K., Van Diepeningen, A.D., Varga, J., Hoekstra, R.F., Dyer, P.S., Debets, A.J.M., 2007. Sexual and vegetative compatibility genes in the aspergilli. Stud. Mycol. 59, 19–30. https://doi.org/10.3114/sim.2007.59.03

Payton, M., McCullough, W., Roberts, C.F., 1976. Agar as a carbon source and its effect on the utilization of other carbon sources by acetate non-utilizing (acu) mutants of *Aspergillus nidulans*. J. Gen. Microbiol. 94, 228–33. https://doi.org/10.1099/00221287-94-1-228

Payton, M.A., Roberts, C.F., 1979. Agar as a Carbon Source in Relation to the Isolation of Lactose Non-utilizing Mutants of *Aspergillus nidulans*. J. Gen. Microbiol. 110, 475–478. https://doi.org/10.1099/00221287-110-2-475

Porter, C.L., 1924. Concerning the Characters of Certain Fungi as Exhibited by Their Growth in the Presence of Other Fungi. Am. J. Bot. 11, 168. https://doi.org/10.2307/2435538

Skidmore, A.M., Dickinson, C.H., 1976. Colony interactions and hyphal interference between Septoria nodorum and phylloplane fungi. Trans. Br. Mycol. Soc. 66, 57–64. https://doi.org/10.1016/S0007-1536(76)80092-7

Stephenson, K.S., Gow, N.A.R., Davidson, F.A., Gadd, G.M., 2014. Regulation of vectorial supply of vesicles to the hyphal tip determines thigmotropism in *Neurospora crassa*. Fungal Biol. 118, 287–294. https://doi.org/10.1016/j.funbio.2013.12.007

Thomson, D.D., Wehmeier, S., Byfield, F.J., Janmey, P.A., Caballero-Lima, D., Crossley, A., Brand, A.C., 2015. Contact-induced apical asymmetry drives the thigmotropic responses of *Candida albicans* hyphae. Cell. Microbiol. 17, 342–354. https://doi.org/10.1111/cmi.12369

Trinci, a. P.J., Saunders, P.T., Gosrani, R., Campbell, K. a. S., 1979. Spiral growth of mycelial and reproductive hyphae. Trans. Br. Mycol. Soc. 73, 283–292. https://doi.org/10.1016/S0007-1536(79)80113-8

Trinci, A.P.J., 1971. Influence of the Width of the Peripheral Growth Zone on the Radial Growth Rate of Fungal Colonies on Solid Media. J. Gen. Microbiol. 67, 325–344. https://doi.org/10.1099/00221287-67-3-325

Wang, X., Shi, F., Wösten, H.A.B., Hektor, H., Poolman, B., Robillard, G.T., 2005. The SC3 hydrophobin self-assembles into a membrane with distinct mass transfer properties. Biophys. J. 88, 3434–3443. https://doi.org/10.1529/biophysj.104.057794

Wösten, H. a, 2001. Hydrophobins: multipurpose proteins. Annu. Rev. Microbiol. 55, 625–646. https://doi.org/10.1146/annurev.micro.55.1.625

Chapter 4

Attempts at determining the identity of the extracellular, self-avoidance signal

[Blank page]

4.1 Introduction

Experiments conducted using cryo-electron scanning microscopy revealed that the *A. fumigatus* retains the ability of self-avoidance during germination and germ tube elongation when it is grown on cellophane (Read, 2017; Fig. 4.1). Since hyphae are grown on a semi-permeable membrane, intercellular communication takes place predominantly through air or via signal molecules, which are able to pass through the cellophane. Nutrient depletion may also be sensed through the membrane. Good candidates for a gaseous signal molecule, if it exists, are volatile organic compounds (VOC).

Volatile organic compounds have been previously reported to act as interspecies and intraspecies signal mediators (Jones and Elliot, 2017; Fig. 4.2). Bacteria use a wide variety (low estimate is ~1,000) of low molecular weight compounds (<300 Da) with high volatility and low vapour pressures (0.01 kPa at 20 °C) to communicate with other
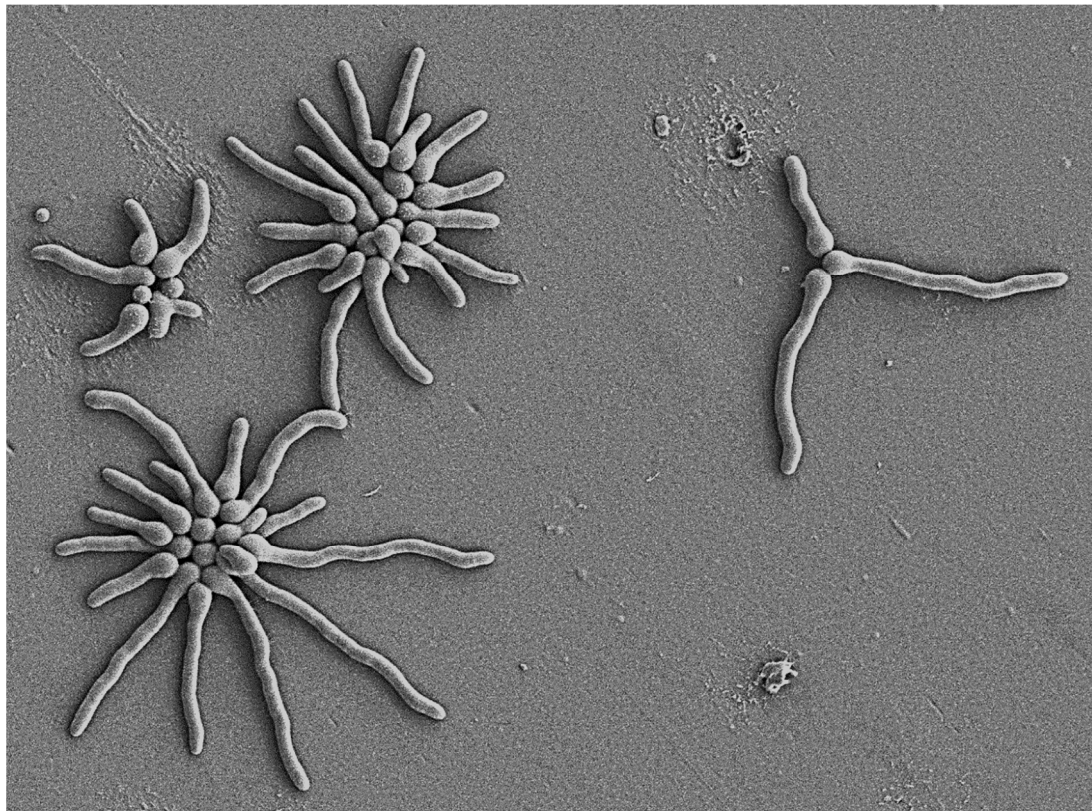
Figure 4.1 Cryo-Scanning Electron Microscopy image of *A. fumigatus* germlings grown on cellophane. Germlings have been grown on a hard surface without any intermediate nutrient, hence interhyphal communication may occur only through air or small molecules permeating the membrane. One of the hypotheses which this observation suggests is that a volatile compound may act as a signal and induce self-avoidance. Reproduced from Read (2017).
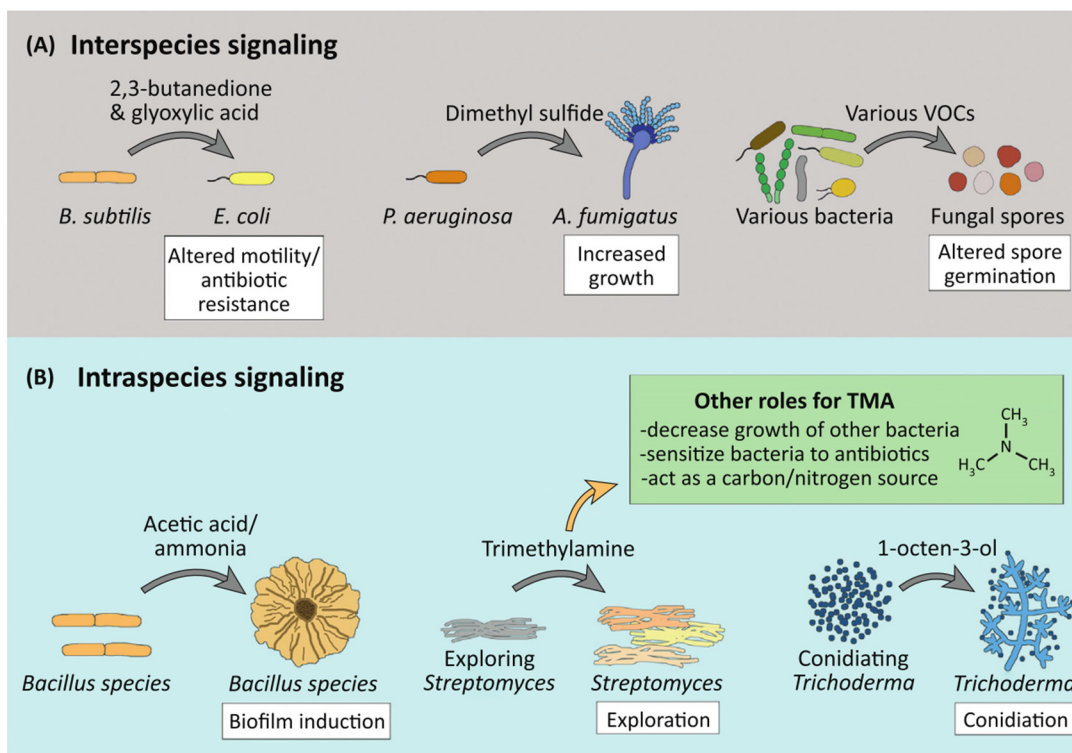
Figure 4.2 Volatile chemical compounds have diverse signalling roles in the microbial world. Their chemical complexity may range from inorganic substances (e.g. ammonia) to complex organic alcohols and acids. Roles may include cell communication between microbial communities of the same species or interspecies communication with mutually beneficial or antagonistic results. Reproduced from Jones and Elliot, 2017).

neighbouring organisms in their immediate environment (Schulz and Dickschat, 2007). The intrinsic chemical properties of VOCs make them ideal signal molecules: a) their high vapour pressure leads to a formation of concentration gradient away from the secreting cell, b) smaller volatile compounds tend to be unstable with a short half-life so they do not saturate the immediate extracellular environment, c) they can evaporate and diffuse through heterogeneous mixtures of solids, liquids and gasses. Previous reports have also shown that small compounds such as nitric oxide (NO) are crucial for the successful fungal infection of plants by fungi (Samalova et al., 2013) and pheromone regulation in plant germination (Šírová et al., 2011). Volatile organic compounds have also been reported to be implicated in the regulation of germination, sexual development and quorum sensing in fungi (reviewed by Albuquerque and Casadevall, 2012; Leeder et al., 2011; Ugalde, 2006; Ugalde and Rodriguez-Urra, 2014). The search for novel VOCs which may act as early infection markers is also of interest as research has shown that volatiles serve as communication signals during microbial infection in human lungs (Barkal et al., 2017). By co-culturing three types of bronchiole cells in custom-designed microfabricated slides, this study showed that there is an increased

cytokine production by bronchioles in response to an *A. fumigatus–Pseudomonas aeruginosa* volatile co-treatment. This greater inflammatory response would suggest that multikingdom (bacterial-fungal-human) indirect interactions are complex factors which contribute to the process of lung infection. Biosynthetic gene clusters (BGCs) of secondary metabolites have been annotated and described in *A. fumigatus* (Inglis et al., 2013; Owens et al., 2014). These gene clusters (26 described to date) encode for a variety of secondary metabolites which provide advantages to the fungus' diverse lifestyle (Bignell et al., 2016). It is evident that analysis of the volatome in *A. fumigatus* strains of interest would contribute to identify potential key VOCs important for growth, development and infection and tie them to described BGCs.

4.1.1 Aims of the chapter

The overall aim of the research described in this chapter was to explore the hypothesis as to whether the potential signal molecule(s) that cause the self-avoidance responses of *A. fumigatus* during germination and growth is a secreted (volatile) compound. To achieve this aim, three main approaches were taken:

1. The scavenging of the gas nitric oxide (NO) to determine if it influenced self-avoidance responses.

2. The direct screening of VOCs previously reported to regulate fungal cell differentiation and growth to determine if any influence self-avoidance responses.

3. A volatome analysis of the *A. fumigatus* wild type and a mutant strain compromised in secondary metabolism grown over a period of 24 hours to identify compounds which may be implicated in self-avoidance responses.

4.2 Results

4.2.1 Scavenging of nitric oxide (NO) does not affect self-avoidance

Nitric oxide (NO) is a small molecule which has been shown to be involved in host-pathogen interactions in bacterial infections (review by Spiro, 2007), microbial symbioses (reviewed by Wang & Ruby, 2011) and germination of pollen seeds (reviewed by Šírová et al. 2011). In filamentous fungi, the work of Samalova *et al.* (2013) has provided insights into the role of NO during infection of rice blast by the fungus

Magnaporthe oryzae. This study provided strong evidence that cytoplasmic NO levels are increased during the germination and appressorium formation of the fungus, suggesting that NO may play a role in the germination and infection of the plant.

To determine whether NO acts as a signalling molecule for negative cell tropisms in *A. fumigatus,* spores were incubated in AMM in the presence of the NO scavenger 2-Phenyl-4,4,5,5-tetramethylimidazoline-1-oxyl 3-oxide (PTIO; Akaike et al., 1993). PTIO is a highly selective nitric oxide scavenger (Goldstein et al., 2003) as shown by the equations below:

$$PTIO + \cdot NO \rightarrow PTI + \cdot NO_2 \qquad (1)$$
$$\cdot NO_2 + \cdot NO \rightarrow N_2O_3 \qquad (2)$$
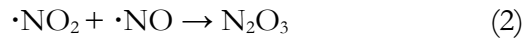
The reaction described by the second equation takes place at low PTIO concentrations (~5 µM) at which both NO_2 and NO are at comparable concentrations. At higher PTIO concentrations, all NO is converted to NO_2. For the purpose of my experiment the following concentrations of PTIO were used: 0 µM (control), 50 µM, 250 µM, and
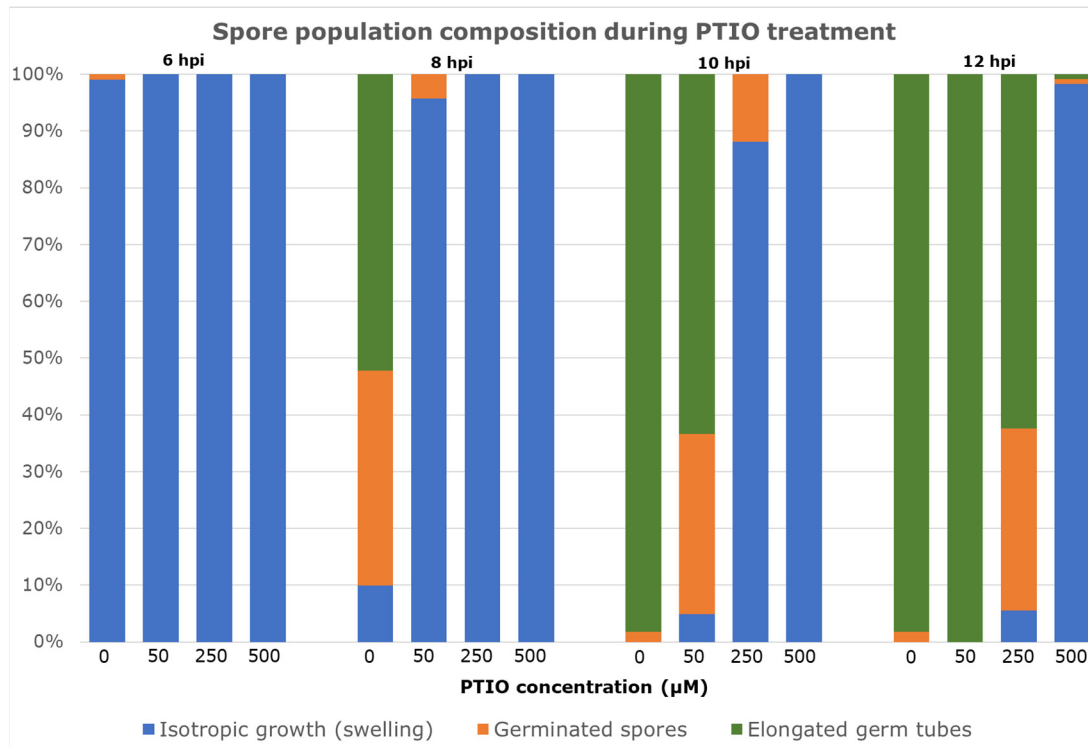
Figure 4.3 The influence of the NO scavenger PTIO on isotropic growth of spores, germination and germ tube growth. Increasing concentrations of the NO scavenger resulted in a successive increase in the inhibition of isotropic growth, spore germination and germ tube growth. Y-axis represents the population percentage.

500 μM. These were similar concentrations of PTIO shown to influence germination and appressorium formation by M. oryzae (Samalova *et al.* (2013). In my analysis, cell germination and growth were imaged in time-lapse, starting at 6 hpi (end of isotropic growth of the spore), using confocal microscopy. To quantify the effect of NO on spore germination, spores were classified as follows:

(1) Spores which are still swelling (i.e. they are still undergoing isotropic growth).

(2) Germinated spores in which there is obvious polarity asymmetry and the germ tube is no longer than 5 μm

(3) Germlings with elongated germ tubes which are longer than 5μm

The time-lapse results show that germination and growth of *A. fumigatus* in the presence of up to and including 250 μM PTIO is gradually delayed compared to the untreated control (Fig. 4.3). At 250 μM of scavenger concentration, germ tube tip growth redirection was still observed in response to cells approaching each other (Fig. 4.4). At 500 μM PTIO the germination process was significantly slower (Fig. 4.3); conidia were reaching the end of the isotropic stage of germination only at the 16-hour mark contrary to the average 6-8 hpi observed in the wild type. These observations provide
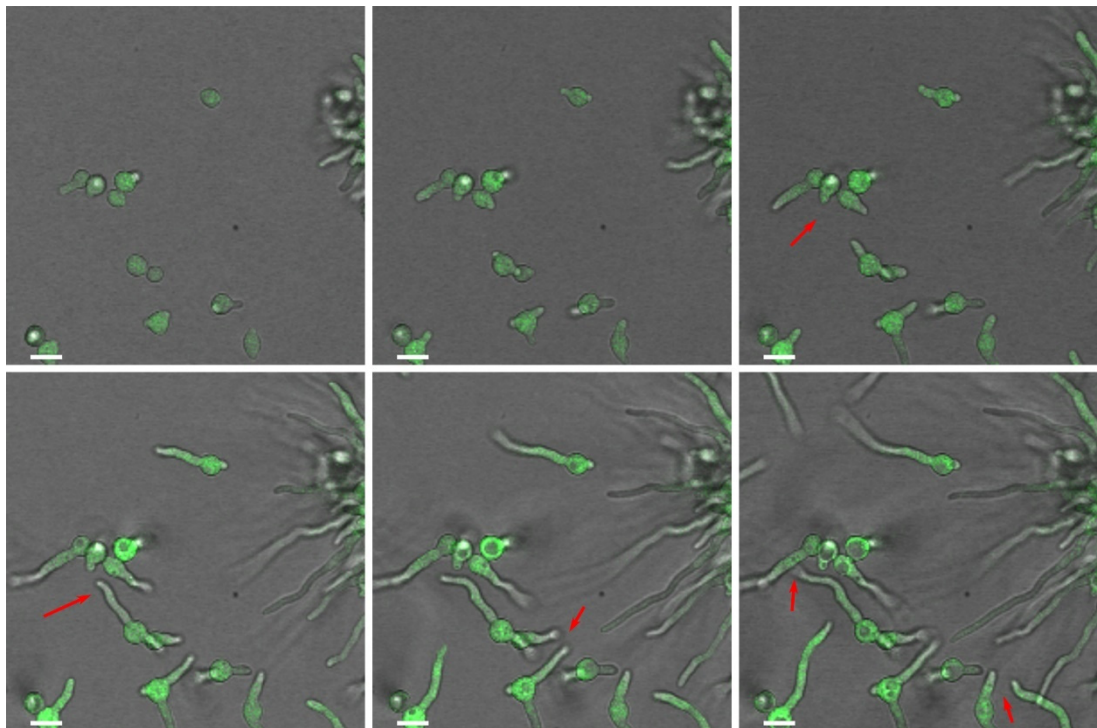
Figure 4.4 Scavenging of NO has no effect on negative autotropisms. Confocal time-lapse imaging of *A. fumigatus* conidia growing in AMM with 250 μM PTIO (NO scavenger) from 10 hpi up to 12 hpi. Spores germinated normally and exhibit self-avoidance when approaching each other (red arrows indicate hyphal reorientation). Scale bar = 5 μm

evidence that NO is not necessary for self-avoidance responses but may be involved in the germination process. The latter observation is consistent with the results reported by Samalova *et al.* (2013) in *M. oryzae.*
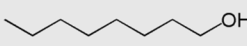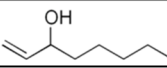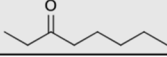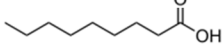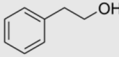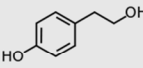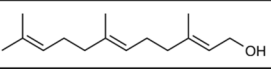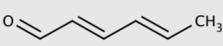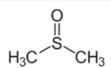
4.2.2 Volatile organic compounds (VOCs) with reported biological activity do not directly induce avoidance responses of *A. fumigatus*

A range of chemical compounds which are VOCs have been reported as playing diverse roles in signalling in the fungal kingdom. These compounds that occur naturally in fungal species, are secreted in detectable amounts and have been associated with several aspects of developmental such as regulation of asexual development, auto-inhibition of germination due to population density, and modulation of growth (Leeder et al., 2011; Ugalde, 2006; Ugalde and Rodriguez-Urra, 2014). My hypothesis was that there is a possible connection between spore germination autoinhibition and the negative autrotropic effect of germ tube emergence from spores, and thus spore germination autoinhibition is another aspect of self-avoidance. To test this hypothesis several compounds previously characterized for their role in germination autoinhibition (Table 4.1) were screened to test their possible tropic effects on germination and determine whether they could induce avoidance of *A. fumigatus* germ tubes. The experimental set up is as described in Section 2.5.1.1 and involved performing high magnification stereomicroscopy of germinating spores in the zone around a filter paper disc soaked in the compound and placed on solid AMMA previously inoculated with conidia.

If the screened chemical compound was indeed an avoidance-inducing factor, then the following avoidance responses might be predicted (Fig. 4.5):

(1) The majority of initial germ site protrusions would be on the spore side away from the highest concentration of the compound.

(2) In a 'zone of inhibition' the emerging germ tubes would grow down the concentration gradient provided that they were unaffected by other factors (e.g. adjacent hyphae).

(3) Some germ tubes in the presence of low concentrations of the compound at the periphery of the zone of inhibition would exhibit directional growth which is more-or-less tangential to the centre of the source of the compound in the filter paper disc.

Table 4.1 Chemical compounds selected for their effect on the self-inhibition of germination and co-ordination of growth in Ascomycota. Also listed, are reference fungal species that the compound is reported to have an effect on. Table adapted from Tables published in Leeder et al. (2011) and Ugalde and Rodriguez-Urra (2004).

Molecule	Structure	Species reported
1-Octanol		*Aspergillus nidulans*
1-Octen-3-ol		*Aspergillus nidulans*
3-Octanone		*Aspergillus nidulans*
Nonanoic acid		*Fusarium oxysporum*
phenylethyl alcohol		*Saccharomyces cerevisiae*
Tryptophol		*Saccharomyces cerevisiae*
2-(4hydroxyphenyl) ethanol		*Candida albicans*
Farnesol		*Candida albicans*
trans,trans-2,4-hexadienal		*Colletotrichum fragariae*
Dimethyl sulfoxide (DMSO)		*Aspergillus fumigatus (?)*

Despite the fact that 1-octanol (Gillot et al., 2016; Herrero-Garcia et al., 2011), 1-octen-3-ol (Chitarra et al., 2004; Herrero-Garcia et al., 2011), and 3-Octanone (Herrero-Garcia et al., 2011) have been reported to be a germination self-inhibitor in other fungi no effect was observed in *A. fumigatus*. Farnesol has been reported to affect the cell wall integrity (CWI) pathway causing apoptosis-like cell death in *A. fumigatus* (Dichtl et al., 2010), and *A. flavus* (Wang et al., 2014). Interestingly, farnesol represses the transition to filamentous form in *C. albicans* (Egbe et al., 2017). In the conducted screen, farnesol did not affect germination after 24 hours, but cells displayed aberrant hyphal growth due to stress as shown in Fig. 4.7.

Of the tested compounds, only tryptophol and nonanoic acid induced changes in overall colony growth compared to the control (ethanol). These compounds induced the formation of zones of inhibition similar to that observed in Kirby-Bauer antibiotic tests (Fig. 4.6). In the presence of 2,4-hexadienal, spores did not germinate for the first 24 hours, but mycelial growth was observed after 48 hours (Fig. 4.9). The zones of
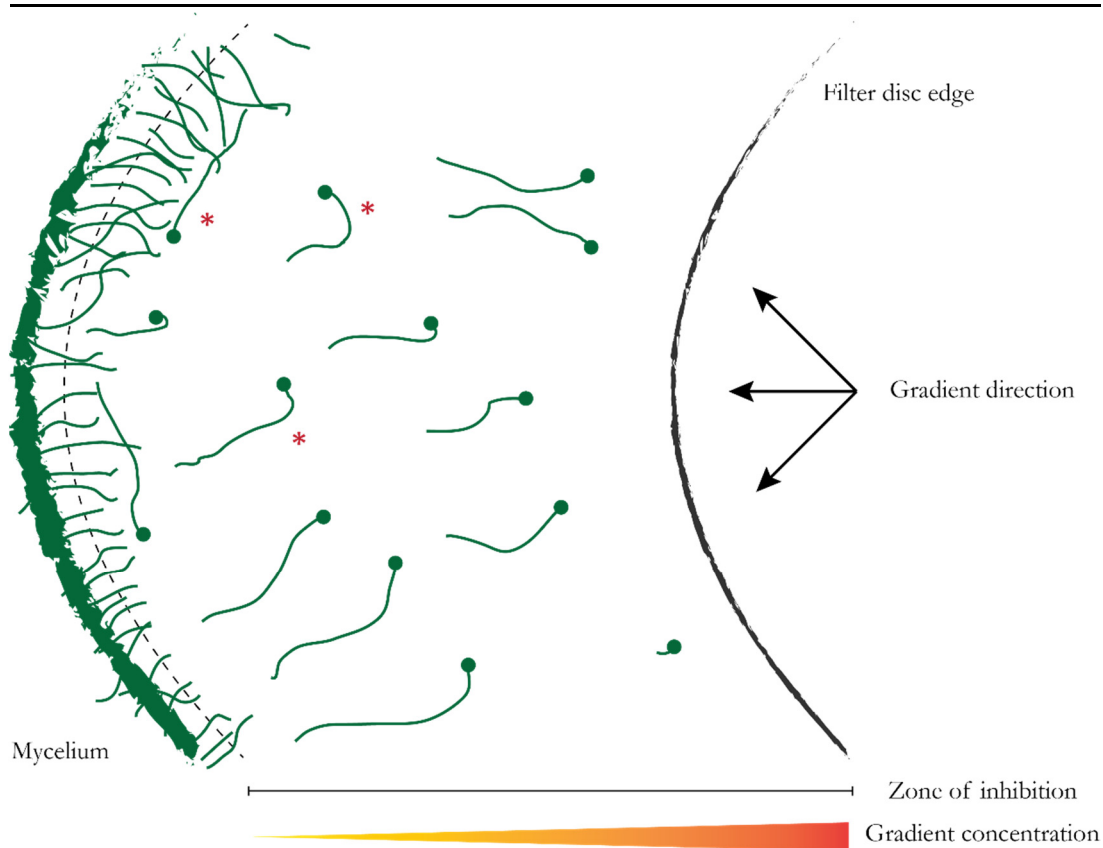
Figure 4.5 Hypothetical model of avoidance to a factor during germination and germ tube growth. Germlings grow away from higher avoidance factor concentrations down the formed gradient. Some germ tubes in the presence of low concentrations of the avoidance at the limits of the zone of inhibition exhibit directional growth which is more-or-less tangential to the centre of the source of the avoidance factor meeting the gradient, avert their growth axis and grow along its interface.

inhibition were further observed under the stereomicroscope to validate if growth follows the hypothetical pattern described in Fig. 4.5. These results are shown in Fig. 4.7.

Compounds were further assessed for their ability to induce the avoidance of mature *A. fumigatus* hyphae. AMMA plates were inoculated with a 4 µl drop containing ~1,200 spores and left to grow for 3 days at 37 °C. A Whatman® Antibiotic Assay Disc was placed on one side of the approaching colony and inoculated with 10 µl of the tested compound (concentration of 1M), and plates were left to incubate for one more day.

Farnesol, tryptophol, nonanoic acid and 2,4-hexadienal notably induced a delay in growth at the interface where hyphae met with high gradients (Fig. 4.7). Stereomicroscopy imaging showed that farnesol and tryptophol treatments resulted in visibly altered growth of hyphae that resulted in denser mycelia. Hyphae approaching
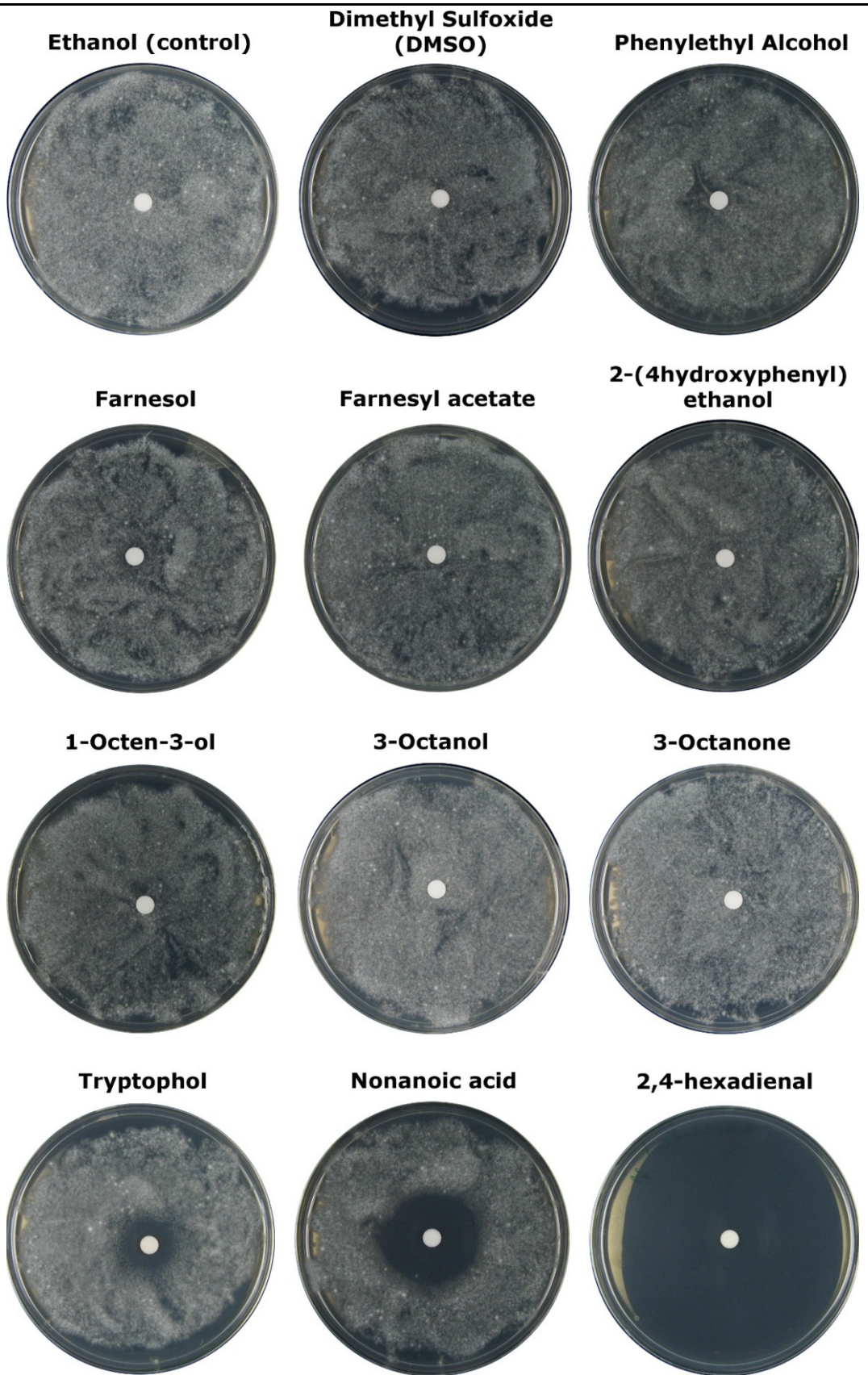
Figure 4.6 Chemical compound screen assay. The activities of selected compounds on germination and self-avoidance of *A.fumigatus* CEA10 was assessed. Tryptophol, nonanoic acid and 2,4-hexadienal showed visible effects on germination compared to the control. Petri dishes were imaged after incubation for 24 hours at 37 °C.

the nonanoic gradient also grew visibly slower compared to the rest of the colony edge but did not have a significantly altered hyphal structure compared to the wild-type and in contrast to the effects of tryptophol. 2,4-hexadienal treatment resulted in the most pronounced growth inhibition of approaching hyphae, which formed a dense mycelial network. None of these compounds displayed growth close to the hypothetical model (Fig. 4.5).

Stereomicroscopy observations of the compound-treated germinating spores showed that farnesol and tryptophol did not affect germination but had an effect on the shape
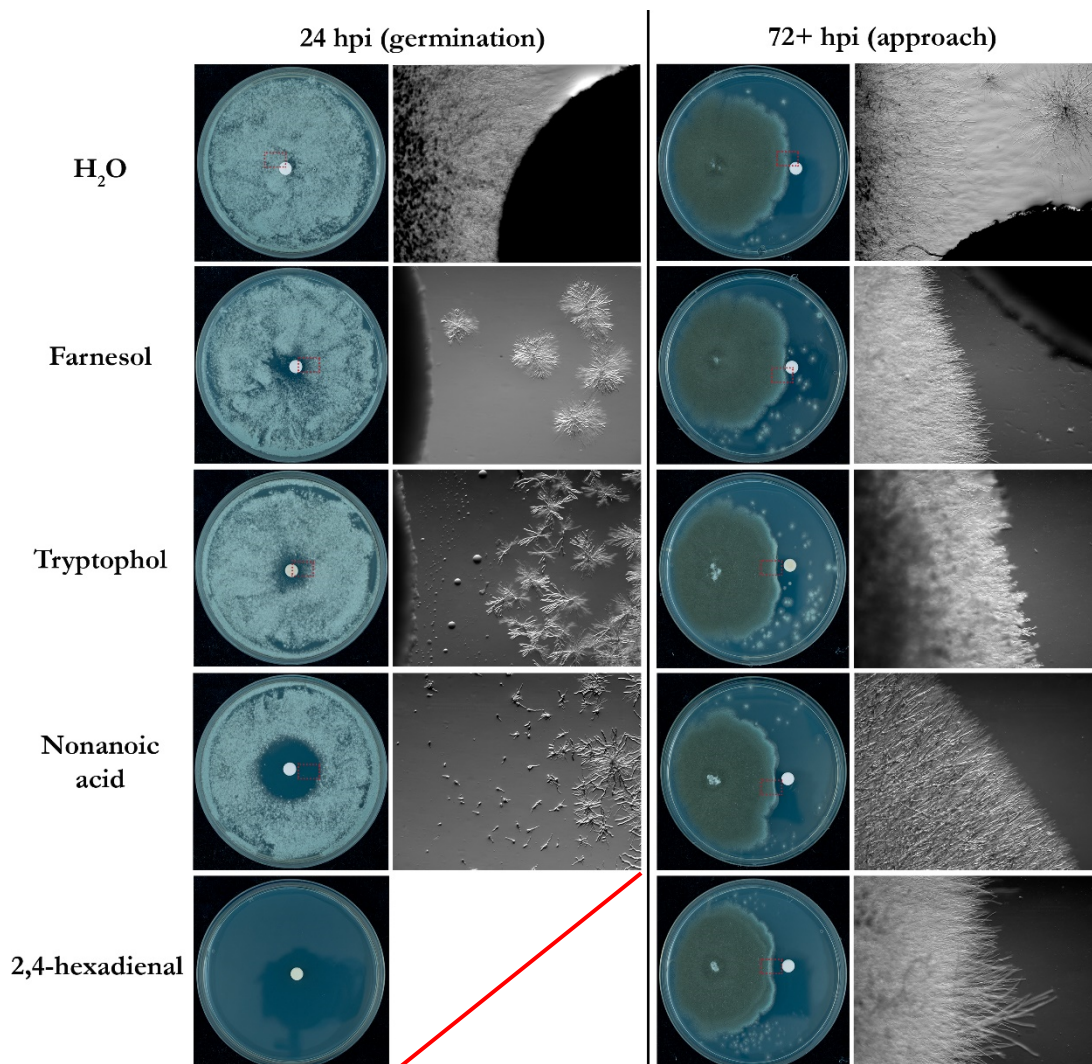
Figure 4.7 Effects of selected compounds on *A. fumigatus* CEA10 morphology and development during germination and vegetative growth. After 24 h, farnesol and tryptophol treatments resulted in the formation of small microcolonies at high concentration gradients. Nonanoic acid affected germination in a dose dependent manner; higher concentrations resulted in the delayed germination. Vegetative hyphae (72+ hpi) approaching the same gradients formed dense mycelial networks on all occasions with visible morphological aberrations of the hyphae approaching the tryptophol gradient.

of fungal microcolonies; their hyphae were noticeably thicker and shorter than the wild type. Out of all the tested compounds trans,trans-2,4-hexadienal displayed the most potent germination inhibitory function on *A. fumigatus*, with no visible germination at 24 hpi. The nonanoic acid gradient resulted in a dose dependent effect on germination; spores in higher gradients germinated slower than the ones in the presence of low concentrations of nonanoic at the periphery of the zone of inhibition. This result suggested that nonanoic acid might be a good candidate compound to further test as a potential avoidance compound.

One of the common VOCs in the preliminary volatome analysis of both strains (wild type and *ΔpptA*) was found to be acetic acid (section 4.2.5), as its presence was detected
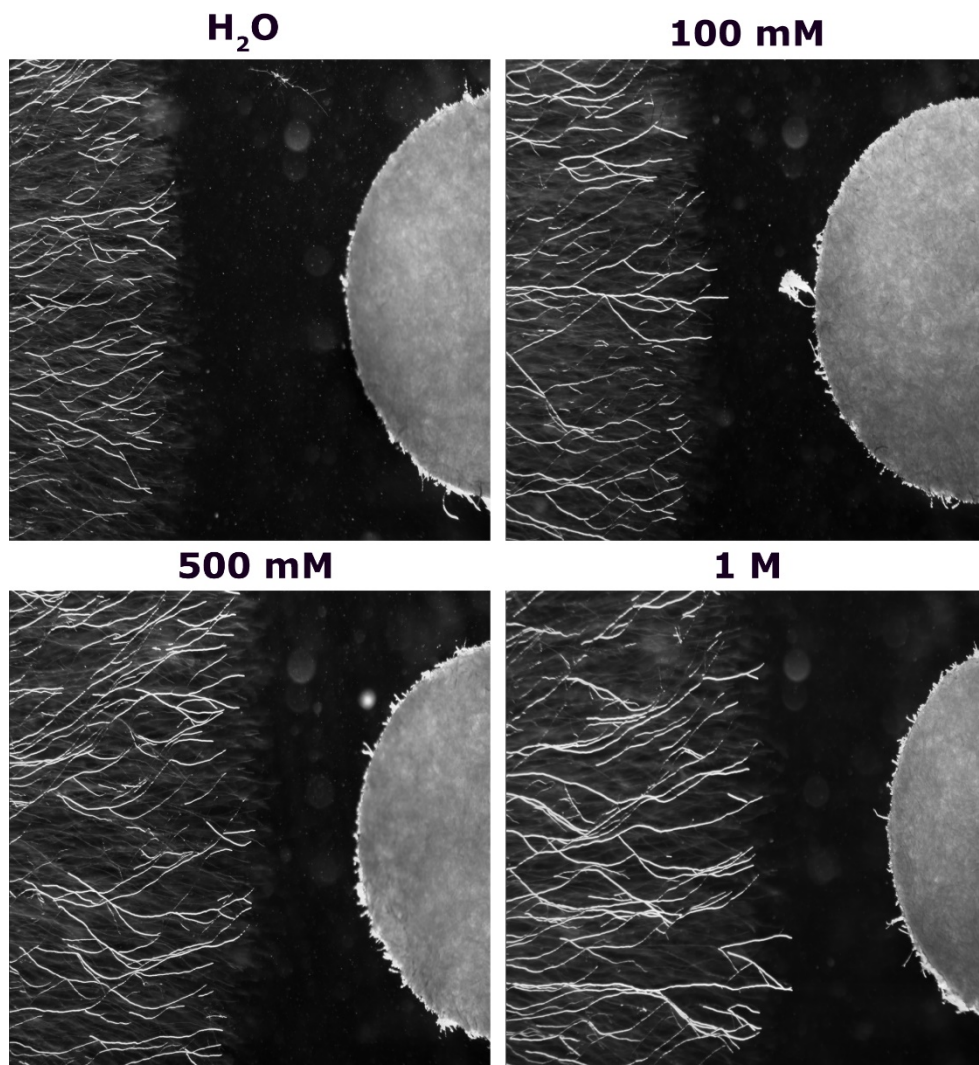
Figure 4.8 Acetate did not induce of avoidance in *A. fumigatus*. Stereomicroscopy images showing that *A.fumigatus* hyphae at the periphery of the fungal colony are not affected by the acetate buffer gradient. Bright white hyphae are cells in focus, while the grey hyphae are underlying hyphae. Whatman® filter disc with acetate buffer is on the right.

in both the culture media and the *A. fumigatus* cultures. To evaluate whether acetate affects hyphal direction, plates were inoculated with *A. fumigatus* spores and incubated for 24 hours at 37 ºC. After 24 hours, a Whatman® Antibiotic Assay Disc was placed 1 cm from the edge of the formed fungal colonies containing 5 µl of sodium acetate buffer (varying concentrations, pH 6.0) and plates were left to incubate for 24 hours. Fungal hyphae approaching the filter disk were imaged using a stereomicroscope. Sodium acetate did not induce negative tropisms in *A. fumigatus* even with gradients generated by high concentration of acetate (1M) on the filter disk (Fig. 4.8). This would suggest that sodium acetate does not affect hyphal orientation in *A. fumigatus* under the tested conditions.

4.2.3 Nonanoic acid induces the formation of synnemeta (coremia) in *A. fumigatus*

To test whether the inhibition zones were a result of delayed germination or a fungistatic effect of the tested compounds described in section 4.2.2, plates were incubated for 24 more hours (total 48 hpi) at 37 °C. Spores on the plates treated with 2,4-hexadienal not only germinated after 24 hours but also grew and sporulated significantly outside the zone of inhibition throughout the plate. A zone of growth inhibition was still observed (Fig. 4.9) after 48 hours (radius ~0,95±10 mm, N=5), compared to the controls (H_2O and ethanol). This suggests that *A. fumigatus* CEA10 has increased sensitivity to 2,4-hexadienal which results in a significant delay of germination.

Plates treated with nonanoic acid retained their zone of inhibition (radius ~0.8±8 mm, N=5). Sporulation on the rest of the media was observed (Fig. 4.10). Unexpectedly, all plates that were treated with nonanoic acid formed specialised aggregated hyphal structures that grew vertically in the air, away from the medium (results of three different experiments, 3-5 different cultures per experiments). Isolation of those structures and observations using confocal microscopy revealed that they consisted of a very tightly meshed mycelium with indiscriminate boundaries (data not shown). After further incubation for 24 h at 37 ºC conidiation was observed at the top of the vertically formed hyphae. These observations combined would suggest that these structures are in fact synnemata (alternatively called coremia; Watkinson, 1979); which are aggregated hyphae that have adhered together to resemble a stalk that bear compact conidiophores at their top (Read, 1994).
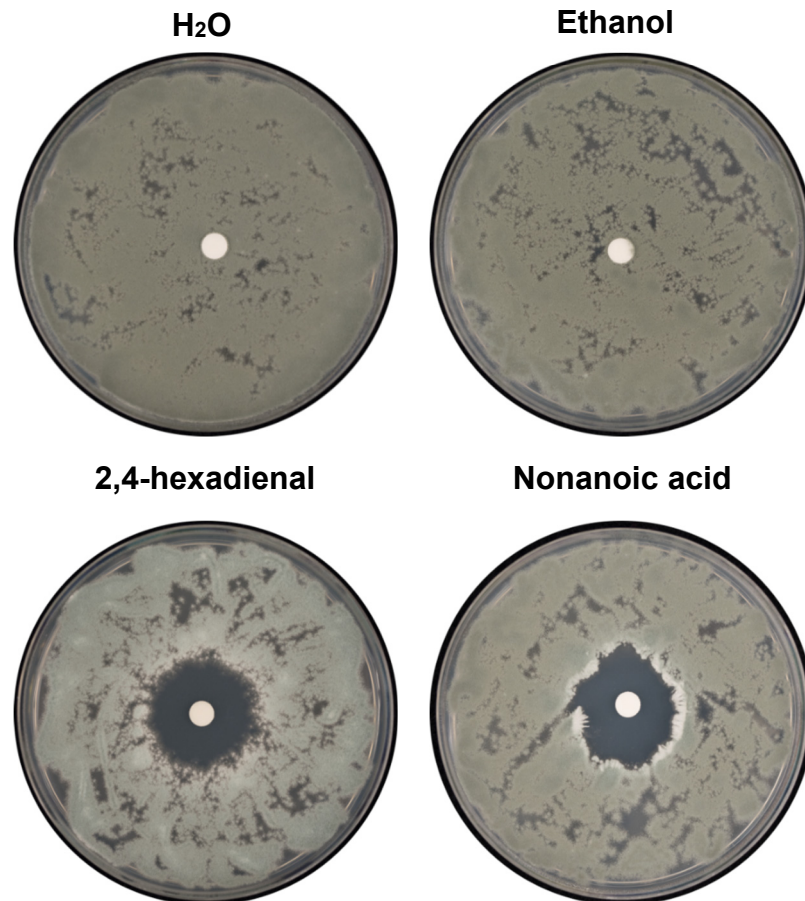
Figure 4.9 Inhibition zones formed by 2,4-hexadienal and nonanoic acid persist after 48 h of incubation. *A. fumigatus* CEA10 spores have germinated, grown and sporulated after 48 h in 2,4-hexadienal treated plates. The inhibition zone formed by the nonanoic acid gradient has persisted after 24h and synnemata have formed at the edge of inhibition ring.
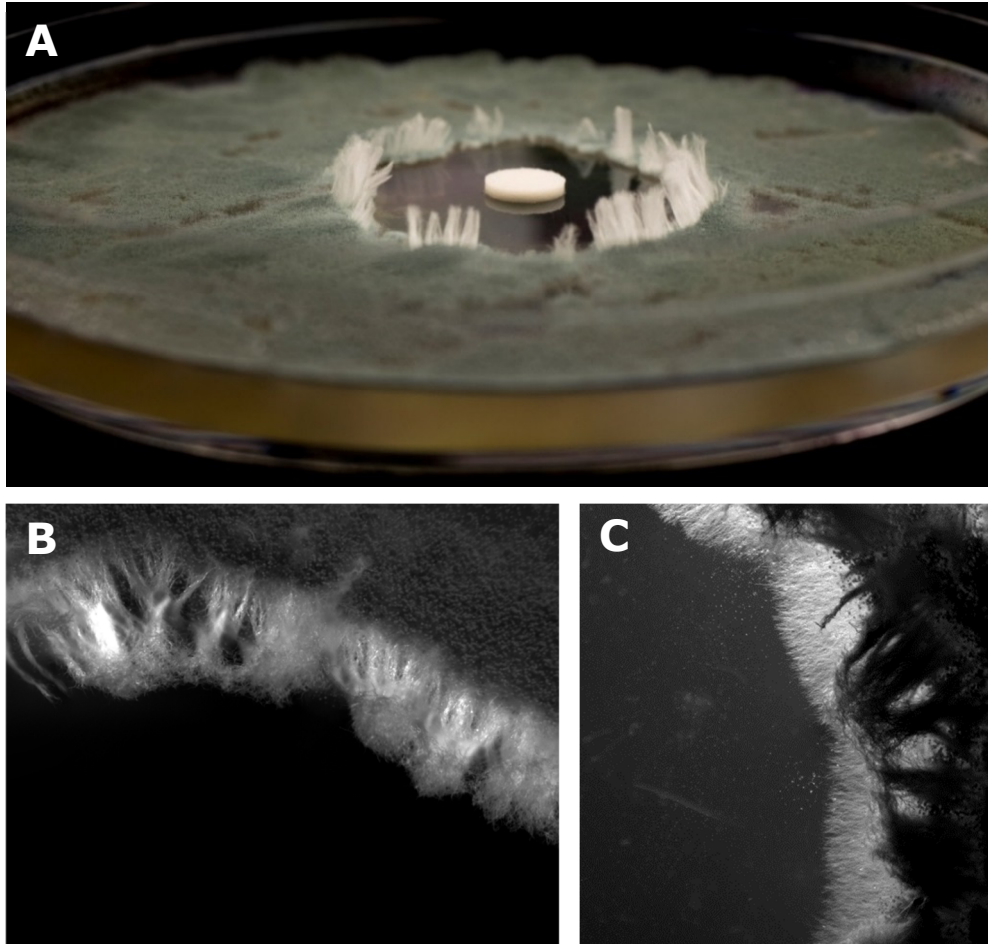
Figure 4.10 Images of the synnematous structures formed in *A. fumigatus*. (A) Synnemata (coremia) are formed after 48 h treatment with nonanoic acid at the edge of the zone of inhibition (photo taken with conventional camera). (B) Stereomicroscopy image of the synnemata (white hyphal structures) using incident lightning from above. (C) Same synnemata (dark hyphal structures on the right of the image) illuminated with transmitted light from below. The structures are thick enough that light cannot pass through as it can with the vegetative hyphae (bright structures.).

4.2.4 Nonanoic acid inhibits germination in *A. fumigatus*

As shown in section 4.2.3, nonanoic acid inhibited germination of *A. fumigatus* spores in a dose-dependent manner. Spores in the zone of inhibition exhibited delayed germination compared to the cells at the zone periphery. To assess if the directionality of germ tube emergence was affected by a concentration gradient formed by nonanoic acid (as the best candidate for inducing self-avoidance, section 4.2.2), hydrogen peroxide (which acts as ROS) and the aldehydes nonanal and decanal were evaluated in disk diffusion experiments.

To this end a compound treatment experiment was carried out in triplicates as described in the previous sections. Nonanal and decanal were found to common VOCs in the preliminary volatome analysis; they were detected in both the culture media and the *A. fumigatus* cultures (section 4.2.6). As they share similar structure to nonanoic acid, they were assessed for their ability to generate the same phenotype as nonanoic acid. Chloroform and itraconazole were used as controls; the former was used as the
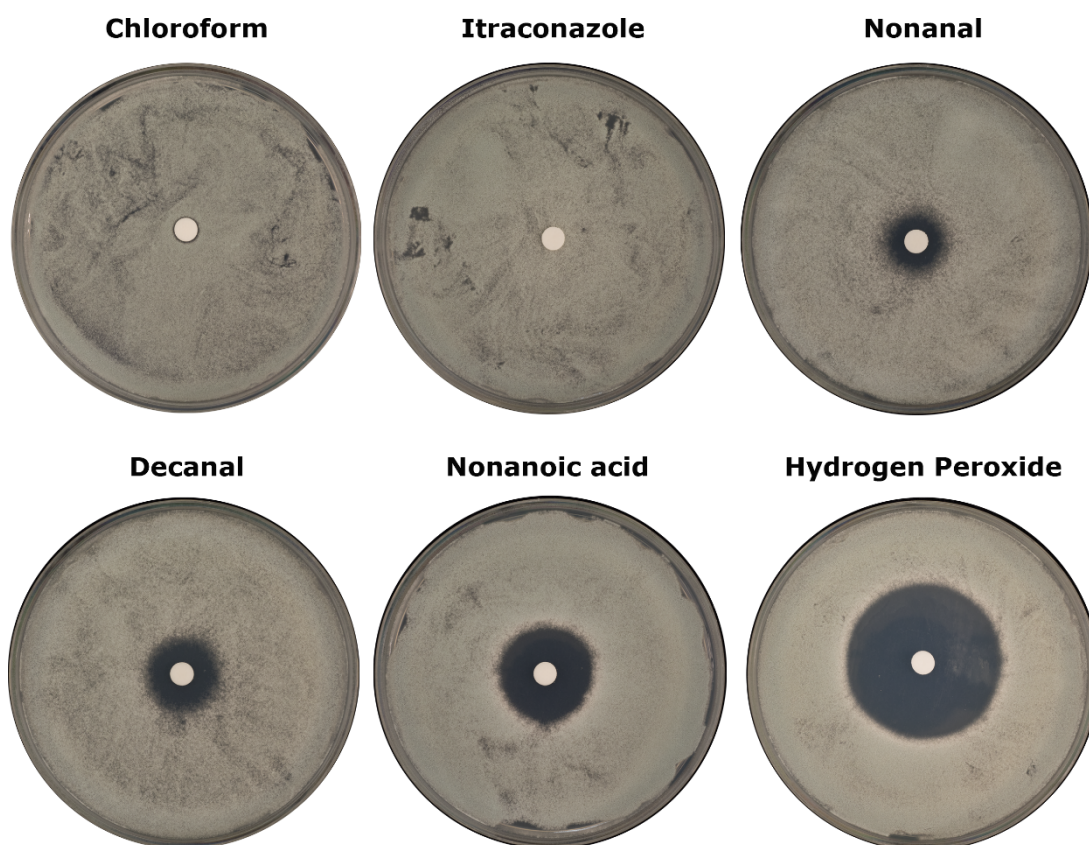
Figure 4.11 Sensitivity of *A. fumigatus* to concentration gradients formed by aldehydes, nonanoic acid and ROS. Nonanal and decanal are aldehydes found in the media and exhibit inhibition of germination at high concentrations. Hydrogen peroxide had a pronounced inhibitory effect compared to the rest of the tested compounds.

(organic) solvent for the tested compounds and itraconazole as a control for generation of zone of inhibition (final conc. 80 µg/ml). Hydrogen peroxide (H_2O_2) was used in an undiluted state (30% w/w), while nonanal, decanal and nonanoic acid were adjusted to 1M concentration. Lines passing through the filter disc centre were drawn with a marker on the back of the Petri dish to have an estimate of the gradient orientation during quantification.

Inhibition zones were formed in all conditions except for the controls (Fig. 4.11). The lack of effect on *A. fumigatus* germination in the controls is rather surprising and unexpected and suggests that the compounds may not have properly diffused through the antibiotic disk. This observation would also apply to the experimental results shown in Figure 4.6. Treatment with hydrogen peroxide results in the largest radius size of all tested compounds (Fig 4.12). Stereomicroscopy observations revealed that at 24 hours fungi spread on the plates with chloroform and itraconazole displayed normal conidiation and no zones of inhibition (Fig. 4.13). Inhibition zones induced by nonanal, decanal and hydrogen peroxide had no intermediate effect on *A. fumigatus* germination; spore germination was inhibited in the inhibition zone up until where the cells grew unrestricted. Minor exceptions of spores germinating inside the inhibition zone induced by nonanal and decanal were observed. These observations would suggest that the zone of inhibition is in fact a zone of dead cells, with a few exceptions being resistant cells.
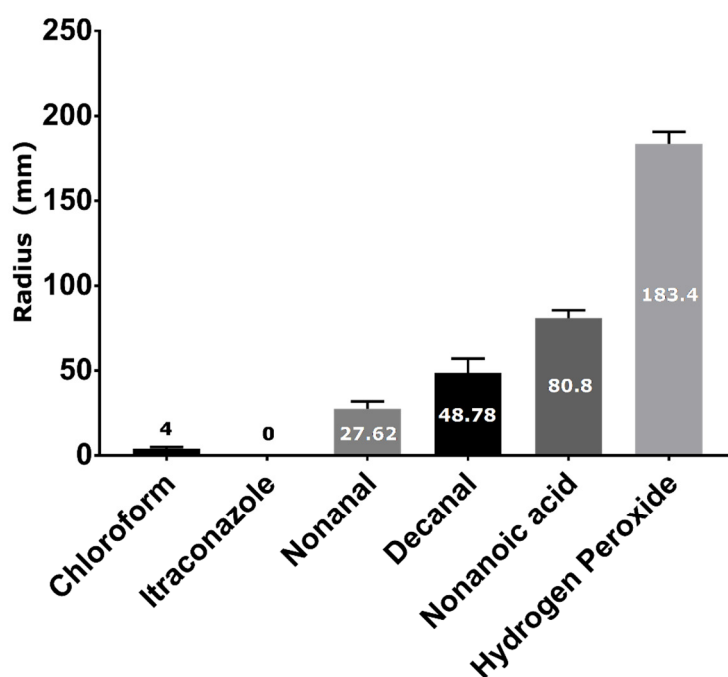
Figure 4.12 Radius of inhibition zone caused by tested compounds. Values are the results of five separate measurements. Error bars depict standard deviations.
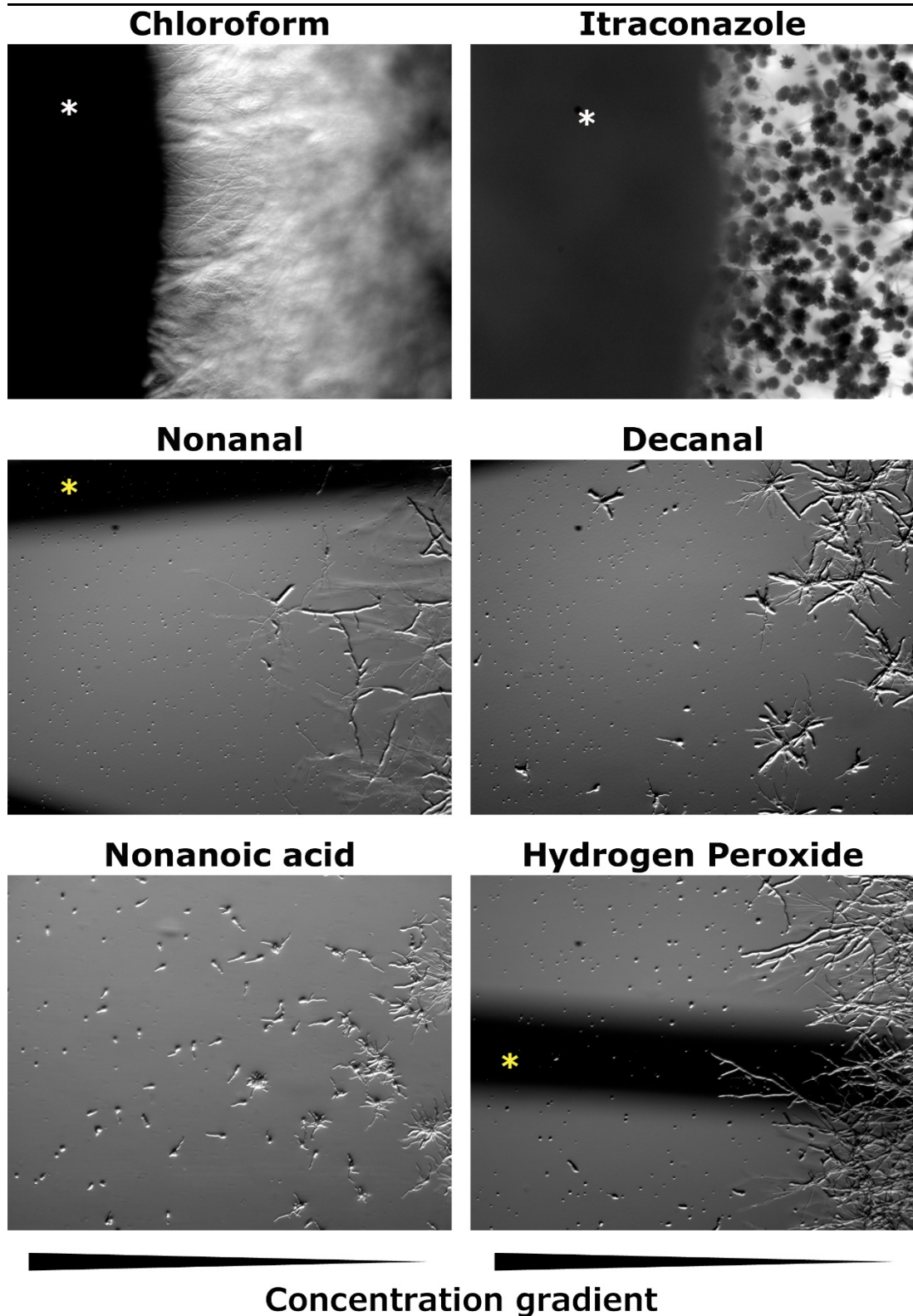
Figure 4.13 Aldehydes, ROS and nonanoic acid affect *A. fumigatus* germination. While nonanal, decanal and hydrogen peroxide completely hindered germination in a cytostatic manner, nonanoic acid displayed a dose dependent effect. White asterisks denote the filter discs, while yellow asterisks show the lines drown to depict the gradient direction.

Cells on the plates treated with nonanoic acid consistently displayed varying degrees of
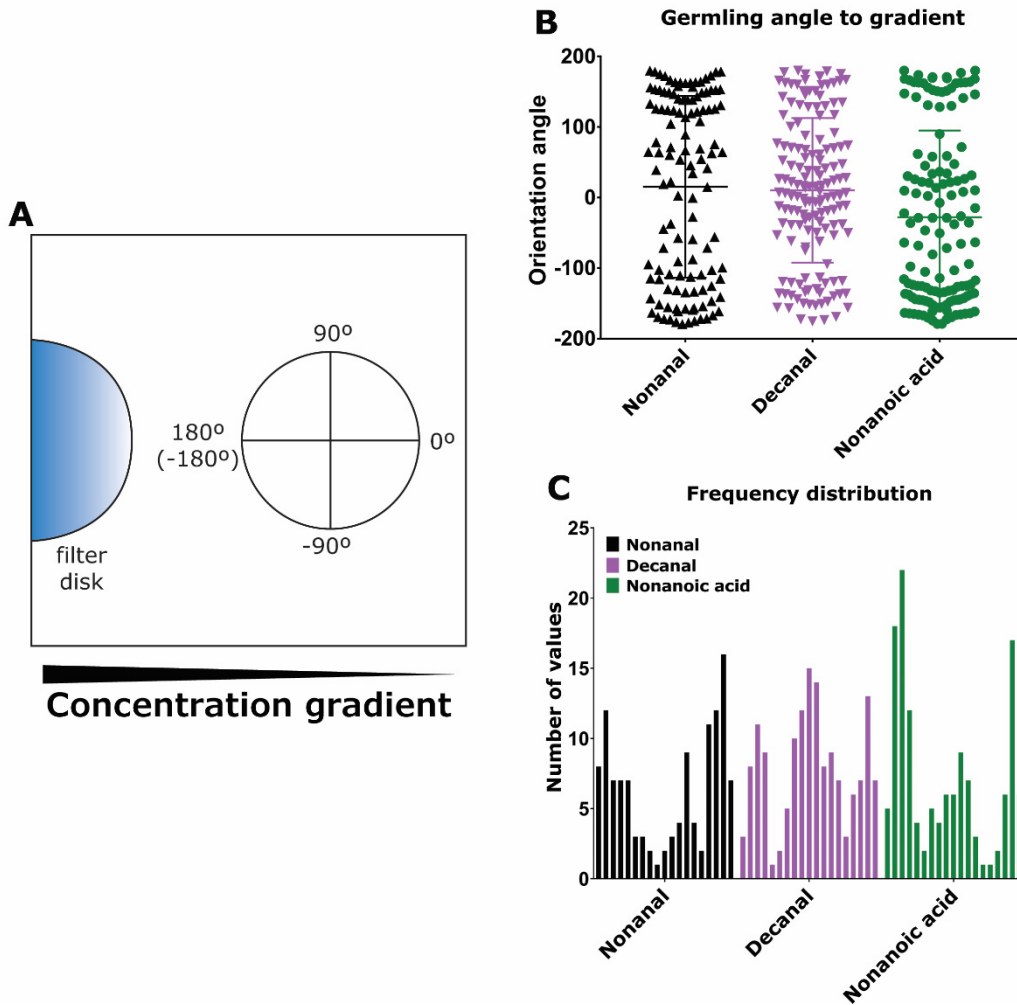
Figure 4.14 Orientation angles of hyphae in respect to VOC gradients. (A) Diagram showing how the angles were calculated. 0° indicates that the measured hypha grows away from the concentration gradient (negative tropism), 180° or -180° denotes growth towards the gradient (chemoattraction). (B) Results of measured angles for nonanal, decanal and nonanoic acid. (C) Frequency distribution of measurements presented in (B). y-axis depicts the angles from -180°→0°→180° per each condition. The frequencies did not follow a normal Gaussian distribution (see text for details).

germination depending on the concentration of the compound, as described in section 4.2.2.

Hyphal orientation of germinated cells in the inhibition zone was quantified in relation to the gradient direction using the FIJI image analysis programme (N =100-120 for each condition). Angles were quantified for germlings found inside the radius of the inhibition zone. Thus, no measurements for chloroform, itraconazole and hydrogen peroxide were conducted.

Orientation angles were measured as the angle formed between the germ tubes and the concentration gradient generated by the filter disk. If the spore is the centre of a circle,

FIJI calculated the orientation angle between 0º-180º as according to the method shown in Fig. 4.14A. Germ tubes extending down the course of the concentration gradient would have a 0º angle and would grow along the gradient, whereas germ tubes growing at a 180º angle would be growing up and thus against the concentration gradient. According to the model described in section 4.2.2, the expected orientation angles of germ tubes growing against an avoidance inducing compound should range from 90º to -90º (zero degrees denoting growth away the concentration gradient). It is apparent from Fig. 4.14B that this is not the case for any of the studied compounds, as angles of 180º were observed. Moreover, the frequency distribution of all observed angles would be expected to be very close to a Gaussian distribution if the chemical compound tested was an avoidance inducer. However, all conditions failed the D'Agostino-Pearson normality test significantly (p value < 0.0001). Statistical comparison of the mean orientation angles (one-way ANOVA) showed that there is statistical significance between nonanoic acid and the other two compounds; p value of 0.0102 and 0.0180 for nonanal and decanal respectively. The mean orientation angles estimated for decanal and nonanal were not significantly different (Fig. 4.14C).

4.2.5 Establishment of a novel fungal volatome extraction methodology

To identify more volatile organic compounds that induce avoidance of *A. fumigatus* hyphae I proceeded to analyse the volatome profile of *A. fumigatus* colonies. Since negative cell autotropisms are evident between germ tubes and between the leading hyphae of mature vegetative hyphae development (discussed in Chapter 3), my hypothesis is that if a VOC is a signal molecule, it would be present in the *A. fumigatus* volatome profile regardless of the fungal colony's age.

To help establish a threshold in which we could subtract volatiles which are potentially not implicated in self-avoidance, a strain which has severe limitations in secondary metabolism was used; *ΔpptA* (Johns et al., 2017). As described in their study, the knockout (deletion mutant) of the phosphopantetheinyl transferase A (PptA) resulted in severe secondary deficiencies and auxotrophies for lysine and iron. However, the *ΔpptA* strain does exhibit negative autotropisms (Fig. 4.15), thus any common compounds between its volatome and the wild type would be candidates for a screen to identify their role (if any) in self-avoidance (Fig. 4.16).
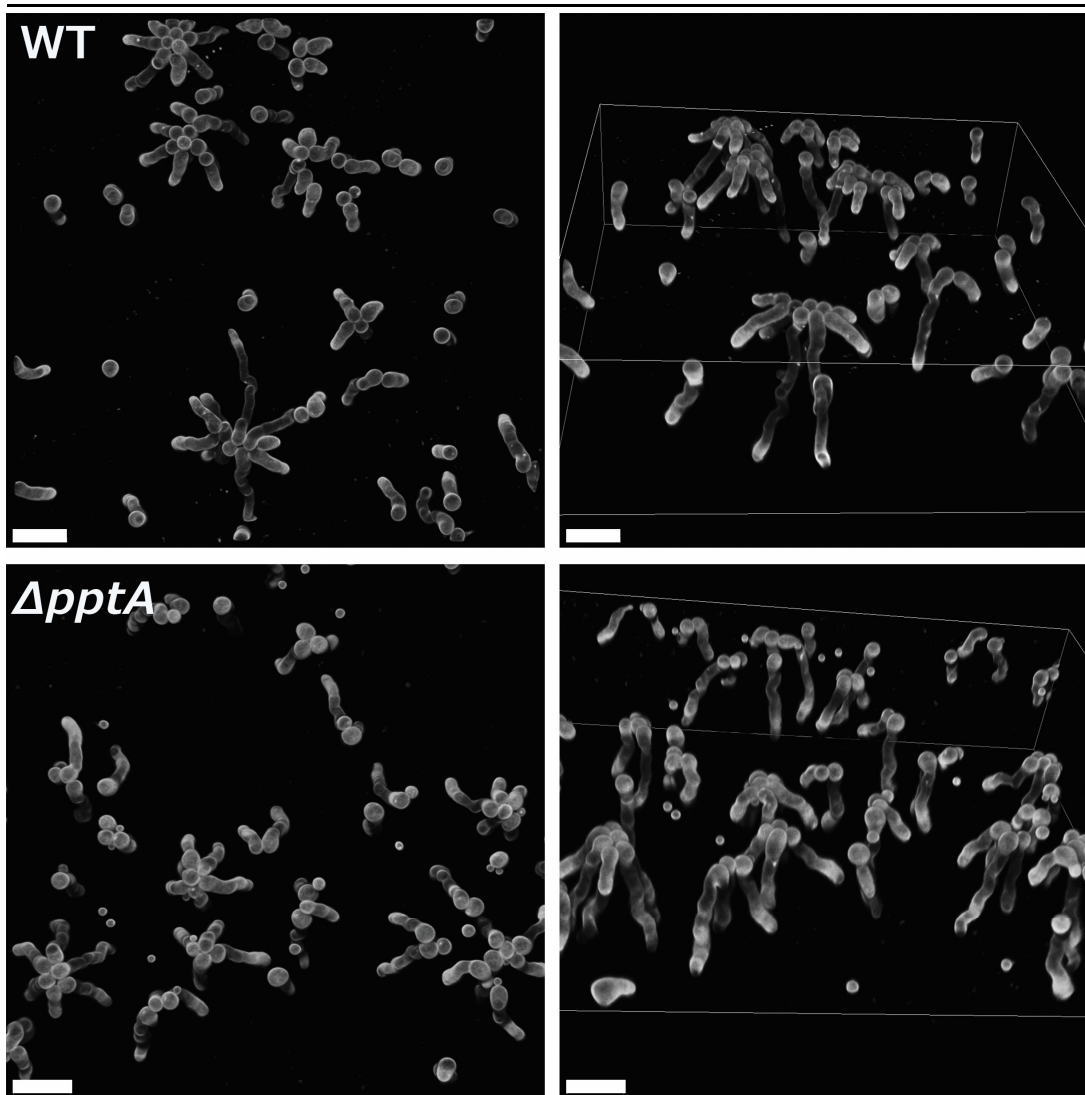
Figure 4.15 The *ΔpptA* strain displays negative cell autotropisms similar to the wild type. The deletion mutant show spread of germ tubes away from one another (left column, upper view of datasets) and the same invasion tropism (right column, side view of the same datasets) described in Chapter 3. Scale bar = 20 μm

To extract and analyse the *A. fumigatus* volatome, a novel approach of sampling was developed. Previous studies have used a solid-phase microextraction (SPME) of the volatome using a polydimethylsiloxane (PDMS) needle to 'passively' collect the headspace, i.e. space above the fungal colony containing vapours (Costa et al., 2016; Heddergott et al., 2014). In my study an alternative approach was taken which involved the sampling of the headspace using thermal desorption tubes. This novel method (described in section 2.6) provides a few advantages over the previously reported ones. More specifically:

    a) any data produced from the GC-MS analysis is semi-quantifiable in relation to initial biomass, since the headspace is cleared with vacuum,
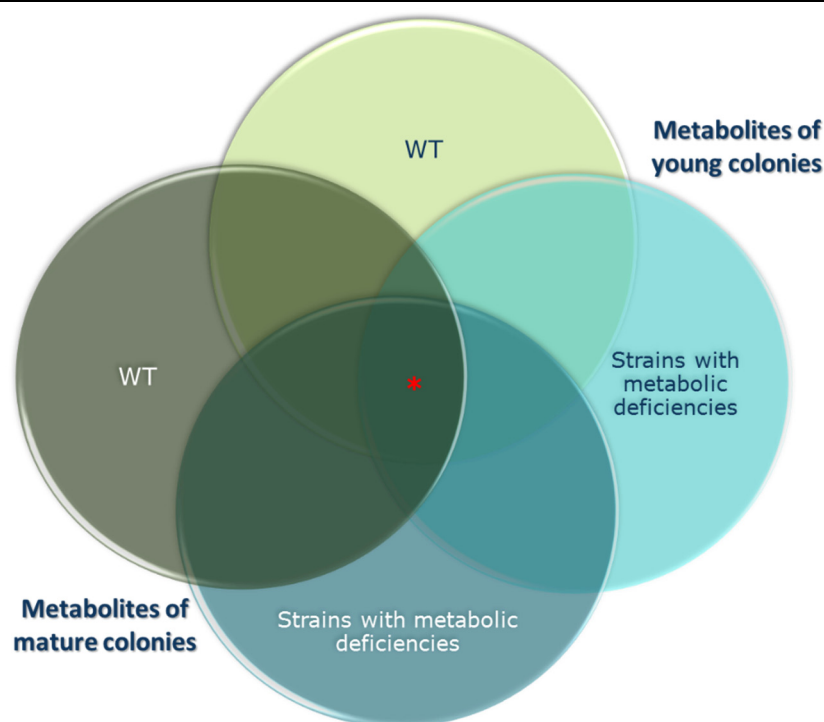
Figure 4.16 Venn diagram showing the target volatiles which may serve as self-avoidance signals. Each circle represents the whole volatome obtained by either a young colony (light) or a mature one (dark). The red asterisk indicates the section containing the target common volatiles for all sampled conditions, which can be signal molecules for negative cell tropisms. For this concept both strains (WT and metabolically deficient) exhibit self-avoidance.

b) transportation and off-line analysis of samples is possible; samples are stored with robust and sealed tubes,

c) headspace is effectively 'reset' after each sampling, producing a volatome profile which is representative of the respective colony stage,

d) most, if not all, volatiles produced by the fungus are sampled in a non-stochastic way, because the sampling is independent of each volatile's vapour pressure,

e) culture aeration conditions remain virtually the same as the flask communicates and is supplied environmental air through its side hose barb. As a result, cells are stressed minimally, and a time-course experiment can be conducted for the same fungal colony.

4.2.6 *A. fumigatus* CEA10 and *ΔpttA* share common VOCs

The volatome of the *A. fumigatus* CEA10 (WT) strain was collected and analysed to identify unique volatile organic compounds. The detailed description of the sampling method, data collection and analysis of the GC-MS results can be found in section 2.6.

GC-MS analysis was carried out by Dr Iain White in the Manchester Institute of Biotechnology (MIB). To identify headspace VOCs related to instrument artefacts (i.e. from TD-GC-MS, sorbent tubes, and headspace apparatus), the list tables of detected compounds from the chromatography analysis were assessed for the presence of any VOCs related to silicone by-products emitted from heating of the analytical equipment or chemical compound leftovers from instrument cleaning and maintenance. A sample chromatogram and its corresponding table from the generated raw data can be found in the Appendix (A.5).

The predominant VOCs were identified as difluoro(dimethyl)silane (1.65 min), ethanol (1.77 min), benzene (2.49), benzoic acid (13.24 min) and several siloxane compounds (contaminants produced from silicone tubing) throughout the retention time range (Cyclotrisiloxane, hexamethyl-, Cyclotetrasiloxane, octamethyl-, Cyclopentasiloxane, decamethyl-, Cycloheptasiloxane, tetradecamethyl-) (Appendix 1). Similarly, assessments were made to identify common VOCs from sterile media control samples. The predominant compounds were identified as acetic acid (2.07 min), benzaldehyde (7.55 min), phenol (7.88 min), acetophenone (10.21 min), nonanal (11.21 min), decanal (13.83 min), 2-ethylhexyl acrylate (14.32 min), and several saturated alkanes (C12-C16).

Unique VOCs were identified in the *A. fumigatus* CEA10 (wild type) cultures at the 12-24-hour time course, present in at least three out of six samples. These included the terpenes cyclopentene (Ret. Time: 1.86 min), himachalene (20.41 min), the terpene precursor molecule α-bergamotene (19.31 min) and the 2-methoxy-furan (4.02 min). VOCs collected with the passive method did not differ significantly from the ones collected actively (data not shown). Unique VOCs were also identified in the *A. fumigatus ΔpptA* strain, namely furan, 2,5-dimethyl- (2.80 min), butanal, 3-methyl- (2.42 min), styrene (5.80 min), and dodecanoic acid (21.93 min).

Several compounds that were common to the *A. fumigatus* CEA10 and the *ΔpptA* strain were identified. Table 4.2 summarises the samples found in at least three out of the six samples analysed per condition and strain for the full culture time-course. Unexpectedly, decanoic acid was detected in the *ΔpptA* cultures, which would imply that the loss-of-function of the PptA palmitoyltransferase is partly recovered so that acetyl-CoA can participate in the fatty acid biosynthesis pathway. Figure 4.17 demonstrates the common compounds in both strains. Due to the limitation of time it

Table 4.2 Common volatiles between the *A. fumigatus* CEA10 and *ΔpptA* strains grown for 12-24 h. Volatiles belong to different chemical functional groups (benzenes, pyrazines, acids, terpenes). Only two compounds (ethyl acetate and himachalane) were produced in significantly different quantities in either strain (Mann-Whitney U test for estimation of *p* value). Data generated by Waqar Ahmed.

VOC	Retention time (*min*)	Molecular weight (*g/mol*)	Mean peak intensity CEA10	Mean peak intensity ΔpptA	*p* value
Ethyl acetate	2.16	88.1	0.16 ± 0.28	1.93 ± 1.52	**0.023**
Butanal, 3-methyl-	2.42	86.1	–	1.03 ± 1.19	0.149
Styrene	5.80	104.1	–	0.61 ± 0.46	0.072
Pyrazine	3.10	80.1	2.17 ± 1.26	3.16 ± 2.28	0.786
Pyrazine, methyl-	4.43	94.1	1.37 ± 0.40	2.10 ± 0.67	0.114
α-Pinene*	6.83	136.2	0.38 ± 0.24	0.25 ± 0.35	0.570
Camphene*	7.25	136.2	0.70 ± 0.13	0.41 ± 0.59	0.441
Limonene*	9.24	136.2	0.62 ± 0.43	0.40 ± 0.60	0.570
Himachalene	20.47	204.4	3.58 ± 3.41	–	**0.026**
Decanoic acid	21.93	172.2646	0.06 ± 0.11	0.58 ± 0.58	0.337

* confirmed identification and retention time using external standard (MS1)
In **bold** = $p < 0.05$

was not possible to test the reported compounds for their ability to influence avoidance in *A. fumigatus,* but it is a question which should be addressed in the future (section 6.4).
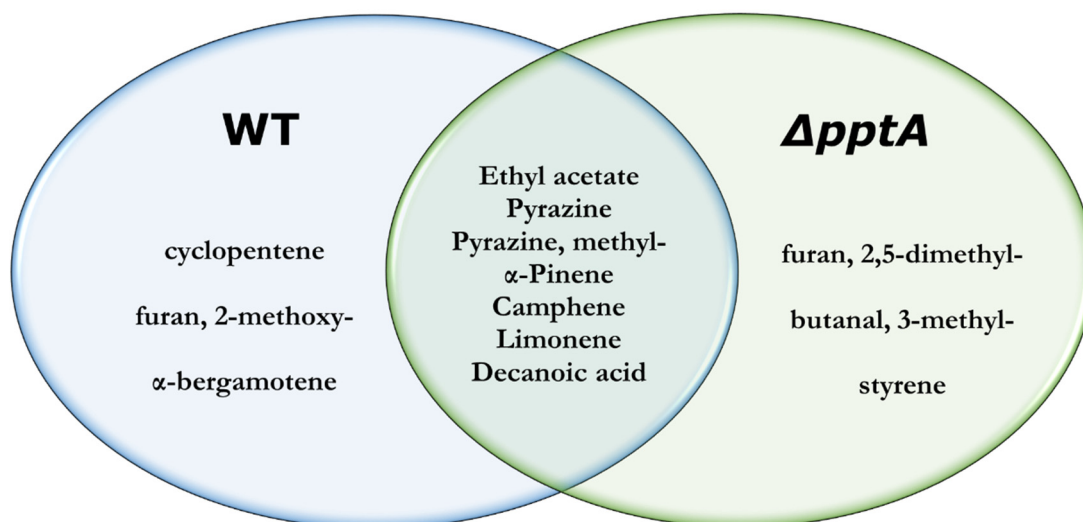
Figure 4.17 Venn diagram showing volatiles in at least 50% of the analysed samples (12-24 hours) of *A. fumigatus* CEA10 and *ΔpptA*. Even though *ΔpptA* has been reported to be limited in producing secondary metabolites, complex metabolites such as limonene and decanoic acid were observed.

4.3 Discussion

The aim of the research described in this chapter was to provide insights into what chemical compound(s) may be acting as extracellular signal molecules to promote negative autotropisms. Previous data has shown that communication between germinating spores and germ tubes growing on cellophane is highly likely to be occurring through air and not via any liquid intermediate (Fig. 4.1). It should be noted that other possible hypotheses which could explain self-avoidance based on this observation (e.g. sensing of and growth toward high nutrient gradients) were not tested. Self-avoidance has also been observed between germlings and spores with intact hydrophobin layer indicating that any communication may be mediated through gases (section 3.2.3). For these reasons, I first chose to investigate whether NO might have negative autotropic properties. However, experiments with a NO scavenger produced no evidence for it having this type of signalling role. In the second study I analysed the inhibitory, tropic and morphological effects of several VOCs on *A. fumigatus* that had previously been characterized as germination autoinhibitors in various fungal species (Table 4.1). From these studies, nonanoic acid turned out to have the most interesting effects but unfortunately without conclusive negative autotropic signal properties. Thirdly, I analysed the volatomes of fungal cultures from 0-24 hours old using a new volatome extraction methodology to gather all the VOCs from the headspace above compounds. Compounds common between two different strains and produced at the different culture times, were identified but none of these was nonanoic acid (Fig. 4.15).

4.3.1 Scavenging of nitric oxide has an impact on germination but does not affect self-avoidance

NO is a small, gaseous, lipophilic molecule able to diffuse freely through the lipid bilayer. Its biochemical traits render it an ideal messenger through Reactive Nitrogen Species (RNS) signalling. Previous studies have provided evidence that NO acts a messenger at key developmental stages in fungi, such as sporulation (Golderer et al., 2001), germination (Samalova et al., 2013) or sexual development (Baidya et al., 2011), in seed germination of plants (Arc et al., 2013; Šírová et al., 2011), and neuron organisation in higher eukaryotes (Grueber and Truman, 1999). Most notably, NO is involved in the antimicrobial response by mononuclear phagocytes (Lowenstein et al., 1994; Stuehr, 2004) and cytotoxic immune response to tumour cells by activated macrophages (Weigert and Brüne, 2008). Nitric oxide radicals have also been shown to provide tolerance towards Amphotericin B (AmB; Vriens et al., 2017). Fungi have developed a NO-homeostasis mechanism using specific proteins, the flavohemoglobins (reviewed by Cánovas et al., 2016) which would also explain the lack of NO involvement in the immune response to *A. fumigatus* conidiospores by pulmonary alveolar macrophages (Michaliszyn et al., 1995), but it would not explain the increased mortality rates of spores in the same fungus by NO donors (Kunert, 1995).

The influence of nitric oxide (NO) on germination and self-avoidance of *A. fumigatus* was assessed in experiments using the NO scavenger, PTIO. Self-avoidance seemed to be unaffected in all tested PTIO concentrations although it did delay germination. As previously mentioned, NO has already been reported to inhibit germination and appressorium formation in *Magnaporthe oryzae* in a similar manner (Samalova et al., 2013). These results thus indicated that NO is not implicated in self-avoidance.

4.3.2 Nonanoic acid influences spore germination in *A. fumigatus*

The effect of organic compounds in germination and self-avoidance was tested by a simple gradient assay using antibiotic filter disks. These involved chemical compounds reported for their use in self-inhibition of germination, and growth modulation (Leeder et al., 2011; Ugalde, 2006; Ugalde and Rodriguez-Urra, 2014). Quite surprisingly, the 8-carbon oxylipins 3-octanol, 1-octen-3-ol, 3-octanone did not show any effect on *A. fumigatus* germination even though they have been reported to inhibit germination in *A.*

nidulans (Herrero-Garcia et al., 2011). Tyrosol [2-(4hydroxyphenyl)ethanol] did not affect germination of *A. fumigatus* either, an expected result as it is a positive germination effector in *C. albicans* (Chen et al., 2004). However, since the controls (chloroform, itraconazole) showed the same unexpected phenotype during the assays, these results suggest that there is a systematic error with how the assay was performed in the first place, rendering these observations untrustworthy at this stage.

Notable compounds with an effect on germination or fungal morphology included farnesol, tryptophol (indole-3-ethanol), nonanal, decanal, hydrogen peroxide, 2,4-hexadienal, and nonanoic acid (Figs. 4.6 and 4.11). Sodium acetate did not induce any avoidance of fungal hyphae at any concentration tested (100 mM – 1M), suggesting that at the tested pH (6.0) sodium acetate is not the self-avoidance signal.

Tryptophol (indole chemical group) and farnesol (sesquiterpene alcohol) gradients did not induce a germination inhibition zone but caused substantial morphological differences in microcolony formation. Notably, microcolonies formed near the antibiotic disk showed reduced growth and thicker hyphae compared to the mycelium at the inhibition zone periphery. Tryptophol also induced a very distinct morphology in the vegetative hyphae compare to the control: stereomicroscopy observations showed that the mycelium is denser and the hyphae thicker. In *S. cerevisiae* it has been reported that tryptophol induces filamentation (Chen and Fink, 2006). Furthermore, a recent study in *N. crassa* has shown that tryptophol is a side-product of the auxin hormone indole-3-acetic acid biosynthesis pathway (Sardar and Kempken, 2018). The reason why tryptophol had different morphological effects on *S. cerevisiae* and *A. fumigatus* are unclear. Farnesol did not seem to affect germination or hyphal growth to the same extent. Although microcolonies were observed near the antibiotic disk where compound concentration is expected to be higher, cells grew normally. This contradicts earlier findings which have reported that farnesol induces apoptosis in *A. fumigatus* (Dichtl et al., 2010) and *A. flavus* (Wang et al., 2014) and limits growth in *C. albicans* and *S. cerevisiae* through translation inhibition (Egbe et al., 2017). It is possible that in the experimental assay farnesol did not diffuse well into the media similar to the controls, thus a concentration gradient was not formed resulting in cells being unaffected by the compound.

The aldehydes nonanal and decanal were present in all the GC-MS samples (media controls and fungal cultures, section 4.2.6), hence they were selected to verify if those compounds present in the media would affect *A. fumigatus* self-avoidance. Hydrogen peroxide has been shown to induce oxidative stress response in filamentous fungi and inhibit germination (Angelova et al., 2005). My results showed that nonanal and decanal affect germination similarly to ROS but in a milder manner (Fig. 4.11-4.12) causing an inhibition zone around the antibiotic disc. Slight differences between the size of the inhibition zone could be attributed to the different diffusion rates of each compound (also applicable to nonanoic acid discussed later). The reason why nonanal and decanal affect *A. fumigatus* germination is unclear since the former has been reported as a germination stimulator in the rust fungus *Puccinia graminis* (Rines et al., 1974). Interestingly, it has also been shown to be an inhibitor of *Arabidopsis thaliana* seed germination (Hung et al., 2014). The aldehyde 2,4-hexadienal, which has also been reported as a germination self-inhibitor in *Colletotrichum fragariae* (Miyagawa et al., 2000), induced a much stronger effect of delayed germination. A possible explanation for the ROS simulated effect of aldehydes (nonanal, decanal, hexadienal) can be found in the aldehydes' chemical properties. Initial VOC concentration placed on the filter disk was high enough to cause autoxidation of the tested aldehyde with environmental oxygen to form peroxides and hydroperoxides. Thus, the observed germination inhibition zone is a secondary effect of the tested aldehydes and does necessarily entail a direct interaction of the compound with the cells.

Of all tested compounds, the most interesting results were obtained from the nonanoic acid assay. Nonanoic acid showed clear intermediate effects on the germination rate of *A. fumigatus*; germination at higher concentrations. This finding is in agreement with previous studies which have shown that nonanoic acid acts as a quorum sensing effector (self-inhibitor) of germination (Breeuwer et al., 1997; Garrett and Robinson, 1969).

4.3.3 Synnematous structure formation is induced in the presence of nonanoic acid

To verify whether the delayed germination in the inhibition zone caused by nonanoic acid recovered, fungal cultures were incubated for a further 24 hours (48 hours total). Although germination did not recover (stereomicroscopy observations not shown), the grown mycelium displayed normal sporulation compared to the control. The most

surprising feature of the mycelium in plates treated with nonanoic acid was the formation of long, white hyphal structures growing almost perpendicularly to the substrate surface (Fig. 4.10). Attempts to image those hyphae using CLSM showed that they are aggregated together into very dense structures. Incubation for a further 24 h resulted in asexual sporulation on top of those structures. These are coremia (or sometimes called synnemata); and are specialised multihyphal aggregates involved in asexual reproduction (Watkinson, 1979; Read, 1994).

Synnemata are characteristic of *Penicillium* species and have been reported formed when mycelia of different strains of the species approach one another in forests (Muntanola-Cvetkovic et al., 2001). Entomopathogen fungi such us *Paecilomyces tenuipes* (Kana-Uchi and Fukatsu, 1999) and *Beauveria bassiana* (Lee et al., 2010), and the nematophagous *Arthrobotrys oligospora* (Werthmann-Cliemas and Lysek, 1986) have been shown to form synnemata. Ordinary saprotrophs such as *Doratomyces stemonitis* have also been shown to produce synnemata (Read, 1994). In addition to a number of *Aspergillus* species described by Raper and Fennell (1965), synnemata have recently been reported in *A. coremiiformis*, *A. togoensis* (Varga et al., 2011), *A. caelatus* (Hubbes, 1975) and an *A. flavus* mutant strain when grown on Murashige-Skoog agar (McAlpin, 2001).

Several attempts have been made to elucidate what promotes the formation of synnemata in filamentous fungi. Studies have shown that the growth media is a determining factor (McAlpin, 2001), and the dark and then light illumination conditions during culture (Kana-Uchi and Fukatsu, 1999). Chemical assays using terpenes and unsaturated acids in *Ceratocystis ulmi* revealed that the most prominent inducer of synnemata formation are linoleic acid ($C_{18}H_{32}O_2$) and, to a lesser extent, limonene ($C_{10}H_{16}$). These chemicals were not tested in *A. fumigatus* to verify their role, if any, in the formation of coremia/synnemata because of the limitation of time. Interestingly, I identified limonene as a VOC secreted by *A. fumigatus* (Fig. 4.17). It is possible that limonene may induce the aggregation and differentiation of hyphae to produce the synnematous structures. To my knowledge this is the first report of coremium formation in *A. fumigatus*. The phenotype is consistent with the formation of an incompatibility reaction associated with vegetative incompatibility (described in section 3.1). This could mean that nonanoic acid may serve as an incompatibility factor between strains of the same species. This hypothesis needs to be tested by further experimentation.

4.3.4 Volatome analysis of *A. fumigatus* CEA10 and *ΔpptA* can provide insight in potential signalling molecules

I found that all tested VOCs that have been reported to effect fungal growth and development (Table 4.1; Leeder et al., 2011; Ugalde and Rodriguez-Urra, 2014) were unsuccessful in inducing avoidance of *A. fumigatus* hyphae. Therefore, it was necessary to identify other VOCs that would be candidate signal molecules for self-avoidance. To achieve this a novel method of volatile headspace sampling was developed with the samples analysed with TD-GC/TOF-MS (section 2.6). The methodology was chosen over the traditional solid phase micro-extraction methods reported before (Costa et al., 2016; Heddergott et al., 2014) due to its greater capacity for trapping VOCs and high durability of materials which allowed storage and transport for off-site analysis. Volatome extraction was achieved by vacuum suction using a specialised pump and was chosen over gas purging (substitution) using inert gases such as CO_2 or N_2 because they resulted in culture disruption by drastically lowering the pH and possibly affecting volatome composition through degradation caused by turbulence inside the headspace chamber. The strain *ΔpptA* was used as an external reference strain because it displayed self-avoidance, yet it is defective in the production of several secondary metabolites (Johns et al., 2017). Hence, common VOCs between the wild type and *ΔpptA* could be potential signals for self-avoidance.

Identified VOCs in *A. fumigatus* CEA10 and *ΔpptA* included monoterpene compounds α-pinene, camphene and limonene. Other identified VOCs of the sesquiterpene class were identified more frequently and in higher abundance in CEA10 (eg. himachalene). Monoterpenes and sesquiterpenes have been reported to be the most prevalent volatiles in *A. fumigatus* (Heddergott et al., 2014) and have also been reported in a study investigating VOCs from human breath as diagnostic markers for invasive pulmonary aspergillosis (Koo et al., 2014). According to the online KEGG database (Ogata et al., 1999) and Heddergott et al. (2014), biosynthesis of terpene VOCs originates from the melvanoate pathway, which is essential for the production of secondary metabolites. Farnesyl diphosphate and geranyl diphosphate act as precursors to monoterpene and sesquiterpene biosynthesis. The suppression of sesquiterpene production in the *ΔpptA* mutant suggests a decreased production of secondary metabolite production. For example, both α-bergamotene and trans-β-bergamotene have been associated with the production of fumagillin (Heddergott et al., 2014), an extracellular metabolite that was absent in the *ΔpptA* LC-MS profiles as shown previously (Johns et al., 2017). Our

results support these observations since α-bergamotene was identified in one CEA10 sample and not at all in *ΔpptA*. Terpene-based compounds are not exclusive to *Aspergillus spp.*; *C. albicans* is known to release the terpenoid farnesol which mediates quorum sensing mechanisms and has been known to inhibit *Pseudomonas aeruginosa* signalling (Cugini et al., 2007; Hornby et al., 2001).

Other compounds common in CEA10 and *ΔpptA* included pyrazines. Pyrazines are nitrogen-containing cyclic compounds are well described for their presence in bacteria metabolism (Schulz and Dickschat, 2007) and have recently gained interest as fungal metabolites (Dickschat, 2017a). Even though pyrazine biosynthesis in *Aspergillus spp.* is not fully understood, pyrazine groups can be found within the chemical structure of some secondary metabolites such as aspergillic acid or gliotoxin (Heddergott et al., 2014), where pyrazines may be released in the headspace during their biosynthesis or degradation.

Ethyl acetate was identified once in CEA10, but significantly more in $\Delta pptA$ (5/6 samples), and has been identified from many fungi (including *A. fumigatus*) in a previous study (Matysik et al., 2009). Butanal, 3-methyl- and decanoic acid were also more frequently identified in $\Delta pptA$. Butanal, 3-methyl-, and a methylated furan were found as discriminatory VOCs in a recent study investigating fungal headspace profiles under hypoxic conditions (Rees et al., 2017). Increased ethyl acetate, butanal, 3-methyl-, decanoic acid, and the identified furan-based compounds in the $\Delta pptA$ strain may be the result of accumulation of these volatile components because of the disruption of fatty acid synthesis due to the absence of PPTase (Dickschat, 2017).

Several VOCs previously reported in *A. fumigatus* (Heddergott et al., 2014) or *A. niger* (Costa et al., 2016) were not identified in our samples, a result which can be explained in several ways. The most important aspect of our analysis was that it aimed at identifying VOCs which are present during early fungal growth (6-12 hours) and during later developmental including early sporulation events (12-24 hours). Besides the aim of identifying novel VOCs which may be self-avoidance signals, there are also medical applications of this analysis. A recent study has demonstrated that communication of microbes via VOCs in human organotypic lung models is possible (Barkal et al., 2017). Therefore, it is important to identify VOCs which are indicative of germination and early fungal growth and can be used as infection markers of timely fungal infection

diagnosis as it has already been shown in studies (Hertel et al., 2015; Rees et al., 2017). For instance, our results demonstrate the absence of terpene compounds from 0 to 8 h, and their presence after 12-24 h. As terpene compounds are thought to be by-products from the production of several secondary metabolites, they may be useful indicators of successful host colonisation or culture growth. In contrast, Heddergott et al. (2014) analysed the volatome of *A. fumigatus* after 48 hpi with the SPME method, which would explain the prevalence of terpene-based VOCs in their results. Another important aspect of the results of my analysis is that they are based on a relatively low number of replicates (6 per condition) which would explain why only few VOCs are consistently present across >50% of the samples.

4.4 Summary

The main results of the research described in this chapter can be summarised as follows:

(1) NO is probably not a VOC involved in signalling negative autotropisms because highly selective scavenging of NO with PTIO does not affect it.

(2) A range of VOCs, which have been previously shown to be shown to cause self-inhibition of spore germination, were tested to determine whether they also affect self-avoidance. However, the results from these experiments proved inconclusive.

(3) Nonanoic acid induced the formation of synnemata (coremia) after 48 hours at the edge of the germination inhibition zone. It was hypothesised that nonanoic may play a role as a vegetative compatibility factor in producing this form of apparent incompatibility reaction.

(4) Several volatiles common to the wild type and a secondary metabolism deficient strain (*ΔpptA*) were identified by GC-MS and need to be assayed further to investigate whether they have a role in self-avoidance.

4.5 References

Akaike, T., Yoshida, M., Miyamoto, Y., Sato, K., Kohno, M., Sasamoto, K., Miyazaki, K., Ueda, S., Maeda, H., 1993. Antagonistic Action of Imidazolineoxyl N-Oxides against Endothelium-Derived Relaxing Factor/*NO through a Radical Reaction. Biochemistry 32, 827–832. https://doi.org/10.1021/bi00054a013

Albuquerque, P., Casadevall, A., 2012. Quorum sensing in fungi a review. Med. Mycol. 50, 337–345. https://doi.org/10.3109/13693786.2011.652201

Angelova, M.B., Pashova, S.B., Spasova, B.K., Vassilev, S. V., Slokoska, L.S., 2005. Oxidative stress response of filamentous fungi induced by hydrogen peroxide and paraquat. Mycol. Res. 109, 150–158. https://doi.org/10.1017/S0953756204001352

Arc, E., Galland, M., Godin, B., Cueff, G., Rajjou, L., 2013. Nitric oxide implication in the control of seed dormancy and germination. Front. Plant Sci. 4, 1–13. https://doi.org/10.3389/fpls.2013.00346

Baidya, S., Cary, J.W., Grayburn, W.S., Calvo, A.M., 2011. Role of nitric oxide and flavohemoglobin homolog genes in *Aspergillus nidulans* sexual development and mycotoxin production. Appl. Environ. Microbiol. 77, 5524–5528. https://doi.org/10.1128/AEM.00638-11

Barkal, L.J., Procknow, C.L., Álvarez-García, Y.R., Niu, M., Jiménez-Torres, J.A., Brockman-Schneider, R.A., Gern, J.E., Denlinger, L.C., Theberge, A.B., Keller, N.P., Berthier, E., Beebe, D.J., 2017. Microbial volatile communication in human organotypic lung models. Nat. Commun. 8, 1770. https://doi.org/10.1038/s41467-017-01985-4

Bignell, E., Cairns, T.C., Throckmorton, K., Nierman, W.C., Keller, N.P., 2016. Secondary metabolite arsenal of an opportunistic pathogenic fungus. Philos. Trans. R. Soc. B Biol. Sci. 371, 1–9. https://doi.org/10.1098/rstb.2016.0023

Breeuwer, P., De Reu, J.C., Drocourt, J.L., Rombouts, F.M., Abee, T., 1997. Nonanoic acid, a fungal self-inhibitor, prevents germination of *Rhizopus oligosporus* sporangiospores by dissipation of the pH gradient. Appl. Environ. Microbiol. 63, 178–185.

Cánovas, D., Marcos, J.F., Marcos, A.T., Strauss, J., 2016. Nitric oxide in fungi: is there NO light at the end of the tunnel? Curr. Genet. 62, 513–518. https://doi.org/10.1007/s00294-016-0574-6

Chen, H., Fink, G.R., 2006. Feedback control of mophogenesis in fungi by aromatic alcohols. Gene Dev. 20, 1150–1161. https://doi.org/10.1101/gad.1411806.sponse

Chen, H., Fujita, M., Feng, Q., Clardy, J., Fink, G.R., 2004. Tyrosol is a quorum-sensing molecule in *Candida albicans*. Proc. Natl. Acad. Sci. 101, 5048–5052. https://doi.org/10.1073/pnas.0401416101

Chitarra, G.S., Abee, T., Rombouts, F.M., Posthumus, M. a, Dijksterhuis, J., 2004. Germination of *Penicillium paneum* Conidia Is Regulated by 1-Octen-3-ol, a Volatile Self-Inhibitor. Appl. Environ. Microbiol. 70, 2823–2829. https://doi.org/10.1128/AEM.70.5.2823-2829.2004

Costa, C.P., Gonçalves Silva, D., Rudnitskaya, A., Almeida, A., Rocha, S.M., 2016. Shedding light on *Aspergillus niger* volatile exometabolome. Sci. Rep. 6, 27441. https://doi.org/10.1038/srep27441

Cugini, C., Calfee, M.W., Farrow, J.M., Morales, D.K., Pesci, E.C., Hogan, D.A., 2007. Farnesol, a common sesquiterpene, inhibits PQS production in *Pseudomonas aeruginosa*. Mol. Microbiol. 65, 896–906. https://doi.org/10.1111/j.1365-2958.2007.05840.x

Dichtl, K., Ebel, F., Dirr, F., Routier, F.H., Heesemann, J., Wagener, J., 2010. Farnesol misplaces tip-localized Rho proteins and inhibits cell wall integrity signalling in *Aspergillus fumigatus*. Mol. Microbiol. 76, 1191–1204. https://doi.org/10.1111/j.1365-2958.2010.07170.x

Dickschat, J.S., 2017a. Fungal volatiles – a survey from edible mushrooms to moulds. Nat. Prod. Rep. 34, 310–328. https://doi.org/10.1039/C7NP00003K

Dickschat, J.S., 2017b. Fungal volatiles – a survey from edible mushrooms to moulds. Nat. Prod. Rep. 34, 310–328. https://doi.org/10.1039/C7NP00003K

Egbe, N.E., Dornelles, T.O., Paget, C.M., Castelli, L.M., Ashe, M.P., 2017. Farnesol inhibits translation to limit growth and filamentation in *C. albicans* and *S. cerevisiae*.

Microb. Cell 4, 294–304. https://doi.org/10.15698/mic2017.09.589

Garrett, M.K., Robinson, P.M., 1969. A stable inhibitor of spore germination produced by fungi. Arch. f??r Mikrobiol. 67, 370–377. https://doi.org/10.1007/BF00412583

Gillot, G., Decourcelle, N., Dauer, G., Barbier, G., Coton, E., Delmail, D., Mounier, J., 2016. 1-Octanol, a self-inhibitor of spore germination in *Penicillium camemberti*. Food Microbiol. 57, 1–7. https://doi.org/10.1016/j.fm.2015.12.008

Golderer, G., Werner, E.R., Leitner, S., Gröbner, P., Werner-Felmayer, G., 2001. Nitric oxide synthase is induced in sporulation of *Physarum polycephalum*. Genes Dev. 15, 1299–1309. https://doi.org/10.1101/gad.890501

Goldstein, S., Russo, A., Samuni, A., 2003. Reactions of PTIO and Carboxy-PTIO with .NO, .NO 2, and O2.-. J. Biol. Chem. 278, 50949–50955. https://doi.org/10.1074/jbc.M308317200

Grueber, W.B., Truman, J.W., 1999. Development and organization of a nitric-oxide-sensitive peripheral neural plexus in larvae of the moth, Manduca sexta. J. Comp. Neurol. 404, 127–141. https://doi.org/10.1002/(SICI)1096-9861(19990201)404:1<127::AID-CNE10>3.0.CO;2-M

Heddergott, C., Calvo, A.M., Latge, J.P., 2014. The Volatome of *Aspergillus fumigatus*. Eukaryot. Cell 13, 1014–1025. https://doi.org/10.1128/EC.00074-14

Herrero-Garcia, E., Garzia, A., Cordobés, S., Espeso, E.A., Ugalde, U., 2011. 8-Carbon oxylipins inhibit germination and growth, and stimulate aerial conidiation in *Aspergillus nidulans*. Fungal Biol. 115, 393–400. https://doi.org/10.1016/j.funbio.2011.02.005

Hertel, M., Hartwig, S., Schütte, E., Gillissen, B., Preissner, R., Schmidt-Westhausen, A.M., Paris, S., Kastner, I., Preissner, S., 2015. Identification of signature volatiles to discriminate *Candida albicans, glabrata, krusei* and *tropicalis* using gas chromatography and mass spectrometry. Mycoses n/a-n/a.

https://doi.org/10.1111/myc.12442

Hornby, J.M., Jensen, E.C., Lisec, A.D., Tasto, J., Jahnke, B., Shoemaker, R., Nickerson, K.W., Tasto, J.J., Dussault, P., 2001. Quorum Sensing in the Dimorphic Fungus *Candida albicans* Is Mediated by Farnesol Appl. Environ. Microbiol. 67, 2982–2992. https://doi.org/10.1128/AEM.67.7.2982

Hubbes, M., 1975. Terpenes and unsaturated fatty acids trigger coremia formation by *Ceratocystis ulmi*. For. Pathol. 5, 129–137. https://doi.org/10.1111/j.1439-0329.1975.tb00456.x

Hung, R., Lee, S., Rodriguez-Saona, C., Bennett, J.W., 2014. Common gas phase molecules from fungi affect seed germination and plant health in *Arabidopsis thaliana*. AMB Express 4, 53. https://doi.org/10.1186/s13568-014-0053-8

Inglis, D., Binkley, J., Skrzypek, M., Arnaud, M., Cerqueira, G., Shah, P., Wymore, F., Wortman, J., Sherlock, G., 2013. Comprehensive annotation of secondary metabolite biosynthetic genes and gene clusters of *Aspergillus nidulans*, *A. fumigatus*, *A. niger* and *A. oryzae*. BMC Microbiol. 13, 91.

Johns, A., Scharf, D.H., Gsaller, F., Schmidt, H., Heinekamp, T., Straßburger, M., Oliver, J.D., Birch, M., Beckmann, N., Dobb, K.S., Gilsenan, J., Rash, B., Bignell, E., Brakhage, A.A., Bromley, M.J., 2017. A Nonredundant Phosphopantetheinyl Transferase, PptA, Is a Novel Antifungal Target That Directs Secondary Metabolite, Siderophore, and Lysine Biosynthesis in *Aspergillus fumigatus* and Is Critical for Pathogenicity. MBio 8, e01504-16. https://doi.org/10.1128/mBio.01504-16

Jones, S.E., Elliot, M.A., 2017. Streptomyces Exploration: Competition, Volatile Communication and New Bacterial Behaviours. Trends Microbiol. 25, 522–531. https://doi.org/10.1016/j.tim.2017.02.001

Kana-Uchi, A., Fukatsu, T., 1999. Light-induced fruit body formation of an entomogenous fungus Paecilomyces tenuipes. Mycoscience 40, 349–351. https://doi.org/10.1007/BF02463879

Koo, S., Thomas, H.R., Daniels, S.D., Lynch, R.C., Fortier, S.M., Shea, M.M., Rearden, P., Comolli, J.C., Baden, L.R., Marty, F.M., 2014. A breath fungal secondary metabolite signature to diagnose invasive aspergillosis. Clin. Infect. Dis. 59, 1733–1740. https://doi.org/10.1093/cid/ciu725

Kunert, J., 1995. Effect of nitric oxide donors on survival of conidia, germination and growth ofAspergillus fumigatus in vitro. Folia Microbiol. (Praha). 40, 238–244. https://doi.org/10.1007/BF02814199

Lee, K.-M., Nam, S.-H., Yoon, C.-S., Jeon, J.-Y., Yeo, J.-H., Lee, K.-G., 2010. Conditions for Formation of Synnemata from *Beauveria bassiana*. Korean J. Appl. Entomol. 49, 43–47. https://doi.org/10.5656/KSAE.2010.49.1.043

Leeder, A.C., Palma-Guerrero, J., Glass, N.L., 2011. The social network: deciphering fungal language. Nat. Rev. Microbiol. 9, 440–451. https://doi.org/10.1038/nrmicro2580

Lowenstein, C.J., Dinerman, J.L., Snyder, S.H., 1994. Nitric oxide: A physiologic messenger. Ann. Intern. Med. 120, 227–237. https://doi.org/10.1146/annurev.bi.63.070194.001135

Matysik, S., Herbarth, O., Mueller, A., 2009. Determination of microbial volatile organic compounds (MVOCs) by passive sampling onto charcoal sorbents. Chemosphere 76, 114–119. https://doi.org/10.1016/j.chemosphere.2009.02.010

McAlpin, C.E., 2001. An *Aspergillus flavus* Mutant Producing Stipitate Sclerotia and Synnemata. Mycologia 93, 552. https://doi.org/10.2307/3761740

Michaliszyn, E., Senechal, S., Martel, P., De Repentigny, L., 1995. Lack of involvement of nitric oxide in killing of *Aspergillus fumigatus* conidia by pulmonary alveolar macrophages. Infect. Immun. 63, 2075–2078.

Miyagawa, H., Inoue, M., Yamanaka, H., Tsurushima, T., Ueno, T., 2000. Chemistry of Spore Germination Self-Inhibitors from the Plant Pathogenic Fungus *Colletotrichum*

fragariae, in: Agrochemical Discovery. pp. 62–71. https://doi.org/10.1021/bk-2001-0774.ch006

Muntanola-Cvetkovic, M., Hoyo, P., Gomez-Bolea, A., 2001. *Penicillium aureocephalum* anam. sp nov. Fungal Divers. 7, 71–79.

Ogata, H., Goto, S., Sato, K., Fujibuchi, W., Bono, H., Kanehisa, M., 1999. KEGG: Kyoto encyclopedia of genes and genomes. Nucleic Acids Res. 27, 29–34. https://doi.org/10.1093/nar/27.1.29

Owens, R.A., Hammel, S., Sheridan, K.J., Jones, G.W., Doyle, S., 2014. A proteomic approach to investigating gene cluster expression and secondary metabolite functionality in *Aspergillus fumigatus*. PLoS One 9. https://doi.org/10.1371/journal.pone.0106942

Raper, K.B.; Fennell, D.I., 1965. The Genus Aspergillus, 1st ed. Williams and Wilkins.

Read, N.D., 2017. Fungal cell structure and organization, in: Kibbler, C., Barton, R., Gow, N.A.R., Howell, S., MacCallum, D., Manuel, R. (Eds.), Oxford Textbook in Medical Mycology. Oxford University Press, p. 400.

Read, N.D., 1994. Cellular nature and multicellular morphogenesis of higher fungi, in: Ingram, D., Hudson, A. (Eds.), In Shape and Form in Plants and Fungi. Academic Press, pp. 254–271.

Rees, C.A., Stefanuto, P.-H., Beattie, S.R., Bultaman, K.M., Cramer, R.A., Hill, J.E., 2017. Sniffing out the hypoxia volatile metabolic signature of *Aspergillus fumigatus*. J. Breath 11, 036003.

Rines, H.W., French, R.C., Daasch, L.W., 1974. Nonanal and 6-methyl-5-hepten-2-one: endogenous germination stimulators of uredospores of *Puccinia graminis* var. tritici and other rusts. J. Agric. Food Chem. 22, 96–100.

Samalova, M., Johnson, J., Illes, M., Kelly, S., Fricker, M., Gurr, S., 2013. Nitric oxide generated by the rice blast fungus *Magnaporthe oryzae* drives plant infection. New Phytol. 197, 207–222. https://doi.org/10.1111/j.1469-8137.2012.04368.x

Sardar, P., Kempken, F., 2018. Characterization of indole-3-pyruvic acid pathway-mediated biosynthesis of auxin in *Neurospora crassa*. PLoS One 13, e0192293. https://doi.org/10.1371/journal.pone.0192293

Schulz, S., Dickschat, J.S., 2007. Bacterial volatiles: the smell of small organisms. Nat. Prod. Rep. 24, 814–842. https://doi.org/10.1039/b507392h

Šírová, J., Sedlářová, M., Piterková, J., Luhová, L., Petřivalský, M., 2011. The role of nitric oxide in the germination of plant seeds and pollen. Plant Sci. 181, 560–572. https://doi.org/10.1016/J.PLANTSCI.2011.03.014

Spiro, S., 2007. Regulators of bacterial responses to nitric oxide. FEMS Microbiol. Rev. 31, 193–211. https://doi.org/10.1111/j.1574-6976.2006.00061.x

Stuehr, D.J., 2004. Enzymes of the L-arginine to nitric oxide pathway. J. Nutr. 134, 2748S–2751S; discussion 2765S–2767S.

Ugalde, U., 2006. Autoregulatory signals in mycelial fungi. Growth, Differ. Sex. 203–213. https://doi.org/10.1007/3-540-28135-5_11

Ugalde, U., Rodriguez-Urra, A.B., 2014. The Mycelium Blueprint: insights into the cues that shape the filamentous fungal colony. Appl. Microbiol. Biotechnol. 98, 8809–8819. https://doi.org/10.1007/s00253-014-6019-6

Varga, J., Frisvad, J.C., Samson, R.A., 2011. Two new aflatoxin producing species, and an overview of *Aspergillus section* Flavi. Stud. Mycol. 69, 57–80. https://doi.org/10.3114/sim.2011.69.05

Vriens, K., Kumar, P.T., Struyfs, C., Cools, T.L., Spincemaille, P., Kokalj, T., Sampaio-Marques, B., Ludovico, P., Lammertyn, J., Cammue, B.P.A., Thevissen, K., 2017. Increasing the Fungicidal Action of Amphotericin B by Inhibiting the Nitric Oxide-Dependent Tolerance Pathway. Oxid. Med. Cell. Longev. 2017, 1–17. https://doi.org/10.1155/2017/4064628

Wang, X., Wang, Y., Zhou, Y., Wei, X., 2014. Farnesol induces apoptosis-like cell death in the pathogenic fungus *Aspergillus flavus*. Mycologia 106, 881–888. https://doi.org/10.3852/13-292

Wang, Y., Ruby, E.G., 2011. The roles of NO in microbial symbioses. Cell. Microbiol. 13, 518–526. https://doi.org/10.1111/j.1462-5822.2011.01576.x

Watkinson Sarah C., 1979. Growth of Rhizmorphs, Mycelial Strands, Coremia and Sclerotia.

Weigert, A., Brüne, B., 2008. Nitric oxide, apoptosis and macrophage polarization during tumor progression. Nitric Oxide - Biol. Chem. 19, 95–102. https://doi.org/10.1016/j.niox.2008.04.021

Werthmann-Cliemas, J., Lysek, G., 1986. Formation of synnematous conidiophores in *Arthrobotrys oligospora*. Trans. Br. Mycol. Soc. 87, 656–658. https://doi.org/10.1016/S0007-1536(86)80112-7

[Blank page]

Chapter 5

Mechanistic investigation of signalling involved in fungal self-avoidance

[Blank page]

5.1 Introduction

Chapter 3 showed that negative autotropisms are important in regulating the morphogenesis of the colony from the point of determining the site of germ tube emergence from spores, and in regulating the directional growth of germ tubes and mature vegetative hyphae relative to those of other germ tubes and vegetative hyphae in their proximity. The mechanistic basis of negative autotropic growth responses in fungi is not understood. The research described in chapter 4 attempted, using several different approaches, to identify the extracellular signal molecule(s) responsible for negative autotropisms. However, no strong candidates for the self-avoidance signal(s) were found.

In this chapter, mutant screening was performed using a collection of deletion (knockout) mutants of *A. fumigatus* that had been generated at the Hans-Knöll Institute (HKI, Jena) and the University of Manchester. These mutants were defective in two classes of proteins: G-coupled protein receptors and protein kinases.

The only studies that have been performed to understand the intracellular signalling involved in negative autotropisms in filamentous fungi have been conducted on *N. crassa* using a fluorescent reporter of active rho GTPases (Lichius et al., 2014). This study provided evidence that these small GTPases, with CDC42 being the most likely candidate, are involved during avoidance between two germ tubes of the same mating type. More specifically, Lichius et al. (2014) showed that as germ tubes approached each other, re-localisation of the small GTPases away from the adjacent germ tubes occurred, and this was followed by the repulsive growth of the germ tube tips resulting in negative autotropisms.

A study in *S. cerevisiae* suggested that a protease, Bar1, secreted by *MAT*a cells can act as a regulator of the pheromone concentration (by degrading the α-factor), enabling *MAT*a cells to recognise and avoid each other. By creating a gradient through degradation of the α-factor, *MAT*a cells move towards *MAT*α cells and away from *MAT*a. The study proposed that this mechanism has been established as a means for efficient mating between yeast cells (Jin et al., 2011).
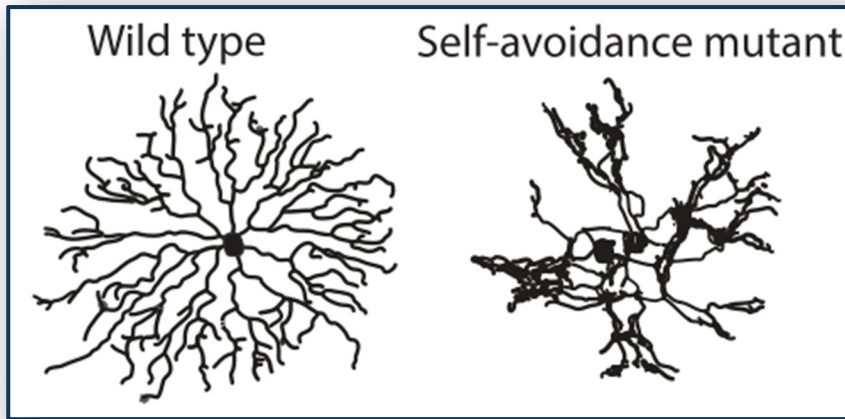
Figure 5.1 Self-avoidance mutant phenotypes in neuron cells. The filamentous axons of a mutant dendrite aggregate resulting in limited coverage of the area in which the cell grows. Reproduced from Lefebvre *et al.* (2015).

The only previous mutant analyses on self-avoidance responses have been made in neuronal cells. It has been previously shown that the mechanistic basis self-avoidance can be described in three stages: (i) (self-)recognition of cells either through pheromones or touch mechanisms by receptors localised on the membrane, (ii) activation downstream signalling cascades which results in (iii) axon rearrangement by actin-polymerisation (reviewed by Guan & Rao, 2003; Lefebvre, Sanes, & Kay, 2015; section 1.3.6.1). Interestingly, the consistent phenotype of self-avoidance dendrite mutants shows that axons tend to aggregate together due to either loss of self-recognition or inability to diverge away from neighbouring structures (Fig. 5.1).

5.1.1 Aims of the research described in this chapter

The overall aim of the research described in this chapter was to perform a phenotypic screen of knockout strain libraries of *A. fumigatus*, to determine components of the signalling pathways involved in the regulation of negative autotropisms. Mutants compromised in the following two classes of proteins were screened:

(1) Sixteen (16) G-protein coupled receptors (GPCRs).
(2) Ninety (90) protein kinases.

5.2 Results

5.2.1 Phenotypic screens performed on GPCR and kinase deletion mutants

To provide evidence for different GPCRs and kinases being involved in regulating negative autotropisms in *A. fumigatus*, deletion mutant collections of 16 GPCRs (provided by Axel Brakhage's group) and 90 protein kinase (provided by the Manchester Fungal Infection Group) were phenotypically screened. Each strain was grown on Aspergillus minimal agar medium (AMMA) and Aspergillus complete agar medium (ACMA) and observed by stereomicroscopy at 24 and 48 hpi as described in section 2.5.4. The screen was conducted with a non-targeted, blind method to eliminate any bias; each strain was assigned a code without prior specific knowledge of its corresponding gene deletion. Imaging was done in triplicates per strain (at least 3 distinct colonies per strain and different Petri dish per colony).

Phenotypes were primarily determined on AMMA 3% w/v to ensure as many hyphae in the same focal plane as possible (see section 3.2.6), as hyphae were more sparsely distributed on this type of media and growth/development patterns were easier to distinguish. Furthermore, the hyphal aggregation phenotype was more obvious on AMMA. For the purposes of the screen two traits were looked into in terms of growth: (i) the ability of the fungus to grow on chemically defined minimal media, and (ii) the presence or lack of avoidance between vegetative hyphae at the periphery of the young colonies or between germ tubes during the early stages of colony initiation. Vegetative hyphal/germ tube aggregation were the morphological phenotypes used as indicators of defective self-avoidance responses.

5.2.1.1 Phenotypic screen of G-protein coupled receptor knockout mutants

G-protein coupled receptors have a central role in extracellular sensing and responses to extracellular signals in fungi and are responsible for the activation of a wide range of signalling pathways (Xue et al., 2008). For this reason, 16 strains which had had their genes encoding for GPCRs deleted were screened to verify if one or more were compromised in negative autotropisms.

All GPCR null mutants displayed normal macroscopic growth phenotypes, as viewed with the naked eye, on both minimal AMMA and complete ACMA media (Fig. 5.3 and 5.4). However, 7 out of the 16 GPCR mutants showed hyphal aggregations compared to the wild type when observed grown on ACMA under the stereomicroscope (Fig. 5.4). These aggregations were regarded as a likely result of defective self-avoidance responses. The lack of self-avoidance was also evident during germination of all of the same 7 GPCR null strains in AMM that were observed to undergo aggregation between vegetative hyphae. The germ tubes of these mutants aggregated and were not equally spaced apart like in the wild type (Fig. 5.5). Table 5.1 summarises the phenotypes of the GPCR mutants in relation to self-avoidance. GPCRs that belonged to Classes I and II (pheromone reception), III (carbon sensing), IV (nitrogen sensing) and VIII (progesterone-like receptors) underwent germ tube and vegetative hyphal aggregation. These Classes of GPCRs are as described in Cabrera *et al.* (2015) and Lafon *et al.* (2006).

To verify quantitively the stereomicroscopic observations, GPCR self-avoidance null mutants were quantified as follows: hyphae grown on AMMA were measured for avoidance and crossover events on both the wild type and the GPCR knockout strains.
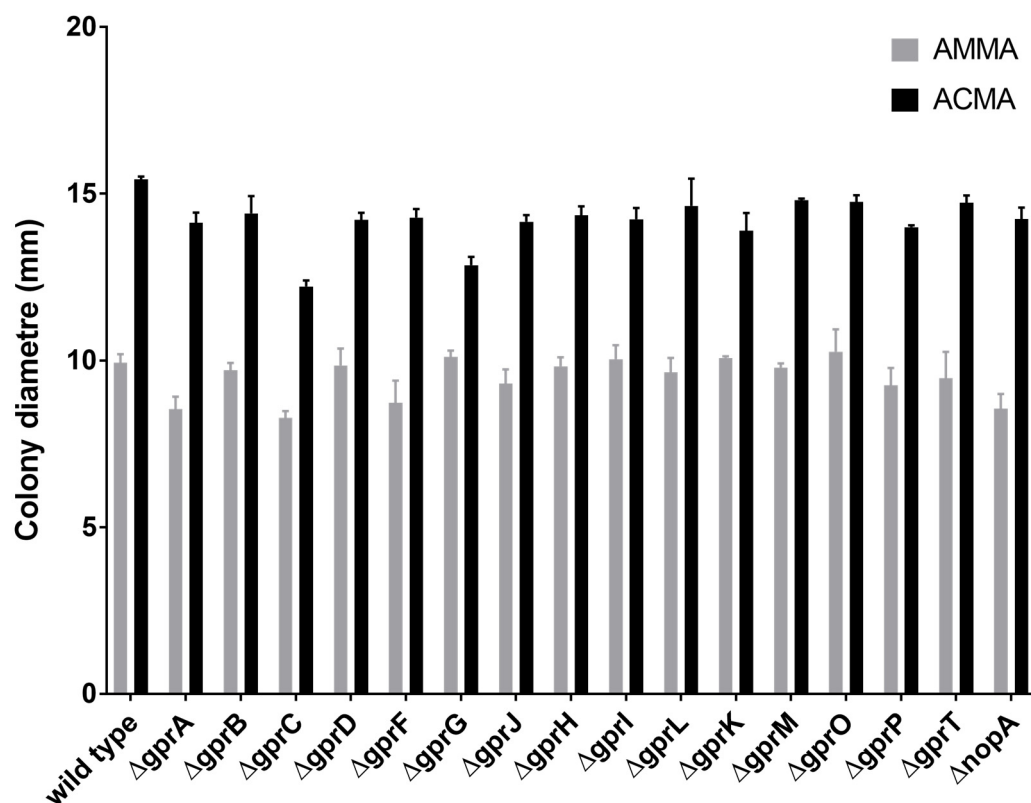
Figure 5.2 Mean colony size of GPCR null strains grown on AMMA and ACMA for 24 hours compared to the wild type. Apart from *ΔgprC* and *ΔgprG* no significant differences were observed. Measurements of five colonies per strain.

Table 5.1 GPCR deletion mutant strains classification in *A. fumigatus* (Lafon *et al.*, 2006), their functions, growth, and their phenotype in relation to defects in the self-avoidance based on the results presented in Figures 5.3-5.4. The self-avoidance null phenotypes were observed when the fungal strains were grown on AMMA for 24 hours. mPR-like/PAQR denotes the progesterone receptors (mPR) belonging to the progestin and adipoQ receptor (PAQR) gene family.

Fungal GPCR Class	Description GPCR Class	*A. fumigatus* gene	*A. fumigatus* Locus	KO exhibits self-avoidance	AMMA Growth (mm)	ACMA Growth (mm)
I	Pheromone receptor-like	*gprA*	AFUB_034900	No	8.53	14.12
II	Pheromone receptor-like	*gprB*	AFUB_055410	No	9.71	14.41
III	Carbon sensor	*gprC*	AFUB_090350	No	8.28	12.22
	Carbon sensor	*gprD*	AFUB_028290	No	9.85	14.21
IV	Nitrogen sensor	*gprF*	AFUB_052610	No	8.73	14.28
	Nitrogen sensor	*gprG*	AFUB_011350	Yes	10.1	12.85
	Nitrogen sensor	*gprJ*	AFUB_007220	No	9.31	14.16
V	cAMP sensor	*gprH*	AFUB_052640	Yes	9.83	14.35
	cAMP sensor	*gprI*	AFUB_047630	Yes	10.04	14.23
	cAMP sensor	*gprL*	AFUB_046660	Yes	9.64	14.63
VI	RGS domain	*gprK*	AFUB_101830	Yes	10.08	13.89
VII	mPR-like/PAQR	*gprM*	AFUB_090880	Yes	9.79	14.8
VIII	mPR-like/PAQR	*gprO*	AFUB_038590	Yes	10.26	14.75
	mPR-like/PAQR	*gprP*	AFUB_073100	Yes	9.25	14
	mPR-like/PAQR	*gprT*	AFUB_096360	No	9.47	14.72
IX	Microbial Opsin	*nopA*	AFUB_088000	Yes	8.56	14.24
		wild type		Yes	9.93	15.43

For the purposes of the quantification only the main hyphae were considered (not lagging hyphal branches, which would *de facto* have a more confined space to grow into). Avoidance events were defined as a pair of hyphae converging and then maintaining visible distance, e.g. grow in parallel. Crossover events were defined as events in which considerable lengths of hyphae (> 20 µm) were growing together, or hyphae forming aggregates, or a pair of hyphae approaching each other and crossing over without any growth redirection. A ratio of crossover to avoidance events was calculated. Data was normalised, and a one-way ANOVA was carried out to test the significance. The results are summarised in Fig. 5.6.
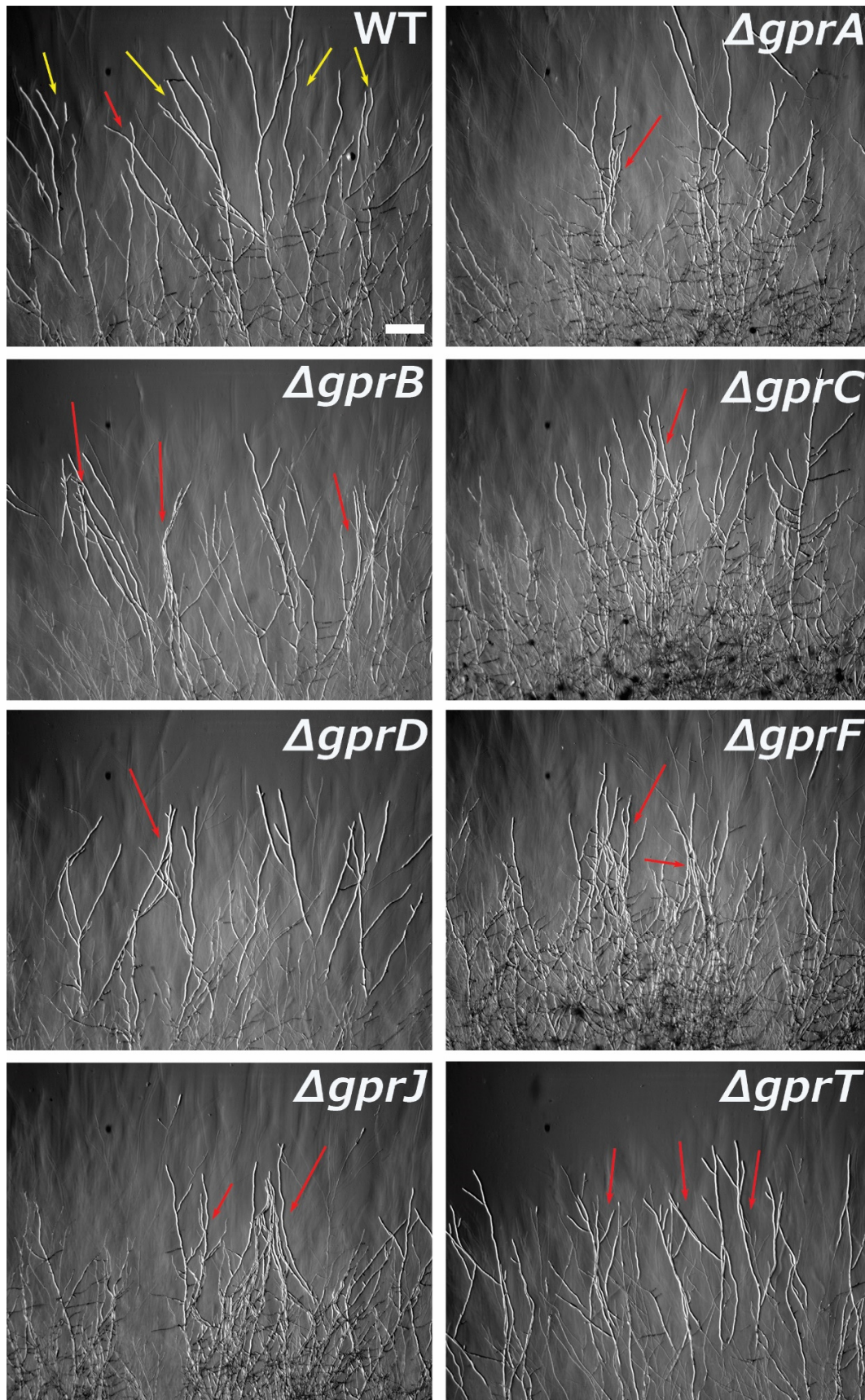
Figure 5.3 Stereomicroscopy images of GPCR deletion mutant strains showing negative autotropisms when grown on AMMA. Red arrows indicate events of hyphal aggregations, while yellow arrows show events of cell avoidance. Scale bar = 100 µm.
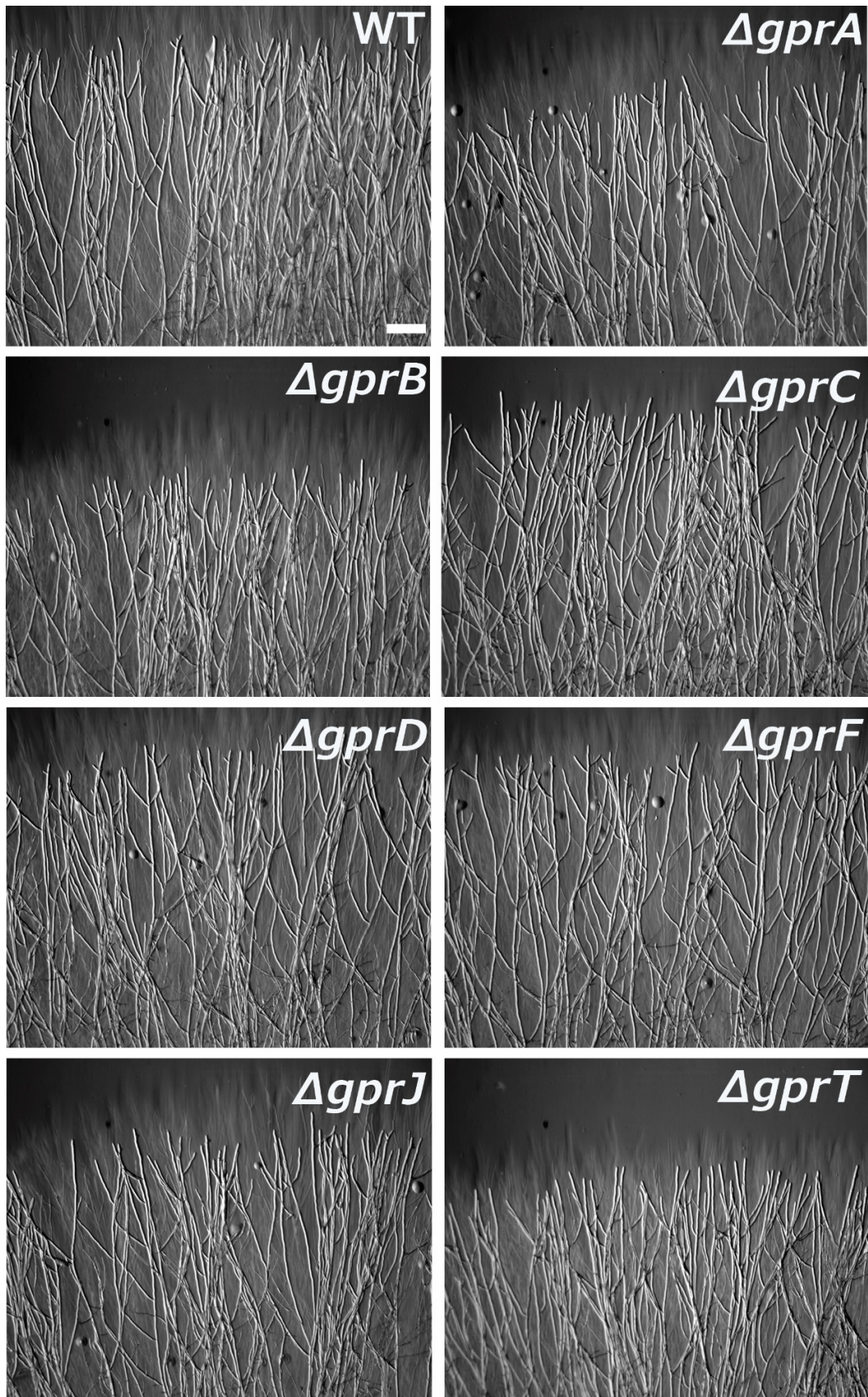
Figure 5.4 Stereomicroscopy images of GPCR deletion mutant strains grown on ACMA. No significant change to phenotype compared to the wild type was observed in these mutant strains. Scale bar = 100 μm.
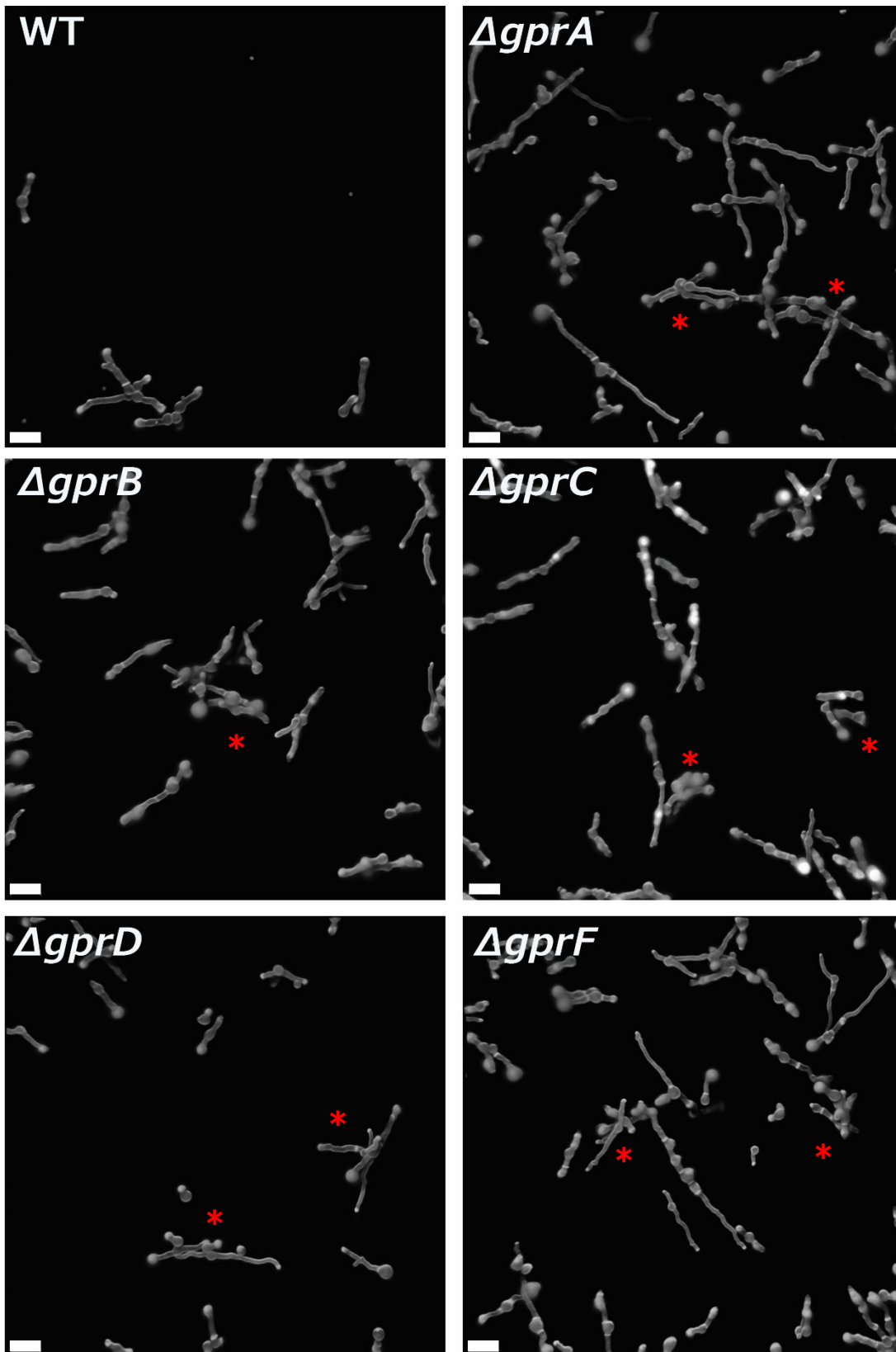
Figure 5.5 Confocal images of GPCR deletion mutant strains grown on AMM (10 hpi). Aggregated germ tubes (red asterisk) during germination were observed compared to the wild type. Cells are stained with calcofluor white. Scale bar = 20 μm.
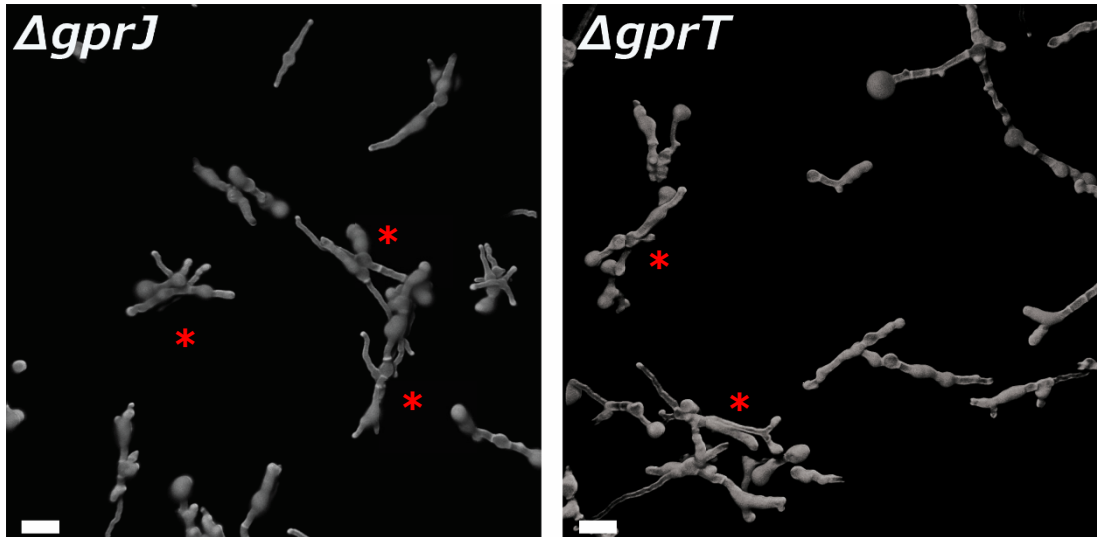
Figure 5.5 (continued) Confocal images of GPCR deletion mutant strains grown on AMM (10 hpi). Hyphal aggregations (red asterisk) during germination are observed compared to the wild type. Cells are stained with calcofluor white. Scale bar = 20 μm.
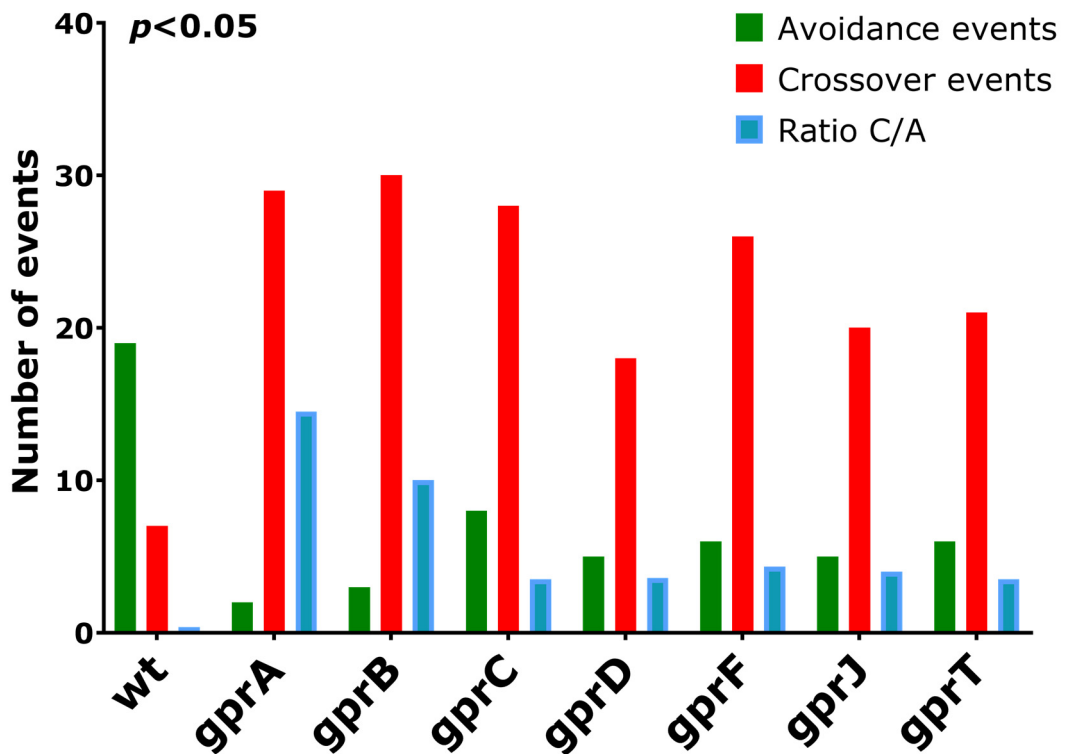
Figure 5.6 Number of avoidance and crossover events between hyphae in the GPCR null strains grown on AMMA. All GPCR strains shown in Fig 5.3 have significantly higher number of crossover events between approaching hyphae than the wild type. Notably, the pheromone receptor-like GPCRs have the highest ratio of crossover to avoidance events. Measurements of 25-30 hyphal pairs per strain.

5.2.1.2 Phenotypic screen of protein kinase deletion mutants

Figure 5.7 summarises the results of the phenotypic screen of protein kinase deletion mutants. Of 115 genes predicted to be encoding for proteins with kinase activity, 25 were essential and could not be obtained after deleting the corresponding gene (Al-Furaiji *et al.*, unpublished). Of the viable strains, 26 exhibited severe growth defects when grown on AMMA either macroscopically at a colony level or microscopically. Thirteen strains exhibited normal growth macroscopically, yet when viewed under the stereomicroscope showed evidence of hyphal aggregation that was commonly accompanied by aberrant patterns of polarized growth, abnormal patterns of branching or an inability to form branches. Common phenotypes were the inability to branch or aberrant branching, and abnormal polarity. Subsequently, the gene products (predict proteins) for each strain were run through 2 distinct BLAST algorithms (blastp and tblastn) for the identification and validation of homologous genes to the knocked-out genes using the reference wild type fungal strains of *Neurospora crassa* OR74A (Galagan et al., 2003), *Candida albicans* SC5314 (Fonzi and Irwin, 1993; Odds et al., 2004) and

KINASE KNOCK-OUT STRAINS PHENOTYPES
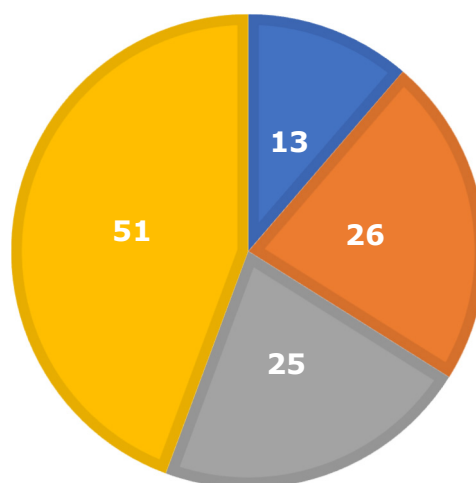
Figure 5.7 Phenotypes of the *A. fumigatus* kinase knock-out strains. Out of 115 genes predicted to be encoding for proteins with kinase activity, 25 were essential and could not be obtained after deleting the corresponding gene (Al-Furaiji *et al.*, unpublished). Of the viable strains, 26 displayed severe growth defects when grown on AMMA either macroscopically at a colony level or microscopically. Thirteen strains exhibited normal growth macroscopically yet showed aberrant polarity and hyphal aggregations when observed under the stereomicroscope.

Saccharomyces cerevisiae S288C (Goffeau et al., 1996) for comparison.

The 13 kinase KO strains exhibiting defective phenotypes in self-avoidance (hyphal aggregation) grew normally on AMMA compared to the wild type (data not shown), but the leading vegetative hyphae at the colony periphery exhibited limited abilities at avoiding neighbouring hyphae.

Table 5.2 provides a list of the self-avoidance defective mutants along with their homologue genes/proteins in the *N. crassa, C. albicans,* and *S. cerevisiae*, while Figures 5.8 and 5.9 provide representative images of each mutant strain considered likely to be defective in self-avoidance. Kinase family classification was carried out by Al-Furaiji *et al.* (unpublished) according to the Kinomer database (Martin et al., 2009). Similar to the phenotypes of self-avoidance mutant cells in neuron studies that exhibited aggregation (Fig. 5.1), fungal hyphae exhibited aggregations with minimal avoidance or in some cases complete insensitivity to their neighbours. In the latter case, hyphae do not diverge at all but instead come in direct contact with the adjacent hyphae and then followed and grew alongside them in pairs. Interestingly, three out of these thirteen self-avoidance genes are homologous to MAP kinases involved in chemotropic mating and self-fusion responses (NRC-1 = MAP kinase kinase kinase; MEK-2 = MAP kinase kinase; MAK-2 = MAP kinase; Read et al., 2009). The homologues of these three MAP kinases in *A. fumigatus* are: ste11/steC = NRC-1; ste7= MEK-2; mpkB/Fus3 = MAK-2 (Table 5.2).   Depending on which kinase is deleted the severity of the phenotype varied. One such example can be identified when the kinase knockout strains of the aforementioned MAP kinase cascade are examined. In both figures 5.8 and 5.9 the *ΔmpkB* strain retains the most prominent self-avoidance phenotype; minimal hyphal coverage over the same field-of-view (FOV).

Of the remaining genes likely to be involved in self-avoidance, in budding yeast the homologues have a diversity of roles in: sensing glucose deprivation (Rim15/ Tak1); the cell cycle (Ms1/Rpk1); cation homeostasis (Hrr25); mRNA metabolism and cation metabolism (Sky1 – there are two homologues of this protein); cell growth and DNA damage response (Cka2); protein kinase C signalling (Pkh3); and telomere regulation (Tel1). Figure 5.10 shows the number of avoidance/crossover events for these strains grown on AMMA, obtained with the methodology described in section 5.2.1.1.
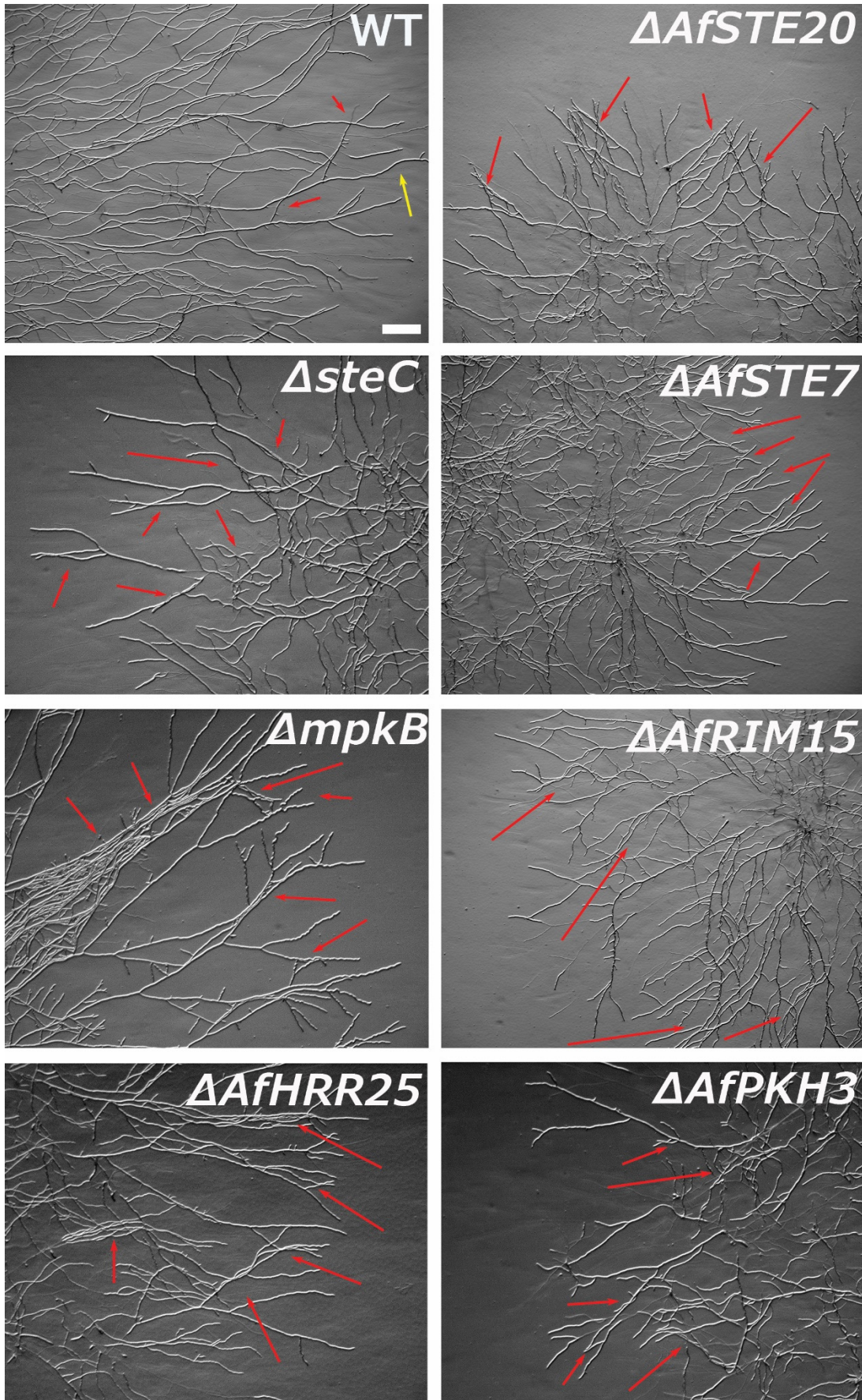
Figure 5.8 Self-avoidance defective strains of *A. fumigatus* grown on *Aspergillus* Minimal Media Agar (AMMA, details on next page).
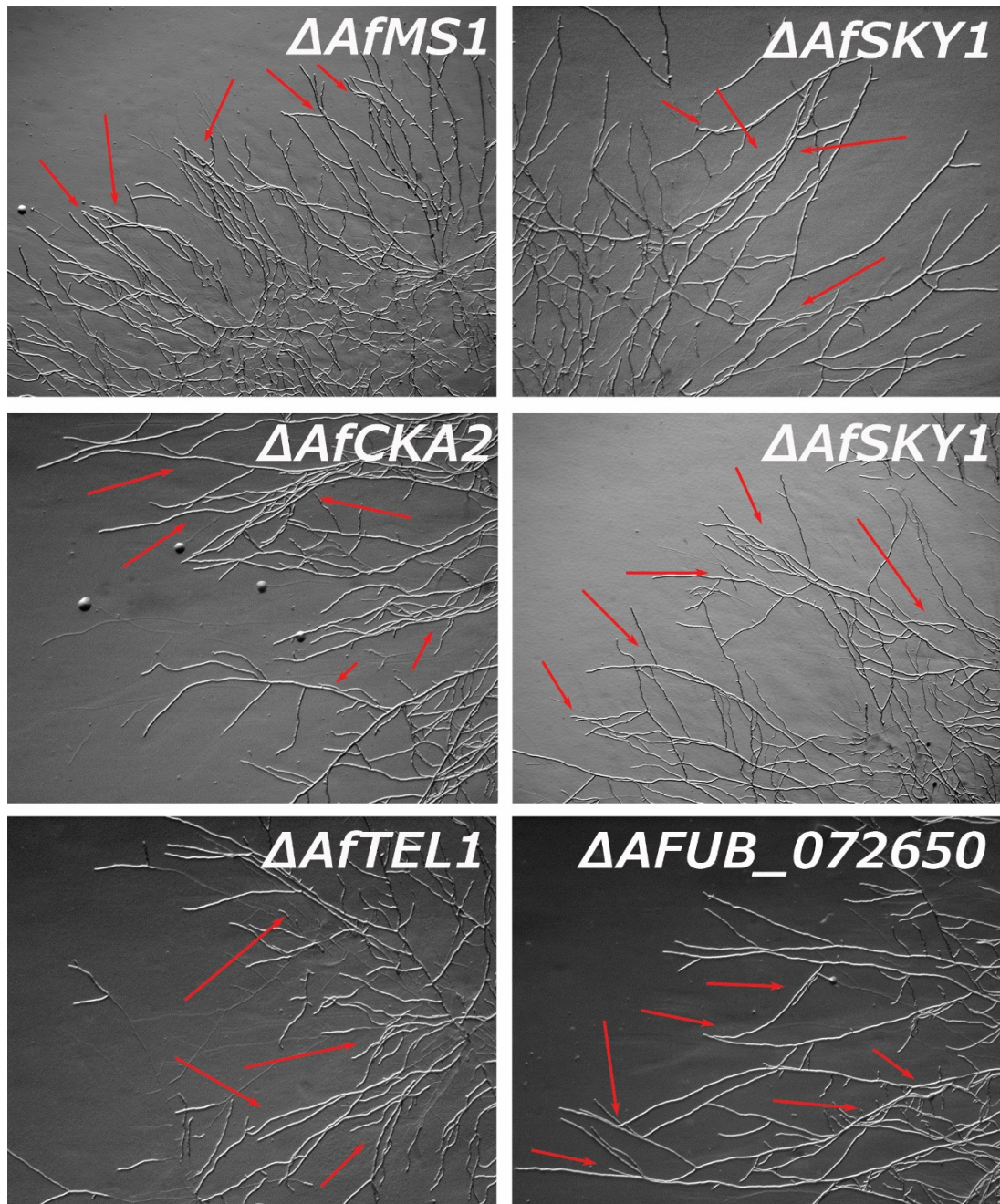
Figure 5.8 (cont.) Self-avoidance defective strains of *A. fumigatus* grown on *Aspergillus* Minimal Media Agar (AMMA). In the wild type (CEA10) there is occasional crossover between hyphae (red arrows), but generally they are well-spaced and avoid one another (yellow arrow). In the self-avoidance defective mutants, hyphal aggregations are prominent (red arrows). These can either lead to many hyphae bundling together and growing alongside in a uniform way or single events where the hypha comes in touch with the obstructing cell before it bounces off (e.g. *ΔAFUB_072650* – kinase of unknown function/homologue). All these phenotypes are very similar to the ones observed in mutant neuron cells defective in negative autotropisms. Scale bar = 100 µm.
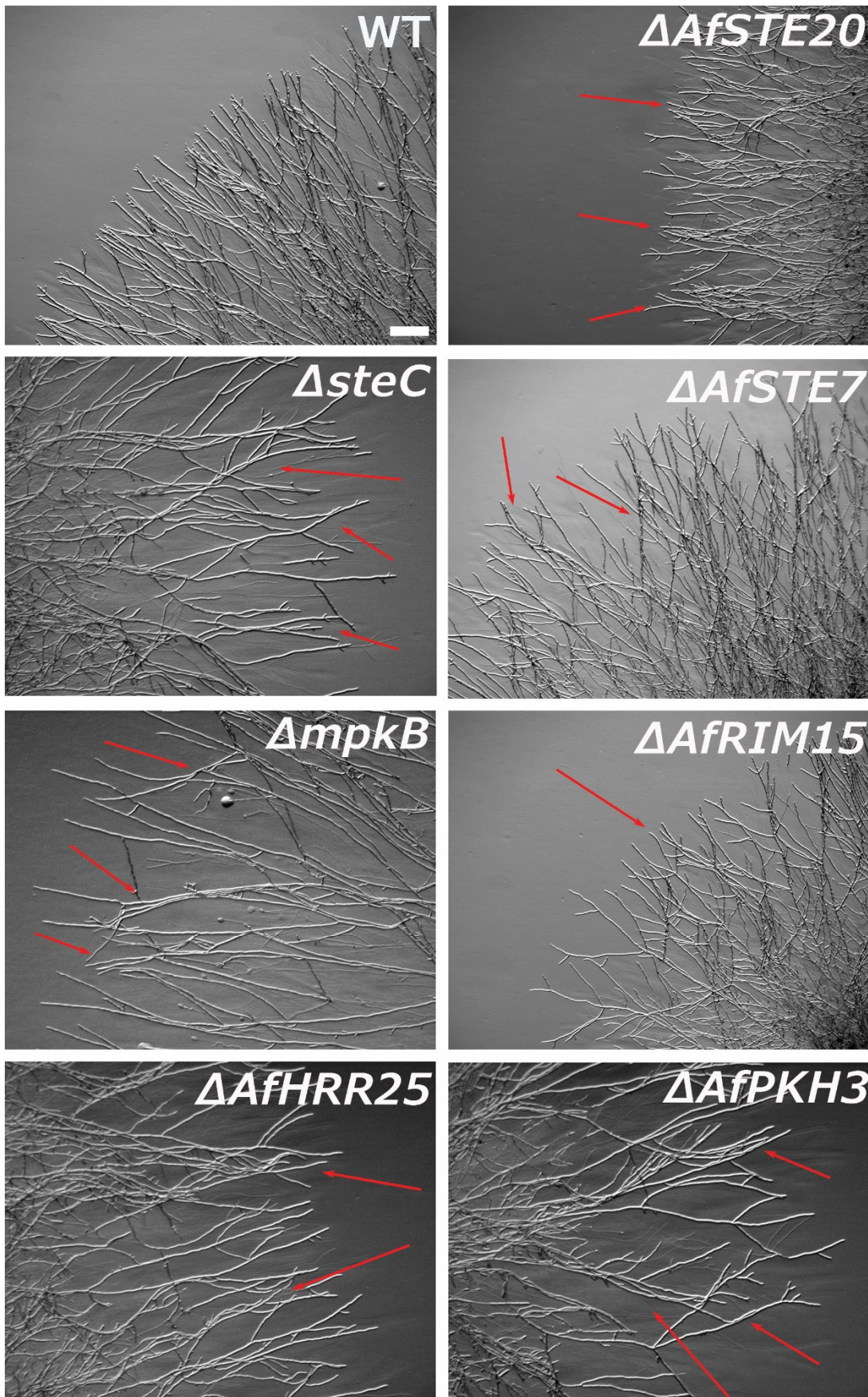
Figure 5.9 Self-avoidance defective strains of *A. fumigatus* grown on *Aspergillus* Complete Media Agar (ACMA, details on next page).
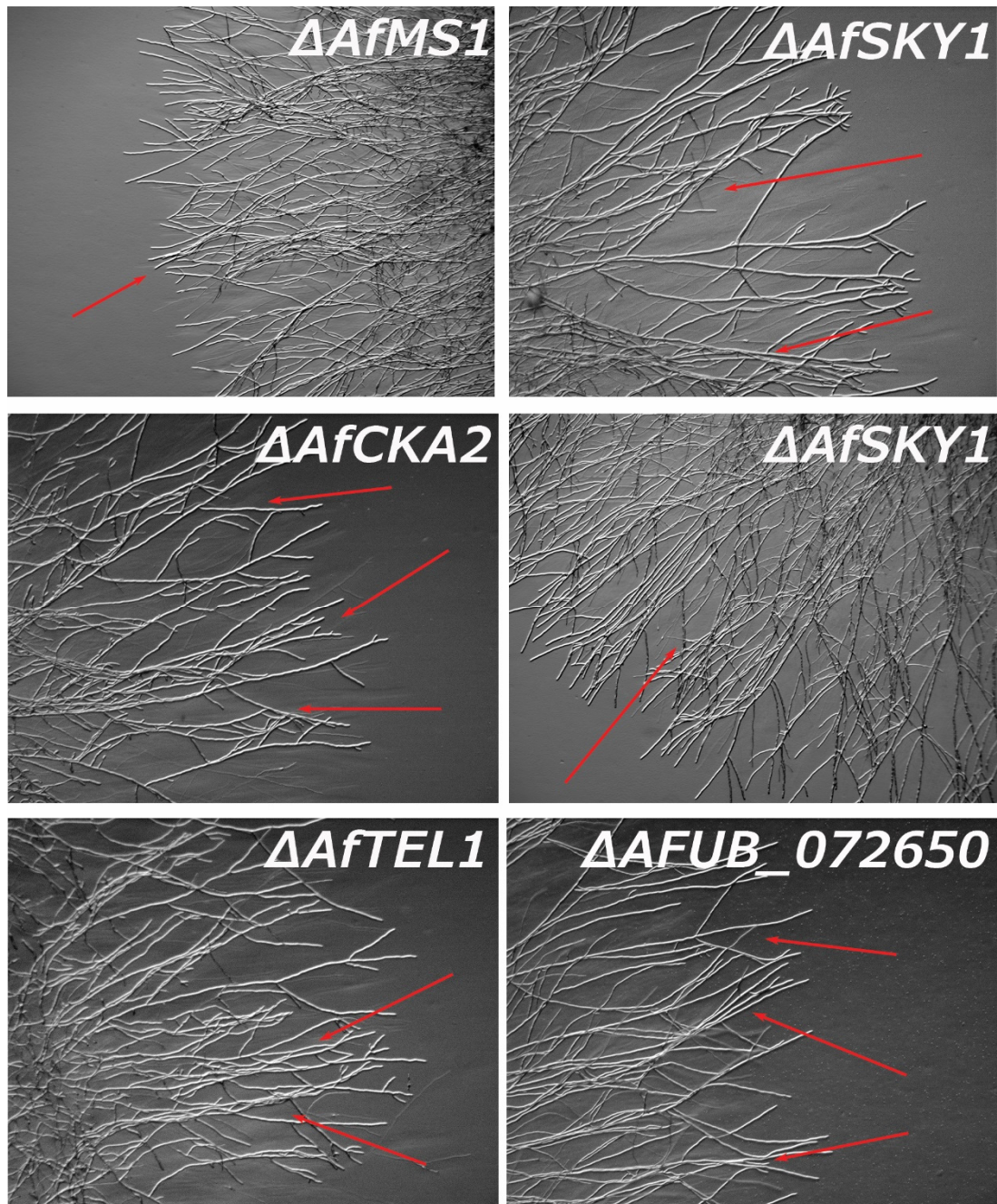
Figure 5.9 (cont.) Self-avoidance defective strains of *A. fumigatus* grown on *Aspergillus* Complete Media Agar (ACMA). The nutrient-rich substrate does not rescue the self-avoidance null phenotype on the tested strains. This suggests that nutrient sensing may be implicated in self-avoidance, as deleted kinases such as the *Af*Ste20, SteC, *Af*Ste7, MpkB (*Af*Fus3) are downstream components of the nutrient sensing pathway in *S. cerevisiae*. Scale bar = 100 μm

Table 5.2 List of the kinase knock-out mutants which are self-avoidance defective and their homologues in *N. crassa*, *C. albicans*, and *S. cerevisiae*. (**AGC:** Protein Kinase A, G and C group, **CAMK:** Calcium/Calmodulin Modulation Kinase activity group, **CK1:** Casein Kinase 1 group, **CMGC:** Kinase group of CDKs, MAPKs, GSK and CDK-like kinases, **STE:** Kinase group including many kinases in the MAPK cascades, **PIKK:** Phosphatidyl-inositol 3' kinase-related kinases)

gene	Aspergillus fumigatus locus	Kinase family	Neurospora crassa gene	locus	Candida albicans gene	locus	Saccharomyces cerevisiae gene	locus	Roles in Saccharomyces cerevisiae
	AFUB_030660	AGC	stk-12	NCU07378	RIM15	I503_05083	RIM15 (TAK1)	YFL033C	Nutrient deprivation (glucose)
	AFUB_041010	AGC		NCU00978	TTK/MPS1	I503_06296	MS1 (RPK1)	YDL028C	Cell cycle
	AFUB_072650	CAMK	stk-19	NCU02245		I503_05638	*unknown*	YPL150W	Unknown role
	AFUB_078920	CK1	ck-1a	NCU00685	HRR25	I503_04795	HRR25	YPL204W	cation homeostasis
	AFUB_045840	CMGC	dsk-1	NCU09202	SRPK3	I503_00596	HRR25	YMR216C	mRNA metabolism, cation homeostasis
Csk	AFUB_082700	CMGC	cka (prd-3)	NCU03124	CKA2-a	503_01943	CKA2	YOR061W	Cell growth, DNA damage response
MpkB/Fus3	AFUB_078810	CMGC	mak-2	NCU02393	CEK2	I503_03961	FUS3	YBL016W	Pheromone response
	AFUB_095720	CMGC	dsk-1	NCU09202	SRPK3	I503_00596	SKY1	YMR216C	mRNA metabolism, cation homeostasis
	AFUB_087320	CMGC	stk-35	NCU05655	PKH3	I503_04600	PKH3	YDR466W	PKC signalling
Ste20	AFUB_021710	STE	stk-4	NCU03894	CST20	I503_04258	STE20	YHL007C	Pheromone response, invasive growth
Ste7	AFUB_043130	STE	mek-2	NCU04612	HST7	I503_02020	STE7	YDL159W	Pheromone response, invasive growth
Ste11/SteC	AFUB_053960	STE	nrc-1	NCU06182	STE11	I503_01825	STE11	YLR362W	Pheromone response
Tel1	AFUB_060320	PIKK	mus-21	NCU00274	TEL1	I503_04830	TEL1	YBL088C	Telomere regulation
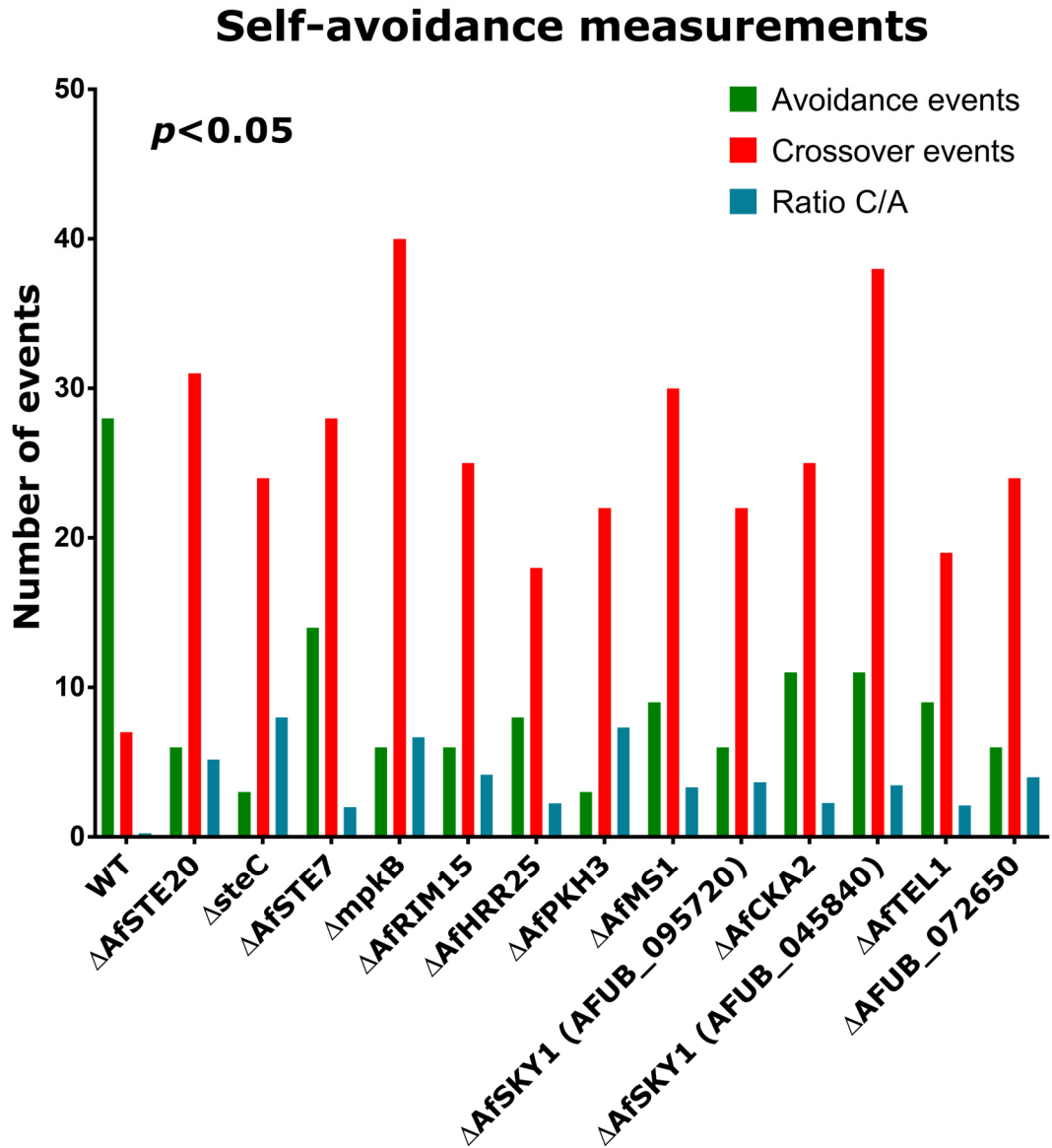
Figure 5.10 Number of avoidance and crossover events between hyphae in the kinase null strains grown on AMMA. All kinase knockout strains shown in Fig 5.8 have significantly higher numbers of crossover events between approaching hyphae than the wild type. Notably, the number of crossover events is consistent across the strains. Measurements of 30-40 hyphal pairs per strain.

5.3 Discussion

5.3.1 GPCRs and negative autotropisms in *A. fumigatus*

My results provide evidence that GPCR genes are not essential for fungal growth on either AMM or ACM (Fig 5.2). The results of the phenotypic screen of GPCR mutants provided very surprising evidence that 7 different GPCRs, belonging to different classes, and involved in pheromone reception, carbon sensing, nitrogen sensing, and the sensing of steroid pheromones resembling progesterone, are involved in self-avoidance responses. These results strongly suggest that multiple extracellular signals are sensed by these GPCRs and that these activated multiple downstream signalling pathways to elicit self-avoidance responses. This finding suggests that the strategy of searching for the identity of single extracellular self-avoidance molecule is flawed because more than one signal may be required to elicit a self-avoidance response.

Nutrient sensing GCPRs have been shown to be important regulator of budded-to-hyphal (BTH) form transition in *C. albicans* through activation of the cAMP-PKA pathway by Gpr1 (Maidan et al., 2005; Midkiff et al., 2011). The nutrient sensor Gpr1 has also been shown to be a regulator of pseudohyphal differentiation in *S. cerevisiae* (Ansari et al., 1999; Lorenz et al., 2000; Tamaki et al., 2000). In *A. nidulans* the GprD acts as a nutrient sensor closely related to the PKA pathway; *ΔgprD* mutants exhibit downregulation of PKA activity (de Souza et al., 2013)(de Souza et al., 2013). In *A. fumigatus* deletion of the genes encoding for GprC and GprD resulted in downregulation of primary metabolism genes and upregulation of genes related to secondary metabolism (Gehrke et al., 2010)(Gehrke et al., 2010). The same study showed that hyphal extension was reduced, and that germination was retarded, two findings which are not in agreement with my observations. In *N. crassa*, deletion of the gene encoding for GPR-4 resulted in lower mass accumulation when the fungus was grown on a variety of different carbon sources (Li and Borkovich, 2006)(Li and Borkovich, 2006). In a study investigating the effect of signalling pathway inhibitors in *C. albicans* and *A. fumigatus* it was revealed that certain GPCR antagonists (e.g. Clozapine) influenced *A. fumigatus* germination (Toenjes et al., 2009). In the same study, antagonists of the Ca^{2+} signalling pathway affected neither germination nor self-avoidance. My results show that nutrient sensing related GPCR knockouts results in limited adaptation of the fungal hyphae and growth aberrations. This would suggest that *A. fumigatus* may be vulnerable to such conditions as it cannot adjust quickly to nutrient limitations and does not grow uniformly as the wild type. These observations

highlight the possibility of nutrient-sensing GPCRs being targets of interest for antifungals, which is further discussed in section 6.2.3.

The loss-of-function of a GPCR which results in lack of self-avoidance can explained as follows: since the GPCR is not transcribed, the related small GTPases (Ga, Gβ) are in a constant unbound state, in which they can be activated by a Guanine Exchange Factor (GEF). As a result, Ste20 and its downstream effectors are constitutively active resulting in abnormal polarity behaviour and lack of avoidance. Since the effect is possibly dependent on a variety of factors, some self-avoidance can still be observed but in general the fungal hyphae have a limited ability to change their polarity in response to neighbouring cells. Consequently, since the regulation of actin polymerisation, hence polarity, is affected hyphal aggregations are formed.

5.3.2 Multiple protein kinases, including one MAP kinase pathway, play roles in self-avoidance

Intracellular kinases are key mediator proteins of the signal transduction between the extracellular environment and a cell's response. Kinases have also been shown to be vital for host-pathogen interactions and cross-kingdom communication (Segorbe et al., 2017; Turrà et al., 2014). Since they are vital components fungal growth, development and adaptation to external environmental cues, I tested whether any kinases are involved in the self-avoidance response of *A. fumigatus* by conducting an unbiased phenotypic screen on different growth conditions.

The results of the phenotypic screen showed that homologues of the principal components of the chemotropic responses during N. crassa mating and during self-fusion between CATs also seem to be involved in regulation of self-avoidance. All these kinases are involved in range of signalling cascades in *S. cerevisiae* such as the mating and pheromone response or the filamentous and invasive growth pathways (Hamel et al., 2012). The MpkB/Fus3 homologue kinase pathway, MAK-2, has also been implicated in cell communication in *N. crassa* with HAM-5 acting as a scaffold protein in the pathway (Dettmann et al., 2014). MAK-2 is also essential for the oscillatory ping-pong communication mechanism during CAT chemostropism up to and including cell fusion in *N. crassa* (Fleissner et al., 2009; Read et al., 2009; Serrano et al., 2017; Weichert et al., 2016). Homologues of the MAPK cascade involved in mating have also been identified in *C. albicans* (Liu, 2001). The results of the phenotypic screen would suggest that this

MAP kinase pathway is involved in two opposing responses in filamentous fungi: hyphal attraction during cell fusion and hyphal repulsion during self-avoidance. Clearly other, yet to be identified, signalling components are involved in regulating which of these two opposing responses is activated. At this stage one can only speculate what these signalling components might be. However, it quite possible that some or all of the proteins listed in Table 5.2, and which when deleted result in a defective self-avoidance response, play a role in this regulation. The fact that multiple extracellular signals and multiple GPCRs may have to be sensed in combination may be a key aspect of how self-avoidance and chemoattraction are differentially regulated. The receptor involved in CAT chemotropisms has not yet identified and is not one of the known GPCRs (Read et al., 2012).

The Pkh3 kinase in *S. cerevisiae*, is a similar kinase to the mammalian phosphoinositide-dependent kinase 1 (PDK1) and yeast kinases Pkh1/Pkh2 which are responsible for the activation of the Pkc1 and Pkc1-effector pathway (Inagaki et al., 1999) and its knockout also results in limited self-avoidance. Pkh1-3 kinases have been shown to affect polarity via the interaction of the TORC and cAMP-PKA signalling pathways in *S. cerevisiae* (Roelants et al., 2002; Voordeckers et al., 2011).

The Hrr25 was initially associated with repair of damaged DNA; its mutation resulted in increased sensitivity to DNA damaging agents (Hoekstra et al., 1991), but it was later identified as the casein kinase 1 (Csk1) homologue and shown to phosphorylate Crz1 both *in vivo* and *in vitro* thus acting as a negative regulator of the Ca^{2+}/calcineurin pathway.

The Rim15 kinase is also affected by the cAMP-PKA nutrient sensing signalling pathway maximising adaptability during the G0-cell cycle stage (Cameroni et al., 2004) and has also been shown to affect kinases Ime1 and Ime2 (Vidan and Mitchell, 1997) which are responsible for pseudohyphal growth in *S. cerevisiae* in nonfermentable carbon sources (Strudwick et al., 2010). The knockout of the latter resulted in severe growth defects in *A. fumigatus* (Appendix 2).

Lastly, of high interest would be the predicted kinase of the AFUB_072650 locus, which has no known homologues in any of the fungal databases that was search against.

Another interesting indication of my mutant screening results was that the regulation of actin cytoskeleton during negative autotropisms is not guided directly through the traditional Cdc42-Wiskott-Aldrich syndrome protein (WASP)-Arp2/3 pathway (Burianek and Soderling, 2013; Tyler et al., 2016), but it is the resultant of more complex interactions of integrated pathways. This is based on the observation that kinase deletion mutants affect polarity and growth axis rearrangement, which are not directly involved in the aforementioned pathway.

5.4 Summary

The results of the research described in this chapter can be summarised as follows:

(1) A screen of 16 GPCR and 115 protein kinase mutants were screened for hyphal aggregation as a phenotypic readout of defects in self-avoidance responses.

(2) Seven G-protein coupled receptors were identified as possibly being involved in negative autotropisms of *A. fumigatus*. They belong belonging to four different classes of GPCRs involved in pheromone reception, carbon sensing, nitrogen sensing, and the sensing of steroid pheromones resembling progesterone.

(3) Thirteen protein kinases were identified as possibly being involved in negative autotropisms of *A. fumigatus*.

(4) The results suggest that multiple extracellular signals are involved in the self-avoidance response.

4.5 References

Ansari, K., Martin, S., Farkasovsky, M., Ehbrecht, I.M., Küntzel, H., 1999. Phospholipase C binds to the receptor-like GPR1 protein and controls pseudohyphal differentiation in *Saccharomyces cerevisiae*. J. Biol. Chem. 274, 30052–30058. https://doi.org/10.1074/jbc.274.42.30052

Burianek, L.E., Soderling, S.H., 2013. Under lock and key: Spatiotemporal regulation of WASP family proteins coordinates separate dynamic cellular processes. Semin. Cell Dev. Biol. 24, 258–266. https://doi.org/10.1016/j.semcdb.2012.12.005

Cabrera, I.E., Pacentine, I. V, Lim, A., Guerrero, N., Krystofova, S., Li, L., Michkov, A. V, Servin, J.A., Ahrendt, S.R., Carrillo, A.J., Davidson, L.M., Barsoum, A.H., Cao, J., Castillo, R., Chen, W.-C., Dinkchian, A., Kim, S., Kitada, S.M., Lai, T.H., Mach,

A., Malekyan, C., Moua, T.R., Torres, C.R., Yamamoto, A., Borkovich, K.A., 2015. Global Analysis of Predicted G Protein-Coupled Receptor Genes in the Filamentous Fungus, *Neurospora crassa*. G3 (Bethesda). 5, 2729–43. https://doi.org/10.1534/g3.115.020974

Cameroni, E., Hulo, N., Roosen, J., Winderickx, J., De Virgilio, C., 2004. The novel yeast PAS kinase Rim15 orchestrates G0-associated antioxidant defense mechanisms. Cell Cycle 3, 462–468. https://doi.org/10.4161/cc.3.4.791

de Souza, W.R., Morais, E.R., Krohn, N.G., Savoldi, M., Goldman, M.H.S., Rodrigues, F., Caldana, C., Semelka, C.T., Tikunov, A.P., Macdonald, J.M., Goldman, G.H., 2013. Identification of Metabolic Pathways Influenced by the G-Protein Coupled Receptors GprB and GprD in *Aspergillus nidulans*. PLoS One 8, 1–13. https://doi.org/10.1371/journal.pone.0062088

Dettmann, A., Heilig, Y., Valerius, O., Ludwig, S., Seiler, S., 2014. Fungal Communication Requires the MAK-2 Pathway Elements STE-20 and RAS-2, the NRC-1 Adapter STE-50 and the MAP Kinase Scaffold HAM-5. PLoS Genet. 10. https://doi.org/10.1371/journal.pgen.1004762

Fleissner, A., Leeder, A.C., Roca, M.G., Read, N.D., Glass, N.L., 2009. Oscillatory recruitment of signaling proteins to cell tips promotes coordinated behavior during cell fusion. Proc. Natl. Acad. Sci. U. S. A. 106, 19387–19392. https://doi.org/10.1073/pnas.0907039106

Fonzi, W.A., Irwin, M.Y., 1993. Isogenic strain construction and gene mapping in *Candida albicans*. Genetics 134, 717–728. https://doi.org/10.1111/j.1834-7819.1995.tb03122.x

Galagan, J., Calvo, S., Borkovich, K., Selker, E., Read, N., Jaffe, D., FitzHugh, W., Ma, L.-J., Smirnov, S., Purcell, S., Rehman, B., Elkins, T., Engels, R., Wang, S., Nielsen, C., Butler, J., Endrizzi, M., Qui, D., Ianakiev, P., Bell-Pedersen, D., Nelson, M., Werner-Washburne, M., Selitrennikoff, C., Kinsey, J., Braun, E., Zelter, A., Schulte, U., Kothe, G., Jedd, G., Mewes, W., Staben, C., Marcotte, E., Greenberg, D., Roy, A., Foley, K., Naylor, J., Stange-Thomann, N., Barrett, R., Gnerre, S.,

Kamal, M., Kamvysselis, M., Mauceli, E., Bielke, C., Rudd, S., Frishman, D., Krystofova, S., Rasmussen, C., Metzenberg, R., Perkins, D., Kroken, S., Cogoni, C., Macino, G., Catcheside, D., Li, W., Pratt, R., Osmani, S., DeSouza, C., Glass, L., Orbach, M., Berglund, A., Voelker, R., Yarden, O., Plamann, M., Seiler, S., Dunlap, J., Radford, A., Aramayo, R., Natvig, D., Alex, L., Mannhaupt, G., Ebbole, D., Freitag, M., Paulsen, I., Sachs, M., Lander, E., Nusbaum, C., Birren, B., 2003. The genome sequence of the filamentous fungus *Neurospora crassa*. Nature 422, 859–868. https://doi.org/doi: 10.1038/nature01554

Gehrke, A., Heinekamp, T., Jacobsen, I.D., Brakhage, A.A., 2010. Heptahelical receptors GprC and GprD of *Aspergillus fumigatus* are essential regulators of colony growth, hyphal morphogenesis, and virulence. Appl. Environ. Microbiol. 76, 3989–3998. https://doi.org/10.1128/AEM.00052-10

Goffeau, A., Barrell, B.G., Bussey, H., Davis, R.W., Dujon, B., Feldmann, H., Galibert, F., Hoheisel, J.D., Jacq, C., Johnston, M., Louis, E.J., Mewes, H.W., Murakami, Y., Philippsen, P., Tettelin, H., Oliver, S.G., 1996. Life with 6000 Genes conveniently among the different interna- Old Questions and New Answers The genome . At the beginning of the se- of its more complex relatives in the eukary- cerevisiae has been completely sequenced *Schizosaccharomyces pombe* indicate. Science (80-.). 274, 546–567. https://doi.org/jyu

Guan, K.-L., Rao, Y., 2003. Signalling mechanisms mediating neuronal responses to guidance cues. Nat. Rev. Neurosci. 4, 941–956. https://doi.org/10.1038/nrn1254

Hamel, L.-P., Nicole, M.-C., Duplessis, S., Ellis, B.E., 2012. Mitogen-Activated Protein Kinase Signaling in Plant-Interacting Fungi: Distinct Messages from Conserved Messengers. Plant Cell 24, 1327–1351. https://doi.org/10.1105/tpc.112.096156

Hoekstra, M.F., Liskay, R.M., Ou, a C., DeMaggio, a J., Burbee, D.G., Heffron, F., 1991. HRR25, a putative protein kinase from budding yeast: association with repair of damaged DNA. Science 253, 1031–4. https://doi.org/Doi 10.1126/Science.1887218

Inagaki, M., Schmelzle, T., Yamaguchi, K., Irie, K., Hall, M.N., Matsumoto, K., 1999.

PDK1 homologs activate the Pkc1-mitogen-activated protein kinase pathway in yeast. Mol. Cell. Biol. 19, 8344–8352. https://doi.org/10.1128/MCB.19.12.8344

Jin, M., Errede, B., Behar, M., Mather, W., Nayak, S., Hasty, J., Dohlman, H.G., Elston, T.C., 2011. Yeast dynamically modify their environment to achieve better mating efficiency. Sci. Signal. 4, ra54.

Lafon, A., Han, K.H., Seo, J.A., Yu, J.H., D'Enfert, C., 2006. G-protein and cAMP-mediated signaling in aspergilli: A genomic perspective. Fungal Genet. Biol. 43, 490–502. https://doi.org/10.1016/j.fgb.2006.02.001

Lefebvre, J.L., Sanes, J.R., Kay, J.N., 2015. Development of Dendritic Form and Function. Annu. Rev. Cell Dev. Biol. 31, 741–777. https://doi.org/10.1146/annurev-cellbio-100913-013020

Li, L., Borkovich, K.A., 2006. GPR-4 is a predicted G-protein-coupled receptor required for carbon source-dependent asexual growth and development in *Neurospora crassa*. Eukaryot. Cell 5, 1287–1300. https://doi.org/10.1128/EC.00109-06

Lichius, A., Goryachev, A.B., Fricker, M.D., Obara, B., Castro-Longoria, E., Read, N.D., 2014. CDC-42 and RAC-1 regulate opposite chemotropisms in *Neurospora crassa*. J. Cell Sci. 127, 1953–65. https://doi.org/10.1242/jcs.141630

Liu, H., 2001. Transcriptional control of dimorphism in Candida albicans. Curr. Opin. Microbiol. 4, 728–735. https://doi.org/10.1016/S1369-5274(01)00275-2

Lorenz, M.C., Pan, X., Harashima, T., Cardenas, M.E., Xue, Y., Hirsch, J.P., Heitman, J., 2000. The G protein-coupled receptor Gpr1 is a nutrient sensor that regulates pseudohyphal differentiation in *Saccharomyces cerevisiae*. Genetics 154, 609–622.

Maidan, M.M., Thevelein, J.M., Van Dijck, P., 2005. Carbon source induced yeast-to-hypha transition in *Candida albicans* is dependent on the presence of amino acids and on the G-protein-coupled receptor Gpr1. Biochem. Soc. Trans. 33, 291–3. https://doi.org/10.1042/BST0330291

Martin, D.M.A., Miranda-Saavedra, D., Barton, G.J., 2009. Kinomer v. 1.0: A database of systematically classified eukaryotic protein kinases. Nucleic Acids Res. 37, 244–250. https://doi.org/10.1093/nar/gkn834

Midkiff, J., Borochoff-Porte, N., White, D., Johnson, D.I., 2011. Small molecule inhibitors of the *Candida albicans* budded-to-hyphal transition act through multiple signaling pathways. PLoS One 6. https://doi.org/10.1371/journal.pone.0025395

Odds, F.C., Brown, A.J.P., Gow, N.A.R., 2004. *Candida albicans* genome sequence: A platform for genomics in the absence of genetics. Genome Biol. 5, 5–7. https://doi.org/10.1186/gb-2004-5-7-230

Read, N.D., Lichius, A., Shoji, J.Y., Goryachev, A.B., 2009. Self-signalling and self-fusion in filamentous fungi. Curr Opin Microbiol 12, 608–615. https://doi.org/10.1016/j.mib.2009.09.008

Roelants, F.M., Torrance, P.D., Bezman, N., Thorner, J., 2002. Pkh1 and Pkh2 Differentially Phosphorylate and Activate Ypk1 and Ykr2 and Define Protein Kinase Modules Required for Maintenance of Cell Wall Integrity. Mol. Biol. Cell 13, 3005–3028. https://doi.org/10.1091/mbc.E02-04-0201

Segorbe, D., Di Pietro, A., Pérez-Nadales, E., Turrà, D., 2017. Three Fusarium oxysporum mitogen-activated protein kinases (MAPKs) have distinct and complementary roles in stress adaptation and cross-kingdom pathogenicity. Mol. Plant Pathol. 18, 912–924. https://doi.org/10.1111/mpp.12446

Serrano, A., Hammadeh, H.H., Herzog, S., Illgen, J., Schumann, M.R., Weichert, M., Fleiβner, A., 2017. The dynamics of signal complex formation mediating germling fusion in *Neurospora crassa*. Fungal Genet. Biol. 101, 31–33. https://doi.org/10.1016/j.fgb.2017.02.003

Strudwick, N., Brown, M., Parmar, V.M., Schroder, M., 2010. Ime1 and Ime2 Are Required for Pseudohyphal Growth of *Saccharomyces cerevisiae* on Nonfermentable Carbon Sources. Mol. Cell. Biol. 30, 5514–5530. https://doi.org/10.1128/MCB.00390-10

Tamaki, H., Miwa, T., Shinozaki, M., Saito, M., Yun, C.W., Yamamoto, K., Kumagai, H., 2000. GPR1 regulates filamentous growth through FLO11 in yeast *Saccharomyces cerevisiae*. Biochem. Biophys. Res. Commun. 267, 164–168. https://doi.org/10.1006/bbrc.1999.1914

Toenjes, K.A., Stark, B.C., Brooks, K.M., Johnson, D.I., 2009. Inhibitors of cellular signalling are cytotoxic or block the budded-to-hyphal transition in the pathogenic yeast *Candida albicans*. J. Med. Microbiol. 58, 779–790. https://doi.org/10.1099/jmm.0.006841-0

Turrà, D., Segorbe, D., Di Pietro, A., 2014. Protein Kinases in Plant-Pathogenic Fungi: Conserved Regulators of Infection. Annu. Rev. Phytopathol. 52, 267–288. https://doi.org/10.1146/annurev-phyto-102313-050143

Tyler, J.J., Allwood, E.G., Ayscough, K.R., 2016. WASP family proteins, more than Arp2/3 activators. Biochem. Soc. Trans. 44, 1339–1345. https://doi.org/10.1042/BST20160176

Vidan, S., Mitchell, a P., 1997. Stimulation of yeast meiotic gene expression by the glucose-repressible protein kinase Rim15p. Mol. Cell. Biol. 17, 2688–2697. https://doi.org/10.1128/MCB.17.5.2688

Voordeckers, K., Kimpe, M., Haesendonckx, S., Louwet, W., Versele, M., Thevelein, J.M., 2011. Yeast 3-phosphoinositide-dependent protein kinase-1 (PDK1) orthologs Pkh1-3 differentially regulate phosphorylation of protein kinase A (PKA) and the protein kinase B (PKB)/S6K ortholog Sch9. J. Biol. Chem. 286, 22017–22027. https://doi.org/10.1074/jbc.M110.200071

Weichert, M., Lichius, A., Priegnitz, B.-E., Brandt, U., Gottschalk, J., Nawrath, T., Groenhagen, U., Read, N.D., Schulz, S., Fleißner, A., 2016. Accumulation of specific sterol precursors targets a MAP kinase cascade mediating cell–cell recognition and fusion. Proc. Natl. Acad. Sci. 113, 11877–11882. https://doi.org/10.1073/pnas.1610527113

Xue, C., Hsueh, Y.P., Heitman, J., 2008. Magnificent seven: Roles of G protein-coupled receptors in extracellular sensing in fungi. FEMS Microbiol. Rev. 32, 1010–1032. https://doi.org/10.1111/j.1574-6976.2008.00131.x

[Blank page]

Chapter 6

Final discussion and future perspectives

[Blank page]

6.1 Introduction

During this PhD project I set out to investigate the fungal negative cell autotropisms, analyse them and gain insights into the signalling pathways involved in their regulation. The key motivation for undertaking such a task was that although fungal self-avoidance was one of the first types of tropisms to be identified (Miyoshi, 1894), little progress was made during the 20th century to elucidate the mechanisms regulating this kind of response. It is notable that in the last decade there has only been one study regarding self-avoidance of fungal cells using *S. cerevisiae* (Jin et al., 2011). In contrast, significant advances have been made into understanding self-avoidance of neuron cells. However, self-avoidance responses by these cells seems to be fundamentally different to that in filamentous fungi such as *A. fumigatus* because only in the former are the responses contact-/touch-mediated (summarised in section 1.3.6.1).

Advances in live-cell imaging, rapid generation of fungal gene deletion libraries and improvements in analytical chemistry methods involving GC-MS, have provided powerful new experimental approaches to investigate the phenomenon of cell avoidance (section 1.3.6). The study's experimental organism, *A. fumigatus,* was chosen not only because it is an established experiment system but also for its impact as a human pathogen, as any key components of self-avoidance may have been linked to reported (Abad et al., 2010) or novel virulence genes and/or markers. Figure 6.1 summarises the thought processes of this thesis based on the overall aims raised in section 1.6 and their respective answers to the key questions addressed in these aims.
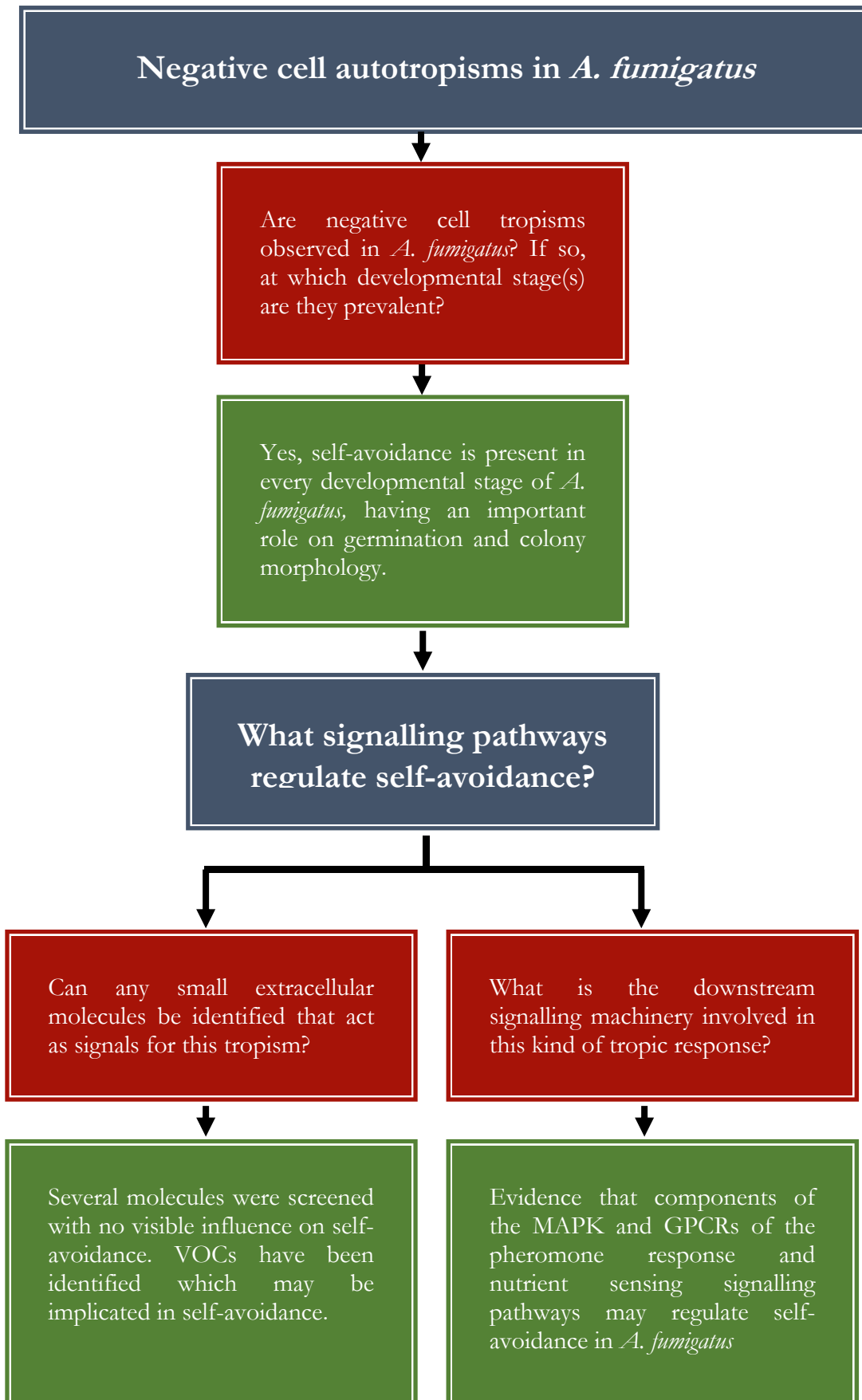
Figure 6.1 Questions addressed in this research thesis. Blue boxes denote general topics, red boxes present the research aims raised in section 1.6, and green boxes provide brief summarised answers to the related aims.

6.2 Key findings

6.2.1 Self-avoidance is a defining factor in *A. fumigatus* germination, colony morphology and expansion

Negative autotropisms of vegetative hyphae and branches at the colony periphery and and positive autotropisms of hyphal branches behind the colony periphery were first shown by live-cell imaging in *Neurospora crassa*. Overall, the vegetative hyphae strongly tended to grow outwards from the colony centre. The specialized hyphal branches undergoing positive autotropisms towards each other in the inner colony regions underwent cell fusion (Hickey et al., 2002). In *A. nidulans* young hyphae tend to avoid one another before they switch to biofilm formation (Stephen Osmani, personal communication). My results showed that in *A. fumigatus* self-avoidance defined the sites of germ tube emergence from spores (section 3.3.2). These germ tubes then averted their growth away from neighbouring spores and adjacent germ tubes (section 3.2.1). This change of direction was also observed in between adjacent mature vegetative hyphae at the colony periphery and between the hyphae of 24-hour approaching colonies (section 3.2.7). Depending on the angle of approach they seemed to be either unaware of each other or they changed their growth course to a parallel one. The observation that the angle of approach may be involved in hyphal sensing and subsequent tropic response is similar to the thigmotropic response observed in *N. crassa* (Stephenson et al., 2014). The barrier zone observed in fungi (Porter, 1924; Skidmore and Dickinson, 1976) due to intraspecies vegetative incompatibility or interspecies competition may be attributed to a significant extent to this hyphal avoidance.

Experiments during germination have shown that the original protrusion site during germination was dependent on the site of contact between spores or spores in close proximity, while it was affected to a lesser extent by contact or near contact between spores and inert objects such as polystyrene microbeads (section 3.3). This would suggest that intercellular communication takes place between germinating spores in contact/near contact, probably after the 3-hour mark of isotropic growth when the hydrophobin layer covering each spore has been disrupted (Dague et al., 2008). After the germination site is established and the first germ tube protrudes from the spore, negative autotropisms take effect and tip growth is affected depending on the relative location of the original germination site to the adjacent cells (section 3.2.1). Experiments which involved dead, and dormant cells showed that the self-avoidance responses of germ tube tips require the interaction between living cells (section 3.2.3).

To quantify negative cell autotropisms in *A. fumigatus* a novel 3D image analysis method was developed which measured the angles of spacing between germ tubes early post-germination. Analysis of 3D data and its 2D projections revealed that the z-axis (depth) is a crucial factor which must be considered when assessing the phenomenon when spores are germinated on agar medium. The mean angle of avoidance did not exceed 70.18° ± 5.39° in a pair of spores, which would suggest that any inducing signal loses its potency at greater angles. The propensity of *A. fumigatus* germlings to invade their substratum was also measured. Although the mechanism by which they invade their substrate is still unclear, my results showed that their ability to invade surfaces is inhibited in increased stiffness. This observation may be important in the context of host tissue invasion and the interaction between fungal hyphae and host cells (section 3.2.6).

6.2.2 Screen of VOCs as potential extracellular signals did not reveal any effect on fungal avoidance

The first step in understanding the signalling machinery guiding self-avoidance was to identify the extracellular signal(s) which induce(s) this response. Volatile organic compounds (VOCs) were tested as their biochemical properties make them ideal signal molecules: they are small, then can diffuse through the cell membrane and their half-life is short enough to negate oversaturation of the signal in the hyphal micro-environs. I tested their activity on germination inhibition and self-avoidance.

The effect of nitric oxide scavenging on spore germination and avoidance was investigated with the use of PTIO, a cell permeable NO scavenger. Nitric oxide is a molecule of interest in fungal disease and my results showed that increased PTIO concentrations inhibited spore germination in *A. fumigatus* but did not affect negative autotropisms during germination and germ tube elongation (section 4.2.1). To my knowledge this is the first report of intracellular NO depletion inhibiting germination of *A. fumigatus*.

A wide range of volatile compounds (organic and inorganic) have been reported to influence germination, modulate growth and development in fungi (Leeder et al., 2011; Ugalde and Rodriguez-Urra, 2014). I tested VOCs which have been reported as self-inhibitors of germination in different ascomycetes (section 4.2.2). My hypothesis was that at a low concentration these germination self-inhibitors might act as self-avoidance

signals, especially if self-inhibition of germination is one aspect of self-avoidance. Of all the tested compounds, only nonanoic acid visibly affected inhibition, in a dose-dependent manner. However, self-avoidance was not affected at all. Interestingly, nonanoic acid induced the formation of synnemata (coremia), hyphal aggregations which act as secondary conidiation structures, at the edge of inhibition zone formed by the concentration gradient at 48 hpi (section 4.2.3). Although synnemata have been reported before in *Aspergilli* (Hubbes, 1975; McAlpin, 2001; Varga et al., 2011)*, to my knowledge this is the first report of their presence in *A. fumigatus*.

The technical limitations of the chemical compound screen (i.e. controls not working properly) dictated the necessity to explore other avenues to identify novel compounds which may act as self-avoidance signals. As Chapter 3 detailed (summarised in section 6.2.1), negative autotropisms in *A. fumigatus* are prevalent in all growth and developmental stages: from spore germination to growth of vegetative hyphae. Therefore, if a VOC generates self-avoidance it would be present at both growth stages. For this reason, a novel GC-MS method was developed to analyse the fungal headspace of *A. fumigatus* wild type (CEA10) and a secondary metabolism deficient strain (*ΔpptA*), which was found to exhibit self-avoidance. This method was sensitive enough to detect compounds that consisted of 2-30 carbon atoms. Mass spectrometry results revealed that both strains secreted a diverse range of chemical compounds, though the *ΔpptA* was limited in the production of sesquiterpenes which comprise the majority of the secondary metabolites in *A. fumigatus* (Heddergott et al., 2014). Common volatiles between the two strains were found but were not analysed to determine if they individually elicited self-avoidance responses due to time restrictions (section 4.2.6). These need to be assayed further (section 6.4) to verify whether they are involved in self-avoidance.

6.2.3 Self-avoidance may be the result of multiple extracellular signals

I proceeded to investigate if there are any of the well characterized G-protein coupled receptors (GPCRs) and which protein kinases are involved in negative autotropisms in *A. fumigatus*. To achieve this, 16 GPCR and 90 viable protein kinase deletion mutants were screened for any hyphal aggregations which would be a phenotypic marker of possible defects in self-avoidance responses. Out of the 16 GPCRs, 7 showed hyphal aggregations when grown on minimal nutrients media (AMMA) and abnormal

germination phenotypes when grown in liquid AMM (section 5.2.1.1). These deletion mutants belong to four different classes of fungal GPCRs which are involved in pheromone reception, carbon sensing, nitrogen sensing, or sensing of steroid pheromones in the budding yeast. The wild type phenotype of these strains was recovered when they were grown on ACMA. Colony size was not affected significantly compared to the wild type under either condition. Growth aberrations of the GPCRs belonging to the nutrient sensing pathways were also interesting from a medical/pharmacological perspective, since nutrient GPCRs are fungal specific and can be used in a drug discovery screen (reviewed by Dijck, 2009). More recently, steps have been made in discovering GPCR-selective drugs, covering a wide-range of diseases and conditions, (Hauser et al., 2017), as well as antibodies (Ayoub et al., 2017) and small drugs targeting the GPCR heterotrimeric complex (Ayoub, 2018). Also, of interest is the implication of the GprT belonging to the mPR/PAQR class of GPCRs which are induced by steroid signals. Although the dependency of oxylipin signalling and quorum sensing pathways on GPCRs has been reported (Affeldt et al., 2012), the oxylipins I screened (Chapter 4) did not affect self-avoidance. It would be interesting to see the role of steroid signals on negative autotropisms, as this type of chemical compounds is easily diffusible through the cell membrane.

The relationship between the kinase signalling pathways and self-avoidance was also investigated. To this end, 90 kinase knockout mutant strains were screened for their phenotypic growth patterns. Twenty-six displayed severe growth defects which ranged from aberrations in branching to limited growth rate. Thirteen protein kinases maintained growth similar to the wild type but displayed hyphal aggregations when observed under the stereomicroscopy. Three mutants MAP kinases and homologues of those involved belong to the pheromone response pathway in budding yeast and in self-fusion during conidial anastomosis tube chemoattraction and fusion. Evidence was also obtained for kinases involved in nutrient sensing through regulation of the cAMP-PKA pathway (Fig. 6.2) in *S. cerevisiae* also possibly being involved in self-avoidance. Taken together, the phenotypic screen results indicate that negative autotropisms are the result of multiple extracellular stimuli, the possible equilibrium of which produce self-avoidance responses. This was an unexpected result because in marked contrast, positive tropisms in yeast (shmoos during cell mating) and filamentous fungi (trichogynes during cell mating; CATs during vegetative cell fusion) produce what is

generally believed to be a single pheromone or pheromone-like chemoattractant signal (Fischer-Harman et al., 2012; Merlini et al., 2016).

6.3 Conclusions

6.3.1 Hypotheses explaining the mechanism of negative tropisms in fungi

It is evident that self-avoidance takes place between cells in all developmental stages of a vegetative fungal colony (sections 3.2.1 and 3.2.7). However, the mechanisms of communication during self-avoidance responses are unknown. The results presented in this thesis are consistent with two alternative hypotheses explaining the mechanisms of communication resulting in negative autotropisms determining sites of germ tube emergence from conidia, and self-avoidance between germ tubes and between vegetative hyphae:

(1) Fine-tuned sensing of gradients of extracellular chemicals, that can act as self-avoidance signals, and which are produced and sensed by adjacent hyphae. These chemicals may be antagonistic causing hyphae to grow away (negative tropism) from the highest concentration of the chemical. Alternatively, the chemical (e.g. nutrient) may naturally be in the form of a gradient adjacent to the hyphae as it is consumed or inactivated by the presence of hyphae. In this case the hypha will be undergoing a positive tropism towards it.

(2) Pulsatile release of an antagonistic chemical that alternates between adjacent hyphae. A similar process forms the basis of the 'ping-pong' mechanism during CAT chemotropism which is involved in *N. crassa* except in this case the released chemical is a chemoattractant (Read *et al.,* 2009).

My results provided no evidence for cell-cell contact, as exhibited by neurons (Zipursky & Grueber, 2013; section 1.3.6.1), playing a significant if any role in these negative autotropisms (section 3.2.2).

A novel unifying model connecting the two hypotheses is shown in Figure 6.2. Deletion of certain GPCRs leads to lack of activation and unbinding their related G-proteins which in turn could activate their downstream effectors. In such a case the hyphal tip sensing is compromised, and hyphae cannot readjust growth according to the corresponding external stimulus. My results also indicate that several kinases related to the cAMP-PKA pathway as regulators or downstream effectors are also involved.

Therefore, self-avoidance is a result of potentially two types of external stimuli, the repulsion due to a pheromone secreted by neighbouring cells and the attraction towards high concentration gradients of nutrients. These external stimuli can either be the
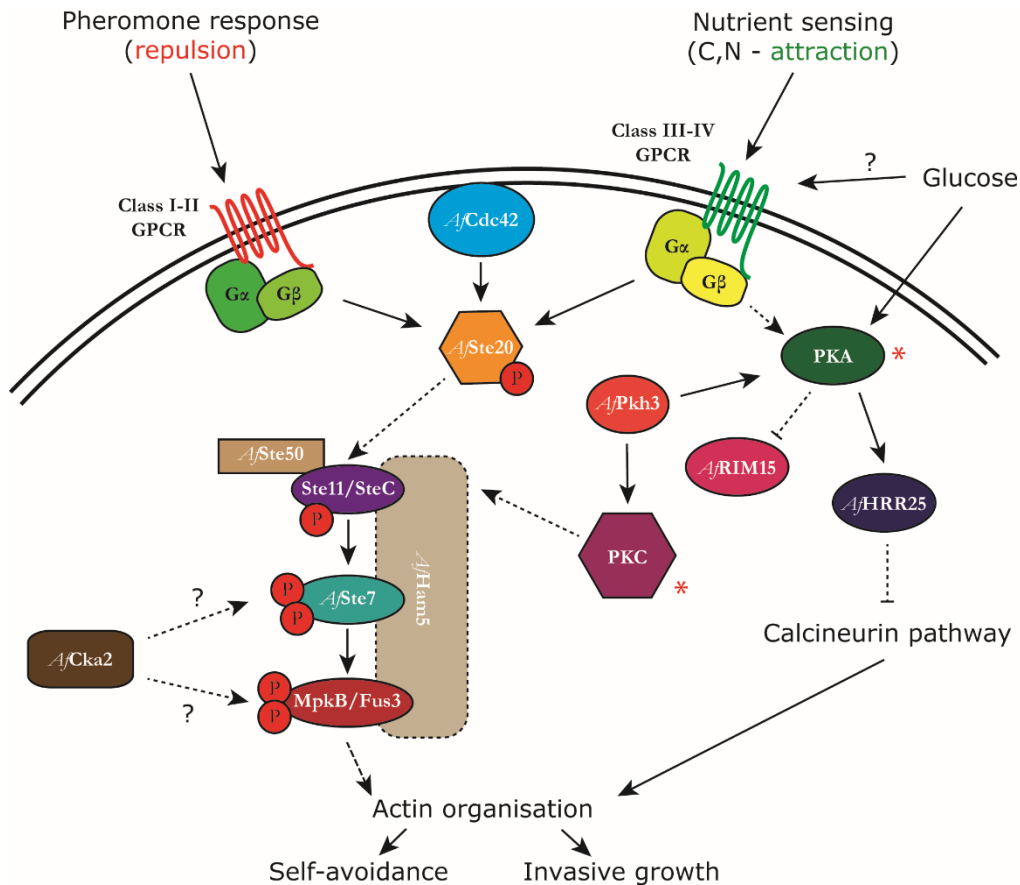
Figure 6.2 Hypothetical model of signalling regulation during self-avoidance in vegetative hyphae at the colony periphery. Relations between signalling components based on literature (see text). Two main types signals may be responsible for self-avoidance: (i) pheromone response and (ii) nutrient availability. In the former case, hyphae may sense a signal molecule which is emitted by neighbouring hyphae. This hypothesis would suggest a 'ping-pong' communication mechanism between the two hyphae, with the signal molecule being emitted in pulses to avoid saturating the gradient around the sensing hyphae. The hyphae would divert its growth from the highest concentration towards the lowest. In the latter mechanism, the hyphal tip grows towards the highest concentration of carbon and nitrogen sources. Since those nutrients are possibly more depleted in the area surrounding neighbouring hyphae, a micro-gradient is formed which can be sensed by the tip of an approaching hypha. Subsequently, the tip may rearrange its growth towards higher concentrations of the sensed nutrient. Thus, what we perceive as negative autotropism may in reality be a positive chemotropism. Based on the balance between the combination of signals received, the fungal cell "decides" where to grow in the form of a self-avoidance response, thus maximising its growth efficiency and therefore fitness to the external environment. Straight lines represent direct interactions, dotted lines represent interactions which include more intermediate components, question marks denote unknown relations, asterisks mark components which are essential for growth in *A. fumigatus*. Model is based on reported interactions in *N. crassa* and *S. cerevisiae* literature. See text for more details.

negative tropism towards a pheromone or the positive tropism towards a nutrient gradient. To my knowledge this is the first time that a proposed model unifies observations and hypotheses made in the past (presented in section 1.3.6).

6.4 Future perspectives

This study has raised a few interesting questions regarding negative autotropisms in *A. fumigatus*. However, several key questions remain unanswered:

(1) What influence do GC-MS identified VOCs have on self-avoidance? As an extension, are there are early growth representative VOCs in *A. fumigatus* which can be identified as early infection markers?

(2) What is the effect of nonanoic acid in other *Aspergilli*? Does it inhibit germination? Does it induce the formation of synnemata in other species of this genus? What other compounds reported to induce synemmata in other filamentous fungi, can also induce them in *A. fumigatus*?

(3) How is the Spitzenkörper, as the primary organelle complex involved in the directional growth of hyphae (Read, 2018), regulated to generate hyphal negative autotropisms in *A. fumigatus*?

(4) Do small rho-GTPases (e.g. CDC42) play a role in regulating the self-avoidance response of determining the site of germination from spores and the vegetative hyphal avoidance response at the colony periphery. This should be analysed using a fluorescent CRIB reporter of active rho-GTPases, as described previously with germ tubes of *N. crassa* (Lichius et al., 2014).

(5) Although, a phenotypic screen of the kinase knockout library was conducted, reverse complementation experiments were not carried out. The effect of induced kinase inhibition was left also left untested. To this extent, an ideal venue of experiments would be to generate mutant strains of the kinases implicated to self-avoidance so they can be tested by chemical genetics through live-cell imaging (Fleißner, 2013; Gregan et al., 2007). Ideally, this should be done in all *A. fumigatus* mating types, as this study used only *MAT1-1* strains.

(6) The phenotypes of GPCR deletion mutant strains on media with different carbon (e.g. sorbitol, sucrose, fructose) and nitrogen (e.g. methionine, urea, uric acid) sources needs to be analysed in order to elucidate whether there is any phenotype rescue under those conditions.

(7) Other prominent signalling pathways, such as the Reactive Nitrogen Species (RNS) and the NADOX complex have not been tested for their possible roles

in negative autotropisms. Breakthroughs in imaging of intracellular ROS in fungi have been made (Marschall and Tudzynski, 2014) which could help verify if intracellular ROS change when adjacent germ tubes/hyphae approach each other.

6.5 References

Abad, A., Fernandez-Molina, J. V, Bikandi, J., Ramirez, A., Margareto, J., Sendino, J., Hernando, F.L., Ponton, J., Garaizar, J., Rementeria, A., 2010. What makes *Aspergillus fumigatus* a successful pathogen? Genes and molecules involved in invasive aspergillosis. Rev Iberoam Micol 27, 155–182. https://doi.org/10.1016/j.riam.2010.10.003

Affeldt, K.J., Brodhagen, M., Keller, N.P., 2012. *Aspergillus* Oxylipin Signaling and Quorum Sensing Pathways Depend on G Protein-Coupled Receptors. Toxins (Basel). 4, 695–717. https://doi.org/10.3390/toxins4090695

Ayoub, M.A., 2018. Small molecules targeting heterotrimeric G proteins. Eur. J. Pharmacol. 826, 169–178. https://doi.org/10.1016/j.ejphar.2018.03.003

Ayoub, M.A., Crépieux, P., Koglin, M., Parmentier, M., Pin, J.P., Poupon, A., Reiter, E., Smit, M., Steyaert, J., Watier, H., Wilkinson, T., 2017. Antibodies targeting G protein-coupled receptors: Recent advances and therapeutic challenges. MAbs 9, 735–741. https://doi.org/10.1080/19420862.2017.1325052

Dague, E., Alsteens, D., Latgé, J.P., Dufrêne, Y.F., 2008. High-resolution cell surface dynamics of germinating *Aspergillus fumigatus* conidia. Biophys. J. 94, 656–660. https://doi.org/10.1529/biophysj.107.116491

Dijck, P. Van, 2009. Nutrient sensing G protein-coupled receptors: Interesting targets for antifungals? Med. Mycol. 47, 671–680. https://doi.org/10.3109/13693780802713349

Fischer-Harman, V., Jackson, K.J., Muñoz, A., Shoji, J. ya, Read, N.D., 2012. Evidence for tryptophan being a signal molecule that inhibits conidial anastomosis tube fusion during colony initiation in *Neurospora crassa*. Fungal Genet. Biol. 49, 896–

902. https://doi.org/10.1016/j.fgb.2012.08.004

Fleißner, A., 2013. Turning the switch: Using chemical genetics to elucidate protein kinase functions in filamentous fungi. Fungal Biol. Rev. 27, 25–31. https://doi.org/10.1016/j.fbr.2013.02.001

Gregan, J., Zhang, C., Rumpf, C., Cipak, L., Li, Z., Uluocak, P., Nasmyth, K., Shokat, K.M., 2007. Construction of conditional analog-sensitive kinase alleles in the fission yeast *Schizosaccharomyces pombe*. Nat. Protoc. 2, 2996–3000. https://doi.org/10.1038/nprot.2007.447

Hauser, A.S., Attwood, M.M., Rask-Andersen, M., Schiöth, H.B., Gloriam, D.E., 2017. Trends in GPCR drug discovery: New agents, targets and indications. Nat. Rev. Drug Discov. 16, 829–842. https://doi.org/10.1038/nrd.2017.178

Heddergott, C., Calvo, A.M., Latge, J.P., 2014. The Volatome of *Aspergillus fumigatus*. Eukaryot. Cell 13, 1014–1025. https://doi.org/10.1128/EC.00074-14

Hickey, P.C., Jacobson, D.J., Read, N.D., Louise Glass, N., 2002. Live-cell imaging of vegetative hyphal fusion in *Neurospora crassa*. Fungal Genet. Biol. 37, 109–119. https://doi.org/10.1016/S1087-1845(02)00035-X

Hubbes, M., 1975. Terpenes and Unsaturated Fatty-Acids Trigger Coremia Formation By Ceratocystis-Ulmi. Eur. J. For. Pathol. 5, 129–137.

Jin, M., Errede, B., Behar, M., Mather, W., Nayak, S., Hasty, J., Dohlman, H.G., Elston, T.C., 2011. Yeast dynamically modify their environment to achieve better mating efficiency. Sci. Signal. 4, ra54.

Lawrence Zipursky, S., Grueber, W.B., 2013. The Molecular Basis of Self-Avoidance. Annu. Rev. Neurosci. 36, 547–568. https://doi.org/10.1146/annurev-neuro-062111-150414

Leeder, A.C., Palma-Guerrero, J., Glass, N.L., 2011. The social network: deciphering fungal language. Nat. Rev. Microbiol. 9, 440–451.

https://doi.org/10.1038/nrmicro2580

Lichius, A., Goryachev, A.B., Fricker, M.D., Obara, B., Castro-Longoria, E., Read, N.D., 2014. CDC-42 and RAC-1 regulate opposite chemotropisms in *Neurospora crassa*. J Cell Sci 127, 1953–1965. https://doi.org/10.1242/jcs.141630

Marschall, R., Tudzynski, P., 2014. A new and reliable method for live imaging and quantification of reactive oxygen species in Botrytis cinerea. Technological advancement. Fungal Genet. Biol. 71, 68–75. https://doi.org/10.1016/j.fgb.2014.08.009

McAlpin, C.E., 2001. An Aspergillus flavus Mutant Producing Stipitate Sclerotia and Synnemata. Mycologia 93, 552. https://doi.org/10.2307/3761740

Merlini, L., Khalili, B., Bendezú, F.O., Hurwitz, D., Vincenzetti, V., Vavylonis, D., Martin, S.G., 2016. Local Pheromone Release from Dynamic Polarity Sites Underlies Cell-Cell Pairing during Yeast Mating. Curr. Biol. 26, 1117–1125. https://doi.org/10.1016/j.cub.2016.02.064

Miyoshi, M., 1894. Über chemotropismus der Pilze. Bot. Zeitung 52, 1–28.

Porter, C.L., 1924. Concerning the Characters of Certain Fungi as Exhibited by Their Growth in the Presence of Other Fungi. Am. J. Bot. 11, 168. https://doi.org/10.2307/2435538

Read, N.D., Lichius, A., Shoji, J. ya, Goryachev, A.B., 2009. Self-signalling and self-fusion in filamentous fungi. Curr. Opin. Microbiol. 12, 608–615. https://doi.org/10.1016/j.mib.2009.09.008

Skidmore, A.M., Dickinson, C.H., 1976. Colony interactions and hyphal interference between *Septoria nodorum* and phylloplane fungi. Trans. Br. Mycol. Soc. 66, 57–64. https://doi.org/10.1016/S0007-1536(76)80092-7

Stephenson, K.S., Gow, N.A.R., Davidson, F.A., Gadd, G.M., 2014. Regulation of vectorial supply of vesicles to the hyphal tip determines thigmotropism in

Neurospora crassa. Fungal Biol. 118, 287–294.
https://doi.org/10.1016/j.funbio.2013.12.007

Ugalde, U., Rodriguez-Urra, A.B., 2014. The Mycelium Blueprint: insights into the cues
that shape the filamentous fungal colony. Appl. Microbiol. Biotechnol. 98, 8809–
8819. https://doi.org/10.1007/s00253-014-6019-6

Varga, J., Frisvad, J.C., Samson, R.A., 2011. Two new aflatoxin producing species, and
an overview of *Aspergillus* section Flavi. Stud. Mycol. 69, 57–80.
https://doi.org/10.3114/sim.2011.69.05

[Blank page]

Appendices

[Blank page]

A.1 – Siloxane products detected in the volatome analysis

Table A.1 Siloxane products detected in fungal headspace analysis

Retention time (min)	Relative abundance	Compound
1.64	6.6625	Sulfur dioxide
1.7	1.775	Silane, difluorodimethyl-
4.26	4.65	Cyclotrisiloxane, hexamethyl-
7.93	3.675	Cyclotetrasiloxane, octamethyl-
11.9	5.35	Cyclopentasiloxane, decamethyl-
16	3.8375	Cyclohexasiloxane, dodecamethyl-
19.82	0.9125	Heptasiloxane, hexadecamethyl-
23.12	0.5375	Hexasiloxane, 1,1,3,3,5,5,7,7,9,9,11,11-dodecamethyl-

A.2 - Table of essential kinases in *A. fumigatus*

Table A.2 Essential kinases in *A. fumigatus*

| Aspergillus fumigatus | | | Neurospora crassa | | Candida albicans | | Saccharomyces cerevisiae | | |
gene	locus	Kinase family	gene	locus	gene	locus	gene	locus	Roles in Saccharomyces cerevisiae
ire1 (put.)	AFUB_002120	AGC	ire-1	NCU02202	IRE1	I503_00775	IRE1 (ERN1)	YHR079C	ER stress response
ark1 (put.)	AFUB_023600	AGC	stk-13	NCU00108		I503_04793	IPL1 (PAC15)	YPL209C	Cell cycle
	AFUB_082830	AGC	stk-9	NCU07399		I503_05403	ENV7	YPL236C	Membrane fusion regulation
	AFUB_095460	AGC	dbf2	NCU09071		I503_02106	DBF20	YPR111W	Cell cycle
	AFUB_068890	AGC	cot-1	NCU07296		I503_01009	CBK1	YNL161W	RAM signalling (polarity, septum, cell integrity)
	AFUB_081870	CAMK	cdc5	NCU09258	CDC5/MSD2	I503_00092	CDC5	YMR001C	Cell cycle
csk1 (put.)	AFUB_019630	CK1	ck-1a	NCU00685		I503_04795	HRR25 (KTI14)	YPL204W	cation homeostasis
cskA	AFUB_072800	CK1	ck-1b	NCU04005	CK1	I503_02255	YCK2	YNL154C	Glucose repression, nutrient sensing
sakA	AFUB_012420	CMGC	os-2 (muk-3)	NCU07024	HOG1	I503_01784	HOG1	YLR113W	Oxidative and/or osmotic stress
prp4 (put.)	AFUB_038640	CMGC	stk-57	NCU10853		I503_01912	YAK1	YJL141C	Nutrient sensing
sgv1 (put.)	AFUB_053070	CMGC	bur-1	NCU01435	BUR1	I503_01938	SGV1 (BUR1)	YPR161C	Transcription regulator
	AFUB_043460	CMGC	cdc7	NCU11410	CDC7	I503_01976	CDC7	YDL017W	Cell cycle
	AFUB_051670	CMGC	stk-47	NCU06685	CTDa	I503_02722	KIN28	YDL108W	Transcription regulator
	AFUB_077790	CMGC	lkh-4	NCU00230		I503_01333	SKY1	YMR216C	mRNA metabolism, cation homeostasis
kin28	AFUB_089250	CMGC	prk-3	NCU03659	KIN28	I503_00655	KIN28	YDL108W	Transcription regulator
vps15	AFUB_077210	CMGC	stk-45	NCU06626		I503_04684	VPS15	YBR097W	Vacuole regulation
	AFUB_054290	CMGC	dsk-1	NCU09202	SRPK3	I503_00596	SKY1	YMR216C	mRNA metabolism, cation homeostasis
	AFUB_079830	CMGC	dsk-1	NCU09202	SRPK3	I503_00596	SKY1	YMR216C	mRNA metabolism, cation homeostasis
mst3-like	AFUB_050750	STE	prk-9	NCU04096	CST20	I503_04258	STE20	YHL007C	Pheromone response, invasive growth
	AFUB_029290	STE	pod-6	NCU11235		I503_01923	KIC1 (NRK1)	YHR102W	Cell integrity and/or morphogenesis
pbs2 (put.)	AFUB_015480	STE	os-5	NCU00587		I503_03108	PBS2	YJL128C	Oxidative and/or osmotic stress
sepH	AFUB_063820	STE	adc-15	NCU01335	CDC15	I503_01959	MKK1	YOR231W	PKC signalling
gcn2	AFUB_054310	STE	cpc-3	NCU01187		I503_05135	GCN2	YDR283C	Nutrient starvation
paf400	AFUB_051100	PIKK	stk-18	NCU01379		I503_04694	TRA1	YHR099W	Transcription regulator
uvsB	AFUB_098230	PIKK	mus-9	NCU11188	MEC1	I503_04422	MEC1	YBR136W	Telomere regulation

A.3 - Table of kinases with growth defects in *A. fumigatus*

Table A.3 Kinase knock-out mutants with defective growth on AMMA.

Aspergillus fumigatus			*Neurospora crassa*		*Candida albicans*		*Saccharomyces cerevisiae*		
gene	locus	Kinase family	gene	locus	gene	locus	gene	locus	Roles/Pathway
pkaC1	AFUB_027890	AGC	*pka-C1*	NCU06240		I503_02157	*TPK2*	YPL203W	Ras-signalling, nutrient sensing
nrc2 (put.)	AFUB_059090	AGC	*nrc-2*	NCU01797		I503_02313	*FPK1*	YNR047W	Membrane asymmetry, pheromone response, TORC
snf1	AFUB_018770	CAMK	*snf-1 (prk-10)*	NCU04566		I503_04165	*SNF1*	YDR477W	Nutrient deprivation (glucose), invasive growth
Ran1 (put.)	AFUB_038630	CAMK	*stk-17 (fi)*	NCU04990		I503_00719	*KSP1*	YHR082C	TORC
	AFUB_039620	CAMK	*camk-2*	NCU02283	*CaMK*	I503_02958	*CMK1*	YFR014C	Cation homeostasis
	AFUB_053520	CAMK	*camk-3*	NCU06177		I503_03743	*TOS3*	YGL179C	Cell cycle, Cytokinesis
	AFUB_007300	CAMK	*stk-22*	NCU03523		I503_03743	*KIN4 (KIN3)*	YOR233W	Cell cycle
kin4 (put.)	AFUB_014350	CAMK	*stk-16*	NCU00914		I503_05638	*PRK1*	YIL095W	Actin cytoskeleton remodelling
	AFUB_006320	CAMK	*stk-38*	NCU06202		I503_02494	*SAK1*	YER129W	Nutrient deprivation (glucose), invasive growth
	AFUB_019930	CAMK	*stk-40*	NCU06249		I503_03173	*PSK2*	YOL045W	Nutrient sensing (sugar flux)
	AFUB_056020	CAMK	*ptk-2*	NCU01940		I503_00662	*NPR1*	YNL183C	TORC
	AFUB_089280	CAMK	*chk2*	NCU02814		I503_02451	*CMK1*	YFR014C	Cation homeostasis
	AFUB_044560	CMGC	*dsk-1*	NCU09202	*SRPK3*	I503_00596	*SKY1*	YMR216C	mRNA metabolism, cation homeostasis
lkh1 (put.)	AFUB_016170	CMGC	*lkh-1*	NCU00230		I503_01333	*KNS1*	YLL019C	TORC
	AFUB_048440	CMGC	*dsk-1*	NCU09292	*SRPK3*	I503_00596	*SKY1*	YMR216C	mRNA metabolism, cation homeostasis
	AFUB_018600	CMGC	*stk-46*	NCU06638		I503_01912	*YAK1*	YJL141C	Nutrient sensing
imeB	AFUB_028770	CMGC	*ime-2 (Prk-8)*	NCU01498	*IME2/SME1*	I503_05741	*IME2 (SME2)*	YJL106W	Cell cycle
	AFUB_017750	CMGC	*lkh-1*	NCU00230		I503_01333	*YAK1*	YJL141C	Nutrient sensing
cdc2	AFUB_073970	CMGC	*cdc-28*	NCU09778		I503_06024	*CDC28*	YBR160W	Cell cycle
mpkA	AFUB_070630	CMGC	*mak-1*	NCU09842	*MKC1*	I503_05440	*SLT2*	YHR030C	CWI, Cell cycle, septum formation
bck1 (put.)	AFUB_038060	STE	*mik-1*	NCU02234		I503_05294	*BCK1*	YJL095W	Cell integrity and/or morphogenesis
sskB (put.)	AFUB_010360	STE	*os-4 (SskB)*	NCU03071		I503_03798	*Ssk2*	YNR031C	Oxidative and/or osmotic stress
ste20-like	AFUB_089870	STE	*mst-1*	NCU00772	*CST20*	I503_04258	*STE20*	YHL007C	Pheromone response, invasive growth
mkk2	AFUB_006190	STE	*mek-1*	NCU06419		I503_02020	*MKK1*	YOR231W	PKC signalling
	AFUB_066030	TK	*stk-51*	NCU08177		I503_00527	*IKS1*	YJL057C	Unknown role
	AFUB_029240	PDHK	*stk-58*	NCU16821		I503_06286	*PKP1*	YIL042C	Mitochondrial kinase

A.4 – Phenotypes of growth defect kinase deletion mutants
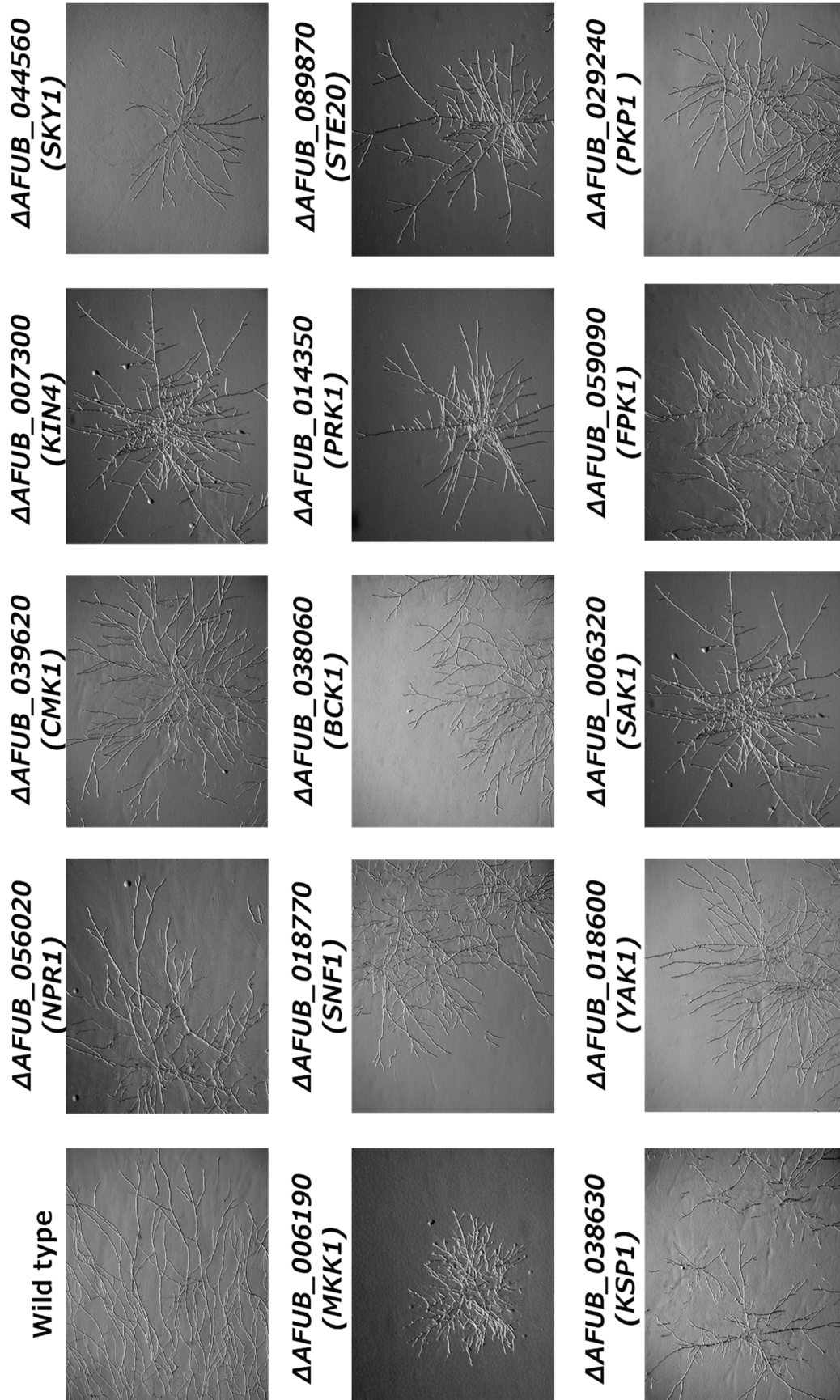
Figure A.1 Phenotypes of kinase with severe growth defects in *A. fumigatus*. In parentheses are the *S. cerevisiae* homologues.

ΔAFUB_016170 (KNS1)

ΔAFUB_073970 (CDC28)

ΔAFUB_019930 (PSK2)

ΔAFUB_010360 (SSK2)

Wild type

ΔAFUB_053520 (TOS3)

ΔAFUB_048440 (SKY1)

ΔAFUB_066030 (IKS1)

ΔAFUB_017750 (YAK1)

ΔAFUB_028770 (IME2)

ΔAFUB_070630 (SLT2)

ΔAFUB_027890 (TPK2)

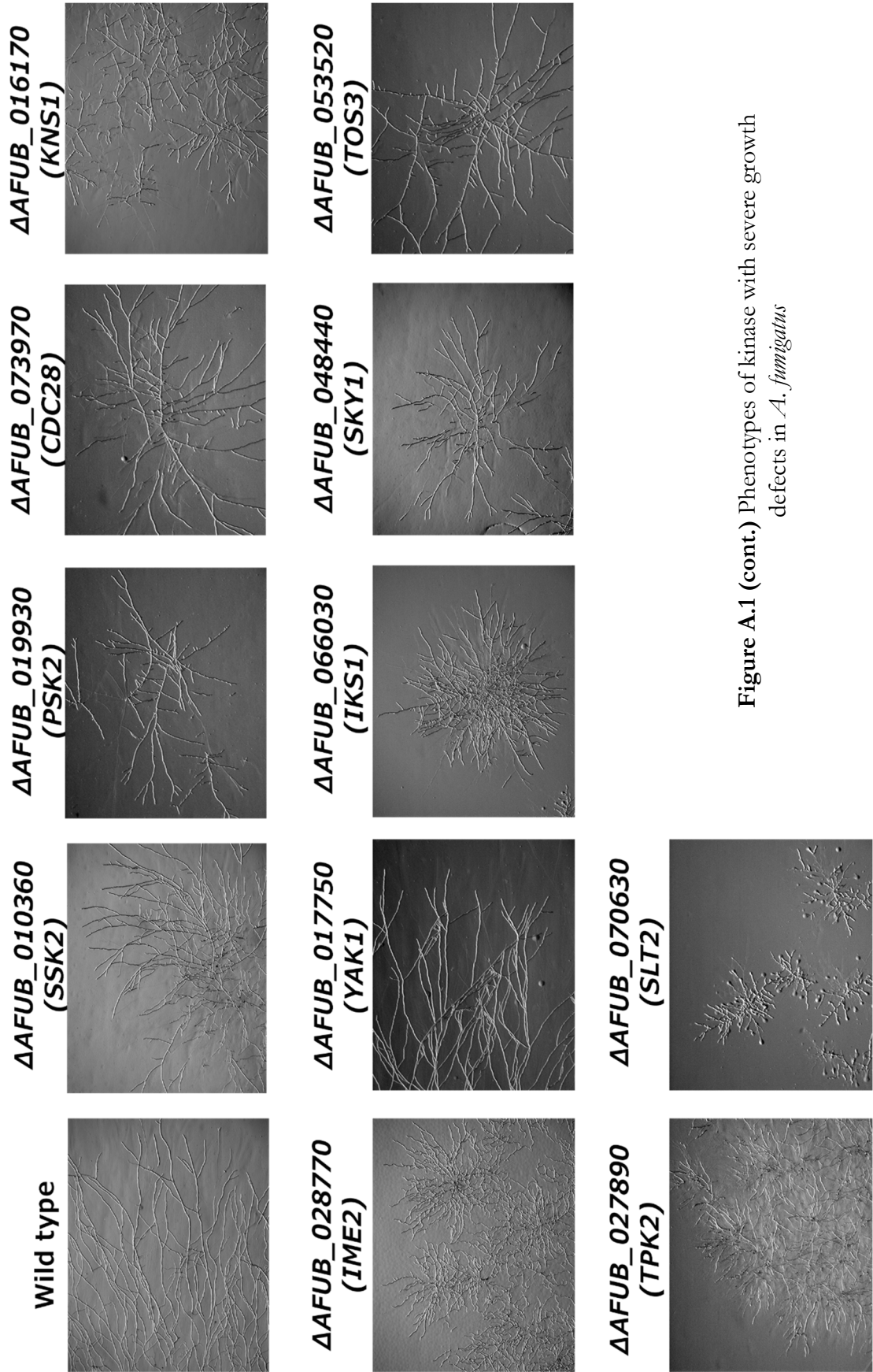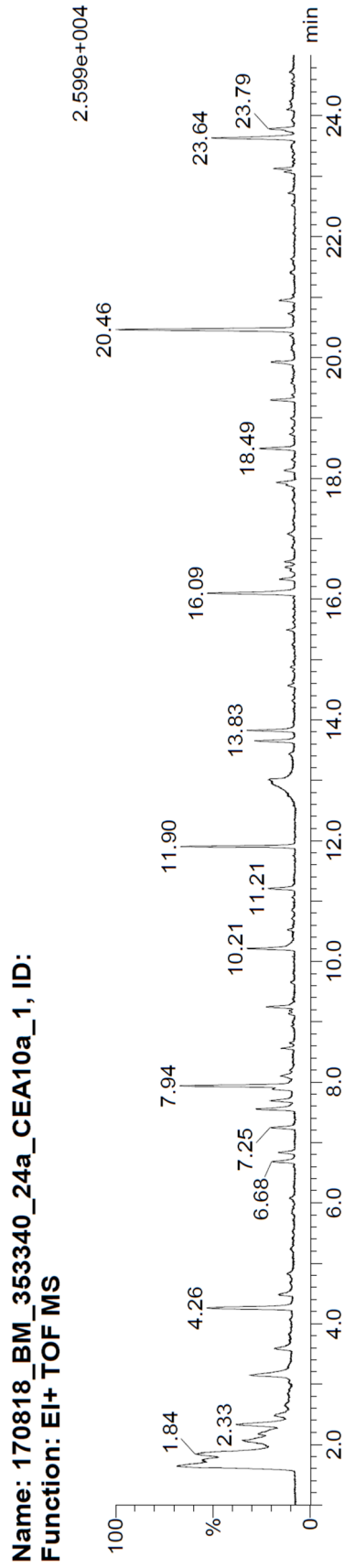**Figure A.1 (cont.)** Phenotypes of kinase with severe growth defects in *A. fumigatus*

A.5 – Sample chromatogram and table from the volatome analysis

Name: 170818_BM_353340_24a_CEA10a_1, ID:
Function: EI+ TOF MS

Figure A.2 Sample hromatogram of *A. fumigatus* volatome extracted at 24 hours.

Table A.4 Results of peaks analysis against NIST-library of Figure A.2. Scan corresponds to the scan ID attributed by the analysis equipment, abundance denotes absolute ion count.

Scan	Ret. Time	Abundance	Compound Name
882	1.62	95	Silane, difluorodimethyl-
895	1.64	881	Aminomethanesulfonic acid
896	1.64	726	Silane, difluorodimethyl-
897	1.65	749	Silane, difluorodimethyl-
915	1.68	341	Silane, difluorodimethyl-
941	1.73	92	1,2-Propanediol, 3,3'-oxydi-, tetranitrate
954	1.75	83	Methane, fluorotrinitro-
961	1.76	466	Dimethyl ether
972	1.78	203	Hydrazine, methyl-
1002	1.84	402	2-Buten-1-ol, 3-methyl-, acetate
1020	1.87	240	2-Propanone, 1-cyclohexyl-
1119	2.05	264	Acetic acid
1120	2.05	246	Hydrazine, 1,2-dimethyl-
1128	2.07	111	Formic acid hydrazide
1270	2.33	298	(Z),(Z)-2,4-Hexadiene
1272	2.33	243	Cyclopentene, 1-methyl-
1718	3.15	240	Pyrazine
1957	3.59	84	Toluene
2319	4.25	280	Cyclotrisiloxane, hexamethyl-
2320	4.26	446	Cyclotrisiloxane, hexamethyl-
2322	4.26	409	Cyclotrisiloxane, hexamethyl-
2442	4.48	96	Pyrazine, methyl-
3643	6.68	83	Benzene, 1-bromo-3-fluoro-
3644	6.68	72	p-Bromofluorobenzene
3646	6.69	72	p-Bromofluorobenzene
3724	6.83	55	ç-Terpinene
3950	7.24	66	Camphene
3952	7.25	80	Camphene
4117	7.55	75	Ethanone, 2,2-dihydroxy-1-phenyl-
4119	7.55	157	Benzaldehyde
4192	7.69	114	Cyclopentane, 1,2-dimethyl-
4298	7.88	120	Phenol
4326	7.93	480	Cyclotetrasiloxane, octamethyl-
4327	7.94	497	Cyclotetrasiloxane, octamethyl-
4328	7.94	441	Cyclotetrasiloxane, octamethyl-
4419	8.11	56	Benzonitrile
5039	9.24	100	D-Limonene
5041	9.25	104	Cyclobutane, 1,3-diisopropenyl-, trans
5565	10.21	218	Phenylglyoxal
5567	10.21	160	Acetophenone
6109	11.21	87	Nonanal
6400	11.74	1	[1,4']Bipiperidinyl-4'-carboxamide, 1'-(4-chlorobenzenesu...
6487	11.90	331	Cyclopentasiloxane, decamethyl-
6488	11.90	345	Cyclopentasiloxane, decamethyl-
6489	11.90	342	Cyclopentasiloxane, decamethyl-

Scan	Ret. Time	Abundance	Compound Name
6490	11.90	348	Cyclopentasiloxane, decamethyl-
7098	13.02	109	Benzoic acid
7099	13.02	81	Benzoic acid
7441	13.65	135	Dodecane
7442	13.65	163	Dodecane
7443	13.65	147	Dodecane
7536	13.82	153	Decanal
7538	13.83	181	Decanal
7776	14.26	0	Terephthalic acid, 4,4-dimethylpent-3-yl pentyl ester
8774	16.09	215	Silane, dimethyl(dimethyl(dimethyl(2-isopropylphenoxy)si...
8775	16.09	289	Cyclohexasiloxane, dodecamethyl-
8776	16.10	334	Silane, dimethyl(dimethyl(dimethyl(2-isopropylphenoxy)si...
10080	18.49	149	Tetradecane
10081	18.49	142	Tetradecane
10521	19.30	72	à-ylangene
11154	20.46	742	ç-HIMACHALENE
11155	20.46	696	ç-HIMACHALENE
11156	20.46	584	ç-HIMACHALENE
12610	23.13	57	Octasiloxane, 1,1,3,3,5,5,7,7,9,9,11,11,13,13,15,15-hexa...
12885	23.63	330	Pentane, 1,1,2,3,4,5-hexachloro-1,2,3,4,5,5-hexafluoro-
12886	23.64	344	Pentane, 1,1,2,3,4,5-hexachloro-1,2,3,4,5,5-hexafluoro-
12887	23.64	281	Pentane, 1,1,2,3,4,5-hexachloro-1,2,3,4,5,5-hexafluoro-
12888	23.64	208	Pentane, 1,1,2,3,4,5-hexachloro-1,2,3,4,5,5-hexafluoro-
12968	23.79	11	Tetrahydropyran Z-10-dodecenoate

A.6 - Publications

Check for updates

Development of an adaptable headspace sampling method for metabolic profiling of the fungal volatome†

Waqar M. Ahmed, ‡[a] Pavlos Geranios,‡[a] Iain R. White,[b] Oluwasola Lawal, [a] Tamara M. Nijsen,[c] Michael J. Bromley,[a] Royston Goodacre, [b] Nick D. Read[a] and Stephen J. Fowler *[a,d]

Pulmonary aspergillosis can cause serious complications in people with a suppressed immune system. Volatile metabolites emitted by *Aspergillus* spp. have shown promise for early detection of pathogenicity. However, volatile profiles require further research, as effective headspace analysis methods are required for extended chemical coverage of the volatome; in terms of both very volatile and semi-volatile compounds. In this study, we describe a novel adaptable sampling method in which fungal headspace samples can be sampled continuously throughout a defined time period using both active (pumped) and passive (diffusive) methods, with the capability for samples to be stored for later off-line analysis. For this method we utilise thermal desorption-gas chromatography-mass spectrometry to generate volatile metabolic profiles using *Aspergillus fumigatus* as the model organism. Several known fungal-specific volatiles associated with secondary metabolite biosynthesis (including α-pinene, camphene, limonene, and several sesquiterpenes) were identified. A comparison between the wild-type *A. fumigatus* with a phosphopantetheinyl transferase null mutant strain (*ΔpptA*) that is compromised in secondary metabolite synthesis, revealed reduced production of sesquiterpenes. We also showed the lack of terpene compounds production during the early growth phase, whilst pyrazines were identified in both early and late growth phases. We have demonstrated that the fungal volatome is dynamic and it is therefore critically necessary to sample the headspace across several time periods using a combination of active and passive sampling techniques to analyse and understand this dynamism.

1. Introduction

Pulmonary aspergillosis (PA) is a group of fungal infections of the respiratory tract which can exacerbate disease in patients with ineffective immune defences, such as those with cystic fibrosis or asthma.[1] The causative pathogens of PA (whether invasive or non-invasive forms) are *Aspergillus* spp. for which the current clinical identification method requires microbial culture or PCR which can be time consuming (up to several days), inefficient, and insensitive. Delays in initiating treatment for these diseases can have a significant outcome on patient mortality.[2] Early and accurate detection of *Aspergillus* spp. colonisation within the lung is therefore crucial for diagnosis of PA.

Volatile organic compounds (VOCs) are known to play a role in intracellular communication between microbes, and between microbes and the host,[3,4] and are largely investigated as potential biomarkers of respiratory disease and for the differentiation of pathogens.[5,6] Exploratory analysis of VOCs emitted by fungi typically involves headspace analysis of *in vitro* cultures, as the headspace gas is a rich source of VOCs and directly indicative of extracellular activity. However, the headspace can be sensitive to several factors including secondary metabolite production,[7] interaction with other fungi or bacteria,[8,9] environmental contaminants or stresses,[10] and sampling and analysis methods.[11] It is therefore important to profile the volatome under a range of conditions, such as at different growth phases, using a suitable sampling method.

In this study we have used *A. fumigatus* CEA10 as the model organism to develop an adaptable and simple headspace

[a]School of Biological Sciences, University of Manchester, UK.
E-mail: Stephen.Fowler@manchester.ac.uk
[b]School of Chemistry, Manchester Institute of Biotechnology, University of Manchester, UK
[c]Philips Research, Royal Philips B.V., The Netherlands
[d]Manchester Academic Health Science Centre, Manchester University Hospitals NHS Foundation Trust, UK
†Electronic supplementary information (ESI) available. See DOI: 10.1039/c8an00841h
‡Equal authorship.

sampling method in which samples may be taken at several time points from the same culture, sampled under active (pumped) or passive (diffusive) sampling means, and where VOCs may be stored and transported for off-line analysis. To demonstrate proof-of-principle of the method we developed, we tested the method's performance by identification of known fungal VOCs from *A. fumigatus* and compared the VOC profile of wild-type *A. fumigatus* to a mutant strain lacking polyketide synthase (PKS) and non-ribosomal-peptide synthase (NRPS) activity and hence with impaired secondary metabolism production.

2. Experimental

2.1. Strains and growth conditions

Two strains of *Aspergillus fumigatus* were used for headspace analysis – a wild-type strain (FGSC A1163) and a phosphopantetheinyl transferase (PptA) null mutant (ΔpptA) derived from the aforementioned wild-type. The ΔpptA strain was recently shown to lack effective secondary metabolite, siderophore, and lysine biosynthesis,[12] rendering the enzyme a potential antifungal target.

A. fumigatus CEA10 ($n = 5$) and ΔpptA ($n = 6$) strains were cultured on Sabouraud Dextrose Agar (Oxoid, Basingstoke, UK) for three to five days at 37 °C. Spores (conidia) were harvested with 10 mL PBS-Tween80 (Sigma-Aldrich, Gillingham, UK) 0.05% v/v (PBS composition in 1 litre: NaCl 8 g, KCl 0.2 g, Na_2PO_4 1.44 g, KH_2PO_4 0.24 g, pH = 7.4). The suspension was subsequently filtered through a sterile double layer of Miracloth (Merck Millipore, Darmstadt, Germany), and the filtrate was centrifuged at 5500g for 10 min. After discarding the supernatant, the precipitate containing the spores was re-suspended in 5 mL of fresh PBS-Tween 80 0.05%. Spores were counted using a Fuchs-Rosenthal haemocytometer and a conventional optical benchtop microscope to optimise the concentration of spores.

2.2. Headspace sampling

The headspace chamber was composed of glass, and the flask opening was sealed with a PTFE stopper (Sigma-Aldrich, Gillingham, UK). A hollow stainless-steel tube was exposed within the headspace chamber, and VOC samples were trapped on a sorbent tube fixed onto a three-way stainless-steel ball valve (Thames Restek, Saunderton, UK) attached to the outside part of the exposed hollow tube. This set up prevented any aerosolised conidia to attach outside of the sample sorbent tube and within the valve. PTFE tape was used as a seal and to prevent fixtures prone to gas leaks.

For the headspace sampling, 100 mL Büchner filter flasks (Scientific Glass Laboratories Limited, Stoke-on-Trent, UK) containing 10 mL of solid *Aspergillus* minimal media (AMM) were inoculated with 1 mL of conidial suspension containing a total of 3×10^5 spores. After gentle shaking to ensure the suspension has covered the entirety of the media surface, the flasks were sealed and incubated at 37 °C. All manipulations

were carried out in a Class 2 microbiological cabinet under aseptic conditions.

During active sampling, headspace gas was drawn out using a low-flow pump (Acti-VOC, Markes International, Llantrisant, UK) with a flow rate of 50 mL min^{-1} for 2 min, resulting in a total sample volume of 100 mL per sample. Headspace was sampled at two time points for germination (0 to 8 h) and maturation or conidiation (12 to 24 h) for all fungal strains and media samples. Passive sampling (*i.e.* diffusive sampling) was performed between 0 and 8 h, and 12 and 24 h. Passive sampling relied upon reaching a pressure-dependant equilibrium; *i.e.*, between the atmospheric pressure within the headspace chamber and the external atmospheric pressure. Headspace gas is drawn out of the chamber with minimal flow (generated by increased pressure), where VOCs are adsorbed onto the sorbent material. The total volume was therefore unknown as the passive flow per minute was not recorded. Although purging the headspace was an option, we chose not to use a gas purge method (*i.e.* with inert gases such as CO_2 and N_2) as induction may disrupt the culture (by drastically lowering the pH, through HCO_3^- in the case of CO_2) and cause turbulence within the headspace chamber. An illustration of active and passive sampling is shown in Fig. 1.

After sampling, flasks were treated with Chemgene HLD$_4$D (Star Lab group, Milton Keynes, UK) for 24 h. After heating to bring the contained media to a melting point, the media was discarded, the flasks were thoroughly washed with water, rinsed with sterile water and autoclaved to be used for subsequent sampling experiments.

2.3. Sample desorption and analysis

Samples were purged through stainless-steel thermal desorption tubes packed with a multi-bed sorbent containing Tenax TA and Carbograph 5TD (Markes International, Llantrisant, UK). The sorbent material was chosen based on the extended trapping range (C_3 to C_{30}) without retaining a high concentration of water molecules.

Tubes were reconditioned at 330 °C for 60 min with a constant dry N_2 flow of 100 mL min^{-1} through the tubes. Sorbent tubes were tightly sealed with brass caps during storage and transportation. After adsorption, sorbent tubes were transported for analysis in an airtight container and stored at 4 °C for no longer than one week before desorption.

Samples were analysed in randomised blocks by Thermal Desorption-Gas Chromatography-*time of flight*-Mass Spectrometry (TD-GC-*tof*-MS). Briefly, tubes were heated in a thermal desorption unit (Unity 2, Markes International, Llantrisant, UK) to 320 °C (5 min hold) before being purged with helium (1 mL min^{-1}). Compounds were transferred onto a cold trap (kept at 0 °C) before being desorbed a second time to 330 °C (3 min hold) and transferred into the GC column for separation. The Agilent DB-5 ms Ultra Inert GC column (30 m length, 0.25 mm internal diameter, 0.25 μm film thickness) within an Agilent 6890 GC oven (Agilent Technologies, West Lothian, UK) had a helium carrier gas flow set to a constant
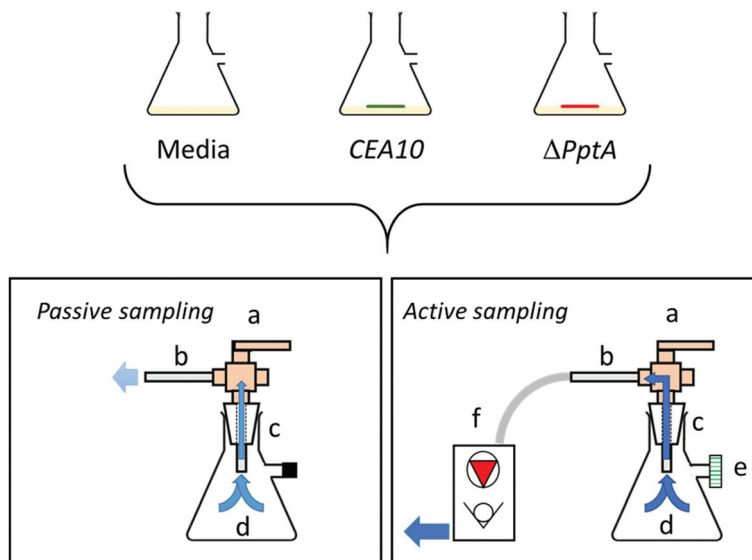
Fig. 1 Illustration of culture samples (media, CEA10, and ΔpptA), and headspace sampling methods (passive sampling and active sampling) where the blue arrows signify headspace gas flow. The headspace sampling apparatus is comprised of several parts, labelled as (a) three way ball valve (brass or stainless steel), (b) thermal desorption tube containing sorbent material, (c) hollow tube (PTFE or stainless steel) and PTFE stopper combination forming an gas tight seal, (d) headspace chamber (glass), (e) input flow filter (in active sampling mode only), and (f) a calibrated and controlled low flow pump.

pressure method (69 kPa), and was subjected to a temperature ramped program starting at 40 °C, first ramp to 170 °C at 6 °C min^{-1}, and the second ramp to 250 °C at 15 °C min^{-1} (total GC run time of 27 min). After chromatographic separation, VOCs were transferred to the mass spectrometer (GCT Premier, Waters Corporation, Manchester, UK) and subjected to electron ionisation (EI) in positive mode (70 eV), before further separation in the *time-of-flight* mass analyser. Mass spectra were acquired in centroid format at a scan rate of 10 scans per s, between m/z 40 and 500.

Each sample was purged with an internal standard to account for analytical variation and to normalise samples (1 ppmv 4-bromofluorobenzene in N$_2$), and each batch run was bracketed by a mixture of VOC standard chemicals (>95% purity, Sigma-Aldrich, Gillingham, UK) to monitor instrument performance. External standards were also run independently to confirm the identification of some VOCs of interest to MSI level 1[13,14] (see Table S1† for further information on the VOC mixture and external standards).

2.4. Data analysis and VOC Identification

Raw GC-MS data files were converted to mzXML format using the MSConvert software (ProteoWizard v. 3.0.8738, Los Angeles, USA). Samples were pre-processed (peak integration and smoothing, baseline correction, and retention time alignment) using both the *XCMS* package[15] through R (R Core Development team, version 3.4.2) and Chromalynx batch analysis using the ApexTrack peak integration algorithm (Masslynx software, Waters Corporation, Manchester, UK). XCMS and Chromalynx parameters were tuned using the VOC standards mixture (Table S1†). The National Institute of

Standards and Technology mass spectral library (NIST version 2014, Gaithersburg, USA) was used for compound identification of chromatographic peaks *i.e.* MSI level 2. In addition, some VOCs were identified with NIST and a chemical standard *i.e.* MSI level 1 (where orthogonal data are used to identify a compound).[13,14]

Peak intensities were normalised by the internal standard for each sample. To test statistical significance between two different sample groups, the non-parametric Mann Whitney-U test was used ($\alpha \leq 0.05$). For multivariate analysis, features with >50% of missing values were removed. Remaining missing values were imputed using the random forest proximity algorithm.[16,17] Features were then range scaled and mean centred.

Principal component analysis (PCA) between strains and time points was carried out to visualise sample separation, batch effects, and identify outliers. If no clear separation was visible between groups, further supervised analysis in the form of Principal component-discriminant function analysis (PC-DFA) was performed using the *adegenet* package.[18] Here, the number of PCs used in the final model were optimised using stratified random sampling (×1000) where data were split into an internal training and validation set (ratio of 75 : 25). From this internal validation, the optimised number of PCs with the lowest root mean squared error (RMSE) from the percentage of successful predicted outcomes was chosen for the final model. PC-DFA loadings from each discriminant function were extracted and features were identified through a NIST library search. The features and identifications were compared to the results of compounds identified through the Chromalynx software.

3. Results

3.1. Headspace sampling method development

Data pre-processing and treatment resulted in a total of 1450 features (*m/z* fragment ions at a specific retention time), which served as input into multivariate analysis. Clusters of discriminatory features were extracted and a total of 35 compounds were identified, 11 of which were identified to MSI level 1 (*i.e.* with a NIST library search and chemical standards).

Headspace sampling was performed to assess the impact of different hardware materials on volatile profiles obtained from tissue culture flasks. The selected materials were glass for the chamber, stainless-steel to channel VOCs towards the sorbent trap, and polytetrafluoroethylene (PTFE) material to seal flask openings. Chromatograms of headspace samples from an empty plastic cell culture flask compared to an empty glass flask are shown in the ESI (Fig. S1†), where a larger number of contaminant VOCs were present from the cell culture flask.

Sampling was performed within the incubator to minimise changes in temperature and pressure, where any fluctuation in these would alter the vapour pressure of headspace VOCs. The sampling volume was chosen based on headspace volume clearance. In our case, this was set to 50 mL min^{-1} for 2 min to clear a headspace volume of approximately 80 mL. Headspace gas was replaced by ambient air through the flask side arm. Active sampling resulted in increased number of VOCs identified, the most significant being sesquiterpenes, when compared to passive sampling (see chromatograms in Fig. S2†).

From blank control samples of the apparatus, known VOCs associated with instrument artefacts (*i.e.* from the analytical instrument, sorbent tubes, cleaning and maintenance, and headspace apparatus) were identified as difluoro(dimethyl)

silane (1.65 min), ethanol (1.77 min), benzene (2.49 min), benzoic acid (13.24 min) and several siloxane compounds throughout the retention time range which, through process of elimination, were thought to originate from the borosilicate glass flask (cyclotrisiloxane, hexamethyl-, cyclotetrasiloxane, octamethyl-, cyclopentasiloxane, decamethyl-, cycloheptasiloxane, tetradecamethyl-). VOCs from AMM media control samples were identified as acetic acid (2.07 min), benzaldehyde (7.55 min), phenol (7.88 min), acetophenone (10.21 min), nonanal (11.21 min), decanal (13.83 min), 2-ethylhexyl acrylate (14.32 min), and several saturated alkanes (C_{12}–C_{16}). A typical chromatogram of a media-only control sample is shown in ESI Fig. S2.† These compounds were excluded from further analysis for the identification of discriminatory fungal VOCs.

3.2. Fungal VOC profiles

The sum of all peak intensities *i.e.* the total ion count was assessed for whole sample reproducibility between replicate headspace samples for each strain. Across CEA10 replicates, passive sampling showed an increased relative standard deviation (RSD) between active (0–8 h = 13.82%, 12–24 h = 14.13%) and passive sampling (0–8 h = 19.66%, 12–24 h = 19.24%), whereas ΔpptA samples showed higher variation between replicates overall compared to that CEA10 for all both active (0–8 h = 36.03%, 12–24 h = 28.60%) and passive (0–8 h = 18.06%, 12–24 h = 50.93%) sampling methods, except 8 h passively collected samples (CEA10 = 19.66%, ΔpptA = 18.06%).

No clear class separation was shown by PCA and therefore supervised analysis was performed. Fig. 2 shows a PC-DFA scores plot between wild-type CEA10 and mutant ΔpptA strains (6 PCs, Total Explained Variance: 82.3%) for both
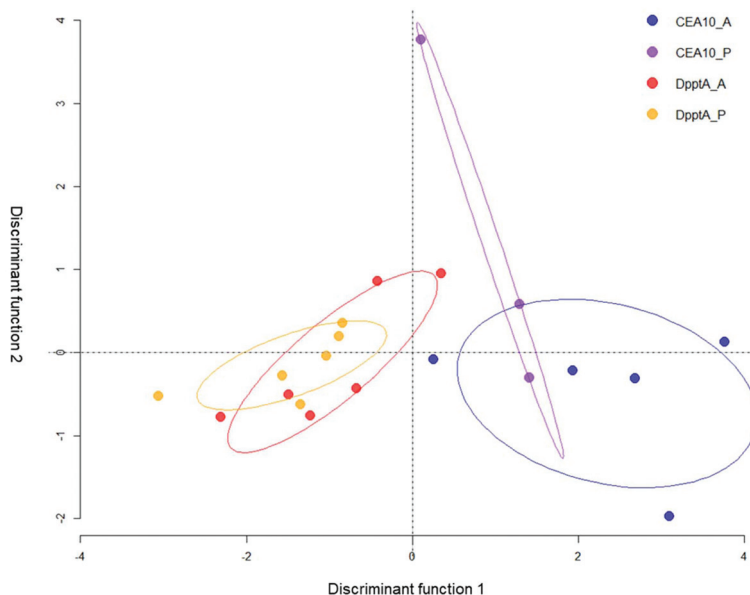

Fig. 2 PC-DFA scores plot (nPCs: 6, TEV: 82.3%) of *A. fumigatus* CEA10 (CEA10-active in blue, and CEA10-passive in purple) and ΔpptA strains (ΔpptA-active in red, and ΔpptA-passive in orange) sampled from 12 to 24 h. Ellipses are drawn as a guide and are have no statistical significance.

Table 1 Fungal volatile organic compounds identified from CEA10 and ΔpptA strains

VOC	Average retention time (min)	Molecular weight (g mol^{-1})	Mean peak intensity ± SD CEA10	ΔpptA	p value
Ethyl acetate	2.16	88.1	0.16 ± 0.28	1.93 ± 1.52	**0.023**
3-Methylbutanal	2.42	86.1	—	1.03 ± 1.19	0.149
Styrene	5.80	104.1	—	0.61 ± 0.46	0.072
Pyrazine	3.10	80.1	2.17 ± 1.26	3.16 ± 2.28	0.786
Methylpyrazine	4.43	94.1	1.37 ± 0.40	2.10 ± 0.67	0.114
α-Pinene[a]	6.83	136.2	0.38 ± 0.24	0.25 ± 0.35	0.570
Camphene[a]	7.25	136.2	0.70 ± 0.13	0.41 ± 0.59	0.441
Limonene[a]	9.24	136.2	0.62 ± 0.43	0.40 ± 0.60	0.570
Himachalene	20.47	204.4	3.58 ± 3.41	—	**0.026**
Decanoic acid	21.93	172.3	0.06 ± 0.11	0.58 ± 0.58	0.337

[a] Confirmed identification to MSI Level 1 by retention time and m/z fragmentation using external standards; all other identifications are MSI Level 2. Some VOCs were not identified in the other sample (signified by a em dash). SD = standard deviation.

passive and active sampling methods (total of four classes: CEA10 *active*, CEA10 *passive*, ΔpptA *active*, and ΔpptA *passive*). PC-DFA loadings from the first discriminant function (DF1, Fig. S3†) revealed VOCs unique to CEA10, identified as cyclopentene, 2-methoxyfuran, α-bergamotene, and himachalene. Additional sesquiterpene VOCs were identified in *A. fumigatus* CEA10 and included isocaryophillene and α-bisabolene from one CEA10 strain sample. Differential VOCs from DF1 were also identified for ΔpptA, identified as 2,5-dimethylfuran, 3-methylbutanal, styrene, and dodecanoic acid. In addition, a sesquiterpene identified as cis-thujopsene was identified from one ΔpptA strain sample. VOCs ($n = 4$) were also identified in at least one sample from both strains, namely ethyl acetate, α-pinene, camphene, and limonene.

Eleven VOCs were identified across a minimum of three replicates (in either or both CEA10 and ΔpptA strains from the 12 to 24 h time point using active sampling) and are listed in Table 1, along with mean peak intensities and p value following statistical testing between CEA10 and ΔpptA sample groups.

3.3. Volatiles specific to germinating and maturing colonies

PC-DFA was also carried out on headspace samples (10 PCs, TEV: 93.5%) collected between 0 to 8 h (*i.e.* during germination) and between 12 to 24 h time periods (Fig. 3) using both active and passive sampling techniques, hence resulting in four classes used in the model. No fungal VOCs were found for samples collected passively between 0 and 8 h, whereas using
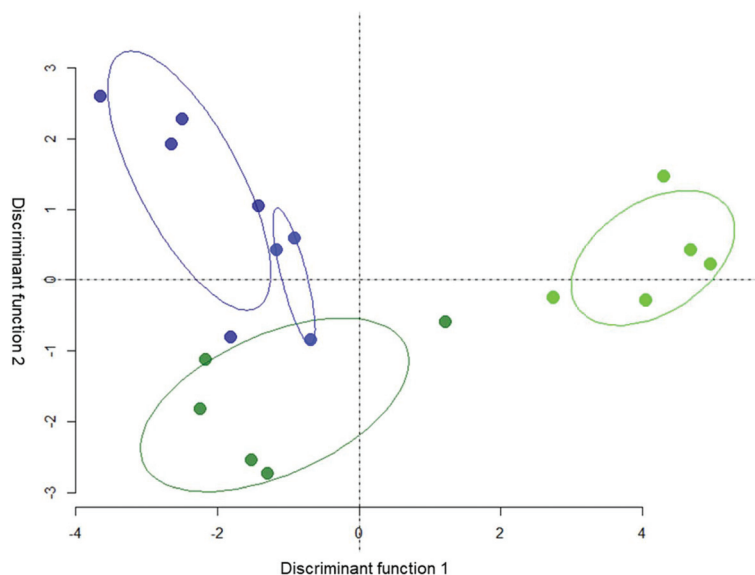

Fig. 3 PC–DFA scores plot (nPCs: 10, TEV: 93.5%) of *A. fumigatus* CEA10 headspace sampled at 0 to 8 h, where samples collected passively are coloured light green and samples collected actively are coloured dark green. Also shown are samples collected between 12 to 24 h, where samples collected passively are coloured light blue, and samples collected actively are coloured dark blue. Ellipses are drawn as a guide and are have no statistical significance.

active sampling at 8 h contained methylpyrazine and pyrazine. These compounds were also present in 12 to 24 h passive and active samples with no difference between the two time-points for both pyrazine (p = 0.383) or methylpyrazine (p = 0.200). PC-DFA Loadings from DF2 revealed the presence of terpene-based compounds (α-pinene, camphene, limonene, and himachelene) in the 12 to 24 h samples.

4.   Discussion

We have developed a headspace sampling method for off-line analysis of the fungal volatome, allowing continuous sampling of a culture over several time-points with passive and/or active sampling methods. Materials were tested and chosen to minimise instrument artefacts and contaminants. As thermal desorption tubes are used to pre-concentrate headspace VOCs, storage and transport of samples between laboratories and off-line analysis by TD-GC-MS is possible. In addition, the sorbent material, flask volume, and gas flow can be changed. Together with metabolomic-driven data processing and supervised analysis, a time segmented non-targeted profile for an extended coverage of the fungal volatome is possible.

To test the method, we have demonstrated proof-of-concept through sampling and identification of known VOCs associated with *A. fumigatus* (Table 1), which included monoterpene compounds α-pinene, camphene, and limonene identified in both *A. fumigatus* CEA10 and ΔpptA strains. The sesquiterpene himachalene was identified more frequently and in higher abundance in the wild-type strain CEA10 (MSI level 2) compared to other sesquiterpenes. Sampling metabolically-derived VOCs is generally difficult, and we have shown that some compounds were not identified across all replicates of a either CEA10 or ΔpptA strains.

Monoterpenes and sesquiterpenes have been identified from *A. fumigatus* headspace by Heddergott *et al.*[19] and in a recent study investigating breath VOCs as diagnostic markers for invasive PA.[20] As described by in both studies, and through the online KEGG database,[21] biosynthesis of terpene-based VOCs originates from the melvanoate pathway, essential for the formation of secondary metabolites, in which farsenyl diphosphate and geranyl diphosphate are the precursors to the biosynthesis of monoterpenes and sesquiterpenes, respectively. The suppression of sesquiterpenes in the ΔpptA mutant is consistent with the role of pptA in activating NRPS and PKS enzymes. Sesquiterpenes are precursors for the production of some secondary metabolites.[19] It is important to note that terpene compounds are not exclusive to *Aspergillus* spp. and may be released by other fungi species such as *Candida*. Terpenes are also common in plant-based diets – an important consideration for clinical biomarker studies.

Pyrazines are nitrogen-containing cyclic compounds and their presence in bacterial metabolism is well described.[22] Recently, pyrazine compounds have gained interest as fungal metabolites.[23] In our study, we were able to identify pyrazine and methylpyrazine in both the CEA10 and ΔpptA strains. The

biosynthesis of pyrazines by *Aspergillus* spp. is not fully understood, however pyrazine groups can be found within the chemical structure of some secondary metabolites such as aspergillic acid or gliotoxin,[19] in which pyrazines may be released in the headspace during their biosynthesis or degradation. As pyrazines share a similar chemical structure to azoles, they may have an inhibitory role in cellular growth. Styrene, another cyclic compound, was also identified from ΔpptA. Although styrene has been identified in other Aspergilli,[24] and to our knowledge this is the first description of it being identified in *A. fumigatus*.

Ethyl acetate was identified only once in CEA10 and 5/6 ΔpptA samples, and has been identified from fungal headspace (including *A. fumigatus*) in a previous study.[25] 3-Methylbutanal and decanoic acid were also more frequently identified in ΔpptA. 3-Methylbutanal, and a methylated furan were identified in a recent study investigating fungal headspace profiles under hypoxia conditions.[10] Increased ethyl acetate, 3-methylbutanal, decanoic acid, and the identified furan-based compounds may be indicative of fatty acid biosynthetic intermediates in the ΔpptA strain, due to the inactivation of fatty acid synthases.

To demonstrate the versatility of the headspace sampling method, we identified VOCs released during the early growth phase of *A. fumigatus*, which included pyrazine and methylpyrazine using active and passive sampling techniques. As mentioned earlier, pyrazine compounds are known fungal VOCs. However, in many studies headspace samples were collected during a single time point and usually at a mature stage of growth (for example 48 h to 96 h). It is therefore important to recognise that some VOCs are suggestive of early cellular growth, and therefore useful in the early indication or diagnosis of aspergillosis, as shown by previous studies.[10,26] Furthermore, VOCs can be transiently present within the headspace (depending on their partition coefficient) and sampling at different time periods is necessary to capture VOCs only present during a particular growth phase. For instance, in this study we showed the absence of terpene compounds from 0–8 h, and their presence in 12–24 h. As terpene compounds are thought to be by-products from the production of secondary metabolites, they may be useful indicators of successful host colonisation or culture growth.

Several VOCs that have been reported in literature were not identified within our samples, for which there may be several reasons, such as the use of different strains, different culture conditions (*e.g.* incubation temperature, growth media) or different sampling time-points to those previously used. In addition, several VOCs were identified in the media (such as alkanes, aldehydes/ketones, and alcohols). These were excluded from further analysis as quantitative analysis would require a higher number of replicates to determine their increased or decreased level of production.

Alternative methods are available for headspace analysis, such as direct mass spectrometric analysis without chromatographic separation, but these do not allow resolution of isobaric chemical species. Techniques such as off-line SPME may be

an alternative to this method.[19,27] Future work would involve comparing different sorbents and developing denatured headspace profiles of several species, and global metabolome coverage between both headspace and liquid matrices.

5. Conclusions

In this study we have demonstrated a novel proof-of-concept for the sampling and analysis of fungal culture headspace using *A. fumigatus* as the test organism. The presence of known fungal VOCs from acquired TD-GC-MS data shows feasibility of the method for profiling the *in vitro* volatome, towards a biological understanding of fungal metabolism. In addition, we have shown that volatile metabolites are indicative of germination, which has potential benefits for clinical diagnostics. Finally, we have shown the dynamic nature of the fungal volatome and how important it is to sample the fungal headspace at different times using active and passive sampling techniques to analyse and understand the significance of this dynamism.

Author contributions

Conflicts of interest

The authors declare no conflicts of interest.

Acknowledgements

References

1 G. D. Brown, D. W. Denning, N. A. R. Gow, S. M. Levitz, M. G. Netea and T. C. White, Hidden killers: Human fungal infections, *Sci. Transl. Med.*, 2012, **4**, 1–10.

2 D. Kontoyiannis and G. Bodey, Invasive aspergillosis in 2002: An update, *Eur. J. Clin. Microbiol. Infect. Dis.*, 2002, **21**, 161–172.

3 L. J. Barkal, C. L. Procknow, Y. R. Álvarez-Garciá, M. Niu, J. A. Jiménez-Torres, R. A. Brockman-Schneider, J. E. Gern, L. C. Denlinger, A. B. Theberge, N. P. Keller, E. Berthier and D. J. Beebe, Microbial volatile communication in human organotypic lung models, *Nat. Commun.*, 2017, **8**, 1770.

4 P. Albuquerque and A. Casadevall, Quorum sensing in fungi a review, *Med. Mycol.*, 2012, **50**, 337–345.

5 L. D. Bos, P. J. Sterk and S. J. Fowler, Breathomics in the setting of asthma and chronic obstructive pulmonary disease, *J. Allergy Clin. Immunol.*, 2016, **138**, 970–976.

6 W. M. Ahmed, O. Lawal, T. M. Nijsen, R. Goodacre and S. J. Fowler, Exhaled Volatile Organic Compounds of Infection: A Systematic Review, *ACS Infect. Dis.*, 2017, **3**, 695–710.

7 S. U. Morath, R. Hung and J. W. Bennett, Fungal volatile organic compounds: A review with emphasis on their biotechnological potential, *Fungal Biol. Rev.*, 2012, **26**, 73–83.

8 B. Briard, C. Heddergott and J. P. Latgé, Volatile compounds emitted by *Pseudomonas aeruginosa* stimulate growth of the fungal pathogen *Aspergillus fumigatus*, *mBio*, 2016, **7**, 1–5.

9 A. H. Neerincx, B. P. Geurts, M. F. J. Habets, J. A. Booij, J. van Loon, J. J. Jansen, L. M. C. Buydens, J. van Ingen, J. W. Mouton, F. J. M. Harren, R. A. Wevers, P. J. F. M. Merkus, S. M. Cristescu and L. A. J. Kluijtmans, Identification of *Pseudomonas aeruginosa* and *Aspergillus fumigatus* mono- and co-cultures based on volatile biomarker combinations, *J. Breath Res.*, 2016, **10**, 16002.

10 C. A. Rees, P.-H. Stefanuto, S. R. Beattie, K. M. Bultaman, R. A. Cramer and J. E. Hill, Sniffing out the hypoxia volatile metabolic signature of Aspergillus fumigatus, *J. Breath Res.*, 2017, **11**, 36003.

11 J. F. Cavalli, X. Fernandez, L. Lizzani-Cuvelier and A. M. Loiseau, Comparison of Static Headspace, Headspace Solid Phase Microextraction, Headspace Sorptive Extraction, and Direct Thermal Desorption Techniques on Chemical Composition of French Olive Oils, *J. Agric. Food Chem.*, 2003, **51**, 7709–7716.

12 A. Johns, D. H. Scharf, F. Gsaller, H. Schmidt, T. Heinekamp, M. Straßburger, J. D. Oliver, M. Birch, N. Beckmann, K. S. Dobb, J. Gilsenan and B. Rash, A Nonredundant Phosphopantetheinyl Transferase, PptA, Is a Novel Antifungal Target That Directs Secondary Metabolite, Siderophore, and Lysine Biosynthesis in Aspergillus fumigatus and Is Critical for Pathogenicity, *mBio*, 2017, **8**, 1–22.

13 L. W. Sumner, A. Amberg, D. Barrett, M. H. Beale, R. Beger, C. A. Daykin, T. W.-M. Fan, O. Fiehn, R. Goodacre, J. L. Griffin, T. Hankemeier, N. Hardy, J. Harnly, R. Higashi, J. Kopka, A. N. Lane, J. C. Lindon, P. Marriott, A. W. Nicholls, M. D. Reily, J. J. Thaden and M. R. Viant,

Proposed minimum reporting standards for chemical analysis, *Metabolomics*, 2007, **3**, 211–221.

14 O. Fiehn, D. Robertson, J. Griffin, M. van der Werf, B. Nikolau, N. Morrison, L. W. Sumner, R. Goodacre, N. W. Hardy, C. Taylor, J. Fostel, B. Kristal, R. Kaddurah-Daouk, P. Mendes, B. van Ommen, J. C. Lindon and S.-A. Sansone, The metabolomics standards initiative (MSI), *Metabolomics*, 2007, **3**, 175–178.

15 C. A. Smith, E. J. Want, G. O'Maille, R. Abagyan and G. Siuzdak, XCMS: Processing Mass Spectrometry Data for Metabolite Profiling Using Nonlinear Peak Alignment, Matching, and Identification, *Anal. Chem.*, 2006, **78**, 779–787.

16 P. S. Gromski, Y. Xu, H. L. Kotze, E. Correa, D. I. Ellis, E. G. Armitage, M. L. Turner and R. Goodacre, Influence of missing values substitutes on multivariate analysis of metabolomics data., *Metabolites*, 2014, **4**, 433–452.

17 D. J. Stekhoven and P. Bühlmann, Missforest-Non-parametric missing value imputation for mixed-type data, *Bioinformatics*, 2012, **28**, 112–118.

18 T. Jombart, Adegenet: A R package for the multivariate analysis of genetic markers, *Bioinformatics*, 2008, **24**, 1403–1405.

19 C. Heddergott, A. M. Calvo and J. P. Latge, The Volatome of Aspergillus fumigatus, *Eukaryotic Cell*, 2014, **13**, 1014–1025.

20 S. Koo, H. R. Thomas, S. D. Daniels, R. C. Lynch, S. M. Fortier, M. M. Shea, P. Rearden, J. C. Comolli, L. R. Baden and F. M. Marty, A Breath Fungal Secondary Metabolite Signature to Diagnose Invasive Aspergillosis., *Clin. Infect. Dis.*, 2014, **59**, 1733–1740.

21 H. Ogata, S. Goto, K. Sato, W. Fujibuchi, H. Bono and M. Kanehisa, KEGG: Kyoto encyclopedia of genes and genomes, *Nucleic Acids Res.*, 1999, **27**, 29–34.

22 S. Schulz and J. S. Dickschat, Bacterial volatiles: the smell of small organisms., *Nat. Prod. Rep.*, 2007, **24**, 814–842.

23 J. S. Dickschat, Fungal volatiles – a survey from edible mushrooms to moulds, *Nat. Prod. Rep.*, 2017, **34**, 310–328.

24 Z. Cheng, M. Li, P. J. Marriott, X. Zhang, S. Wang, J. Li and L. Ma, Chemometric analysis of the volatile compounds generated by aspergillus carbonarius strains isolated from grapes and dried vine fruits, *Toxins*, 2018, **10**, 1–17.

25 S. Matysik, O. Herbarth and A. Mueller, Determination of microbial volatile organic compounds (MVOCs) by passive sampling onto charcoal sorbents, *Chemosphere*, 2009, **76**, 114–119.

26 M. Hertel, S. Hartwig, E. Schütte, B. Gillissen, R. Preissner, A. M. Schmidt-Westhausen, S. Paris, I. Kastner and S. Preissner, Identification of signature volatiles to discriminate *Candida albicans, glabrata, krusei* and *tropicalis* using gas chromatography and mass spectrometry, *Mycoses*, 2015, **59**, 117–126.

27 C. P. Costa, D. Gonçalves Silva, A. Rudnitskaya, A. Almeida and S. M. Rocha, Shedding light on Aspergillus niger volatile exometabolome, *Sci. Rep.*, 2016, **6**, 27441.